5.11 IMPACTS OF MITIGATION MEASURES ON THE TEMPERATURE FIELD AND THEIR RANKING AT THE REGIONAL SCALE

In the following sections, the impacts of mitigation measures on the temperature field are presented. It is important to note that the ranking of various measures in terms of their cooling potential can differ by area and time interval (i.e., hour or range of hours). Thus, the implementation and deployment of measures (e.g., selecting the top priorities) depends on the goal to be achieved at a particular locale. For example, if the goal were to reduce daytime maxima in temperature, then the ranking could differ from if all-hour temperature averages were to be reduced or if, for some reason, nighttime temperature were to be modified.

We note again here that case02 is an extreme scenario of vegetation canopy increase in urban areas and should perhaps be disregarded in some parts of this analysis – it is included here as a maximum possible effect from urban reforestation (per request from project participants). As discussed earlier, case01 is likely an upper bound for realistic implementation of canopy-cover measures.

Thus, aside from case02, the other mitigation levels evaluated at the 2-km level are realistic and relatively moderate. Furthermore, the localized impacts (e.g., cooling) and ranking (i.e., relative effectiveness) of various measures and levels can differ from on subdomain to another because the advective effects are significant at this scale. Recall that this analysis is for current climate (MJJAS 2013 – 2016) and for current land-use conditions and urbanization levels.

5.11.1 Impacts on the temperature field at 0600 PDT

In Figure 5-17, the average temperature reductions at 0600 PDT are presented. This is temperature reduction averaged over all 0600-PDT hours (in each period) and over the urban grid cells in each specified sub-domain. It can be seen that the ranking (i.e., the order of measures' effectiveness listed at right on each figure) at this hour is consistent across all regions but that the magnitudes of reductions in temperature differ by location. Furthermore, the intra-measure differences within each area are also different, i.e., how close or far apart are the reductions from different measures.

Whereas Figure 5-17 shows the variations in cooling levels across different time periods (for each region), Figure 5-18 summarizes the averages of those effects. It can be seen that the effects of canopy-cover are larger than those of albedo, as expected, since there is no significant amount of sunlight at 0600 PDT. The cooling effects associated with albedo measures at this hour are mostly carry-overs from the previous day's daytime hours, i.e., smaller long-wave re-radiation of heat at night. The areas in Davis, Sacramento, Woodland, and Yuba City have larger cooling at this hour and larger inter-quartile ranges (spread) of cooling effects. The most effective scenario, excluding case02, is the combination case31.

Figure 5-17: Average temperature reduction (°C) at 0600 PDT. Time periods are identified on the horizontal axis and the ranking of measures on the right side of each graph.

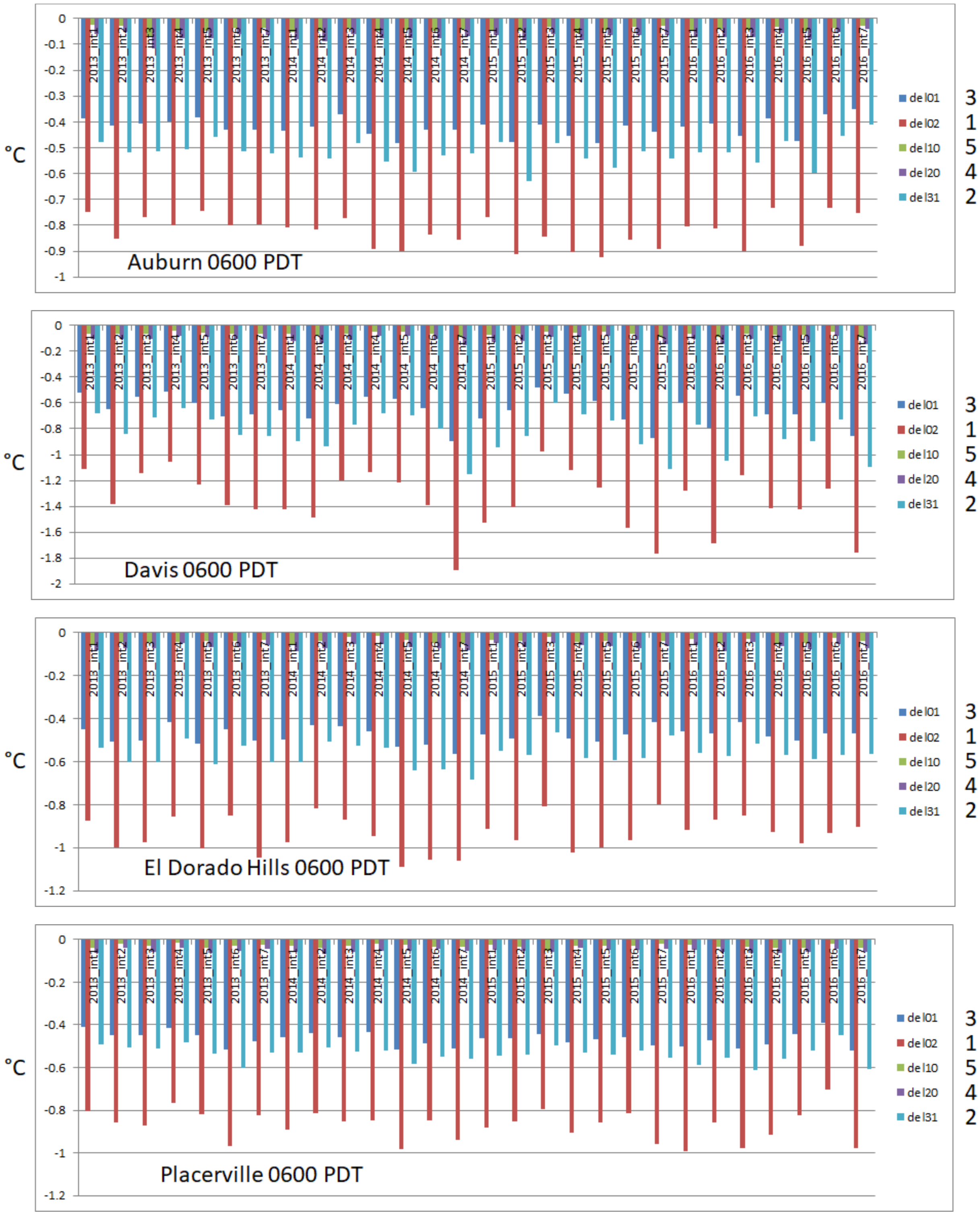

Figure 5-17, continued.

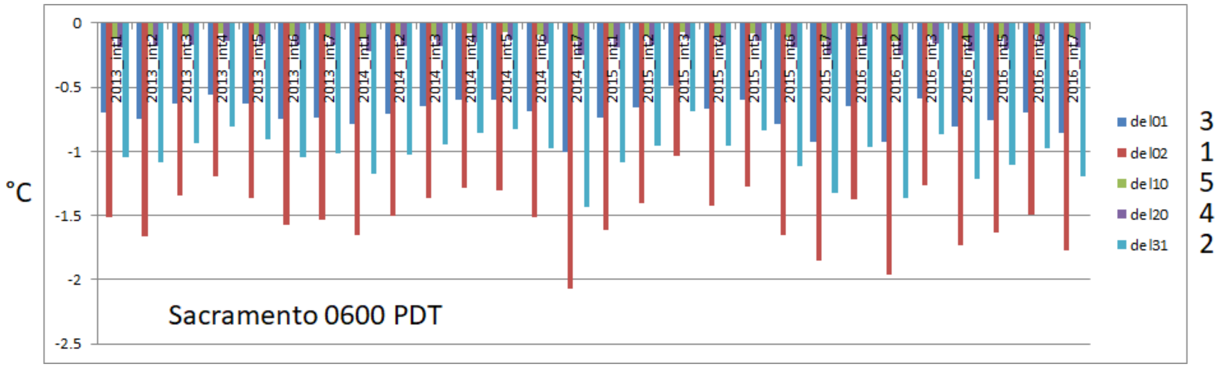

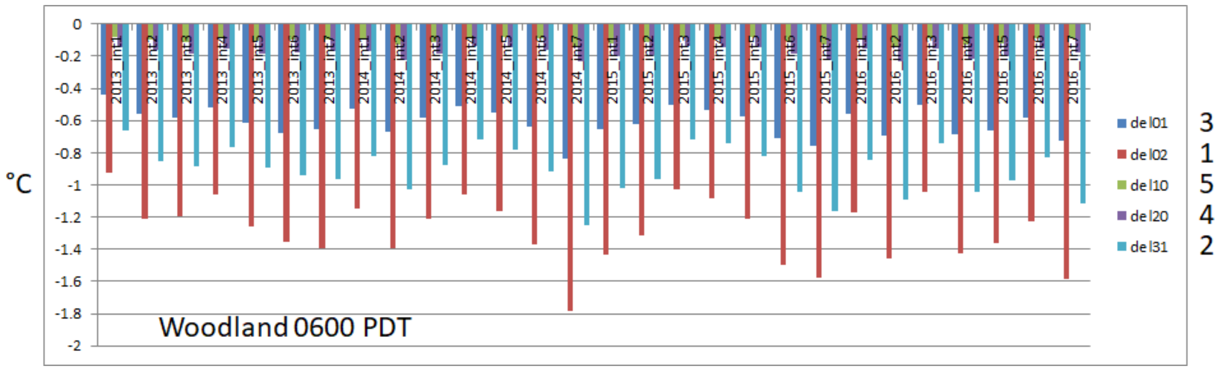

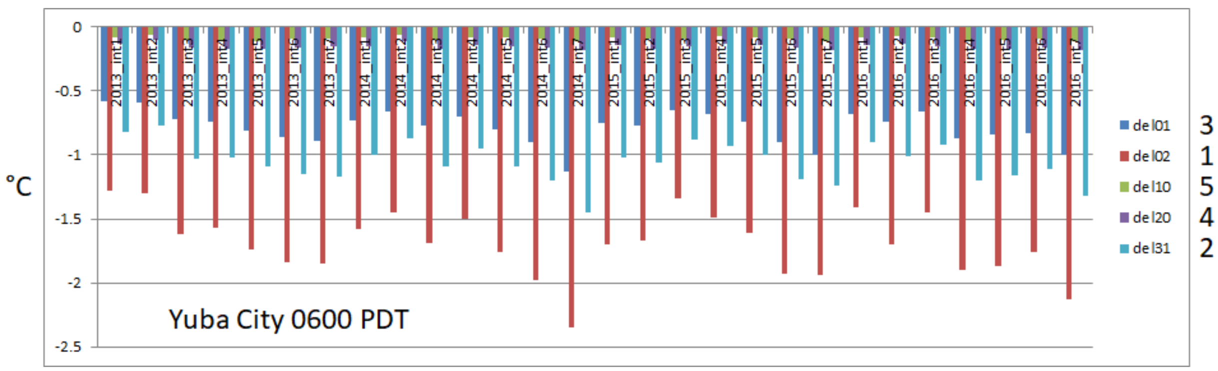

Figure 5-18: Summary of averaged temperature impacts at 0600 PDT. Median, quartiles, and maxima/minima are shown with box and whisker plots.

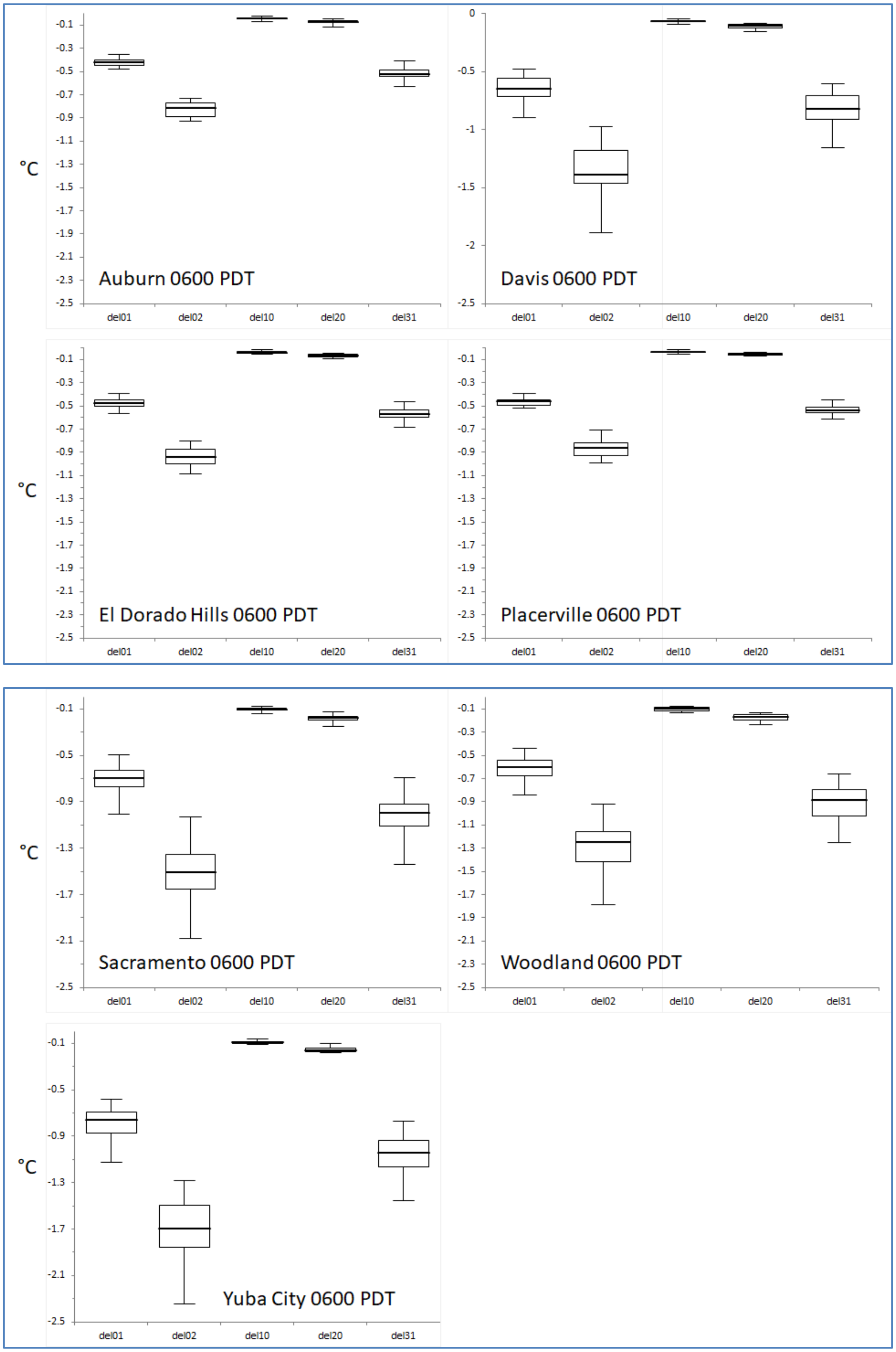

5.11.2 Impacts on the temperature field at 1300 PDT

In Figure 5-19, the average temperature reductions at 1300 PDT are shown (i.e., reductions averaged over all 1300 PDT hours in each time period) and also averaged over urban grid cells in each specified sub-domain. The figure shows that the ranking (i.e., the order of measures' effectiveness) at this time interval is (1) different from that at 0600 PDT, discussed above, and (2) varies across different regions, unlike at 0600 PDT where they were similar across all sub-domains. As this is a daylight hour close to solar noon (1300 PDT), the effects of albedo measures are larger than those of canopy cover. The magnitudes of reductions in temperature differ by location and so do the intra-measure differences within each area, i.e., how close or far apart are the reductions from different measures. There are also situations where some of the measures are tied in terms of their cooling potentials, as seen in Figure 5-19 (e.g., case01 and case20 in Placerville, as indicated by the bracket at the right end of the figure).

Figure 5-20 summarizes the averages of those effects at 1300 PDT over all time periods. The areas in El Dorado Hills, Sacramento, and Woodland have some of the larger cooling effects at this hour as well as the larger inter-quartile ranges of temperature reductions. At 1300 PDT, the albedo measures are more effective than canopy-cover increases (excluding the extreme case02), which is the inverse of the ranking at 0600 PDT. The albedo effects can also be larger than case02 in some domains, i.e., Sacramento and Woodland. Finally, the most effective scenario is case31.

Figure 5-19: Average temperature reduction (°C) at 1300 PDT. Time periods are identified on the horizontal axis and the ranking of measures on the right side of each graph.

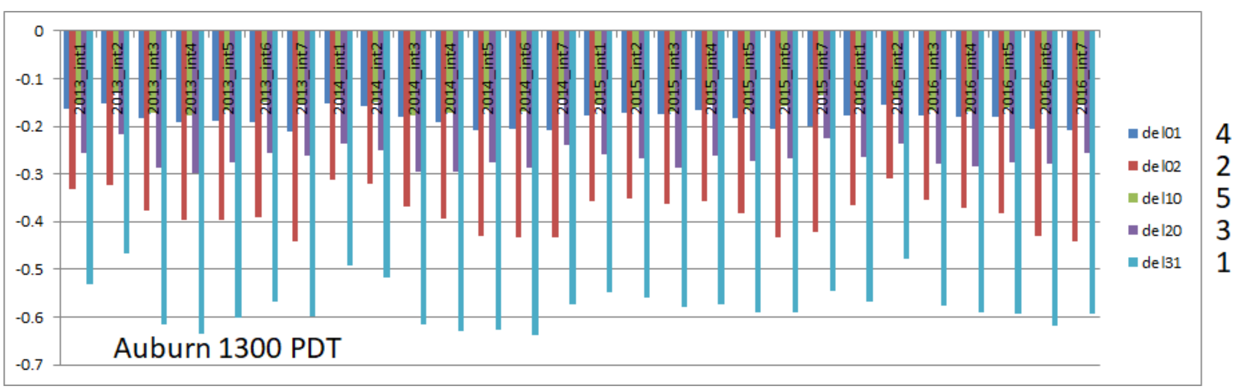

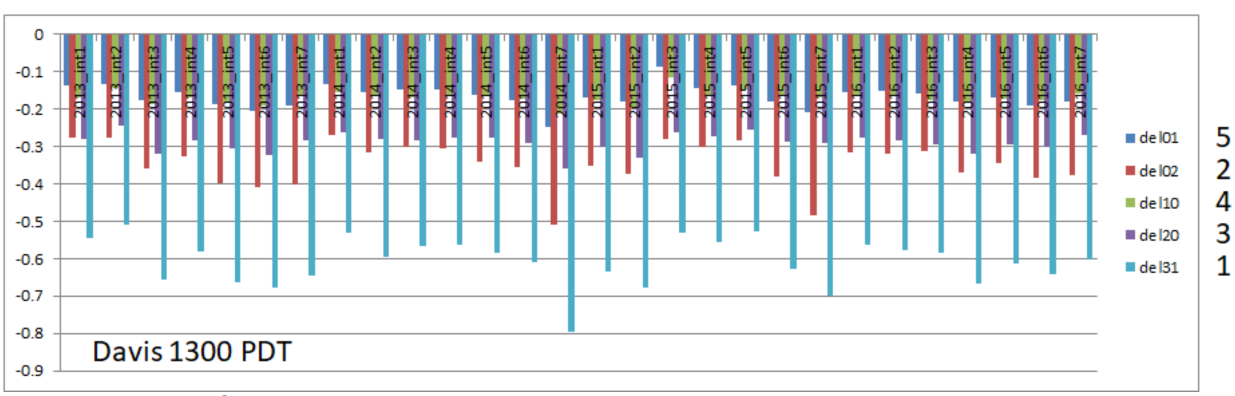

Figure 5-19, continued.

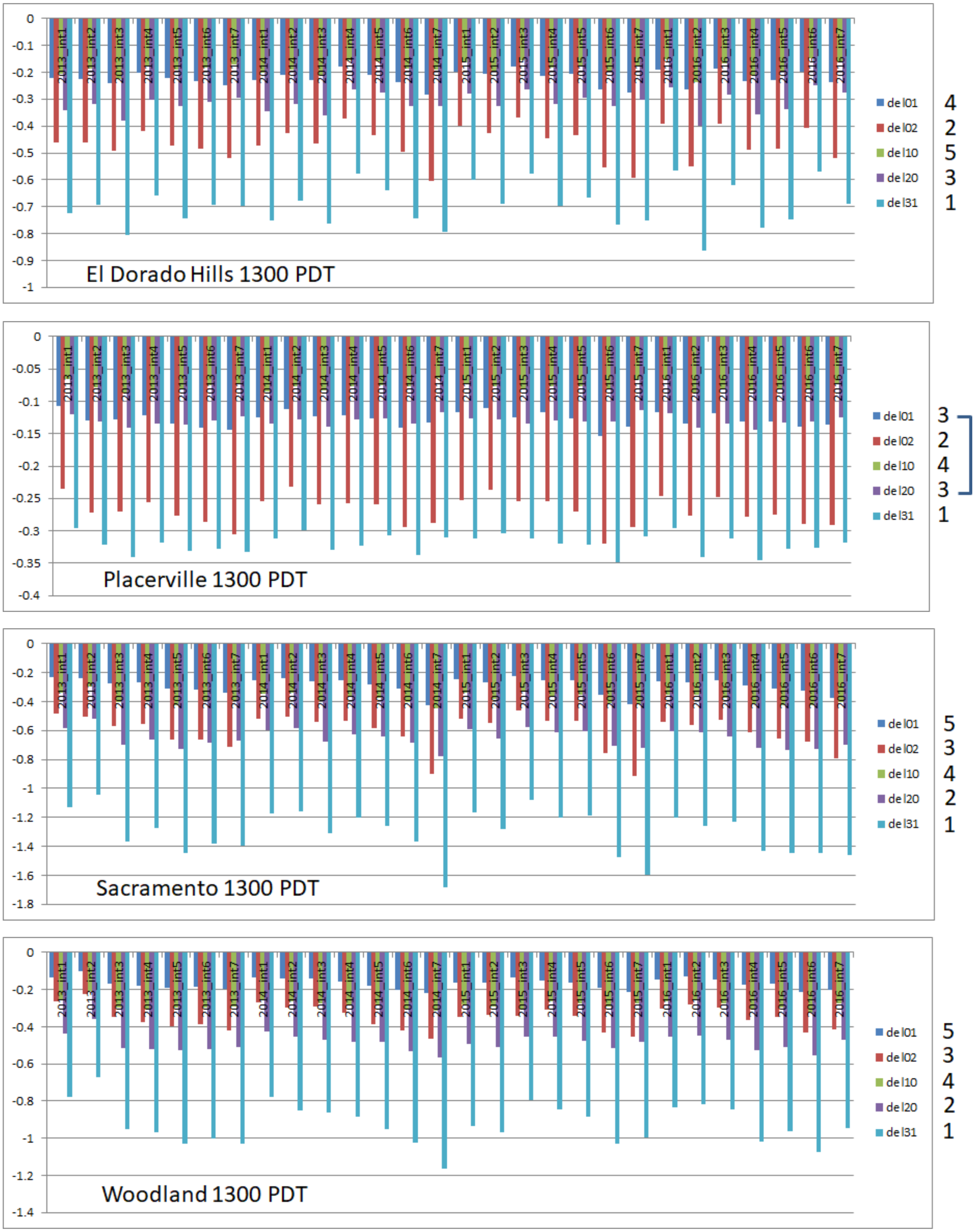

Figure 5-19, continued.

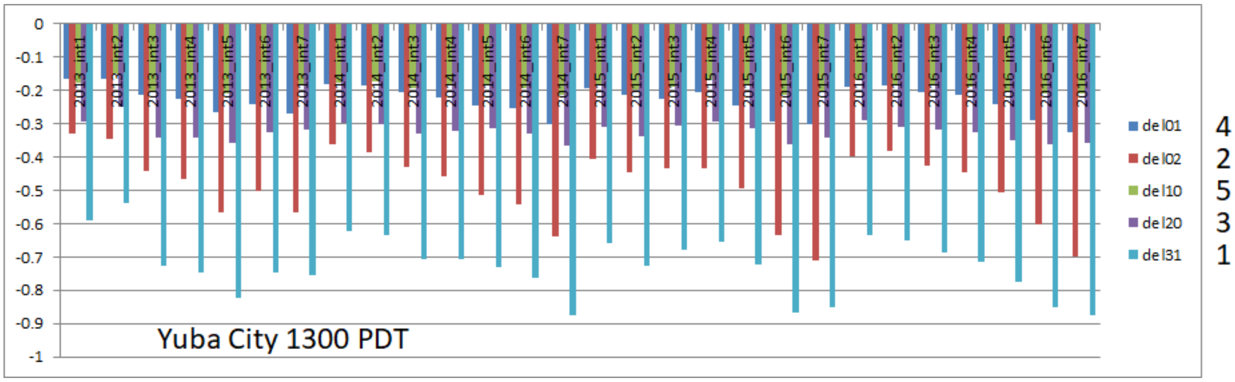

Figure 5-20: Summary of averaged temperature impacts at 1300 PDT. Median, quartiles, and maxima/minima are shown with box and whisker plots.

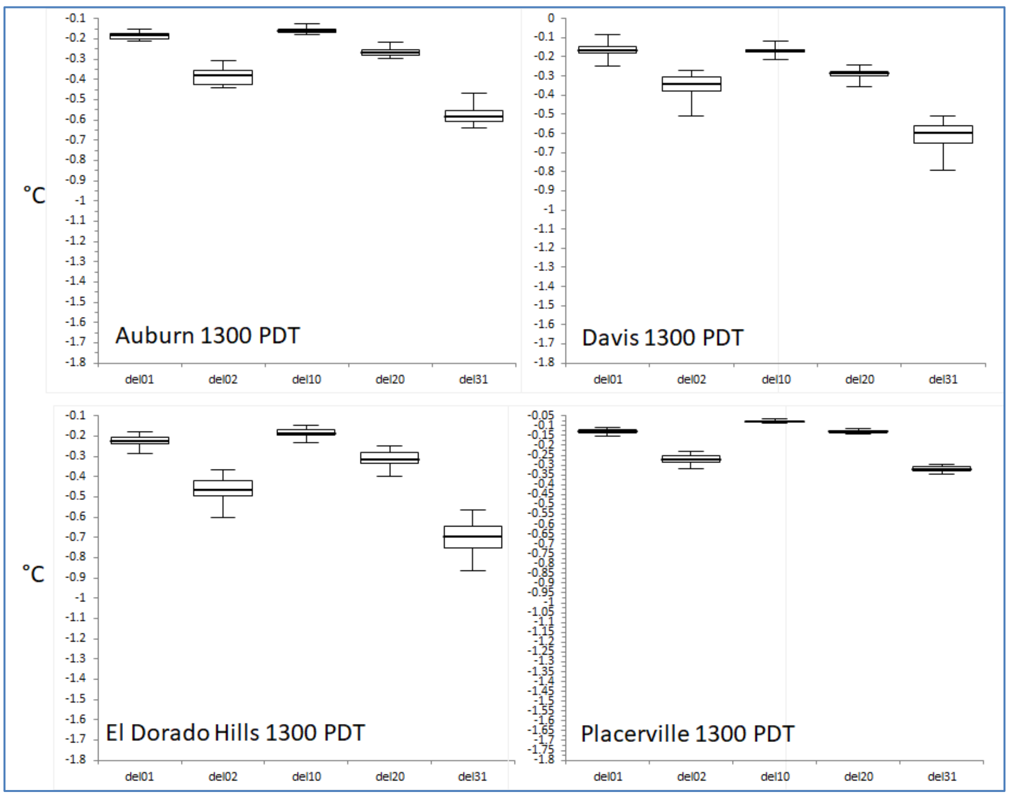

Figure 5-20, continued.

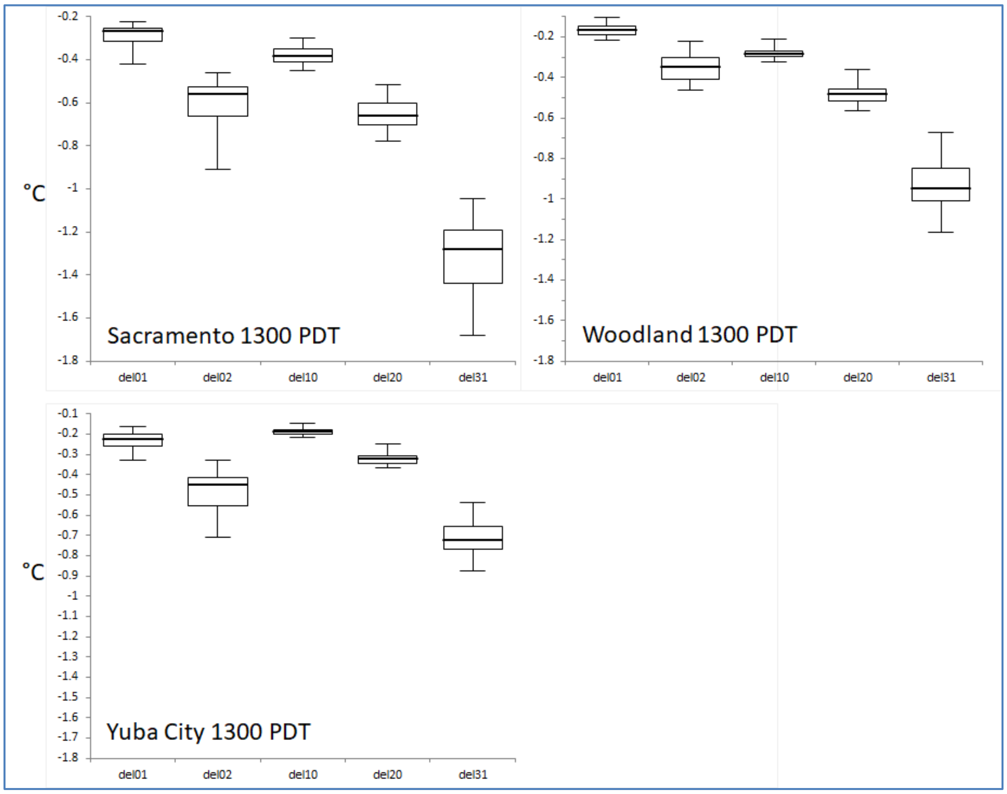

5.11.3 Impacts on the temperature field during hours 1400 – 2000 PDT

Figure 5-21 shows the average temperature reductions for the hour range 1400 - 2000 PDT (i.e., temperature reductions averaged over all 1400 to 2000 PDT hours in each time period) and also averaged over urban grid cells in each specified sub-domain. This range of hours is of interest to local utilities, i.e., SMUD, for peak electric load planning and management. The figure shows that the order of measures' effectiveness during this hourly range is (1) different from that at 0600 and 1300 PDT (although more similar to 1300 PDT) and (2) also varies across different regions, unlike at 0600 PDT. During this range of hours (1400 – 2000 PDT), the effects of albedo measures again are larger than those of canopy cover, excluding case02, because of it being mostly daylight. The magnitudes of reductions in temperature and the intra-measure differences within each area differ by location, as was seen at hour 1300 PDT, above, in Section 5.1.2. There are also instances where some of the measures are tied in terms of their cooling potentials, as seen in Figure 5-21 (e.g., case02 and case20 in Woodland). This indicates that the effects of albedo are very significant during this range of hours (and are equivalent to the effects of an extreme canopy-cover measure).

Figure 5-22 summarizes the cooling effects averaged for the hours 1400 – 2000 PDT over all time periods. In this case, the cooling effects are more uniform across all regions (less contrasts) although some areas, such as Sacramento, see the largest cooling. During this hourly range, the albedo and vegetation measures, when averaged over all periods, have relatively the same cooling potential (excluding case02). Albedo scenario case20 produces larger cooling than vegetation scenario case01, and the most effective measure is, again, the combined scenario case31.

Figure 5-21: Average temperature reduction (°C) during hours 1400 – 2000 PDT. Periods are identified on the horizontal axis and the ranking of measures on the right side of each graph.

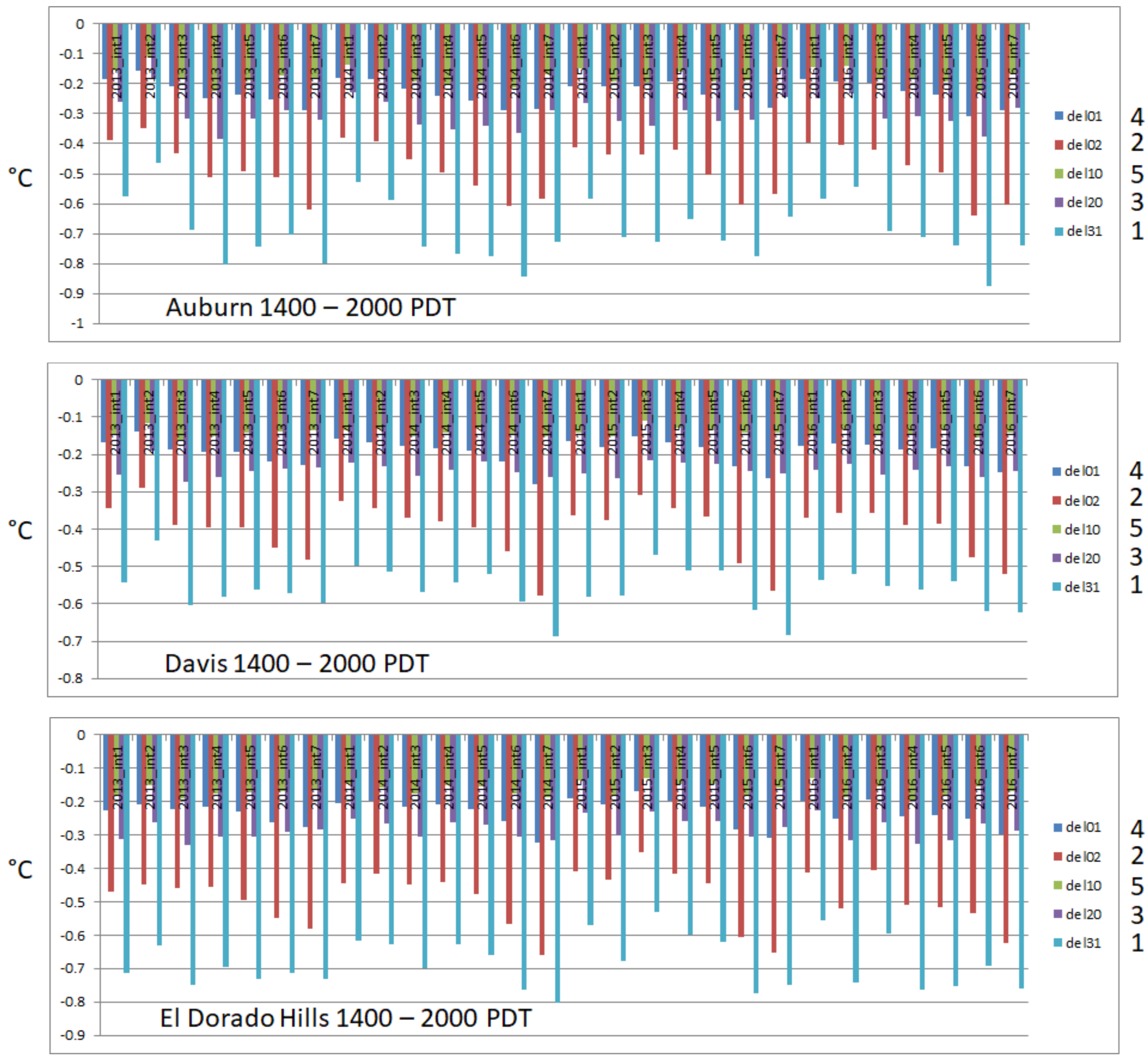

Figure 5-21, continued.

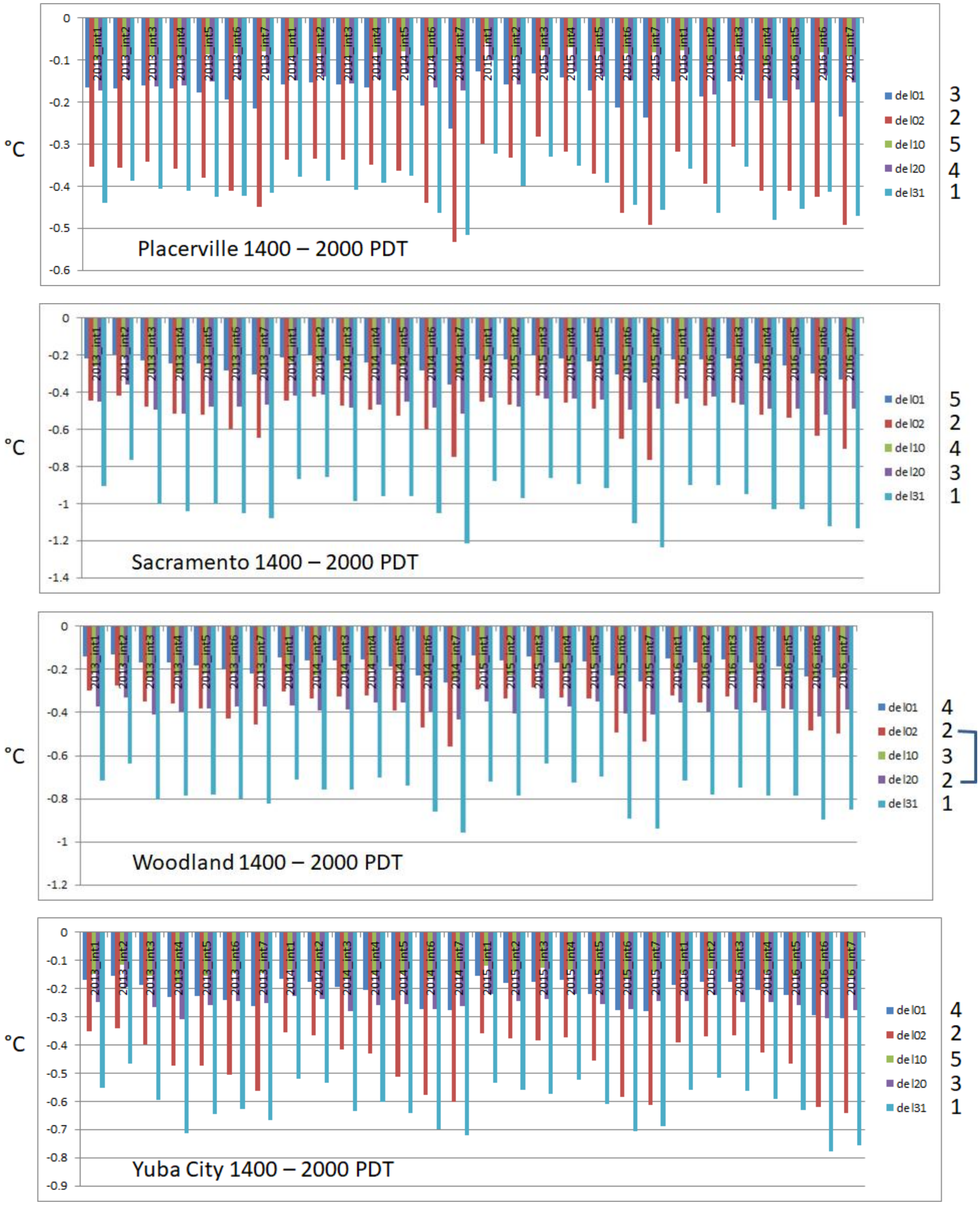

Figure 5-22: Summary of averaged temperature impacts at 1400 - 2000 PDT. Median, quartiles, and maxima/minima are shown with box and whisker plots.

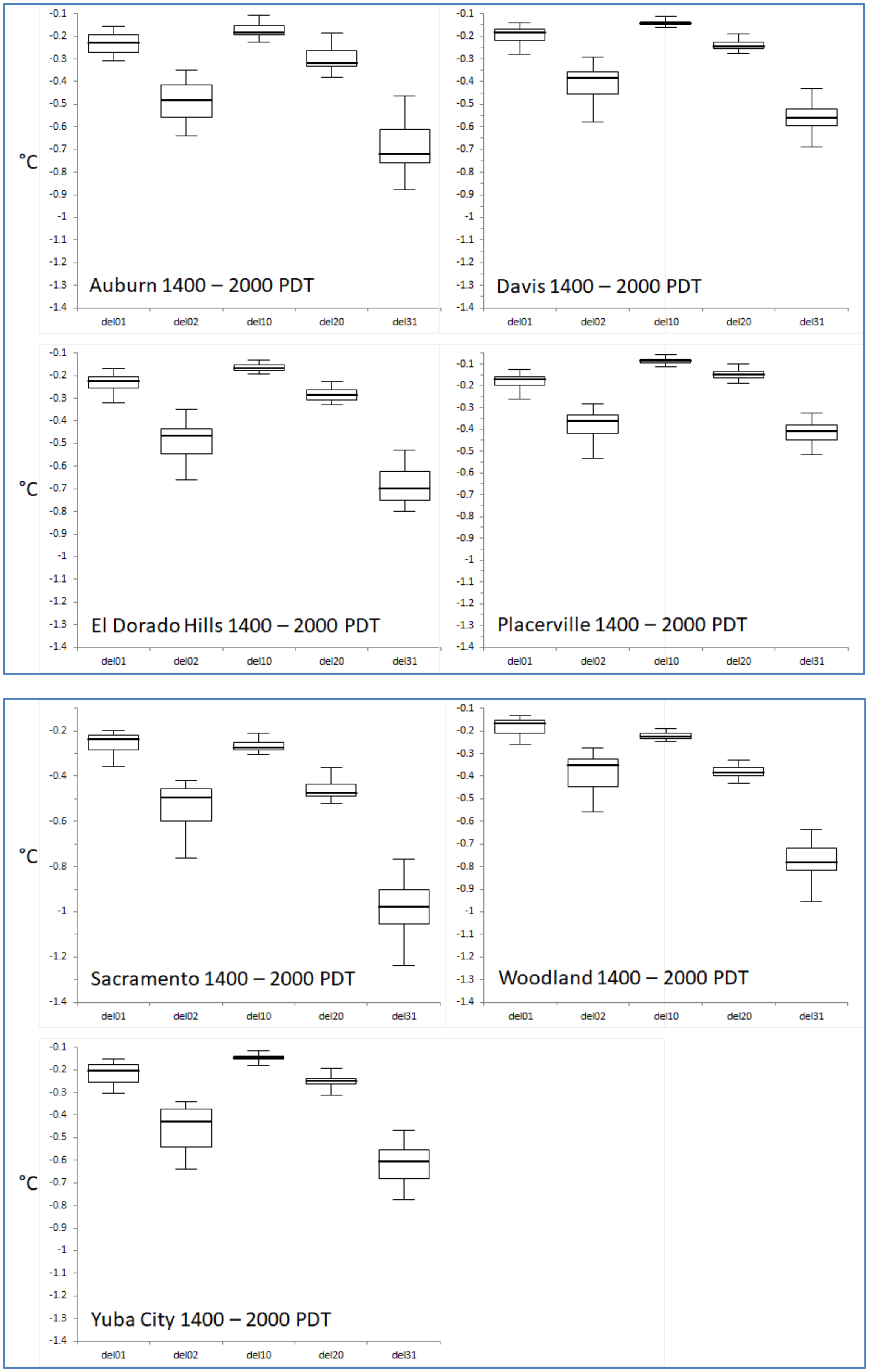

5.11.4 Impacts on the temperature field at 1500 PDT

An analysis similar to that for 1300 PDT (~solar noon) was repeated for 1500 PDT, which is closer to the time of peak air temperatures. Figure 5-23 shows the average temperature reductions at this hour (i.e., reductions averaged over all 1500-PDT hours in each period) that are also averaged over urban grid cells in each specified sub-domain. The ranking of measures at 1500 PDT is relatively similar to that at 1300 PDT, although differences do exist. At 1500 PDT, the effects of albedo measures during this daylight hour are larger than those of canopy cover (excluding case02). Some albedo measures (case20) even have a larger cooling effect than the extreme canopy cover scenario (case02). The magnitudes of reductions in temperature and the intra-measure differences within each area, i.e., how close or far apart are the reductions from different measures, also differ from one area to another. There also are cases with ties in terms of cooling potential, as seen in Figure 5-23 (e.g., case01 and case10 in Auburn, El Dorado Hills, and Yuba City).

Figure 5-24 provides a summary of the averaged effects at 1500 PDT. The areas in El Dorado Hills, Sacramento, and Woodland see relatively larger cooling effects at this time interval – these are also the areas with the larger inter-quartile ranges (spread) of temperature reductions. At this time interval, the albedo measures are more effective than canopy measures and the most effective scenario is the combination case31.

Figure 5-23: Average temperature reduction (°C) at 1500 PDT. Periods are identified on the horizontal axis and the ranking of measures on the right side of each graph.

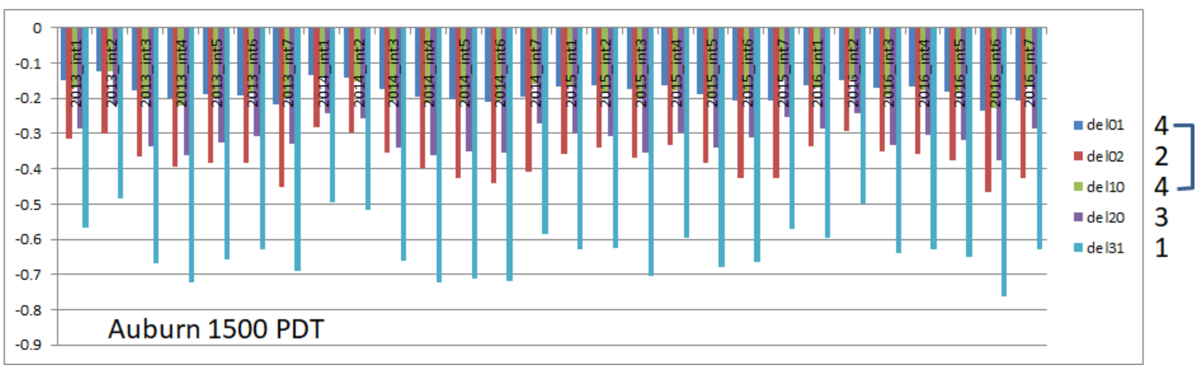

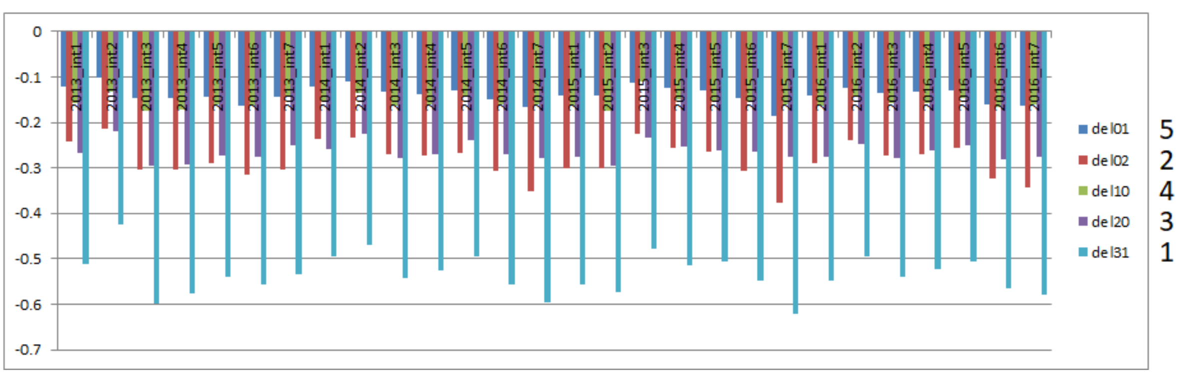

Figure 5-23, continued.

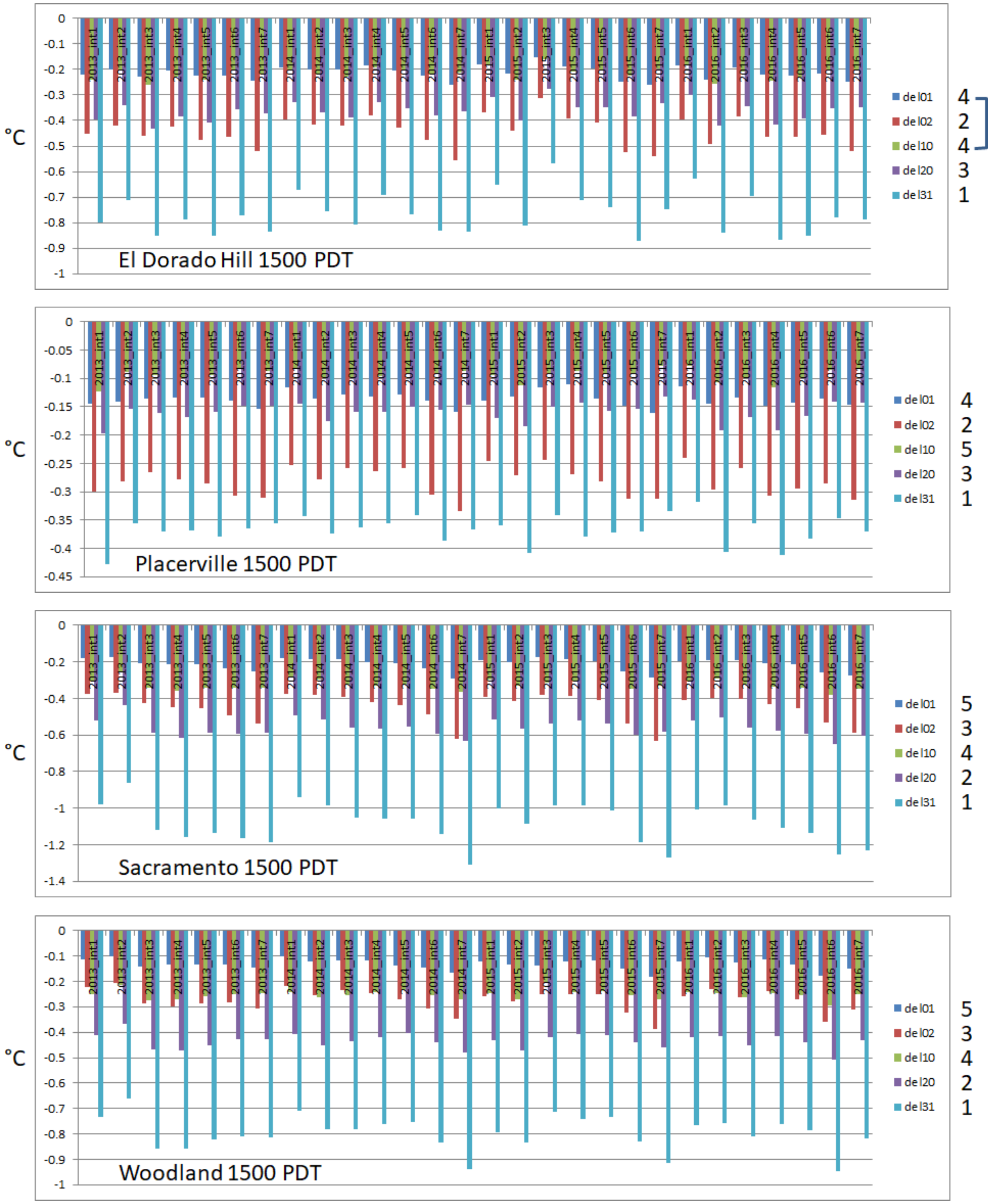

Figure 5-23, continued.

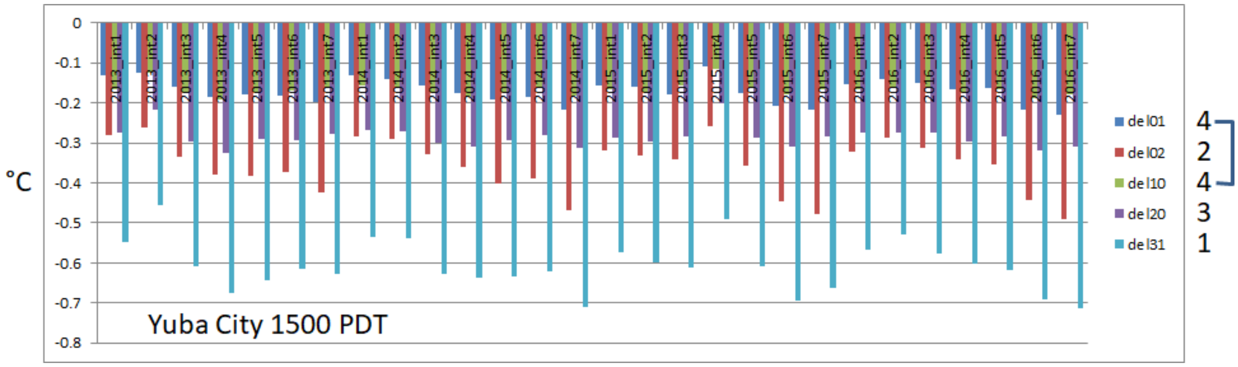

Figure 5-24: Summary of temperature impacts at 1500 PDT. Median, quartiles, and maxima/minima are shown with box and whisker plots.

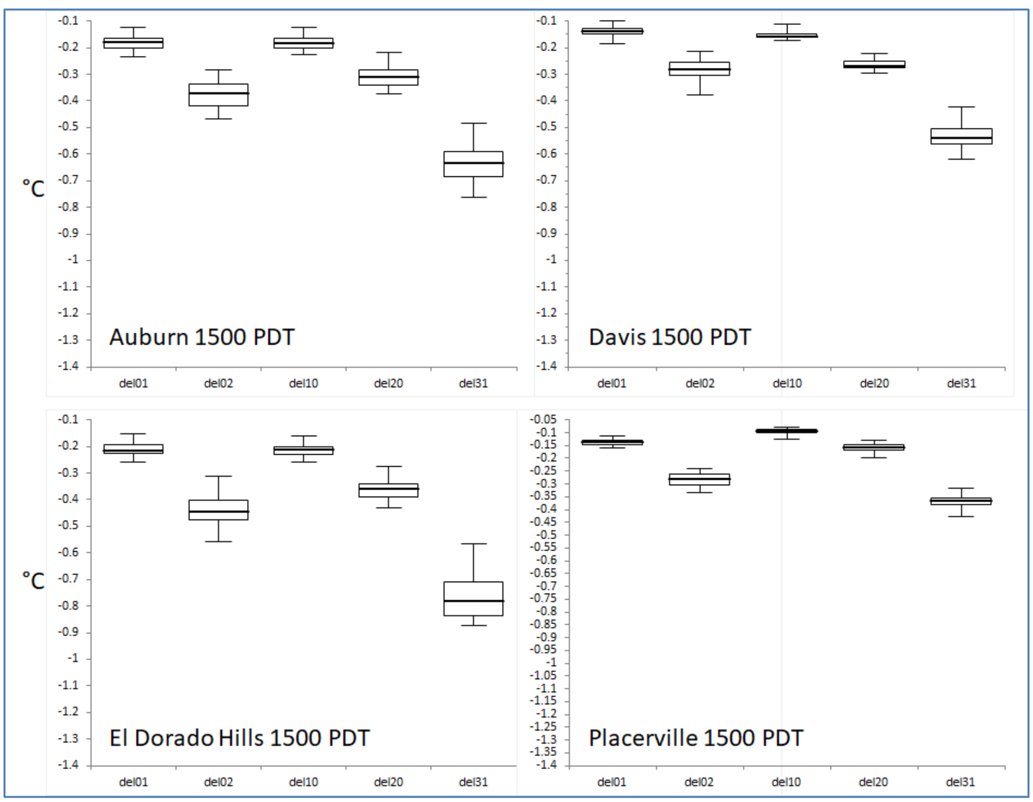

Figure 5-24, continued.

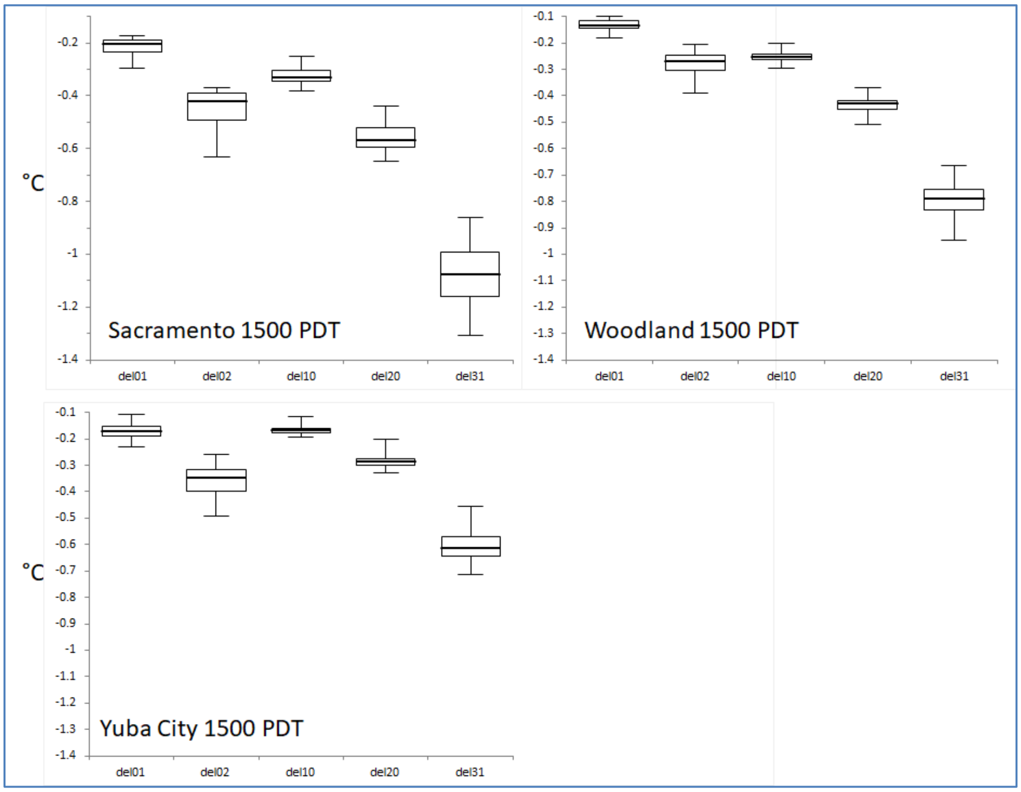

5.11.5 Impacts on the all-hours temperature field

Figure 5-25 shows the all-hours average temperature reductions (i.e., averaged over all hours in each period) and also averaged over urban grid cells in the specified sub-domains. The ranking of measures for this range of hours is biased towards (influenced by) nighttime effects of vegetation cover and thus may not be a good indicator for use in daytime urban heat-reduction planning. In fact, as the figure shows, and except for one or two instances, the ranking (i.e., the order of measures' effectiveness) at all hours is same as the ranking at 0600 PDT (the magnitude is different, however).

Figure 5-26 summarizes the all-hours cooling effects averaged again over all modeled periods. The areas of Davis, Sacramento, Woodland, and Yuba City see the larger cooling effects, which is comparable to 0600 PDT. The most effective scenario is case02 – if this scenario is excluded, then the next most effective one is the combination measure (case31).

Figure 5-25: Average all-hours temperature reduction (°C). Periods are identified on the horizontal axis and the ranking of measures on the right side of each graph.

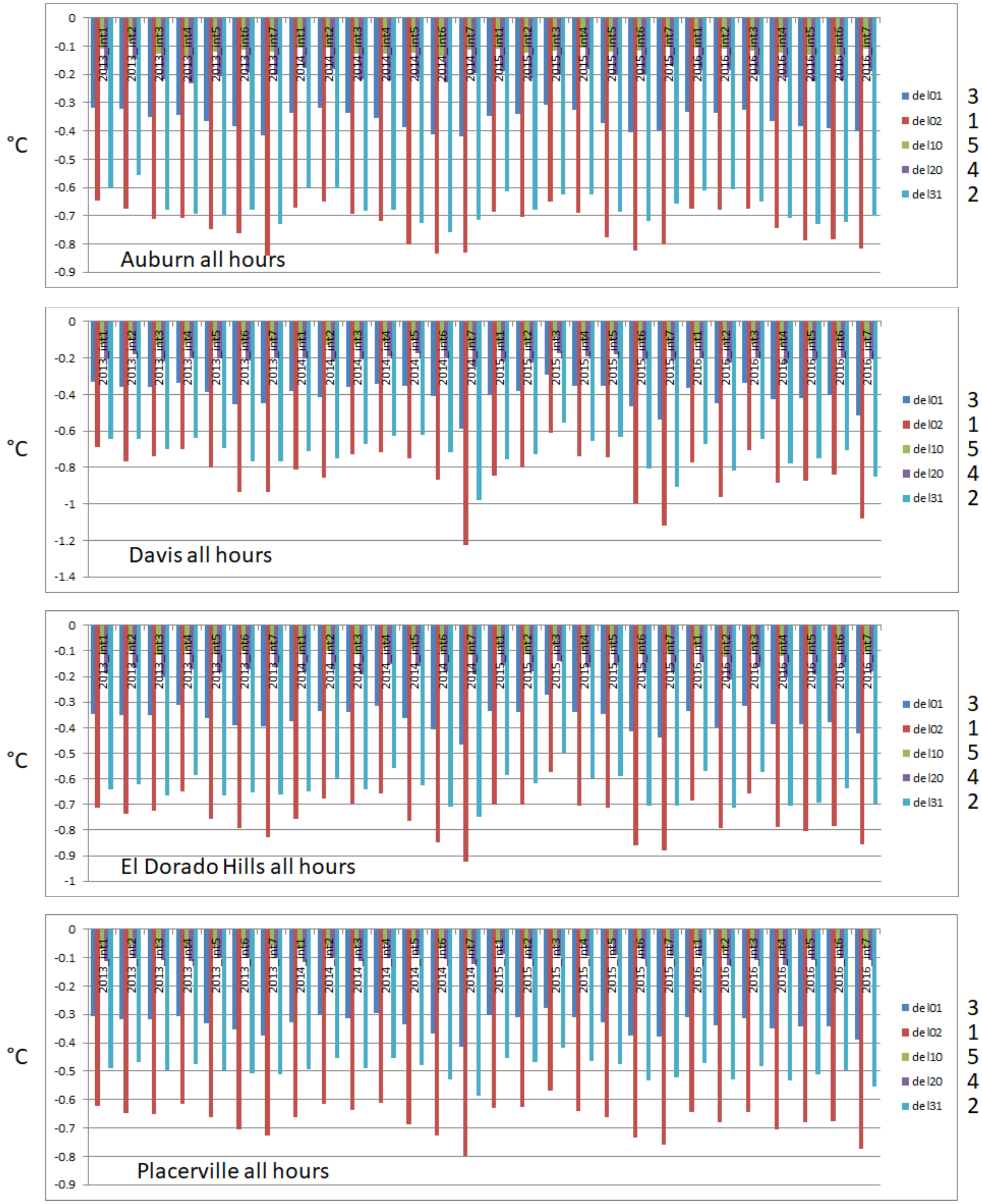

Figure 5-25, continued.

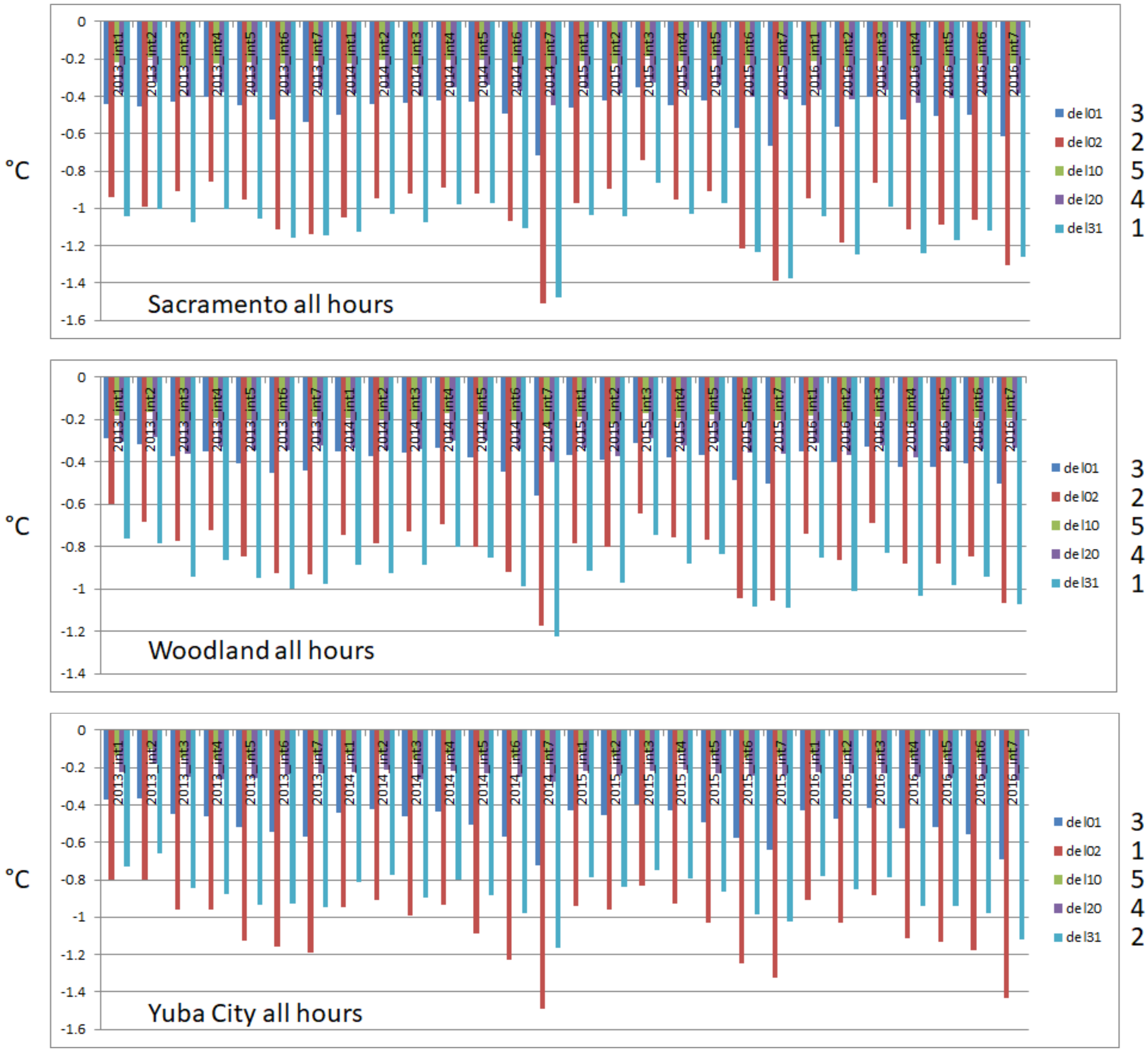

Figure 5-26: Summary of all-hour average temperature impacts. Median, quartiles, and maxima/minima are shown with box and whisker plots.

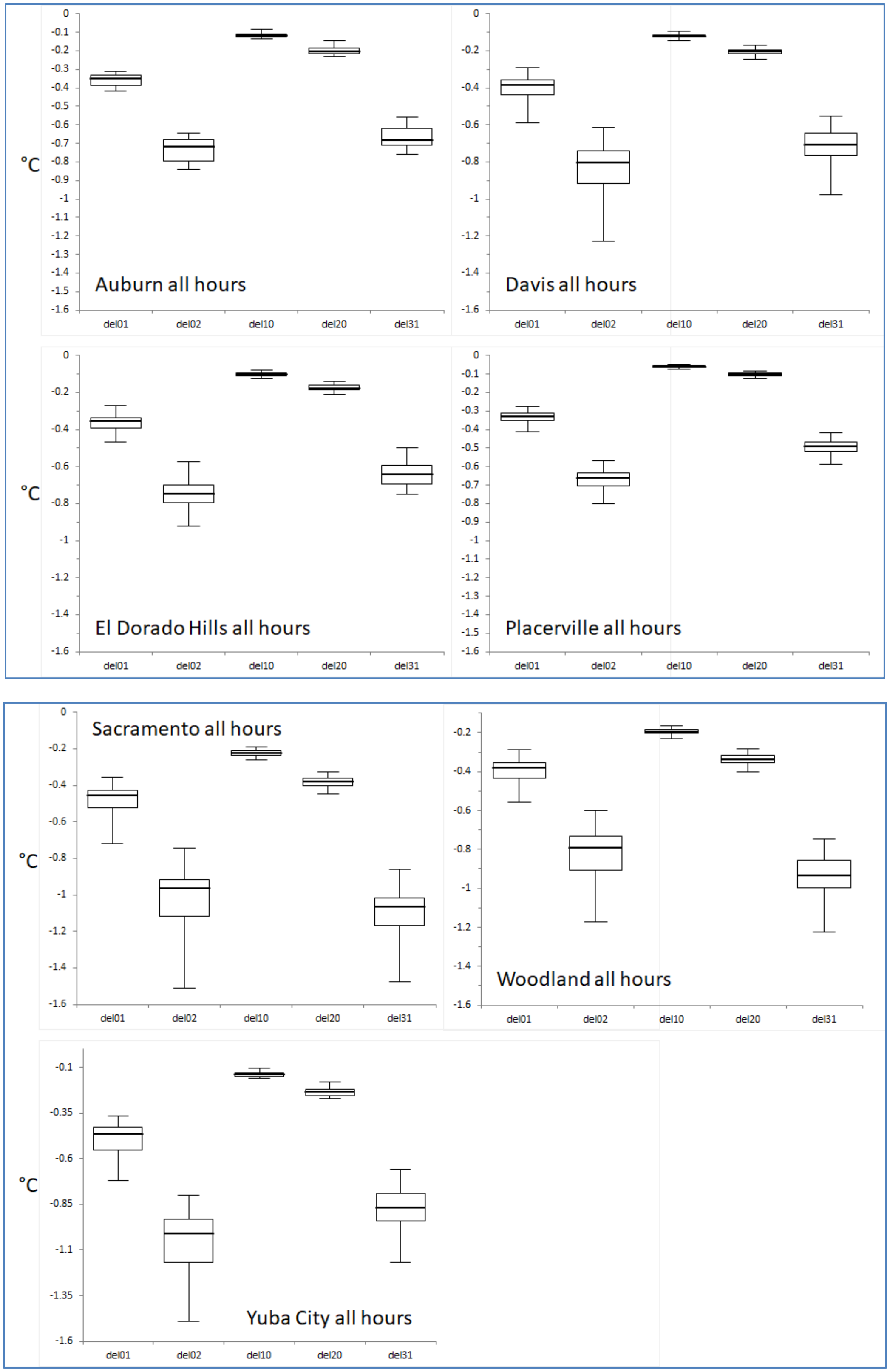

5.12 SUMMARY OF RANKINGS

To provide an "at a glance" comparison among various scenarios, Chart 5-1 summarizes the ranking of the five measures (defined earlier) in each region and for various hours or times of day. This is a high-level summary of the UHI-mitigation potentials of these measures in current climate and land-use / land-cover conditions. As explained earlier, case02 is an extreme scenario of vegetation-cover increase and should be disregarded. It is included here only as a test for upper bounds, i.e., largest cooling, per suggestions from local tree organizations.

Chart 5-1: Summary of urban-heat mitigation potential: ranking of measures case01 through case31 by cooling effectiveness in current climate (1 – 5, darker to lighter gray = largest to smallest cooling). Note that case02 should be excluded in some analysis. Also note that these are impacts on temperature, not UHII.

		Auburn	Davis	El Dorado Hills	Placerville	Sacramento	Woodland	Yuba City
0600 PDT	case01	3	3	3	3	3	3	3
	case02	1	1	1	1	1	1	1
	case10	5	5	5	5	5	5	5
	case20	4	4	4	4	4	4	4
	case31	2	2	2	2	2	2	2
1300 PDT	case01	4	5	4	3	5	5	4
	case02	2	2	2	2	3	3	2
	case10	5	4	5	4	4	4	5
	case20	3	3	3	3	2	2	3
	case31	1	1	1	1	1	1	1
1400 - 2000 PDT	case01	4	4	4	3	5	4	4
	case02	2	2	2	2	2	2	2
	case10	5	5	5	5	4	3	5
	case20	3	3	3	4	3	2	3
	case31	1	1	1	1	1	1	1
1500 PDT	case01	4	5	4	4	5	5	4
	case02	2	2	2	2	3	3	2
	case10	4	4	4	5	4	4	4
	case20	3	3	3	3	2	2	3
	case31	1	1	1	1	1	1	1
allHRS	case01	3	3	3	3	3	3	3
	case02	1	1	1	1	2	2	1
	case10	5	5	5	5	5	5	5
	case20	4	4	4	4	4	4	4
	case31	2	2	2	2	1	1	2

The chart does not provide information on the spread (e.g., inter-quartile ranges) of the cooling effects from a particular measure nor how close various measures are to each other (or how far apart they are in terms of cooling effects). It simply shows the ranking even if differences between one measure and another can be very small or almost tied in some instances. Cases (scenarios) that are tied are indicated by a repeated number (and color code). It is important to note that the rankings are based on temperature changes averaged over 2-km. These rankings can differ at the finer scales

(500 m) and the magnitudes of the temperature reductions also get larger when averaged at finer resolutions. In Chart 5-1, the various time bands may be of interest to different applications. For example, the 0600 PDT and allHRS bands could be of interest from a heat-wave perspective, the 1400-2000 PDT band may be of interest to utilities, the 1500-PDT band could be used in relation to peak cooling demand analysis, and the band at 1300 PDT is of relevance to assessments of measures around solar noon.

The modeling of future climates, e.g., year 2050 RCP 4.5 and RCP 8.5, discussed later, shows that except for a number of instances, the current-climate ranking (and ordering) of measures remains generally unchanged into the future. That is, the ranking of measures in terms of their cooling effectiveness in current climates and LULC remains relatively the same in the future. While the ranking (order) can be relatively similar in current and future years, the magnitudes of the cooling effects differ. Table 5-7 provides the numerical values of the cooling associated with Chart-1 (values are averaged over all grid cells in each region and for the given time period), with case02 excluded. The additional chart below the table simply is a graphical representation of the values listed.

Table 5-7: Temperature changes (°C) corresponding to Chart 5-1 (case02 has been excluded).

		Auburn	Davis	El Dorado Hills	Placerville	Sacramento	Woodland	Yuba City
0600 PDT	case01	-0.40	-0.60	-0.50	-0.50	-0.70	-0.60	-0.75
	case10	-0.08	-0.15	-0.09	-0.09	-0.10	-0.10	-0.10
	case20	-0.10	-0.20	-0.10	-0.10	-0.20	-0.20	-0.20
	case31	-0.50	-0.90	-0.60	-0.55	-1.00	-0.90	-1.00
1300 PDT	case01	-0.20	-0.18	-0.22	-0.12	-0.25	-0.18	-0.22
	case10	-0.20	-0.20	-0.20	-0.08	-0.40	-0.30	-0.20
	case20	-0.30	-0.30	-0.30	-0.12	-0.65	-0.50	-0.33
	case31	-0.60	-0.60	-0.70	-0.32	-1.30	-0.95	-0.70
1400 - 2000 PDT	case01	-0.22	-0.19	-0.22	-0.18	-0.23	-0.16	-0.20
	case10	-0.20	-0.15	-0.15	-0.10	-0.25	-0.22	-0.15
	case20	-0.32	-0.25	-0.30	-0.15	-0.47	-0.35	-0.25
	case31	-0.72	-0.55	-0.70	-0.40	-1.00	-0.76	-0.60
1500 PDT	case01	-0.18	-0.14	-0.21	-0.14	-0.20	-0.13	-0.17
	case10	-0.18	-0.15	-0.21	-0.10	-0.33	-0.25	-0.18
	case20	-0.30	-0.27	-0.36	-0.16	-0.55	-0.45	-0.30
	case31	-0.64	-0.52	-0.80	-0.37	-1.10	-0.80	-0.60
allHRS	case01	-0.35	-0.40	-0.35	-0.32	-0.45	-0.38	-0.47
	case10	-0.12	-0.17	-0.10	-0.05	-0.20	-0.20	-0.15
	case20	-0.20	-0.20	-0.18	-0.10	-0.37	-0.33	-0.22
	case31	-0.65	-0.70	-0.60	-0.50	-1.06	-0.92	-0.85

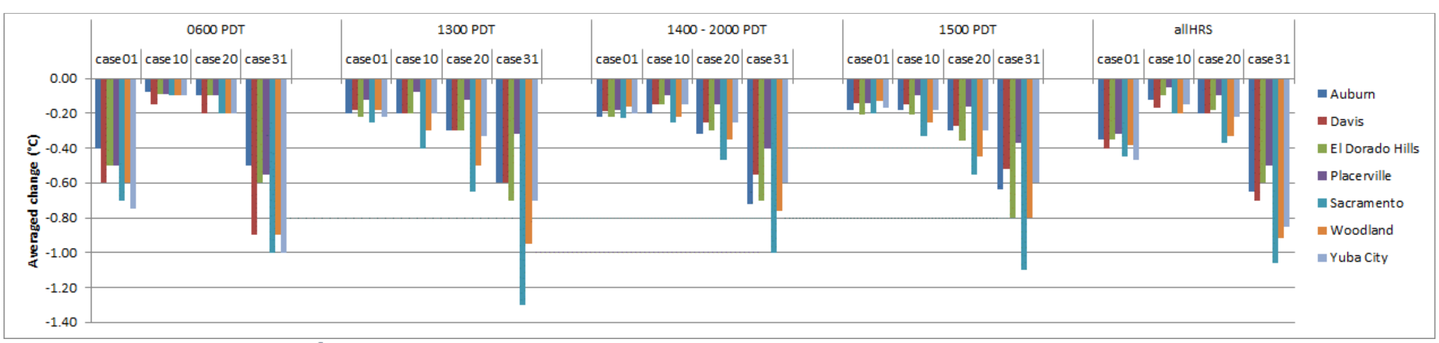

Table 5-7 excludes case02 to provide a fairer comparison among measures. At the finer scales (i.e., specific projects evaluated at 500-m resolution), the cooling effects are significantly larger than the 2-km averaged effects reported here.

It can be concluded from this discussion (Chart 5-1 and Table 5-7) that albedo scenarios (e.g., cool roofs and cool pavements) are the top choice for reducing daytime urban air temperature. Because the vegetation canopy cover can cool the air both during the day and at night, its impacts are dominant in the 24-hour average metrics and early-morning averages.

5.13 IMPACTS OF COOLING MEASURES ON THE URBAN HEAT ISLAND INDEX IN CURRENT CLIMATE

Following the calculations and establishment of the UHII for the Capital region, as discussed earlier in Section 5.3, the potential of various mitigation measures in offsetting or mitigating the index was quantified. In this section, an overview is presented for the regional scale (2 km) for current climate and LULC. A similar assessment will be presented at the fine scale (500 m), later in this report.

The examples shown here are for cases 01, 02, 10, 20, and 31, as defined earlier, for hours 0600 PDT, 1500 PDT, and the all-hour average UHII. It is reiterated that the maps shown in this discussion are composites (not a continuous field) made up of six different tiles, each with its own upwind reference points (see Section 5.3). It is equally important to note here that the changes discussed in the following sections are changes in the UHII (which, itself, is a temperature *difference*) not in absolute temperature.

5.13.1 Impacts on the UHII at 0600 PDT

Figures 5-27 and 5-28 summarize the potential of heat-mitigation measures for fully or partially offsetting the UHII at 0600 PDT. Figure 5-27 also shows the spatial characteristics of the UHII offsets, i.e., where the cooling effect is largest within each of the tiles. A temperature equivalent (DH hr^{-1} in units of C·hr hr^{-1}) is also provided on each figure. This example is for the period July 16 – 31, 2015.

As discussed earlier, all cases are presented in Figure 5-28, however, vegetation-canopy scenarios above case01 may not be realistically feasible at this time. It can be seen from Figure 5-28 that at 0600 PDT, the most effective measures are those that include canopy-cover increase, which, as previously highlighted, is because (1) the effects of albedo changes are small, as there is little solar radiation at this hour -- except for reduced long-wave re-radiation of heat at night, and (2) that vegetation canopies cool the air continuously during the day and night.

While all regions benefit from significant UHII offset at this hour, the areas of Woodland, Davis, and Sacramento see the largest reductions, percentage-wise (Figure 5-28). The largest reduction is produced by case31 (up to -2.1 ºC in temperature equivalent) as seen in the last graph of Figure 5-27.

Figure 5-27: Change in 0600-PDT UHII (composite 2 km domain). Example for period July 16 – 31, 2015 (DH = °C · hr)

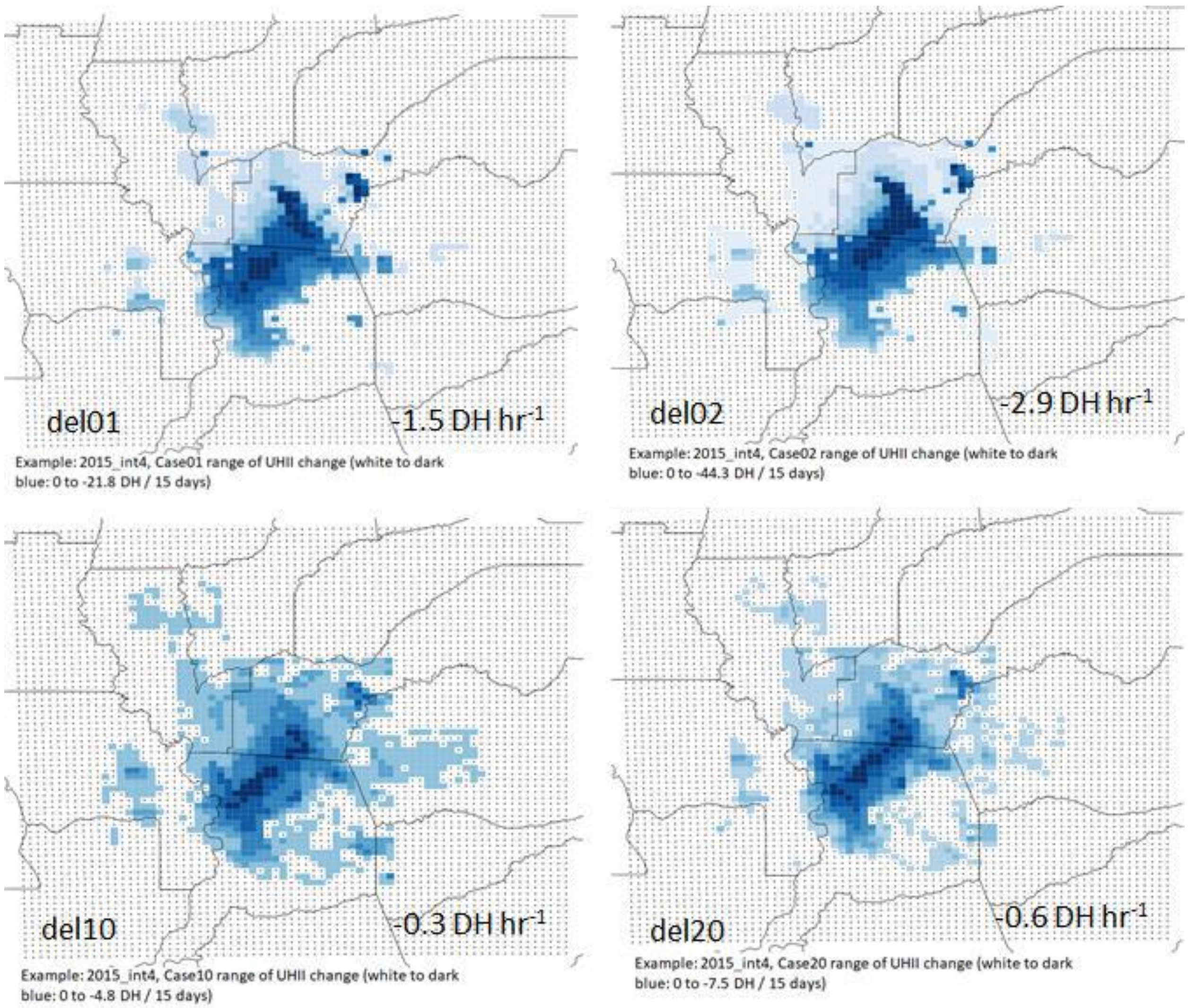

Figure 5-27, continued.

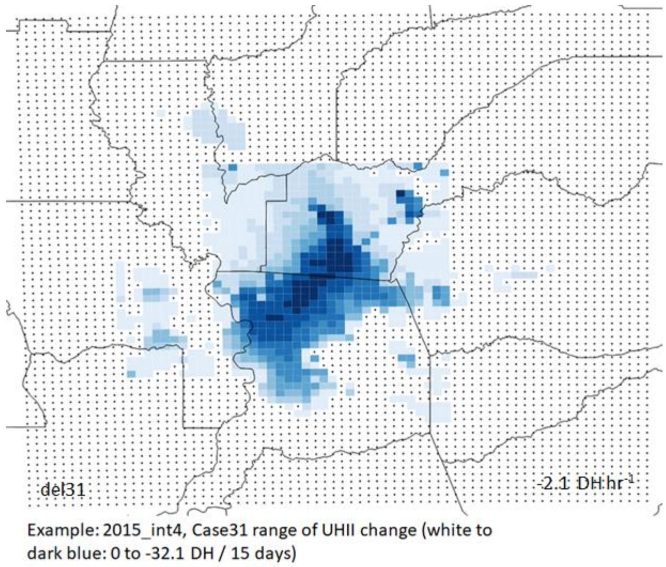

Figure 5-28: Reduction (%) in 0600-PDT UHII for the period July 16 – 31, 2015 (DH = °C · hr)

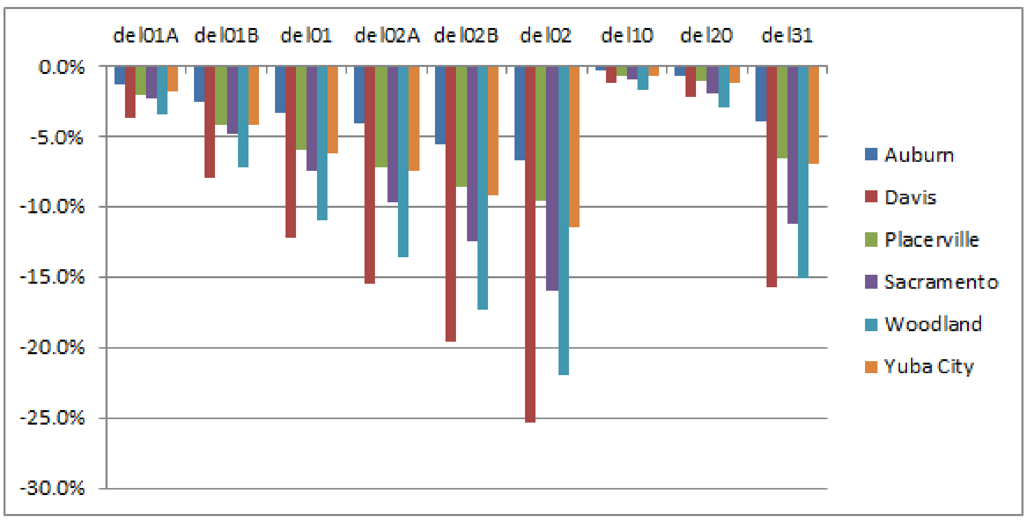

5.13.2 Impacts on the UHII at 1500 PDT

In a similar manner, Figures 5-29 and 5-30 summarize the potential of heat-mitigation measures in offsetting the UHII at 1500 PDT for an example period (July 16 – 31, 2015). Figure 5-29 shows the spatial characteristics of UHII offsets – the effects of albedo measures are now dominant during daylight hours, which is the reverse of what occurs at 0600 PDT (Section 5.13.1). Furthermore, the spatial characteristics of cooling at this hour are more varied than at 0600 PDT because the effects of albedo are more pronounced than the effects of canopy cover. As discussed earlier, features such as the American River and surrounding areas, for example, now appear conspicuously in the figures, since these are areas where albedo changes are the smallest, because of small impervious cover.

In Figure 5-30, it can be seen that albedo measures are more effective than canopy measures during daylight hours (excluding case02 and similar). The most effective scenario at reducing the UHII is that of a combination of measures (case31). While the UHII offset is significant in all areas, Sacramento, Auburn, and Placerville see the larger reductions (percentage wise) in the UHII, which is different from the areas at 0600 PDT.

There also is a negligible increase in the UHII in case01B in Yuba City (Figure 5-30). In past studies, e.g., Taha (2013a,b), such increases were observed resulting from non-linear effects and attributed to changes in the wind and mixing fields under certain daytime conditions. But the occurrence is negligible (as seen in the figure) and the area affected by the increase is small, as discussed earlier in Section 5.10.

Figure 5-29: Change in 1500-PDT UHII (composite 2 km domain). Example for period July 16 – 31, 2015 (DH = °C · hr)

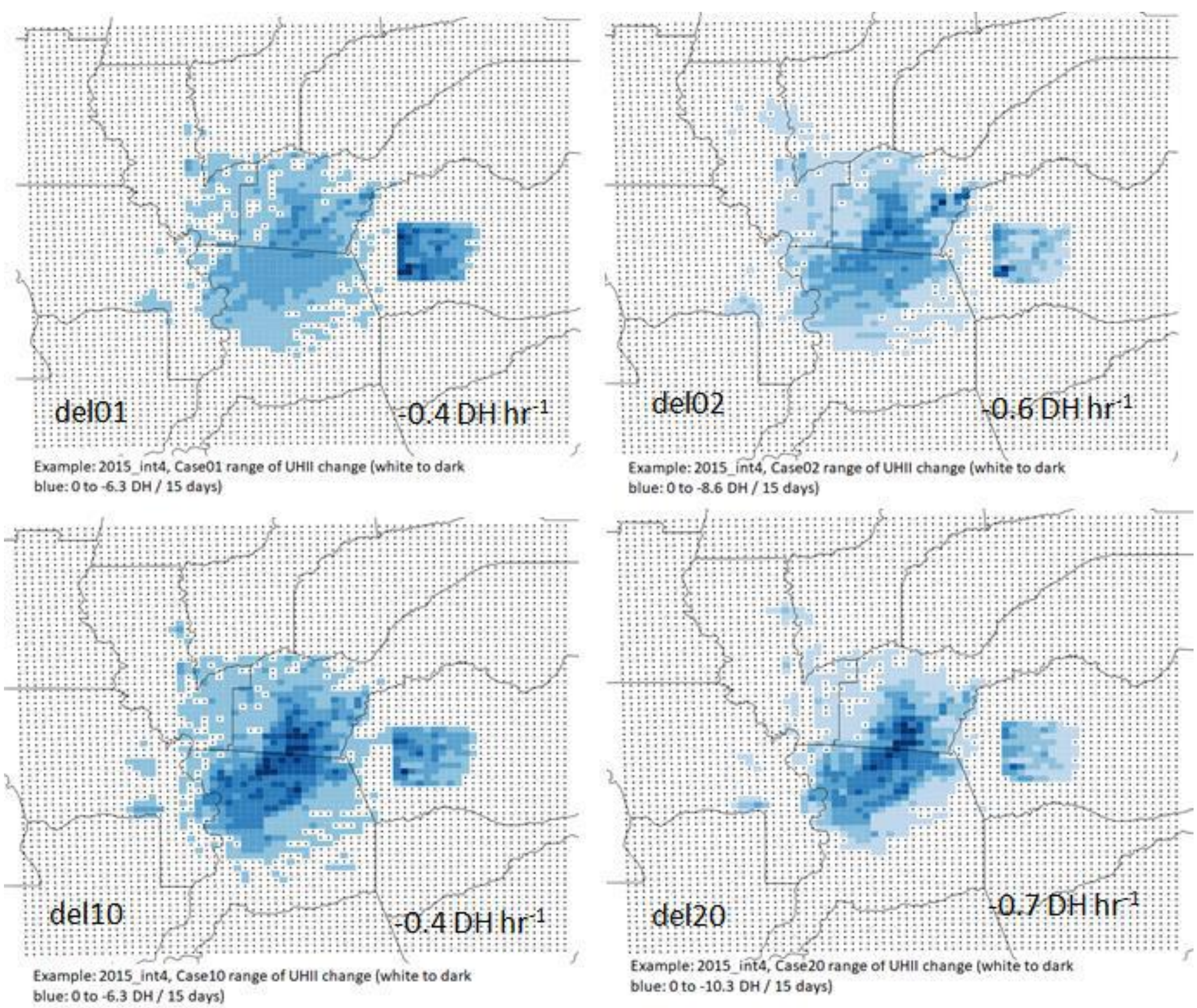

Figure 5-29, continued.

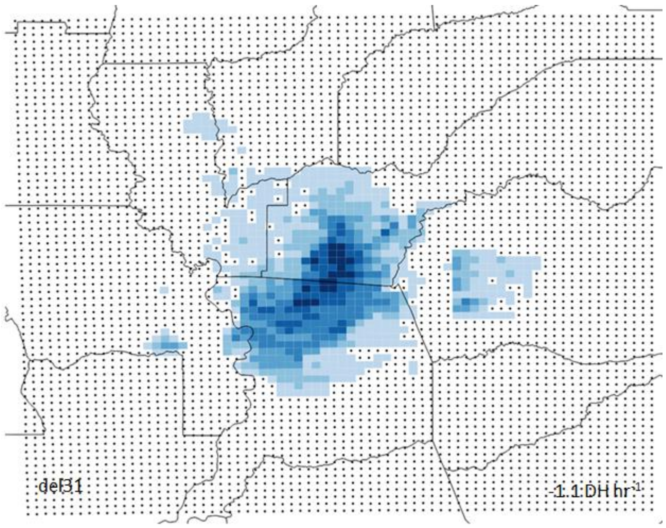

Example: 2015_int4, Case31 range of UHII change (white to dark blue: 0 to -15.9 DH / 15 days)

Figure 5-30: Reduction (%) in 1500-PDT UHII for the period July 16 – 31, 2015 (DH = °C · hr)

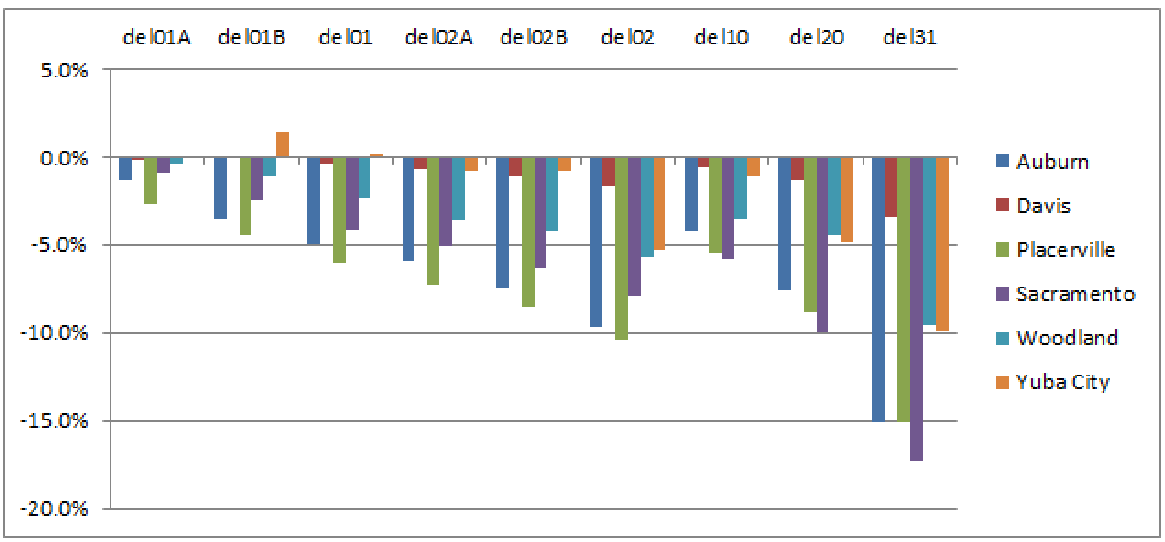

5.13.3 Impacts on the all-hours UHII

Some aspects of the all-hours UHII mitigation are presented in this section. Figures 5-31 and 5-33 summarize the potential of heat-mitigation measures in offsetting the UHII as an all-hour average for the sample period July 16 – 31, 2015. Figure 5-31 shows the spatial characteristics of UHII offsets which, again, are skewed relatively more towards the effects of canopy cover (since they include nighttime effects). For comparison, Figure 5-32 is the Cal/EPA all-hours UHII (Taha

2017). One can see that (1) the spatial pattern of UHII mitigation is in general such that the greater offsets are in locations of larger UHII (which is both expected and desirable) and (2) that case31 (as well as case02) can offset most if not all of the all-hours UHII in terms of temperature equivalent (DH hr^{-1}).

The most effective measures (excluding case02 and similar) are the combination scenario and the vegetation-cover case01. The albedo measures are still effective and significant, but because this metric includes nighttime effects, vegetation canopy has a more dominant effect. Finally, while all areas benefit significantly from mitigation measures at all hours, Woodland, Sacramento, and Davis see the largest (percentage-wise) reductions in the all-hours UHII.

Figure 5-31: Change in all-hours UHII (composite 2 km domain). Example for period July 16 – 31, 2015 (DH = °C · hr)

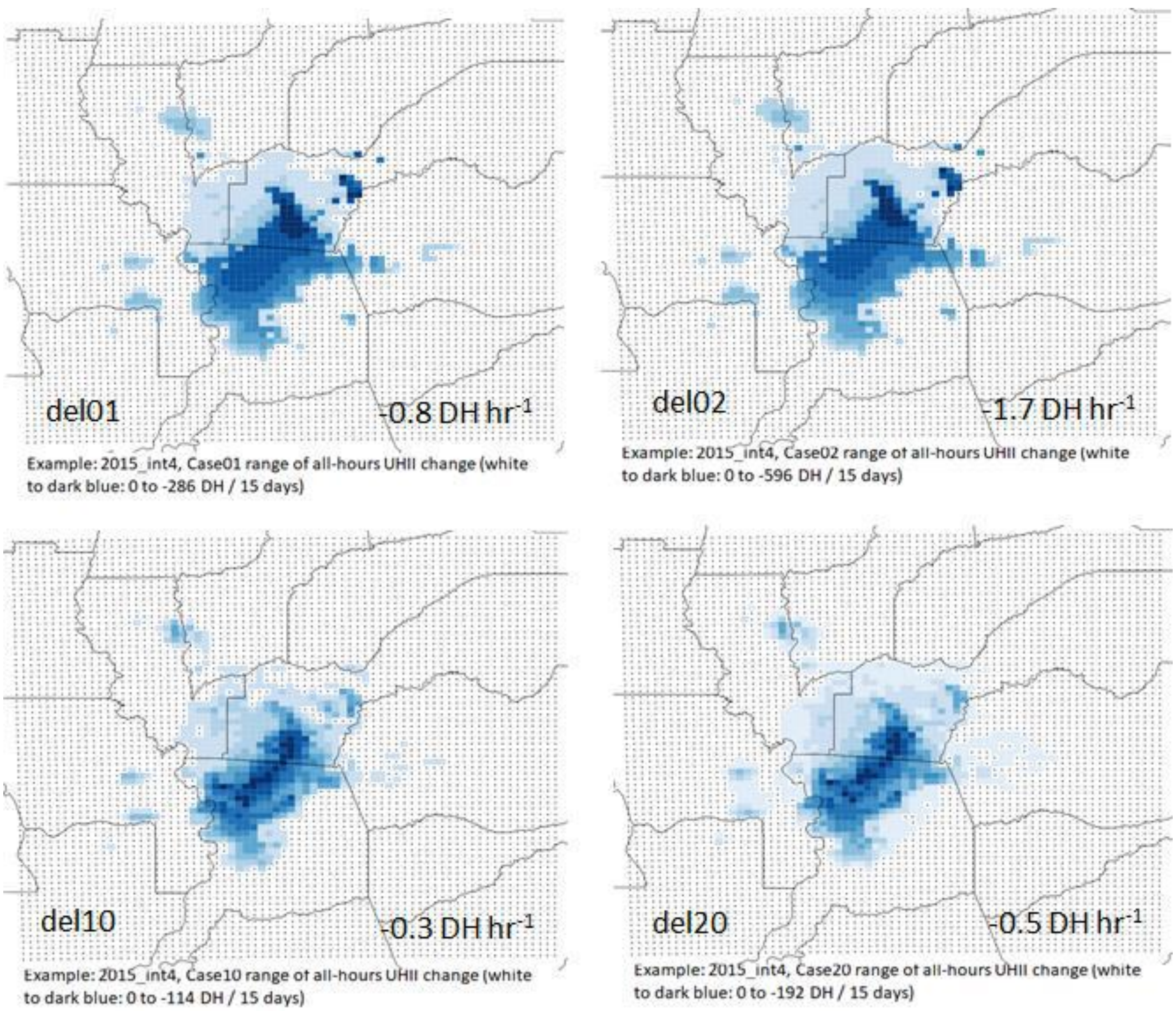

Figure 5-31, continued.

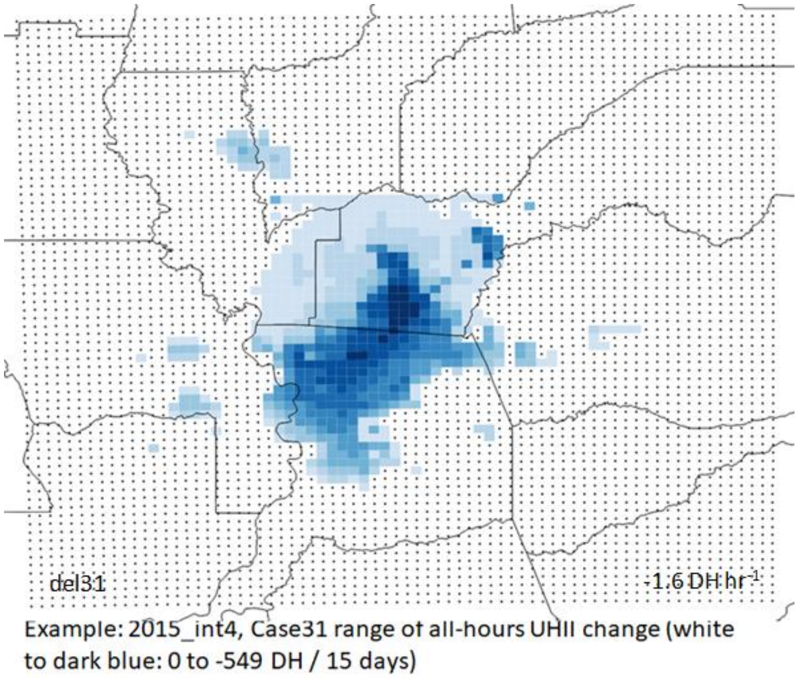

Figure 5-32: Level-1 Cal/EPA UHII (Taha 2017; Taha and Freed 2015), not encompassing the entire 6-counties region. Areas with the largest UHII also have some of the largest potentials for cooling.

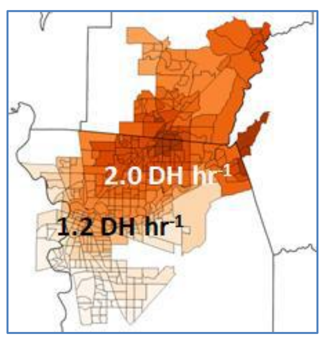

Finally, Figure 5-34 summarizes the reductions in the UHII (DH exceedances) relative to 35 °C (95 °F) which is a threshold commonly used by the electric utilities in calculating summertime cooling loads. The pattern of reductions in UHII (DH) above this threshold looks generally similar to the pattern of reductions in the all-hours UHII (see Figure 5-33). Excluding the extreme case02 and related scenarios, the most effective measure at reducing UHII above 35 °C is again case31 followed by albedo (case20) and vegetation-canopy cover (case01). Here, they are both of relatively similar magnitudes. However, the order of areas with most benefits (percentage-wise) is Placerville, Auburn, and Sacramento.

It is important to reiterate again that the changes discussed in this section are changes in UHII not in absolute temperature.

Figure 5-33: Reduction (%) in all-hours UHII for the period July 16 – 31, 2015 (DH = °C · hr)

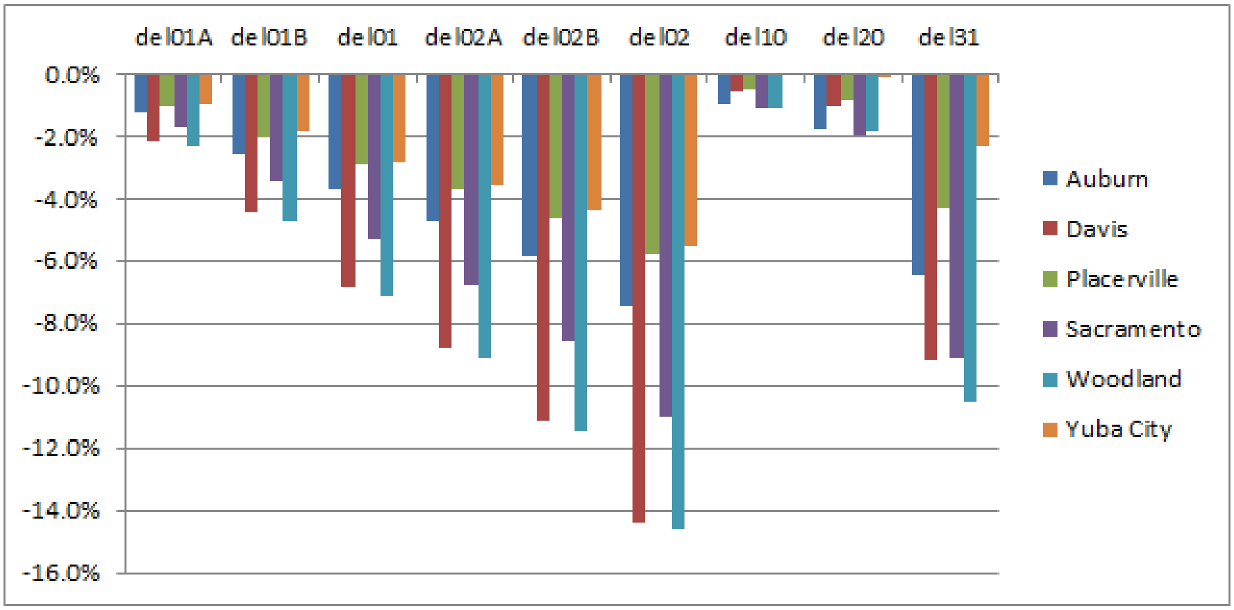

Figure 5-34: Reduction (%) in UHII above a 35 °C threshold, for all periods.

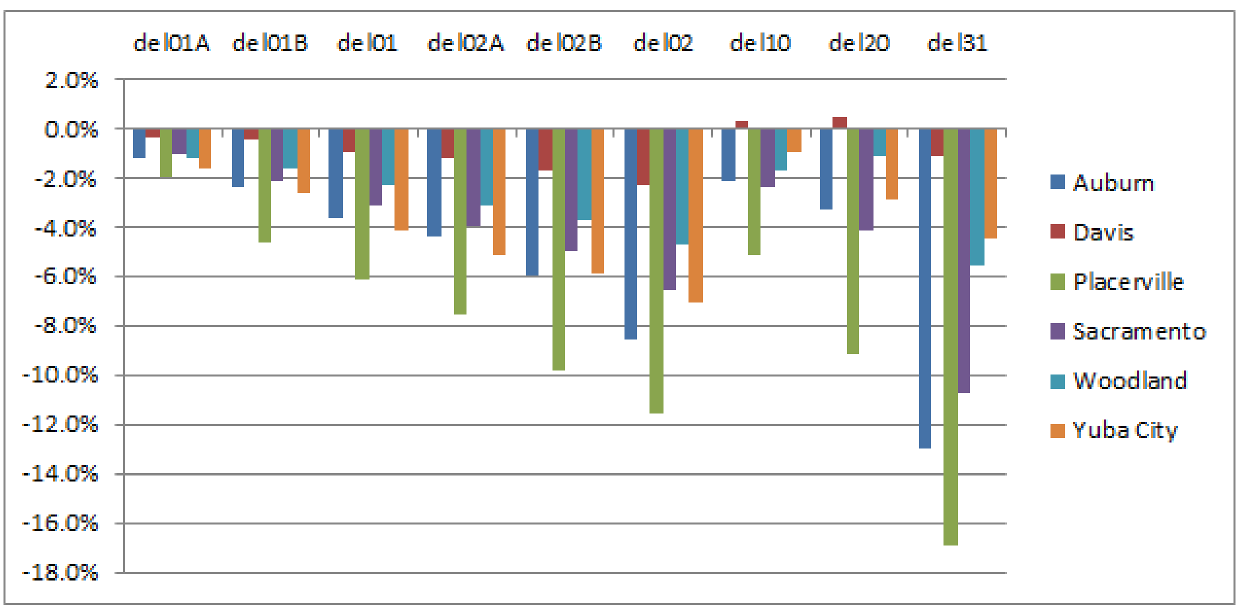

5.14 CHANGES IN TEMPERATURE EXCEEDANCES OVER THRESHOLDS

In this section, the changes in temperature, e.g., cumulative DH, above thresholds of 35 and 38 °C are presented. It is noted here that this analysis of temperature (DH) versus thresholds is different from a similar analysis of DH in terms of the National Weather Service Heat Index (NWS HI, discussed in Section 5.15) in that the NWS HI also includes humidity in the calculations. Thus, the analysis in this section may be more useful to applications by utilities -- the threshold of 38 °C, for example, is of interest to utilities in the region (SMUD) in planning for electric demand. On the other hand, the NWS HI analysis is used in the assessment of potential heat-health impacts of mitigation measures.

35 °C threshold

Figure 5-35 shows the degree-hour (ºC·hr) exceedances above 35 °C in the sub-domains of interest and for all modeled times. For each time period, indicated on the horizontal axis, a base case and five scenarios or measures are plotted to provide an indication as to their heat-mitigation potentials. While the range of exceedances (absolute values) varies by region, certain features are consistent across all domains. For instance, the periods 2013_int3, 2014_int3, and 2016_int4 have consistently larger exceedances than other time periods in all sub-domains (these are periods containing heat-wave/heat-event days, as discussed in Section 5.15, Table 5-12). Also, relative to the base scenario, it can be seen that all measures can reduce exceedances by a significant amount.

Table 5-8 summarizes the percentage-wise reductions in exceedances averaged over all periods for each region. Excluding case02 (an extreme scenario), it can be seen that the albedo measures are either similar in effect to or better than the vegetation-canopy measures since the 35 ºC threshold is a daytime-high temperature (i.e., a time of day when albedo measures are effective). The scenario producing the largest reductions in exceedances is case31, which is consistent with results from other analysis of metrics and threshold.

Figure 5-35: Temperature exceedance (DH) over a 35 °C threshold, for all periods.

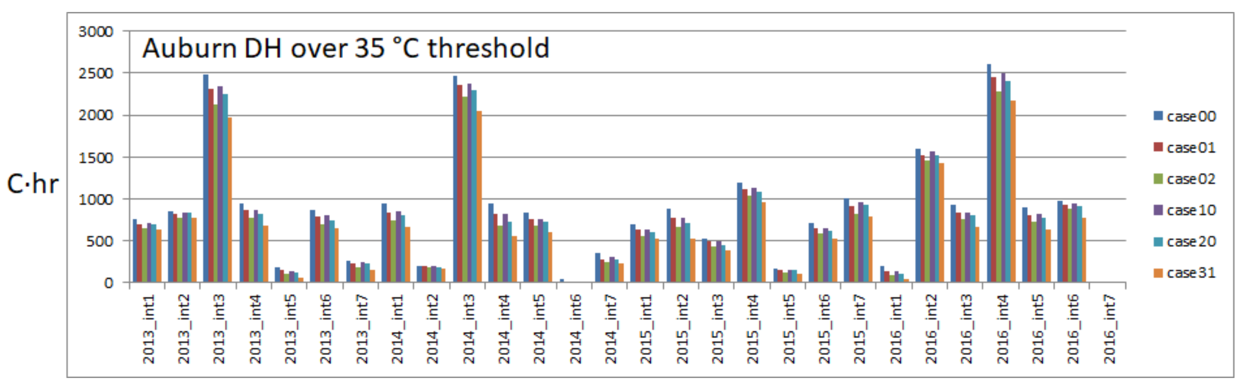

Figure 5-35, continued.

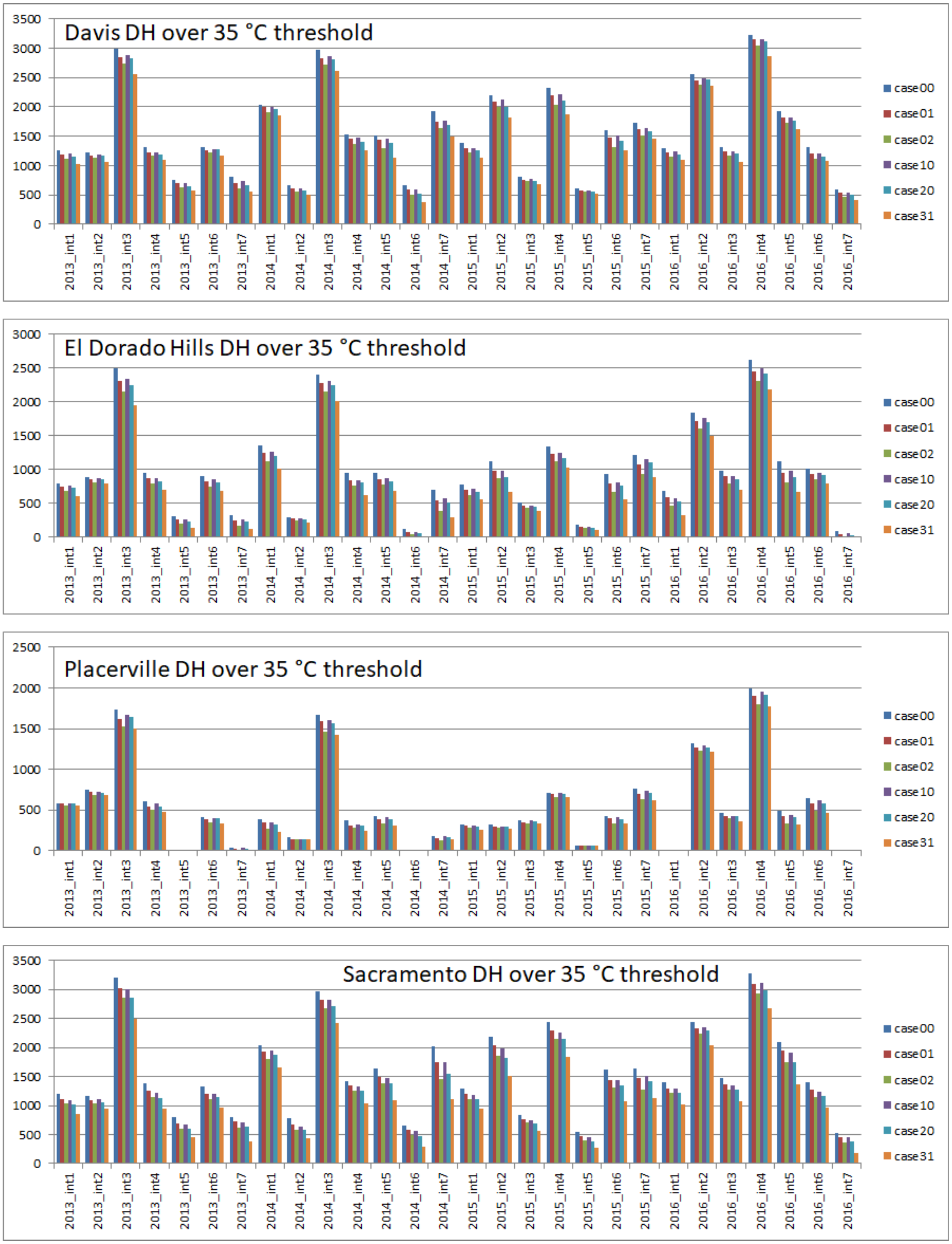

Figure 5-35, continued.

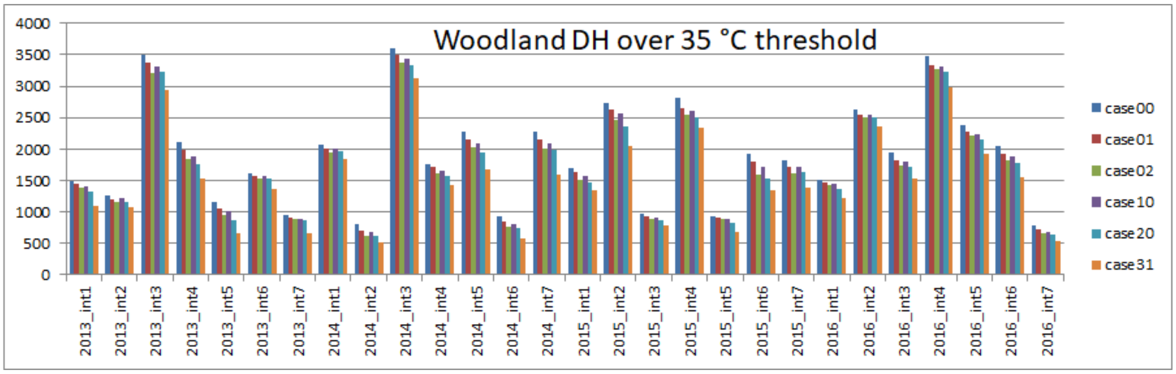

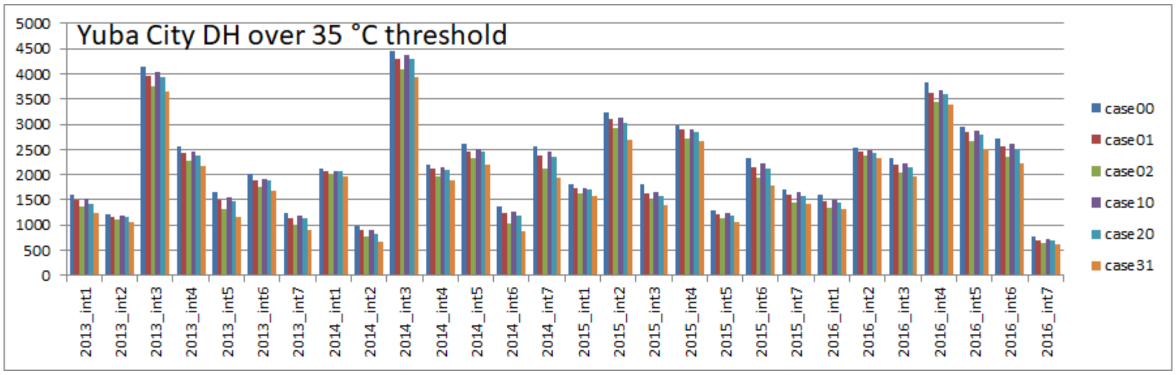

Table 5-8: Reduction in exceedances over 35 °C, current climate, averaged over all intervals and years (2013 – 2016) and over urban areas in the given sub-domains.

	Canopy scenarios		Albedo scenarios		Combination
	del01	del02	del10	del20	del31
Auburn	-8.1%	-16.3%	-6.8%	-11.2%	-23.7%
Davis	-5.4%	-10.9%	-4.5%	-7.9%	-16.7%
El Dorado Hills	-9.6%	-18.6%	-7.7%	-12.6%	-27.4%
Placerville	-6.9%	-14.1%	-3.9%	-6.7%	-16.4%
Sacramento	-7.7%	-15.2%	-8.5%	-14.1%	-28.9%
Woodland	-4.7%	-9.5%	-6.6%	-11.3%	-21.3%
Yuba City	-5.4%	-12.1%	-3.9%	-6.9%	-16.5%

38 °C threshold

Figure 5-36 represents the degree-hour (ºC·hr) exceedances above 38 °C in all sub-domains and for all time intervals. As in the preceding discussion, for each time interval a base case and five scenarios or mitigation measures are plotted. As discussed above, certain features are consistent across all domains, e.g., periods 2013_int3, 2014_int3, and 2016_int4 (heat-wave/heat events) have consistently larger exceedances than other time periods in all sub-domains.

In Table 5-9, the percentage-wise reductions in exceedances above 38 °C, averaged over all periods for each region, are summarized. It is to be noted, as elsewhere in this analysis, that case del02 is an extreme and that case31 represents a more realistic level of canopy cover increase paired with a relatively high, but realistic increase in albedo. Thus, excluding case02, one can see that the albedo measures are either similar to (in effect) or better than the vegetation-canopy measures, as this is a daytime temperature threshold. Furthermore, the scenario producing the largest reductions in exceedances is case31, which is consistent with other results presented earlier in this report.

Figure 5-36: Temperature exceedance (DH) over a 38 °C threshold, for all periods.

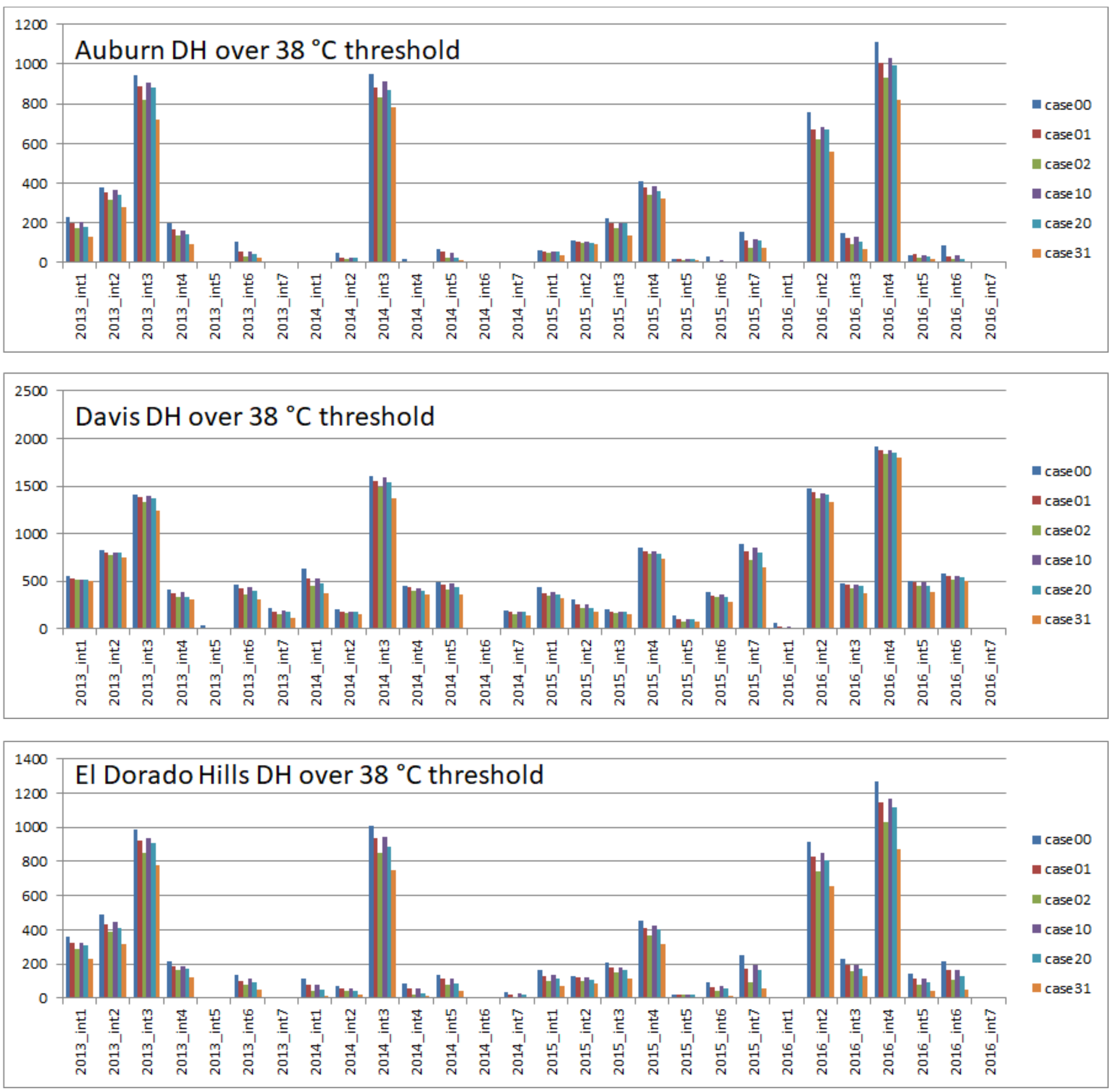

Figure 5-36, continued.

Table 5-9: Average reduction in exceedances over 38 °C, current climate, averaged over all intervals and years (2013 – 2016).

	Canopy scenarios		Albedo scenarios		Combination
	del01	del02	del10	del20	del31
Auburn	-11%	-21%	-10%	-15%	-31%
Davis	-6%	-12%	-5%	-9%	-19%
El Dorado Hills	-13%	-25%	-11%	-18%	-38%
Placerville	-12%	-25%	-8%	-15%	-32%
Sacramento	-10%	-20%	-11%	-19%	-36%
Woodland	-6%	-12%	-10%	-16%	-28%
Yuba City	-7%	-14%	-6%	-10%	-20%

5.15 REDUCTIONS IN THE NATIONAL WEATHER SERVICE HEAT INDEX (NWS HI) WARNING LEVELS

One interesting aspect of UHI-mitigation measures, at least in theory, is their potential to improve public heat health among other benefits. To characterize these effects, the potential of measures in reducing exposure to excessive heat, e.g., above various warning levels of the National Weather Service Heat Index (NWS HI), was quantified in this study. The NWS HI was defined earlier in Section 5.9.1 (Equation 5-8) – it is computed based on both temperature and humidity but reported in degrees F (i.e., as an effective temperature).

The goal of the analysis presented in this section was to quantify the potential of heat-mitigation measures in "shifting down" the NWS HI from one warning level to a lower one, e.g., from "Danger" to "Extreme Caution" or from "Extreme Caution" to "Caution", and to reduce exposure to heat-wave conditions (see Glossary). Several metrics are discussed below that provide an assessment of these potential effects – some are specific to certain time intervals; others are more general indicators of averages. These metrics were calculated at a number of probing locations identified in Figure 5-37.

As an example, Table 5-10 shows the number of hours at 1700 PDT (through all intervals in 2013-2016) that are over the "Danger" and "Extreme Caution" levels and how that number is reduced with a scenario of combined albedo increase and canopy cover (case31). It can be seen that the number of hours above the "Danger" level can be reduced by half or more and that the number of hours above the "Extreme Caution" level can be reduced by between 18% and 35% with case31.

As discussed below and shown in Table 5-12, the mitigation measures can also reduce the number of heat-wave days and the exposure to heat-wave conditions.

Figure 5-37: Locations of probing points for the analysis of changes in the NWS Heat Index.

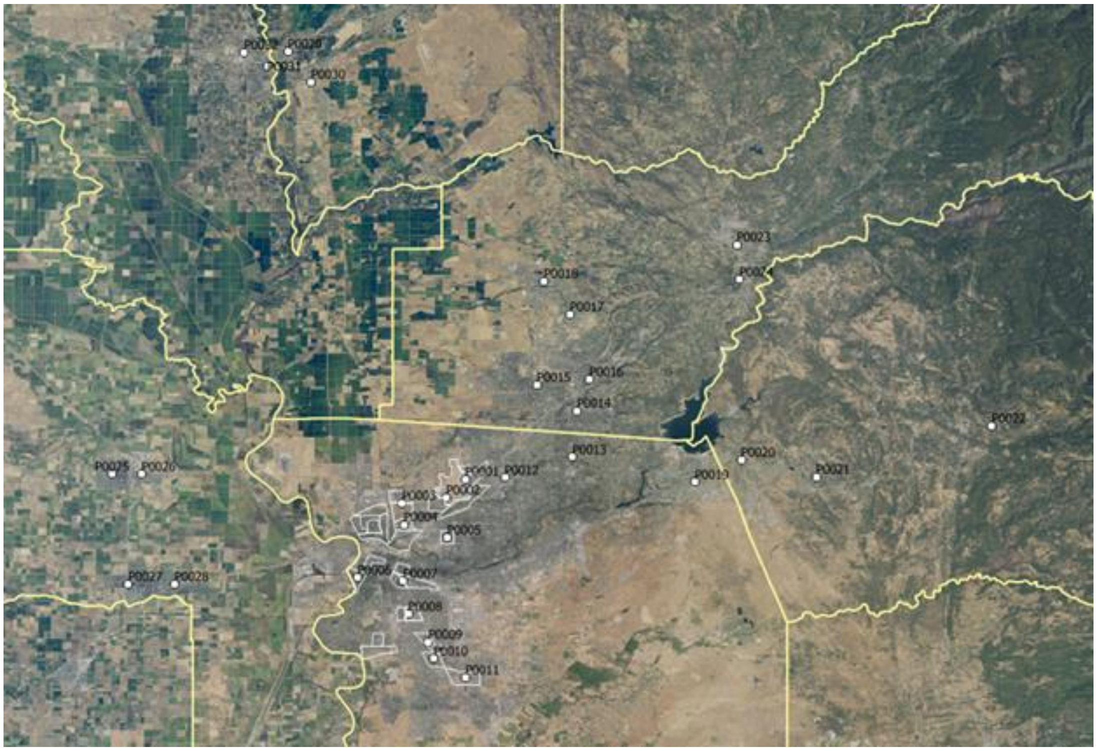

Table 5-10: Changes in the number of hours when the NWS Heat Index exceeds the specified thresholds for "Danger" and "Extreme Caution".

Probing station	Number of hours above NWS HI "Danger" **		Number of hours above NWS HI "Extreme Caution" **		Reduction
	case00	case31	case00	case31	Case31-00
P0001 AB617 (SAC)	4	2	180	124	31%
P0004 AB617 (SAC)	3	2	171	123	28%
P0008 AB617 (SAC)	2	1	140	98	30%
P0011 AB617 (SAC)	1	1	124	90	27%
P0013 Citrus Heights	6	2	177	119	33%
P0014 Roseville	7	2	189	122	35%
P0018 Lincoln	8	2	210	154	27%
P0020 El Dorado Hills	2	1	114	78	32%
P0022 Placerville	1	1	40	31	23%
P0026 Woodlands	6	2	193	151	22%
P0028 Davis	2	2	149	122	18%
P0029 Marysville	13	6	245	192	22%
P0032 Yuba City	13	4	251	178	29%

** At 1700 PDT hours during the period 2013 – 2016 intervals 1 – 7.

The NWS HI "Danger" level is defined as above the threshold of 106 °F (41.1 °C) and "Extreme Caution" above a threshold of 91 °F (32.8 °C). The "Caution" level is set at 80 °F (26.7 °C). These thresholds are shown as dashed lines in Figure 5-38. A heat wave is defined when the NWS HI is within or exceeds 105-110 ºF for at least two consecutive days. Per this definition, and as seen in Figure 5-38, the model correctly captures heat events/heat waves in the Capital region during the intervals of (1) June 30 – July 4, 2013 (day counter 30-34 in Figure 5-38), (2) June 30 – July 1, 2016 (day counter 345-346), and (3) July 28 – 29, 2016 (day counter 373-374).

Two types of information can be gleaned from Figure 5-38:

1. whether there are exceedances above certain HI warning levels or thresholds, e.g., above the dashed lines. For example, in the first graph of Figure 5-38, there are exceedances in 1700-PDT HI above 106 °F between June 30th and July 4th, 2013 (day counter 30-34), which is one of three heat waves identified above, and there are several exceedances above 91 °F, some of which are highlighted with the vertical green arrows; and
2. whether there are instances where the cooling measure (case31) "shifts down" the HI from one warning level to a lower one. Some such instances are shown at the locations of the green arrows in the first graph of Figure 5-38 where the HI goes from the "Extreme Caution" level (blue series) to the "Caution" level (red series). The cumulative HI reductions (e.g., DH above thresholds) are discussed later in this section.

Figure 5-38: NWS HI at all 1700-PDT hours (for case00, case31) for JJAS at probing locations identified in Figure 5-37.

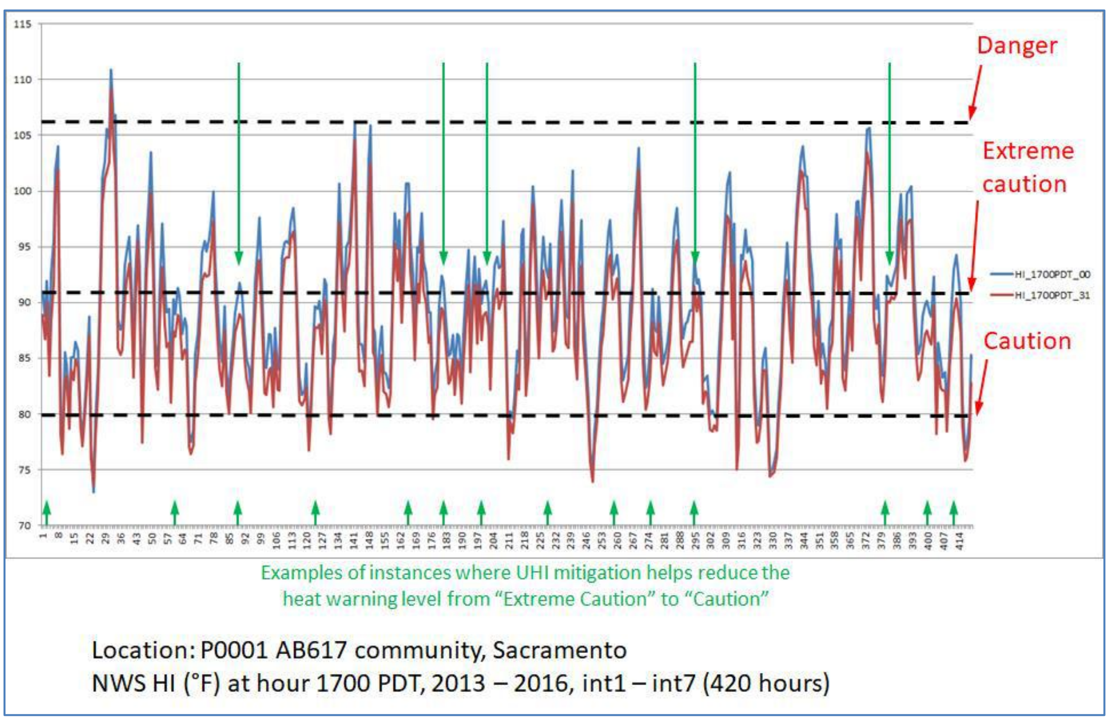

Figure 5-38, continued.

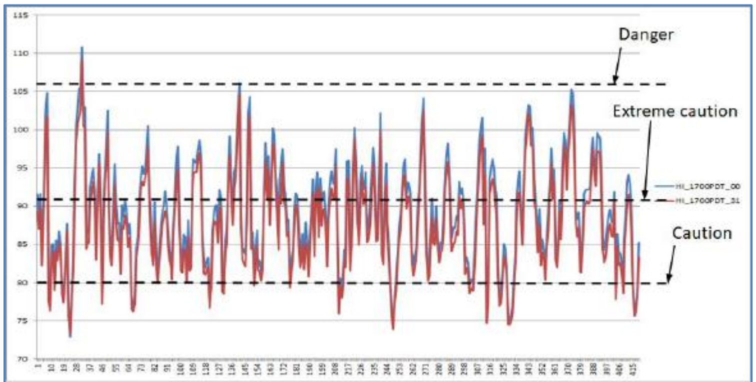

Location: P0004 AB617 community, Sacramento
NWS HI (°F) at hour 1700 PDT, 2013 – 2016, int1 – int7 (420 hours)

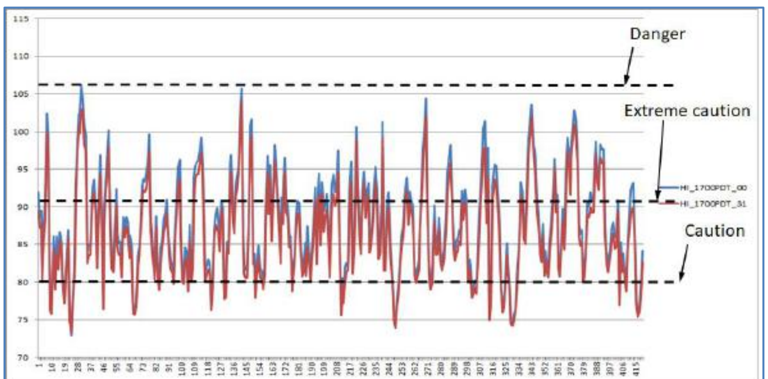

Location: P0008 AB617 community, Sacramento
NWS HI (°F) at hour 1700 PDT, 2013 – 2016, int1 – int7 (420 hours)

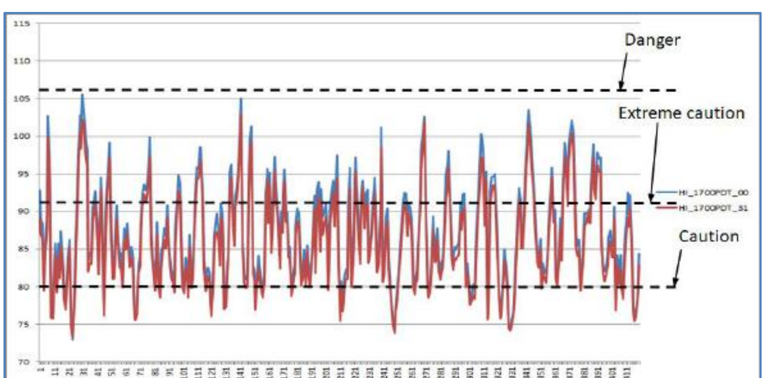

Location: P0011 AB617 community, Sacramento
NWS HI (°F) at hour 1700 PDT, 2013 – 2016, int1 – int7 (420 hours)

Figure 5-38, continued.

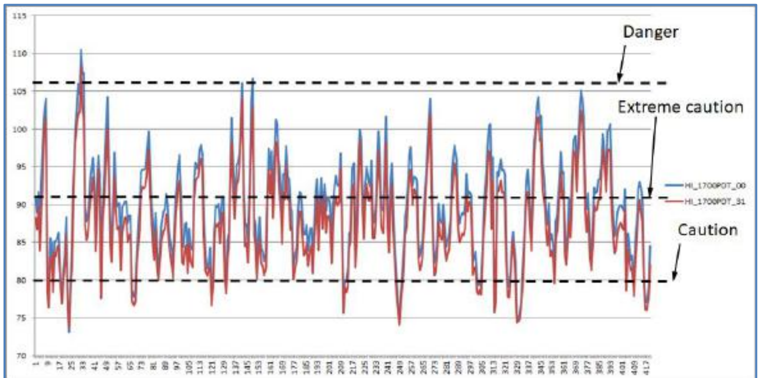

Location: P0013 Citrus Heights
NWS HI (°F) at hour 1700 PDT, 2013 – 2016, int1 – int7 (420 hours)

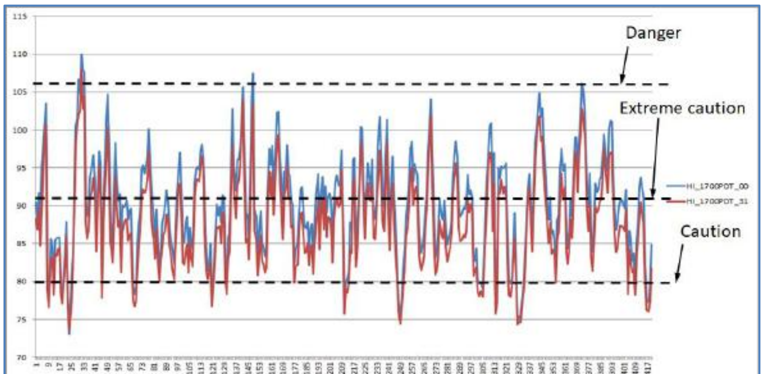

Location: P0014 Roseville
NWS HI (°F) at hour 1700 PDT, 2013 – 2016, int1 – int7 (420 hours)

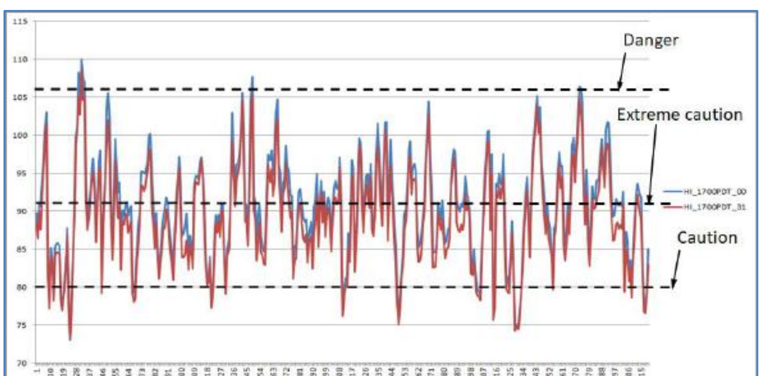

Location: P0018 Lincoln
NWS HI (°F) at hour 1700 PDT, 2013 – 2016, int1 – int7 (420 hours)

Figure 5-38, continued.

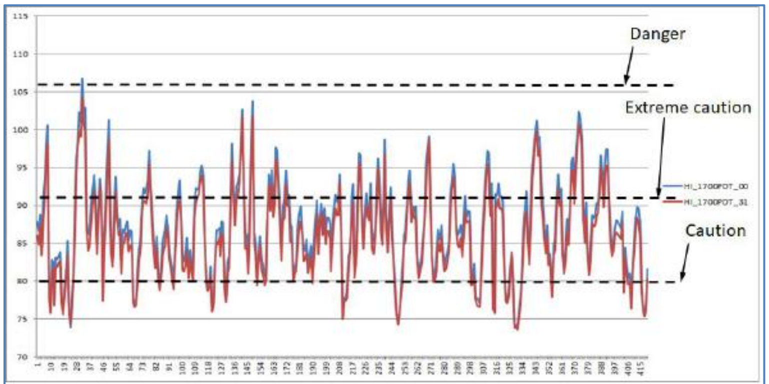

Location: P0020 El Dorado Hills
NWS HI (°F) at hour 1700 PDT, 2013 – 2016, int1 – int7 (420 hours)

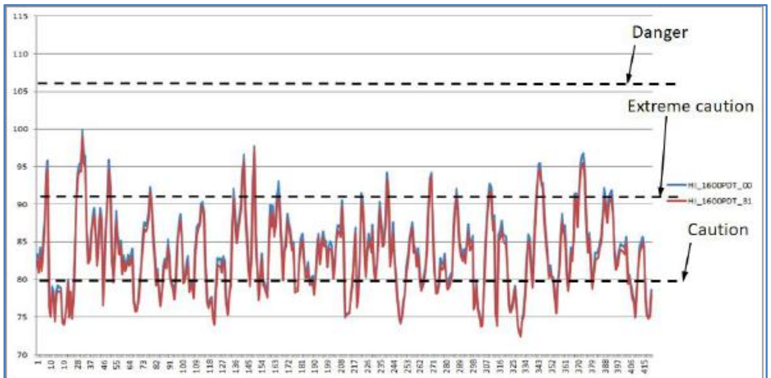

Location: P0022 Placerville
NWS HI (°F) at hour 1600 PDT, 2013 – 2016, int1 – int7 (420 hours)

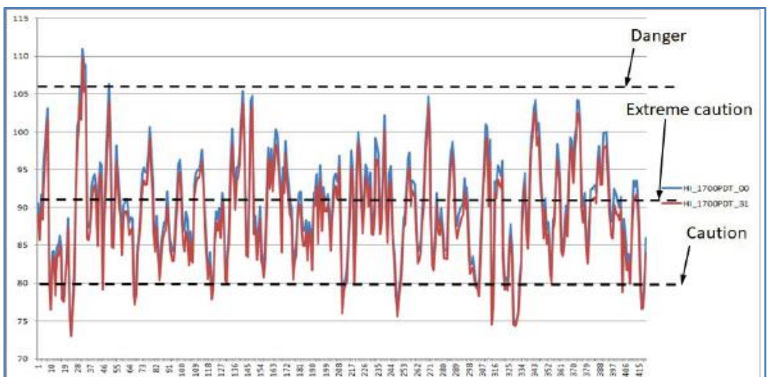

Location: P0026 Woodlands
NWS HI (°F) at hour 1700 PDT, 2013 – 2016, int1 – int7 (420 hours)

Figure 5-38, continued.

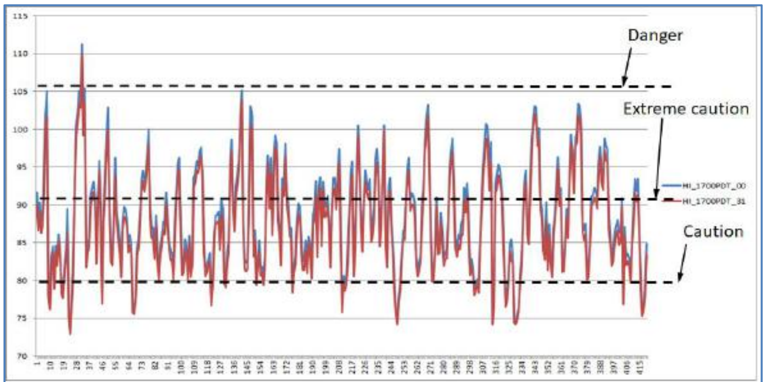

Location: P0028 Davis
NWS HI (°F) at hour 1700 PDT, 2013 – 2016, int1 – int7 (420 hours)

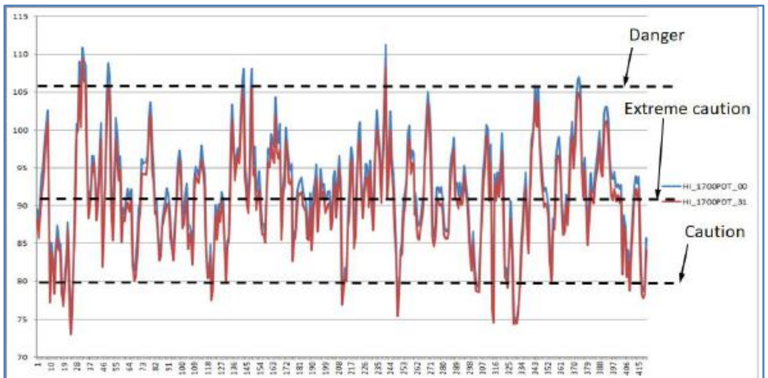

Location: P0029 Marysville
NWS HI (°F) at hour 1700 PDT, 2013 – 2016, int1 – int7 (420 hours)

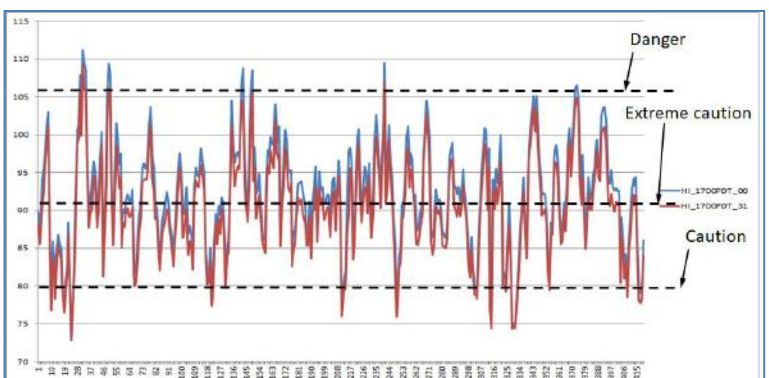

Location: P0032 Yuba City
NWS HI (°F) at hour 1700 PDT, 2013 – 2016, int1 – int7 (420 hours)

Table 5-11 provides additional information for the hours at 1700 PDT in terms of exceedances and potentials for reduction of the NWS HI levels by the mitigation measures (in this example, case31). In this table, cumulative metrics (i.e., % change in degree-hours above the thresholds) are provided. Thus, for each selected probing point (P0001 through P0032), the first three rows provide the percentages of DH above the given thresholds and the following three rows give the percent reduction in DH above those thresholds. Thus, it can be seen that the mitigation measure (case31) has a significant impact and can reduce exceedances above 106 °F by between 50% and 100% (except for one location) and the exceedances above 91 °F by between 18% and 36%.

Table 5-11: Exceedances (DH) above three NWS HI levels (1700 PDT averages over all intervals) in current climate for selected probing locations (P####) defined in Figure 5-37. All numbers in the table are percentages. (Note: DH = °F · hr).

	HI threshold	Probing location						
		P0001	P0004	P0008	P0011	P0013	P0014	P0018
% of DH above thresholds	>80 °F (%)	93.0	92.8	90.6	90.1	92.3	93.4	93.9
	> 91 °F (%)	45.6	43.5	36.0	32.1	44.8	47.7	52.7
	> 106 °F (%)	0.9	0.6	0.3	0.0	1.4	1.7	2.0
% reduction in DH above thresholds	>80 °F (% ↓)	-5.8	-5.0	-5.2	-9.4	-4.9	-6.1	-4.7
	> 91 °F (%↓)	-31.9	-28.6	-30.5	-28.0	-33.5	-36.2	-27.0
	> 106 °F (%↓)	-66.2	-49.7	-100.0	N/A	-79.8	-83.2	-85.5

	HI threshold	Probing location					
		P0020	P0022	P0026	P0028	P0029	P0032
% of DH above thresholds	>80 °F (%)	89.0	71.3	94.1	92.1	94.6	94.8
	> 91 °F (%)	29.3	10.4	48.7	38.2	61.0	62.5
	> 106 °F (%)	0.3	0.0	1.4	0.3	3.4	3.4
% reduction in DH above thresholds	>80 °F (% ↓)	-4.8	-4.8	-4.2	-4.8	-2.6	-3.5
	> 91 °F (%↓)	-31.9	-23.3	-22.3	-18.7	-22.1	-29.5
	> 106 °F (%↓)	-100.0	N/A	-79.7	-1.1	-58.7	-75.6

In terms of locally countering or offsetting the effects of excessive heat events or heat waves (per above definitions), Table 5-12 provides a summary of the mitigation potential for case31. The table shows the number of days with NWS HI of 105 – 110 ºF at each selected probing location and for the three heat-wave events identified above. The table also shows the reduction in the number of heat-wave days at each location as a result of implementing case31 – the heat-wave effects are-locally offset everywhere except for one period in each of the Yuba City and Marysville locations.

During the 6/30 – 7/3, 2013 heat wave, case31 reduces the number of heat-wave days from 5 or 4 to 1 or 0 in most locations, except for Marysville and Yuba City. During the 6/30 – 6/31, 2016 heat event, case31 reduces the number of days to zero at all locations. The same occurs during the interval 7/29 – 7/30, 2016, i.e., heat-wave days are reduced to zero, except for Marysville and Yuba City where they are reduced from 3 to 2 and from 3 to 1, respectively.

Table 5-12: Number of consecutive days with NWS HI 105 – 110 ºF in three time periods.

		Number of days with NWS HI 105 – 110 ºF					
Probing location	Heat wave?	6/30 – 7/4, 2013		6/30 – 6/31, 2016		7/28 – 7/30, 2016	
		base	case31	base	case31	base	case31
P0001 AB617 (Sac)	yes	5	1	0	0	2	0
P0004 AB617 (Sac)	yes	3	1	0	0	2	0
P0008 AB617 (Sac)		1	0	0	0	0	0
P0011 AB617 (Sac)		1	0	0	0	0	0
P0013 Citrus Heights	yes	5	1	1	0	1	0
P0014 Roseville	yes	5	2	1	0	2	0
P0018 Lincoln	yes	4	3	1	0	2	0
P0020 El Dorado Hills		1	0	0	0	0	0
P0022 Placerville		0	0	0	0	0	0
P0026 Woodland	yes	3	0	0	0	0	0
P0028 Davis	yes	4	0	0	0	0	0
P0029 Marysville	yes	4	4	2	0	3	2
P0032 Yuba City	yes	4	4	2	0	3	1

Whereas some of the foregoing discussion, e.g., Figure 5-38 and Table 5-11, summarized the effects of UHI mitigation in terms of the 1700-PDT NWS HI, Figure 5-39 provides additional information for the hours from 1400 to 2000 PDT. Thus, the following charts summarize the average reductions (percentage-wise) in DH exceedances above the three warning thresholds of the NWS HI (Caution, Extreme Caution, and Danger) for case31 at thirteen selected probing points (defined earlier) and for seven individual hours (from 1400 to 2000 PDT) averaged over all such hours in the modeled periods (i.e., a total of 420 hours for each computed hour average). In other words, Figure 5-39 provides an average for all 1400-PDT hours during JJAS of 2013-2016, all 1500-PDT hours during JJAS 2013-2016, and so on, as identified in the legend of each figure. If no data is shown for certain hours in the graphs, this means that there were no exceedances of the thresholds to begin with.

From Figure 5-39, it can be seen that the mitigation measure can offset exceedances above various thresholds at all locations and hours, sometimes fully (100%) offsetting the exceedances over the "Danger" threshold. Furthermore, and except for the "Danger" level, the reductions in the other two levels exhibit a rough "inverted U" pattern suggesting that the cooling measure decreases the

HI relatively more on both sides of 1700 PDT. That is, the HI is reduced most (percentage-wise) at 1400 and 2000 PDT, then at 1500 and 1900 PDT, then at 1600 and 1800 PDT, and finally at 1700 PDT. Thus, in a way, the foregoing discussion of the hour at 1700 PDT might in fact be a presentation of the smallest beneficial effects of the cooling measures (i.e., the benefits can be larger at other hours, or it could be because the heat index is smaller at those hours than at 1700 PDT). For the "Danger" level, this argument does not apply as there is no clear pattern in HI reductions and the cooling measure can be equally effective at different hours.

Figure 5-39: Percentage-wise reductions in the NWS HI exceedances (DH) over the specified thresholds for case31 relative base scenario for all hours during JJAS at probing locations identified in Figure 5-37.

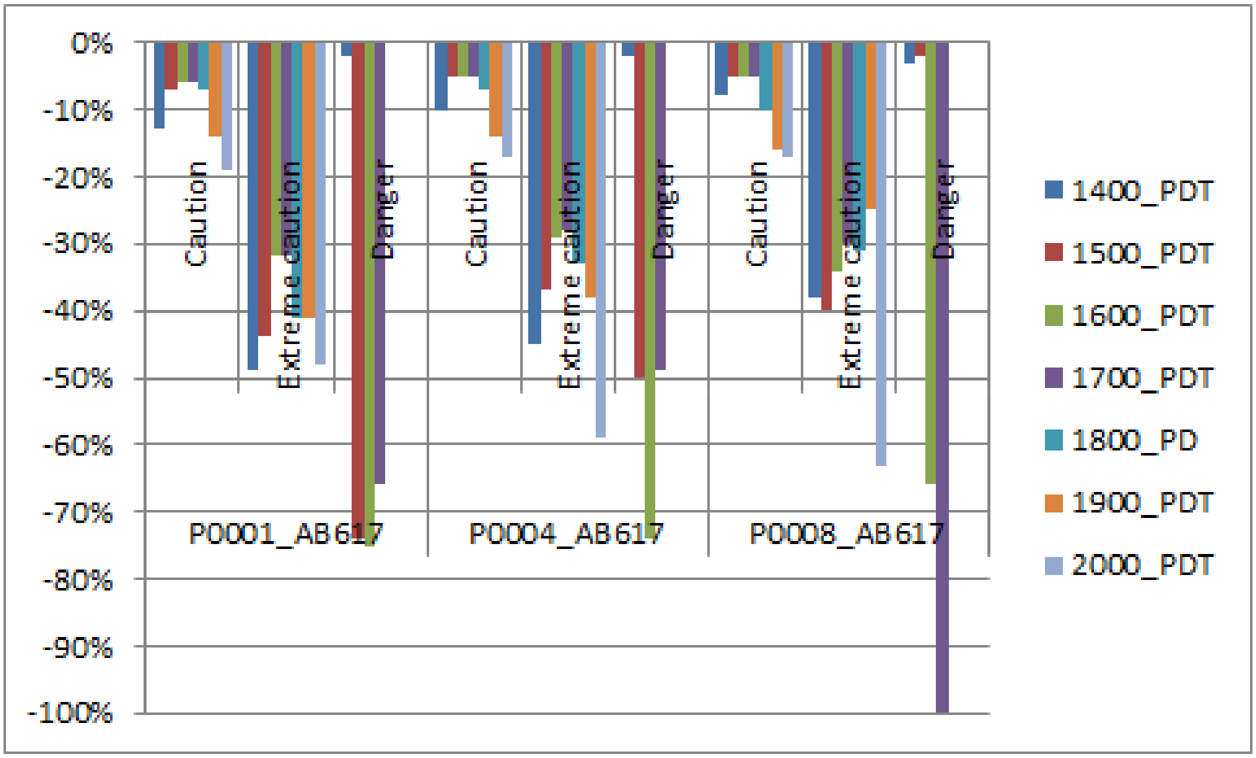

Figure 5-39, continued.

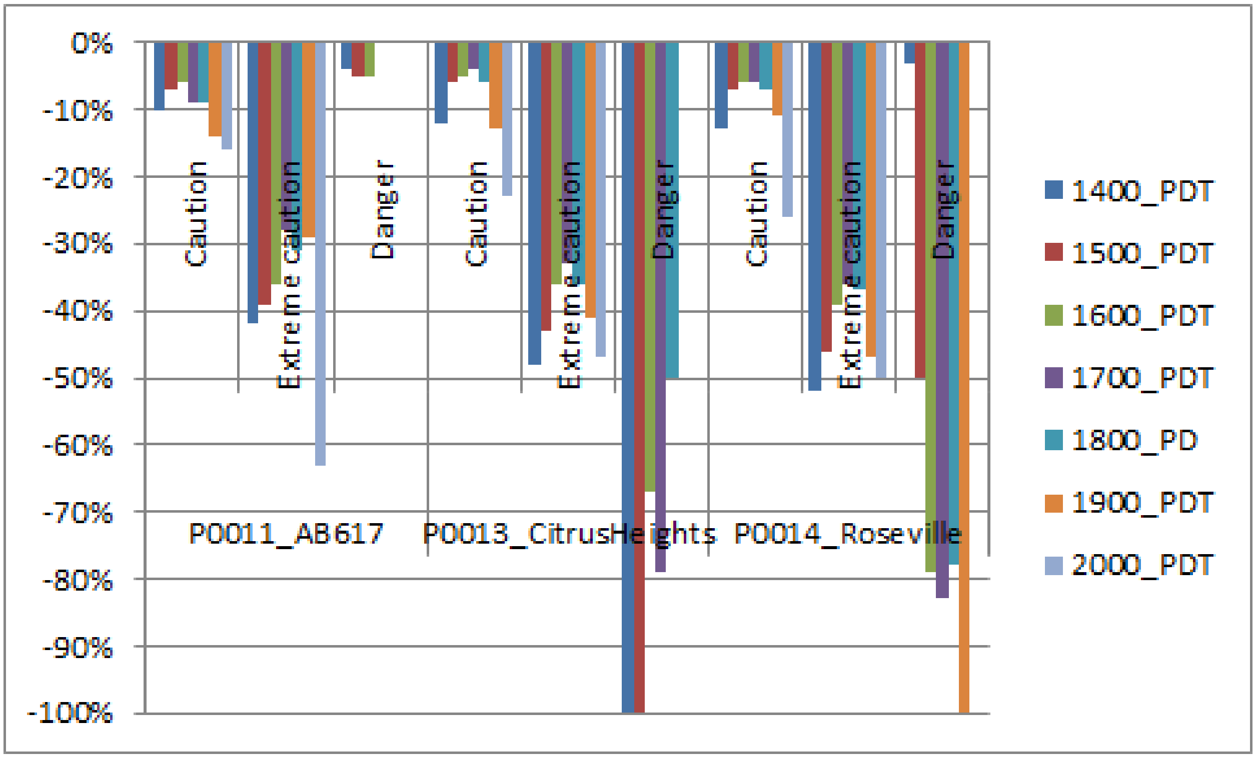

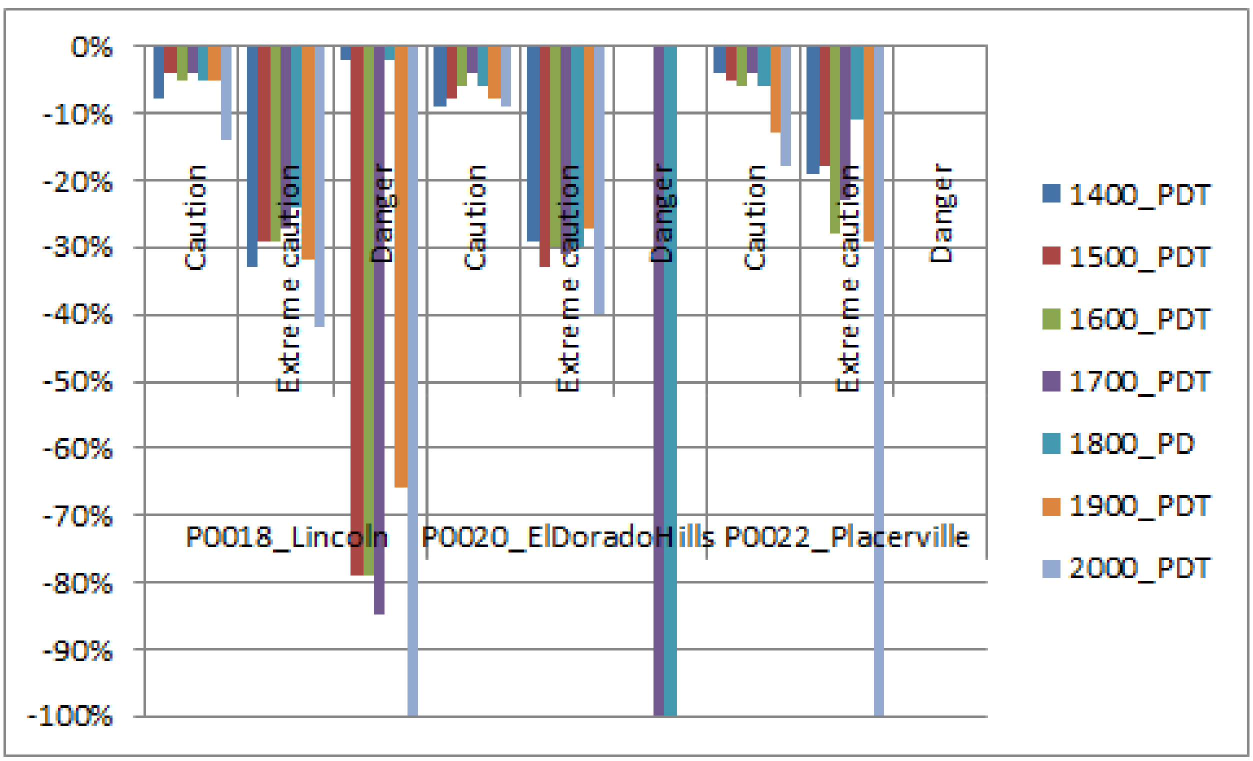

Figure 5-39, continued.

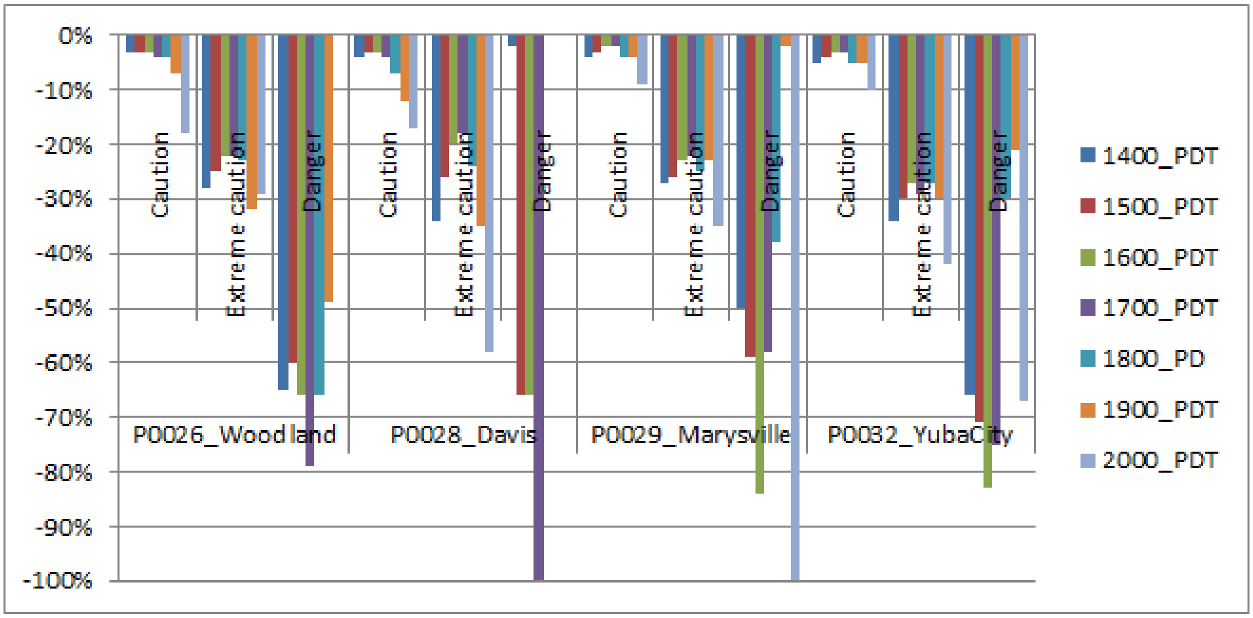

5.16 IMPACTS OF INCREMENTAL INCREASES IN CANOPY COVER

In this section, the impacts of incremental increases in canopy cover on air temperature are discussed in addition to providing an estimate of the corresponding water usage. The increase in cover could be a result of canopy growth and/or planting additional urban trees over time. For this purpose, additional, intermediate scenarios to case01 and case02 (that were presented earlier in Section 5-5) were introduced and modeled. These are cases 01A, 01B, 02A, and 02B, as defined in Table 5-13.

Table 5-13: Definition of canopy-cover incremental cover.

Scenario	01A	01B	**01**	02A	02B	**02**
Cover **increase** (percent of cell area)	3.4%	7.7%	12.0%	16.3%	20.6%	25.0%
Possible equivalent time frame	2018	2022	2026	2030	2033	2037

It is re-iterated here that scenarios with tree cover increases larger than case01, i.e., 02A, 02B, and 02, are likely not feasible at this time as they will require a very large amount of tree planting. As alluded to earlier, case01 can be considered an upper bound that includes increasing canopy cover by 12% (area-wise) and bringing the total cover in many areas to about 14% which is the average of the established canopy cover in Sacramento. By comparison, case02 would bring the total cover to 35%, which, while technically doable, is a relatively more extreme scenario. Nevertheless, all of the cases are considered in the analysis to provide various estimates of cooling effects and water consumption.

The following tabulations and figures summarize the effects in each sub-domain of the 6-counties Capital region. These are averages (spatially) over each area as well as temporally over the specified hours or hourly intervals during years 2013-2016 and intervals 1-7 within each. Information is also provided to show the degree-hours (°C·hr) exceedances over specified thresholds, e.g., 35 and 38 °C, and percent-wise changes (reductions) relative to these thresholds for each canopy scenario.

The results presented in this section are for a few sample hour intervals during daylight as well as over all-hour periods. This is an important point to keep in mind since the effects of canopy cover are continuous (during day and night) unlike the effects of albedo that occur during the day or the effects of vehicle electrification and heat-emission control that are seen mostly during rush hours. This is also important from heat-health / heat-wave perspectives since nighttime cooling can contribute to relieving heat stress.

Table 5-14 is a listing of average base and perturbation-scenario temperatures and average reductions resulting from the various incremental canopy scenarios. This information is also presented graphically in Figure 5-40, where it can be seen that as canopy cover increases, the net cooling effect becomes larger, which is what is generally expected. However, the increase is not linear although it appears to be close to that.

Modeling the incremental increases in canopy cover suggests different sensitives in temperature response to changes in cover (Figure 5-40). To discuss this point, we examine the changes in all-hours average cooling (which is the last graph in Figure 5-40) as an example. In Auburn (for instance), going from a 3.4% increase in canopy cover (percent of cell area) to 25% increase, that is, going from case01A to case02, results in all-hours average cooling going from 0.1 to 0.7 °C. On the other hand, the same canopy cover increase, i.e., going from +3.4% to +25% in Sacramento, results in all-hours average cooling going from 0.15 to 1.0 °C, meaning a larger response or sensitivity to the same changes in canopy cover. The main reason, aside from geographical, LULC, and microclimatic differences, is the size of the urban area affected by canopy-cover increase. In Sacramento, larger areas are affected by tree cover than in Auburn and, thus, areas in Sacramento can benefit from the transport of cooler air from upwind locations, hence the additional cooling benefit. The same observation applies to other time intervals and hours.

Table 5-14: Average temperature and change (°C) from incremental increase in canopy cover

1300 PDT

1300PDT	case00	case01A	case01B	case01	case02A	case02B	case02	del01A	del01B	del01	del02A	del02B	del02
Auburn	29.3128	29.256	29.1965	29.1356	29.0867	29.0269	28.9451	-0.05676	-0.11624	-0.17717	-0.22603	-0.2859	-0.36762
Davis	31.3363	31.2855	31.2319	31.1764	31.1315	31.0769	31.0011	-0.05087	-0.10443	-0.15992	-0.20483	-0.25944	-0.33524
El Dorado Hills	29.5428	29.4745	29.4024	29.3275	29.2682	29.1946	29.0935	-0.06836	-0.14045	-0.21537	-0.27462	-0.34822	-0.44933
Placerville	28.8258	28.786	28.7448	28.7022	28.6677	28.6253	28.566	-0.03978	-0.08095	-0.12362	-0.15803	-0.20047	-0.25978
Sacramento	30.8787	30.7906	30.6966	30.5997	30.5218	30.4253	30.292	-0.08811	-0.18218	-0.279	-0.35689	-0.4534	-0.58672
Woodland	31.8151	31.7639	31.7083	31.6526	31.6083	31.5533	31.4742	-0.05126	-0.10678	-0.1625	-0.20679	-0.26181	-0.34088
Yuba City	31.5444	31.4748	31.3992	31.3216	31.2603	31.1831	31.0765	-0.06962	-0.1452	-0.22281	-0.28407	-0.36129	-0.46788

1400 to 2000 PDT

1400 to 2000PDT	case00	case01A	case01B	case01	case02A	case02B	case02	del01A	del01B	del01	del02A	del02B	del02
Auburn	30.33	30.2598	30.1842	30.1063	30.0437	29.9676	29.8617	-0.07017	-0.14583	-0.22366	-0.28628	-0.36245	-0.46828
Davis	31.5302	31.4704	31.4081	31.3434	31.2918	31.2281	31.1418	-0.05983	-0.1221	-0.18676	-0.23845	-0.30207	-0.38837
El Dorado Hills	30.4984	30.4277	30.3522	30.2737	30.2102	30.1326	30.0244	-0.07071	-0.14621	-0.2247	-0.28819	-0.36575	-0.47393
Placerville	28.9496	28.8949	28.8364	28.7765	28.7272	28.6663	28.5821	-0.05469	-0.11319	-0.17315	-0.22241	-0.28332	-0.36751
Sacramento	31.8764	31.7998	31.7182	31.6339	31.5662	31.4824	31.3658	-0.07659	-0.15819	-0.24249	-0.31024	-0.39398	-0.51064
Woodland	32.4665	32.411	32.3526	32.292	32.2442	32.1839	32.1013	-0.05547	-0.11393	-0.17449	-0.22231	-0.28258	-0.36517
Yuba City	33.2518	33.1866	33.1154	33.0444	32.9852	32.9123	32.8106	-0.06526	-0.13648	-0.20748	-0.26661	-0.33951	-0.44126

1500 PDT

1500PDT	case00	case01A	case01B	case01	case02A	case02B	case02	del01A	del01B	del01	del02A	del02B	del02
Auburn	31.0863	31.0314	30.9729	30.9126	30.8646	30.8077	30.7264	-0.05497	-0.11345	-0.17372	-0.22176	-0.27869	-0.35997
Davis	33.063	33.0208	32.976	32.9288	32.8929	32.8488	32.7894	-0.04219	-0.08707	-0.13417	-0.17012	-0.21426	-0.27366
El Dorado Hills	31.4745	31.4091	31.3396	31.268	31.2114	31.1418	31.0453	-0.06536	-0.13486	-0.20646	-0.26306	-0.3327	-0.42916
Placerville	30.0235	29.9812	29.9371	29.8914	29.8563	29.8119	29.7508	-0.04223	-0.08633	-0.13203	-0.16715	-0.21151	-0.27262
Sacramento	33.0852	33.0199	32.9501	32.8785	32.8207	32.7497	32.651	-0.06529	-0.13514	-0.20671	-0.26453	-0.33548	-0.43419
Woodland	33.7661	33.7267	33.6823	33.6387	33.6041	33.5592	33.5003	-0.03941	-0.08379	-0.12739	-0.16202	-0.20694	-0.26577
Yuba City	33.9507	33.8995	33.8422	33.7855	33.7388	33.6811	33.6046	-0.05114	-0.10845	-0.16514	-0.21191	-0.26953	-0.34612

All hours

allHRS	case00	case01A	case01B	case01	case02A	case02B	case02	del01A	del01B	del01	del02A	del02B	del02
Auburn	26.3181	26.2066	26.0893	25.9703	25.8753	25.7615	25.608	-0.11159	-0.22879	-0.34786	-0.44286	-0.55666	-0.7101
Davis	25.1114	24.989	24.8585	24.724	24.616	24.4835	24.301	-0.12239	-0.25288	-0.38736	-0.49535	-0.62788	-0.8104
El Dorado Hills	25.7303	25.6179	25.4992	25.378	25.2816	25.1641	25.0053	-0.11241	-0.23114	-0.35234	-0.44876	-0.56621	-0.725
Placerville	25.4063	25.3032	25.1945	25.0848	24.9993	24.8962	24.7585	-0.10307	-0.21177	-0.32151	-0.40698	-0.51014	-0.64776
Sacramento	25.7256	25.5786	25.4209	25.2567	25.124	24.9594	24.7307	-0.14699	-0.30467	-0.46885	-0.60159	-0.76621	-0.99484
Woodland	25.6928	25.5717	25.4429	25.3115	25.2053	25.0744	24.8944	-0.12108	-0.24985	-0.38128	-0.48749	-0.61838	-0.79832
Yuba City	27.0336	26.8848	26.723	26.5552	26.4187	26.2497	26.0161	-0.14887	-0.31061	-0.47847	-0.61496	-0.78393	-1.01756

Figure 5-40: Average reduction in air temperature (ºC) for various intervals, canopy scenarios, and regions. Time periods are given a top left of each graph. Vertical axis is degrees C.

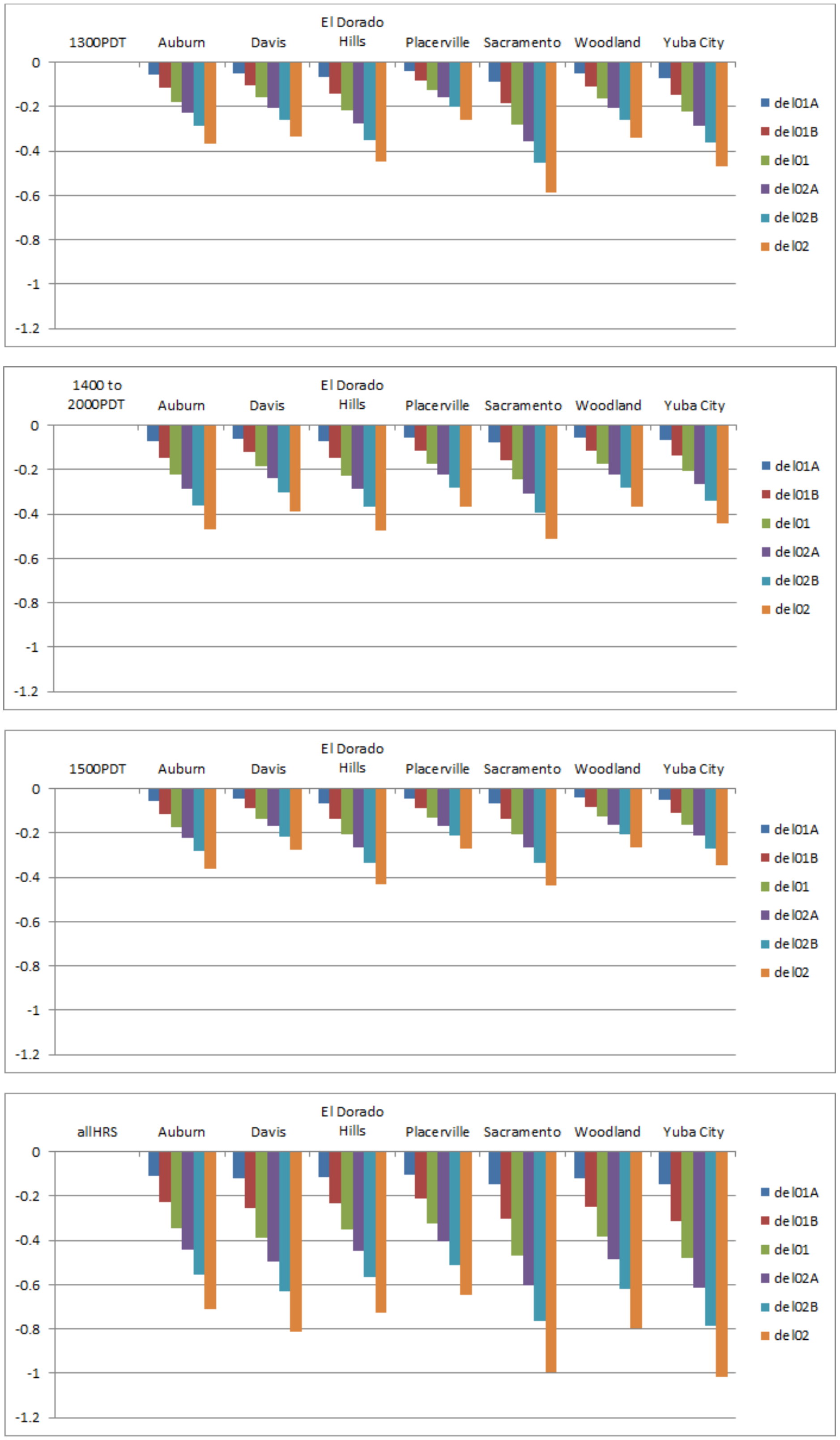

Table 5-15 summarizes the cumulative exceedances (DH) above 35 and 38 °C and their changes (reductions) for various canopy-cover incremental scenarios. The reductions (percentage-wise) of total DH above thresholds are also represented in Figure 5-41. In general, the pattern in these figures is similar to those in Figure 5-40 (average reductions in temperature). The urban-cooling measures can decrease the DH exceedances above 35 °C by up to 18% and above 38 °C by up to 25%, depending on region.

Table 5-15: Degree-hours (ºC · hr) and changes from incremental canopy cover over specified thresholds

Threshold: 35 °C

totDH above 35	case00	case01A	case01B	case01	case02A	case02B	case02	del01A	del01B	del01	del02A	del02B	del02
Auburn	846.87	825.321	801.814	778.072	760.713	739.514	708.931	-21.5493	-45.0556	-68.7983	-86.1566	-107.356	-137.939
Davis	1511.72	1483.96	1456.31	1429.56	1408.89	1382.86	1346.71	-27.7615	-55.4101	-82.1601	-102.838	-128.861	-165.018
El Dorado Hills	961.836	932.987	902.124	869.72	848.722	821.346	782.901	-28.8486	-59.7119	-92.1156	-113.114	-140.49	-178.935
Placerville	526.077	514.036	499.851	489.87	481.431	467.883	451.701	-12.0406	-26.2261	-36.2069	-44.6463	-58.1943	-74.3753
Sacramento	1537.63	1497.72	1458.12	1419.34	1389.32	1353.65	1303.5	-39.9079	-79.5081	-118.295	-148.311	-183.981	-234.132
Woodland	1845.11	1816.34	1786.45	1758.56	1733.35	1706	1670.69	-28.7717	-58.6578	-86.5431	-111.76	-139.112	-174.422
Yuba City	2160.07	2123.17	2081.81	2042.36	2005.14	1959.6	1898.84	-36.8973	-78.2571	-117.703	-154.924	-200.462	-261.225

Threshold: 38 °C

totDH above 38	case00	case01A	case01B	case01	case02A	case02B	case02	del01A	del01B	del01	del02A	del02B	del02
Auburn	210.152	202.176	194.193	185.563	179.782	173.696	165.93	-7.97576	-15.9589	-24.5886	-30.3697	-36.4562	-44.2216
Davis	543.194	533.002	521.248	509.497	501.32	491.254	476.541	-10.1921	-21.9468	-33.6973	-41.8747	-51.9404	-66.6531
El Dorado Hills	267.096	256.243	244.945	233.087	224.251	214.774	200.056	-10.8531	-22.1518	-34.009	-42.8458	-52.322	-67.0405
Placerville	86.0162	82.1139	78.538	75.6212	73.394	70.9801	66.2296	-3.90225	-7.47823	-10.395	-12.6222	-15.0361	-19.7865
Sacramento	552.711	535.437	516.826	498.535	484.765	467.099	444.554	-17.2742	-35.8851	-54.1766	-67.9465	-85.6122	-108.157
Woodland	658.175	643.615	630.917	616.891	607.585	595.145	579.582	-14.5597	-27.2581	-41.284	-50.5896	-63.0298	-78.5925
Yuba City	806.334	787.241	766.083	748.25	733.734	717.912	692.357	-19.0924	-40.2505	-58.0832	-72.6	-88.4211	-113.976

Figure 5-41: Average reduction in DH exceedances above 35 and 38 ºC for incremental canopy cover.

Total DH above 35 °C

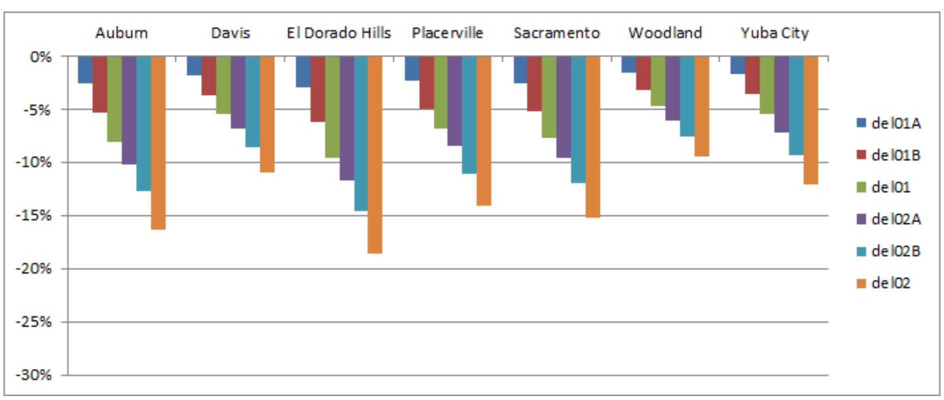

Figure 5-41, continued.

Total DH above 38 °C

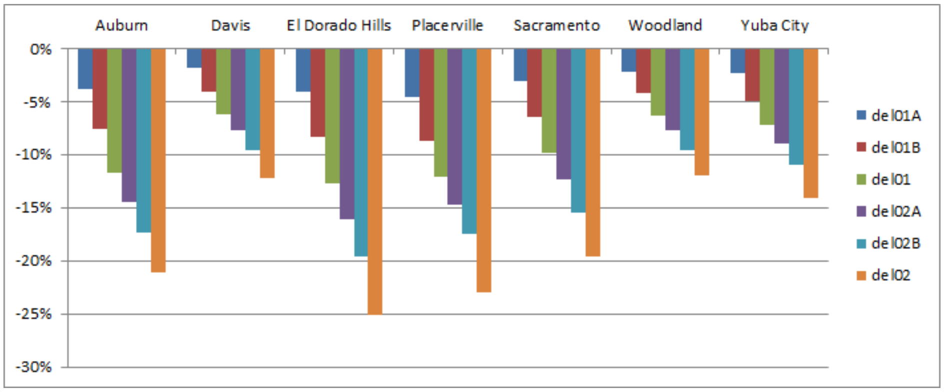

In terms of water usage by the canopy, the following crude estimates were developed via quantification of evapotranspiration. The estimates are provided as water needed by the canopy in order to achieve an all-hours average cooling of 0.5 °C in each of the sub-regions.

While the discussion above clearly indicates a wide range of cooling potential across different scenarios and across different regions, here a cooling of 0.5 °C is used as a common denominator to provide equivalence, i.e., the same basis for comparison across different regions. The 0.5 ºC cooling is an average over all urban cells in the given area and over all hours of the day (not just daytime or specific hour). The corresponding water usage is estimated by calculating evapotranspiration over years 2013-2016 and intervals 1-7 within each year. Table 5-16 is a summary of these estimates, in liters per year (L yr^{-1}) of water per neighborhood. In this calculation, a neighborhood is assumed to cover an area of 0.25 – 0.5 km^2.

Table 5-16: Water use equivalents to achieve an area average of 0.5 °C reduction in all-hours average temperature.

Area	H_2O (L yr^{-1}) per neighborhood (~ 0.25 – 0.5 km^2)
Auburn	117,905,000
Davis	94,500,000
El Dorado Hills	106,276,320
Placerville	118,260,000
Sacramento	74,740,320
Woodland	94,608,000
Yuba City	74,600,200

To put these estimates into some context, we compare against a few examples:

(1) Per U.S. EPA, a typical family of four uses 144,000 gallons of water per year, which is 545,040 liters per year (L yr^{-1}). Thus, the water usage range in Table 5-16 (per neighborhood of 0.25 to 0.5 km^2) would correspond to the annual water usage of some 130 – 200 households. To provide further context, a census tract in urban California is about 1 km^2 on average and has about 5000 people (which is about 1250 households), and the neighborhood calculations at 0.25 – 0.5 km^2 would translate to between 312 and 625 households. Thus, per this calculation, the tree water usage in a neighborhood is equivalent to the annual water usage of some 130 – 200 households out of 312 – 625 households (to achieve an all-hours and area-wide average cooling of 0.5 ºC), which is about one third of the households.

(2) A brief literature review of crops evapotranspiration shows (after various conversions) that, for example, alfalfa uses 350,462,900 L yr^{-1} per 0.25 km^2 per season, which is 3 to 5 times more than the evaporation from the canopy scenarios in table above. For wheat, the usage is 101,634,250 L yr^{-1} per 0.25 km^2.

(3) For the purpose of comparing water-usage estimates, as computed above, against the literature and values from observational studies, the following example is provided. Various organizations have measured or estimated water consumption by trees and found that evapotranspiration is correlated to trunk diameter at breast height (DBH), e.g., Pretzsch et al. (2015). Measurements show that for typical mature large trees with DBH of 30 cm (12 inches), evapotranspiration ranges from 120 to 150 gallons of water per day per tree. This is respectively equivalent to 82,554,240 and 103,192,800 L yr^{-1} per 0.25 km^2 and is of the same magnitude as the values reported in Table 5-16, thus lending additional credence to these estimates.

5.17 IDENTIFYING GEOGRAPHICAL AREAS FOR IMPLEMENTING URBAN-COOLING MEASURES BASED ON THE UHII SCORE

The goal of this analysis is to produce additional layers of information, e.g., that could be used in conjunction with other datasets, including CES 3.0 (OEHHA 2013), to help identify and prioritize geographical areas for deployment of UHI-mitigation measures.

For this purpose, an initial scoring of areas was developed based on the modeled UHII at the regional scale. As with the CES 3.0 score, the higher the UHII score, the worse is urban heat and the higher the priority is for action. The first set of scores (e.g., Figure 5-41) was developed based on the local UHII regardless of absolute air temperature. However, the cooling measures are welcome in all regions, regardless of the score, as residents would benefit from these effects no matter how they rank relative to some other areas. That is, the reductions in absolute temperature are equally welcomed everywhere.

Thus, the purpose of the scoring such as shown in Figure 5-41 is to provide Caltrans and urban planners with additional information when allocating resources. The figure shows five tiers or ranks based on UHII intervals of 1 °C in the 6-counties Capital region (the higher the score, the worse is the condition). The UHII scoring presented here is based on climate as the sole criterion -- no socio-economic factors were taken into consideration. If, for example, the UHII tiers were weighted by CES 3.0 scores (last graph in Figure 5-41), the UHII score would shift relatively more towards central and south Sacramento, in areas with AB617 communities A, B, and D (which occur in UHII Tiers 3 and 4) as well as community C and its surroundings (which occur in UHII Tier 2). Additional information is provided in Appendix D-1.

Thus, if only UHII is used as basis, the areas including Yuba City / Marysville, Woodland, Davis, and Placerville occur in UHII Tiers 1 and 2. Most of north and south Sacramento and AB617 communities C, E, and G and others nearby occur in Tier 2. Central Sacramento, AB617 communities A, B, and D, and an area extending to Folsom and El Dorado Hills occur in Tiers 3 and 4. Northeast Sacramento, Roseville, Rocklin, Granite Bay, Lincoln, parts of Folsom, and areas west Auburn occur in Tier 4. Finally, an area from Roseville to Lincoln and a small area over Auburn fall into Tier 5. Again, the higher the tier (or UHII score), the worse is the UHII. Of note, this also includes some non-urban areas because of heat transport.

Figure 5-41: UHII score for implementing UHI-reduction measures at the regional scale: Tiers 1 through 5 (lowest to highest score) using UHII as the sole criterion.

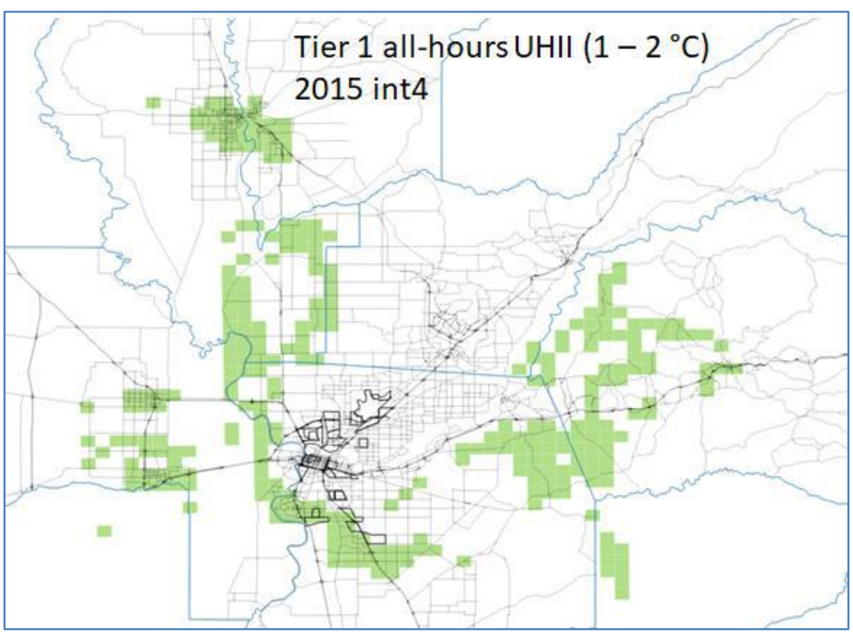

Figure 5-41, continued

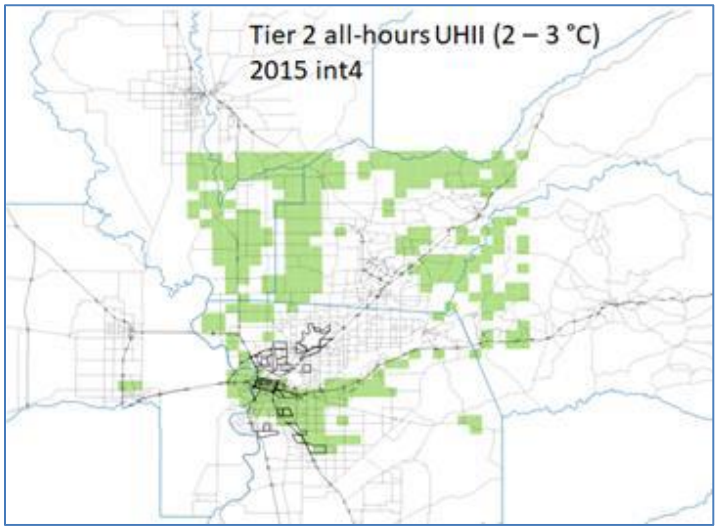

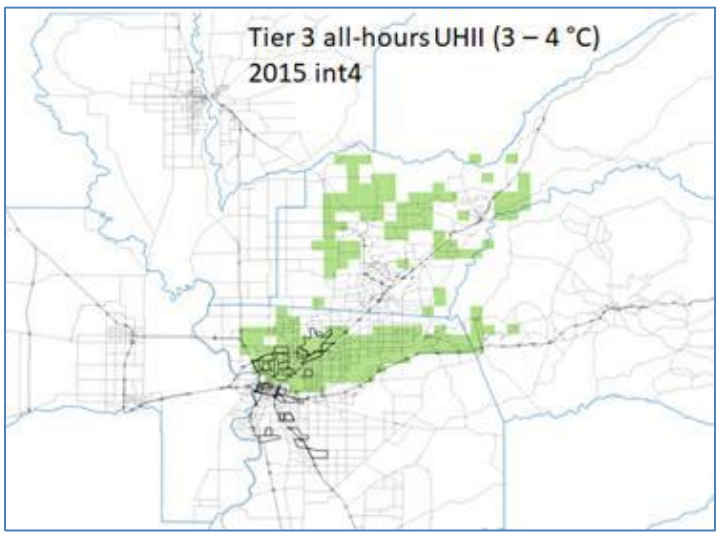

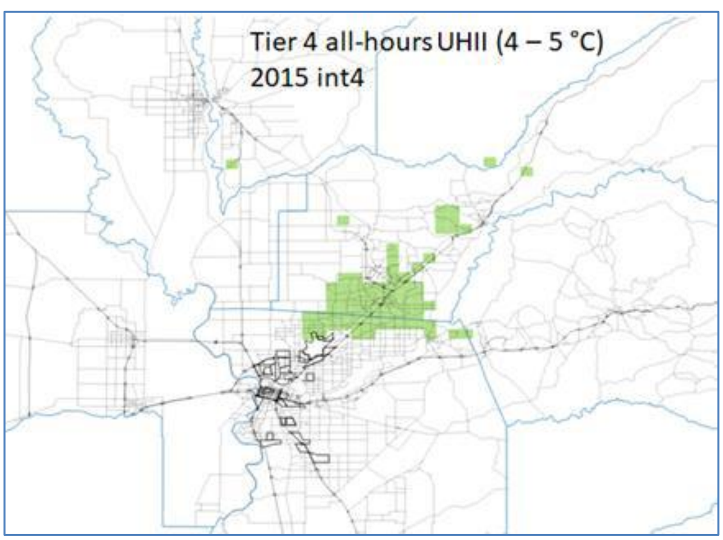

Figure 5-41, continued

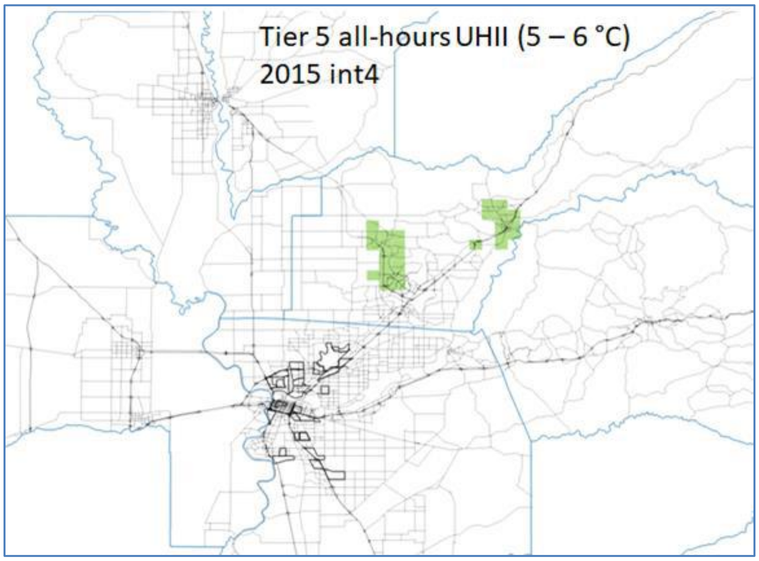

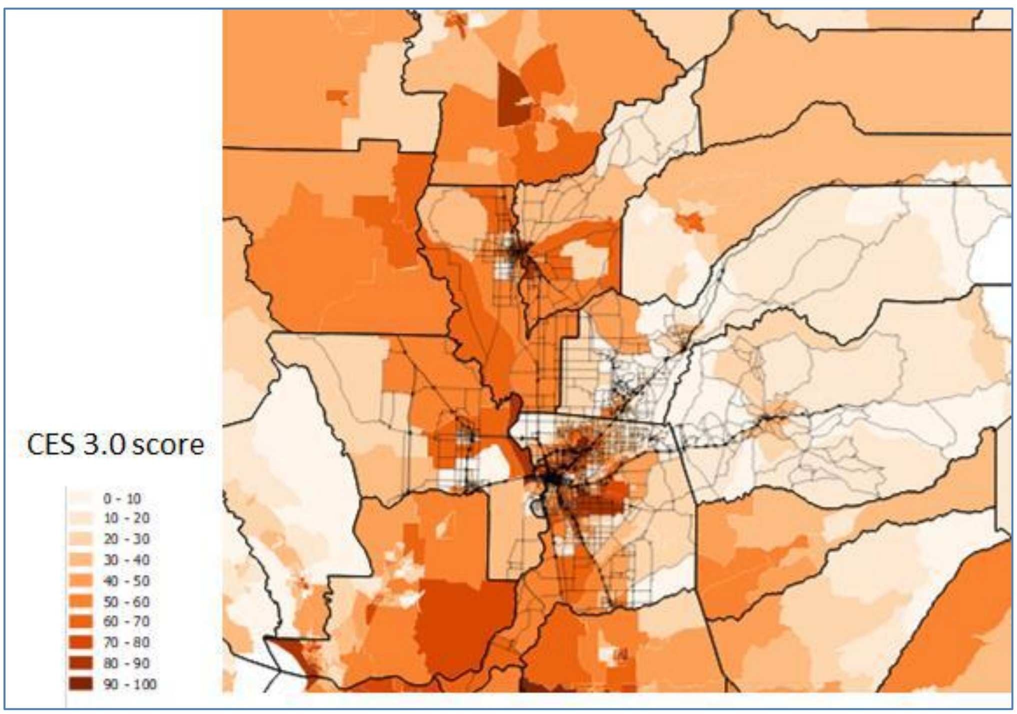

However, using only the UHII as an indicator to mitigation priorities can provide an overall picture that may be counter-intuitive at times. Thus, the above scoring is repeated, but this time using both UHII and absolute air temperature as basis, to provide relatively more intuitive rankings. That is, areas with both large UHII and high absolute temperatures get a higher score than areas with small

UHII and lower temperatures. Of course, a range of possible combinations exists in-between these two ends.

To develop a temperature-weighted UHII score, i.e., *wuSCORE*, (here, for all hours and all intervals) a tier was assigned to each of the UHII and absolute temperature ranges as follows:

$$1.0 \leq UHII < 2.0, \quad UHII_{tier} = 1$$
$$2.0 \leq UHII < 3.0, \quad UHII_{tier} = 2$$
$$3.0 \leq UHII < 4.0, \quad UHII_{tier} = 3$$
$$4.0 \leq UHII < 5.0, \quad UHII_{tier} = 4$$
$$5.0 \leq UHII < 6.0, \quad UHII_{tier} = 5$$

and,

$$25.0 \leq Tair < 26.0, \quad Tair_{tier} = 1$$
$$26.0 \leq Tair < 27.0, \quad Tair_{tier} = 2$$
$$27.0 \leq Tair < 28.0, \quad Tair_{tier} = 3$$
$$28.0 \leq Tair < 29.0, \quad Tair_{tier} = 4$$
$$29.0 \leq Tair < 30.0, \quad Tair_{tier} = 5$$

where, the units of Tair are °C and the units for UHII are ºC·hr hr^{-1}. Then, for cells where UHII > 1 and Tair > 25 ºC, the weighted UHII score (*wuSCORE*) for a given grid cell is computed as:

$$wuSCORE = LOG\,(UHII_{tier} \times Tair_{tier}) \qquad (5\text{-}10)$$

The reason for using *LOG* in Equation 5-10 is simply to damp the range of *wuSCORE* for plotting and scaling purposes. Note that *wuSCORE* is dimensionless and has no physical meaning.

Figure 5-42 shows an example of *wuSCORE* computed based on both all-hour UHII and all-hour absolute temperature averages for all years and intervals modeled in this study (Appendix D-2 provides a larger version of these maps). As can be seen, the pattern differs from that of UHII-only basis in scoring (in Figure 5-41).

The lowest score (Tier 1) includes AB617 communities D, G, H and surroundings, peripheral areas in Woodland and Davis, small areas in Marysville, Placerville, and parts of El Dorado Hills.

The second score (Tier 2) includes south and southeast Sacramento, some western parts of downtown Sacramento and surroundings, areas to the south of the American River, peripheral areas in Yuba City / Marysville, northwest Woodland, and central Davis. Some areas in Granite Bay are also included in this tier.

The next-to-top score (Tier 3) includes AB617 communities A, B, D, north Sacramento and parts of downtown, and an area extending east to include south Folsom and El Dorado Hills. Also included in this tier are parts of Lincoln and Auburn. Finally, the top score (Tier 4) includes parts of AB617 community "D", parts of northeast Sacramento, Folsom, El Dorado Hills, Roseville, Rocklin, Lincoln, central parts of Yuba City / Marysville, and parts of Auburn.

Figure 5-42: Temperature-weighted UHII score (wuSCORE) for implementing UHI-reduction measures at the regional scale: Tiers 1 through 4 correspond to lowest to highest wuSCORE.

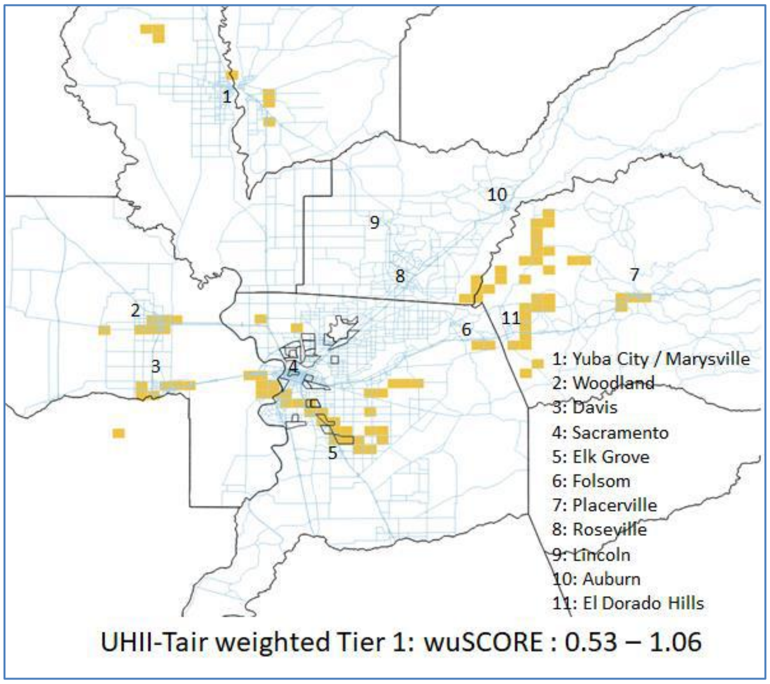

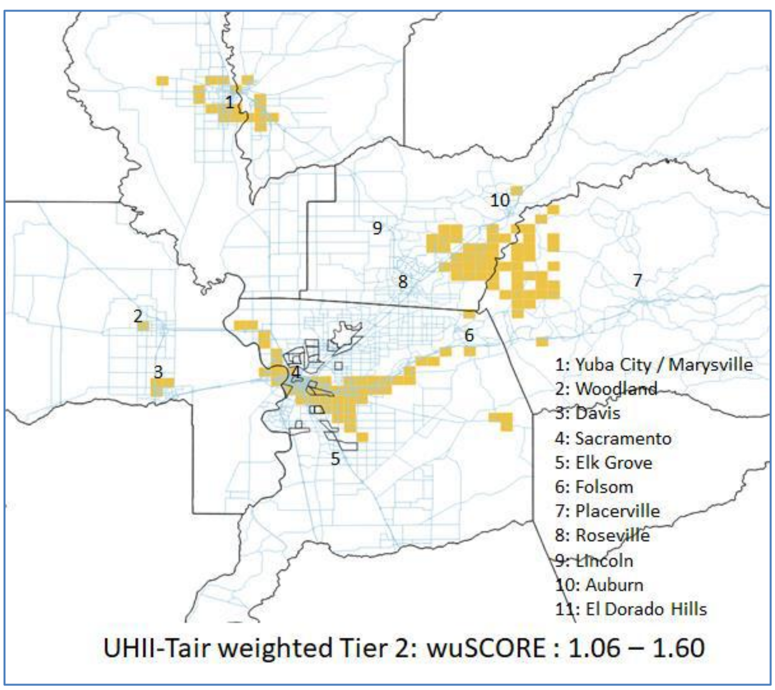

Figure 5-42, continued.

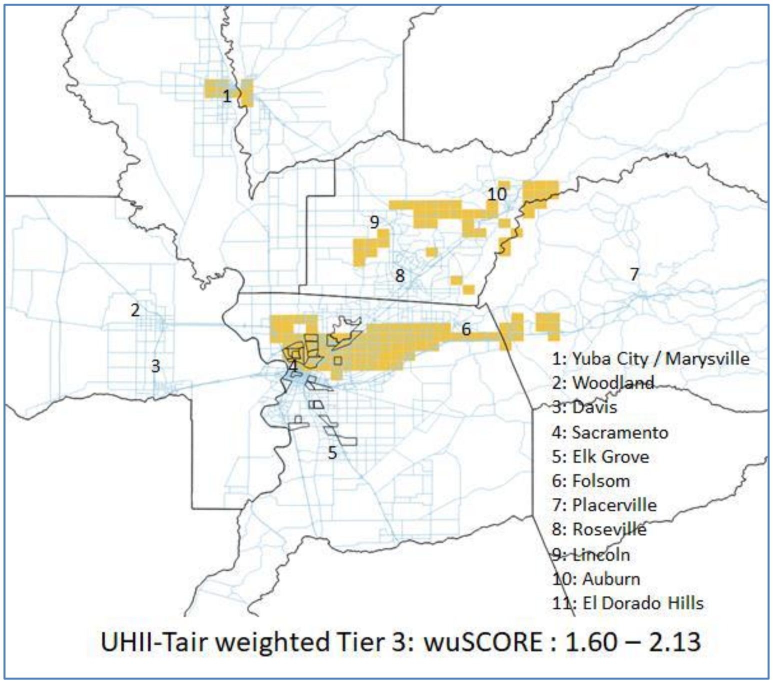

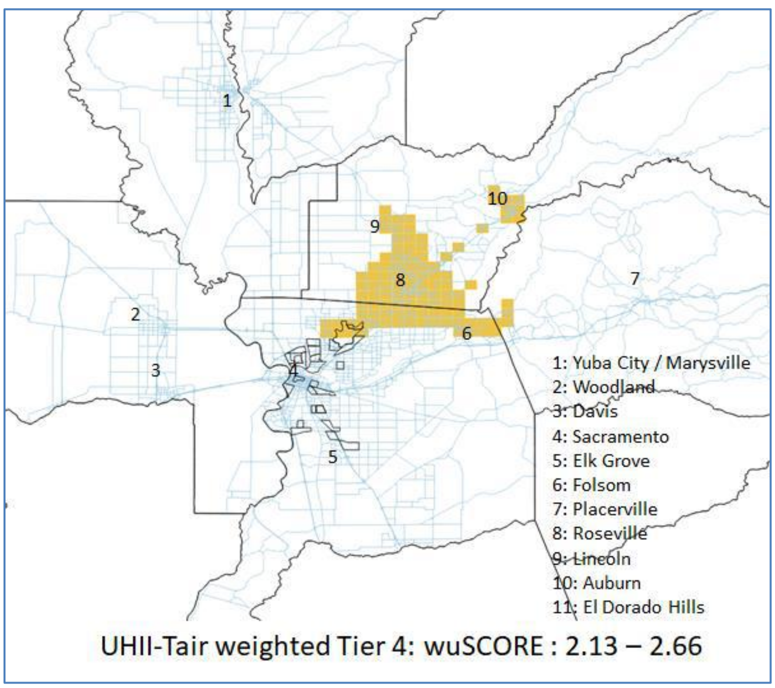

5.18 COMMUNITY-LEVEL, FINE-SCALE MODELING AND ANALYSIS

This section presents results from modeling community-scale or roadway project-specific mitigation measures. The goal of the simulations at 500-m resolution was to provide an assessment of the localized or site-specific changes in microclimate (excluding or including transported effects from neighboring communities) resulting from these measures. It was also the goal of the fine-scale modeling to evaluate certain mitigation strategies that were not tested at the 2-km level because they are project-, site-, or community-specific.

In other words, the simulations presented in this section answer the question: "What happens locally if a neighborhood or community implemented UHI-mitigation measures but the rest of the Capital region didn't do anything?"

The 500-m results were evaluated on a 5-dimensional matrix of:

(**v**)ariable (T_{air}, $T_{surface}$, T_{UCL}, *RH, U, Zi, Solar*);

(**i**)nterval (*year, month, interval*);

(**t**)ime of day or range of hours (*all hours, 0600 PDT, 0700 PDT, 1300 PDT, 1500 PDT, 1700 PDT, 1400-2000 PDT*);

(**m**)easure (*caseAA-00, caseBB-00, caseQF2-00, etc.*, see Section 5.19); and

(**a**)rea/site.

That is, changes from mitigation measures were given by:

$$\Delta_{v,i,t,m,a}$$

5.19 DEFINITIONS OF PROJECT-SPECIFIC AND COMMUNITY-LEVEL SCENARIOS

The following scenarios were modeled at the 500-m scale and in various combinations depending on domain and/or specific requests from the project participants, SMAQMD / LGC, and the project TAC:

- caseAA:
  - For the MTP projects defined by SMAQMD, LGC, the project TAC, or WSP, the roadway albedo was increased from a mean of 0.12 (average of current roadway albedo) to 0.35. The reason for imposing this upper limit was discussed earlier in the report.
  - For the AB617 communities, DAC areas, or other urban areas of interest to cities and project participants, such as downtown areas or specific projects, roof albedo was increased from a current mean of 0.17 to 0.5 and the roadway albedo from a

mean of 0.12 to 0.30 (this is a smaller increase than 0.35 above because these are mostly residential areas, compared to MTP projects that usually comprise major highways and freeways where increases in roadway albedo can be made larger). The reason for imposing these upper limits was discussed earlier in this report.

- caseQF2/QF3:
    - This is a vehicle-electrification scenario. In this case, heat flux from mobile sources was reduced by 25% (per CEC and SMAQMD studies that assume an electric-vehicle ownership of 25%). The maximum reduction (25%) was further modulated by (1) the distribution of urban fraction in the domain and (2) distance from charging stations. Furthermore, the hourly variations in heat emissions from mobile sources were approximated as in the following diurnal profile of traffic intensity (graph below) based on Sailor and Lu (2004). The red vertical line on the graph identifies the rush hour at 1700 PDT.
    - The reductions in mobile-source heat emissions were evaluated along the major highways in the region such as I-5, HWY 99, I-80, HWY 50, etc., depending on the sub-domain being modeled. This will be discussed when presenting results from various 500-m domain simulations in this report.

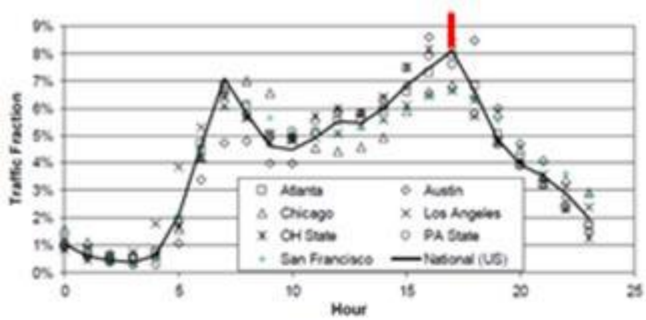

Source: Sailor and Lu (2004).

- caseSMAQMD_ZEV:
    - This is also a vehicle-electrification scenario, like cases QF2/QF3 above, except that the reductions in heat emissions were applied to and evaluated throughout the region, around the various charging stations identified in the SMAQMD's ZEV Readiness Plan (SMAQMD 2018).
    - In this modeling study, the reductions in heat emissions for this scenario were scaled using a Cressman weighting scheme that reduces electrification levels radially outward from each charging station location and further modified as a function of LULC, roadway density, and urban fraction.

- At the charging stations, the reduction in heat emissions was assumed to be 25% (maximum reduction) which was then reduced radially outward of each station following a Cressman weighting scheme. For this analysis, the scheme was applied with a 10-km radius of influence, as discussed later in this report.

- caseBB_evapo:
  - This is a vegetation-canopy scenario that increases cover and evapotranspiration, but is different from canopy-cover cases at the 2 km level (i.e., case01 through case02). Here, the increases in canopy cover were applied to areas of interest defined by the SMAQMD, LGC and project TAC, including AB617 communities, downtown areas, and DACs. This will be discussed on a domain-by-domain basis later in this report.
  - For this case, 310 large trees were added to 0.25 km^2 cells, which is equivalent to an increase of 8% of the cell area. Thus, this is roughly equivalent to or smaller than case01 in domain D04 (2 km grid) but the increase in cover is concentrated in a smaller area (there also is a more extreme test case, caseBB_evapo3, where 940 trees were added to each 500-m cell, which is equivalent to an increase of 24% of cell area, thus roughly corresponding to case02 at the 2-km scale – but this was only a test scenario).
  - Per literature, a large tree is 65 m^2 on average; a medium tree is 30 m^2; and a small tree is 10 m^2. The assumption made here is that the trees being planted are large (upon maturity), thus with a top-down view area of 65 m^2. However, compared to actual established trees, this may not be particularly large. For example, the trees in Cesar Chavez Park (between the LGC and Cal/EPA offices in Sacramento) have a top-down-view area of 120 – 150 m^2, thus twice or close to three times the size of the trees assumed in this modeling study.
  - Another exercise that can help visualize the extent of increased canopy cover in this scenario is to compare to a well-known park, say, Central Park in New York. There are about 20,000 trees in that park and the total park area is ~3.6 km^2. This yields a tree-specific site area of 180 m^2 $tree^{-1}$. Thus, for a 500-m cell, this would translate into 1390 trees. On the other hand, the scenario modeled here adds only 310 trees per 500-m cell, which is quite reasonable.

- caseAA_BBevapo_QF
  - This is a case combining cases AA, BBevapo, and QF2/QF3.
- caseAA_BBevapo_QF_CW:
  - This is a cool-walls scenario where in addition to other measures, the albedo of walls is increased to 0.40 (from an average of 0.15).

- casePV01 through PV20:
    - These are solar PV scenarios explained in detail later in this report.

Out of the total number of grid cells in each 500-m domain D05 through D10, a subset of cells is designated as urban, each with a calculated urban fraction (per LULC analysis). These cells are where the Altostratus-modified modUCM model is triggered, i.e., where the urban fraction exceeds a certain pre-determined threshold. These will be discussed in Section 5.21. Furthermore, a subset of these urban cells was designated for application of the mitigation measures defined above. These cells were defined either by technical potential or by project locations of interest to the project TAC, cities, and communities in the region.

5.20 MODELED PERIODS AT 500 m SCALE

For the community-scale modeling and analysis at 500-m resolution, the following periods are presented in this report:

2013_int3:	Representing hottest periods (daily max: 38 – 45 °C)
2016_int5:	Representing mid-range periods (daily max: 34 – 37 °C)
2015_int1:	Representing lower-end periods (daily max: 27 – 35 °C)

It is to be noted that the hotter weather, e.g., with daily maximum air temperatures in the range of 38 – 45 °C, occurs in only about 10% of the time (out of the total number of hours examined in this study), but is weighted at 33% in this analysis (one of the three periods listed above). As such the results and discussions in the following sections are skewed towards hotter weather, i.e., they represent some of the worst-case conditions of urban heat and the UHII.

5.21 URBAN-CELL TRIGGERS FOR THE 500-m MODEL

As introduced earlier in this report, the fine-scale modeling at 500-m resolution was carried out in this study using modUCM, which is an Altostratus Inc. – modified WRF urban canopy model described in Taha (2008a-c, 2017, 2018). The modified model requires additional surface-characterization parameters as discussed in Section 2.

Per this Altostratus approach, the urban model is triggered (called) at specified grid cells in each domain. These cells can be defined per modeler’s objectives and criteria – an approach that allows the triggering to occur not solely based on a cell’s LULC class, as is done in the standard WRF model (although this is one of many available options) but also based on each cell’s physical properties or combinations of properties (i.e., it often is the case that some areas are defined as urban but in fact have the same physical properties as a non-urban LULC, and vice-versa). Thus, the Altostratus approach offers a more accurate basis for calling the urban modules in modUCM to ensure more area-specific simulations. When the modUCM is called at specified grid cells, various parameters are also weighted by urban fraction and meshed with non-urban properties and parameters based on LULC and physical characteristics in each cell. Figure 5-43 shows the modUCM trigger points for each 500-m domain (D05 through D10) based on urban fraction. Appendix A-2 provides a larger version of these maps.

Figure 5-43: Urban fraction as a modUCM trigger (trigger grid cells in 500-m domains). Note the contrast in urban extents and urban fraction ranges across these domains. Also note that the figures are not to the same scale.

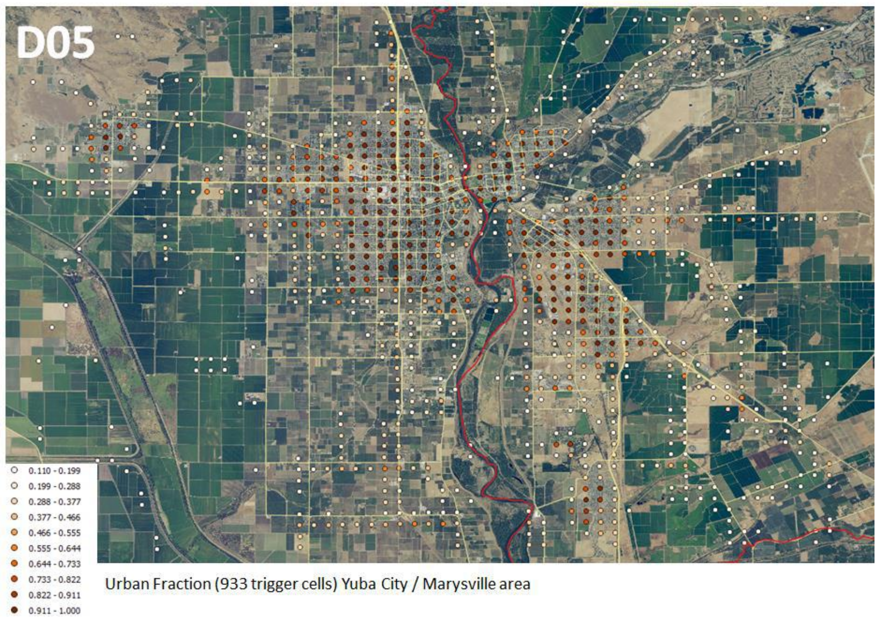

Urban Fraction (933 trigger cells) Yuba City / Marysville area

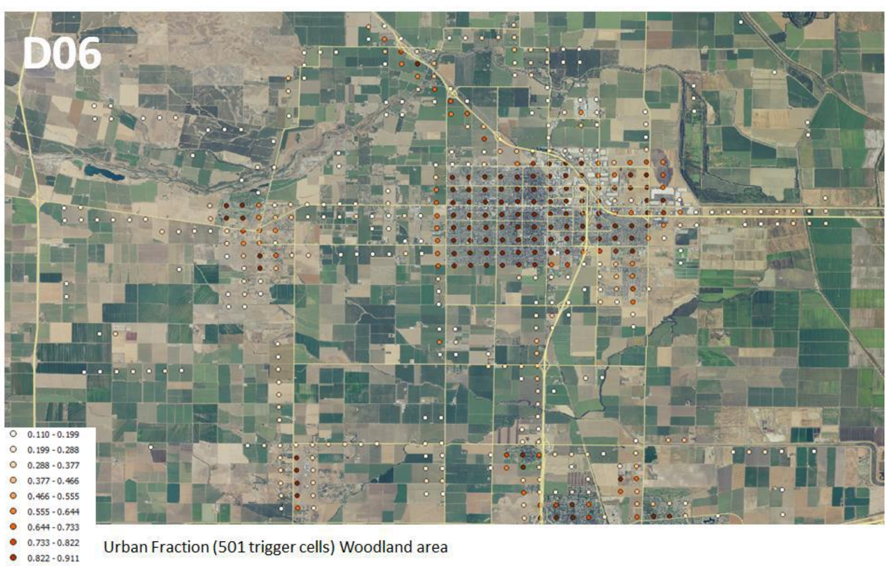

Urban Fraction (501 trigger cells) Woodland area

Figure 5-43, continued.

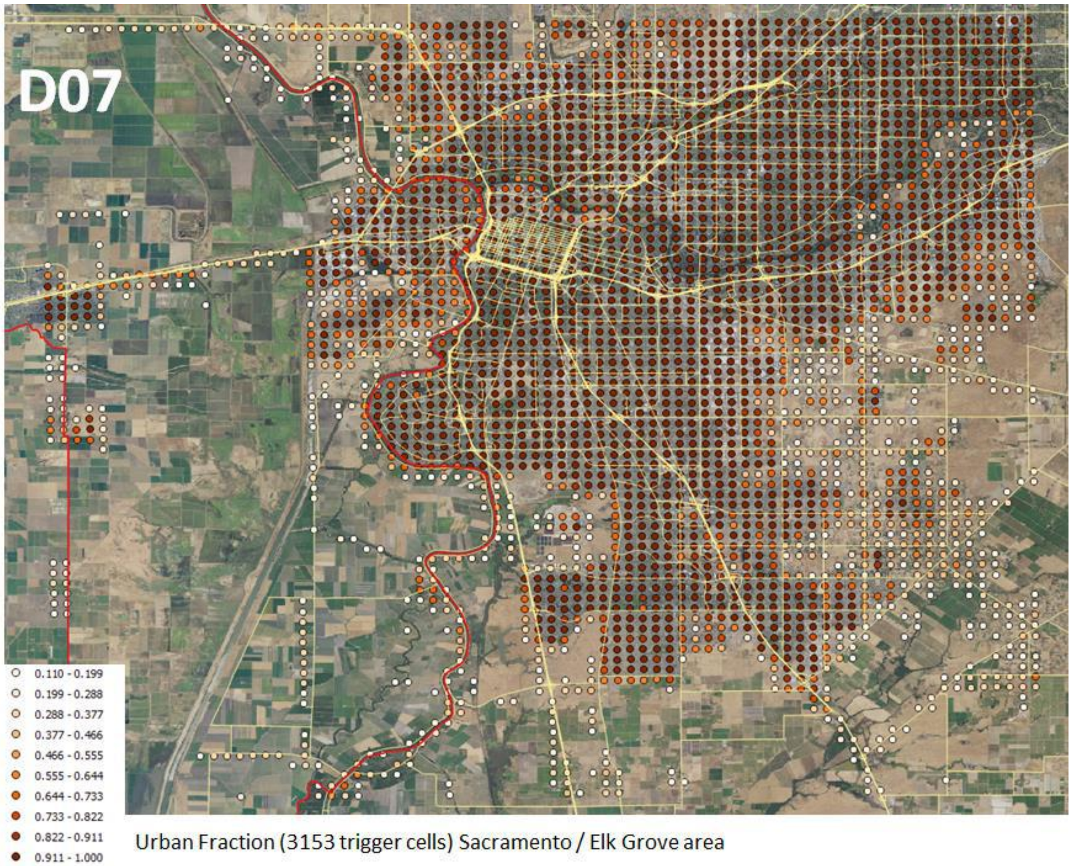

Urban Fraction (3153 trigger cells) Sacramento / Elk Grove area

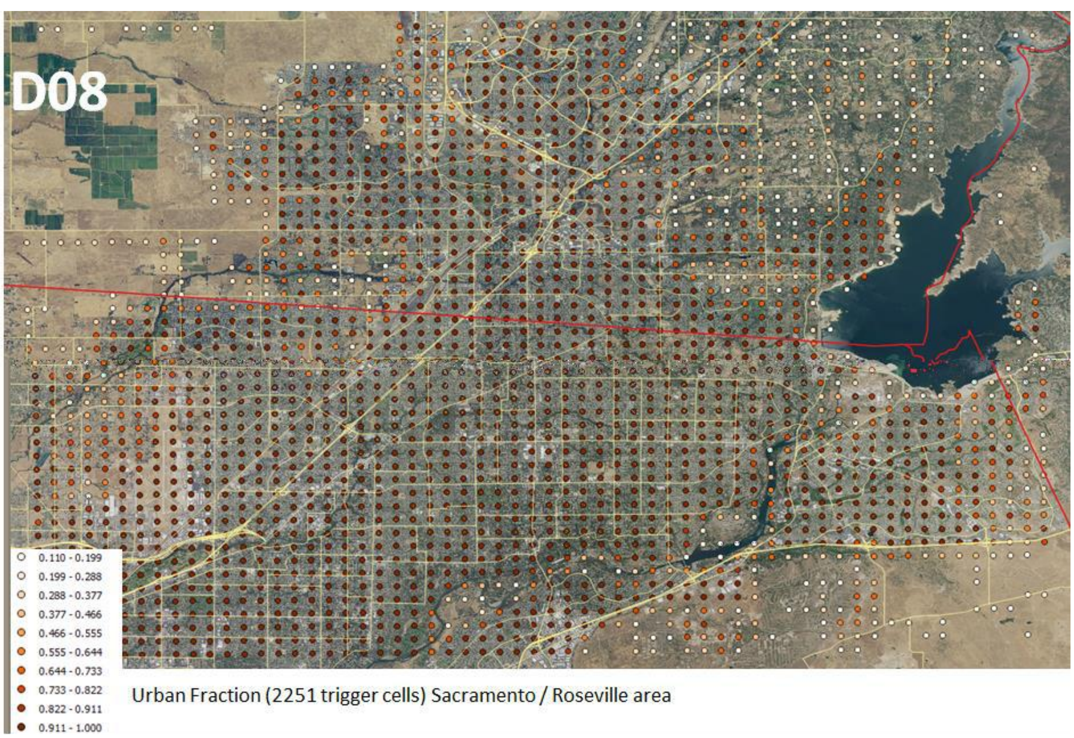

Urban Fraction (2251 trigger cells) Sacramento / Roseville area

Figure 5-43, continued.

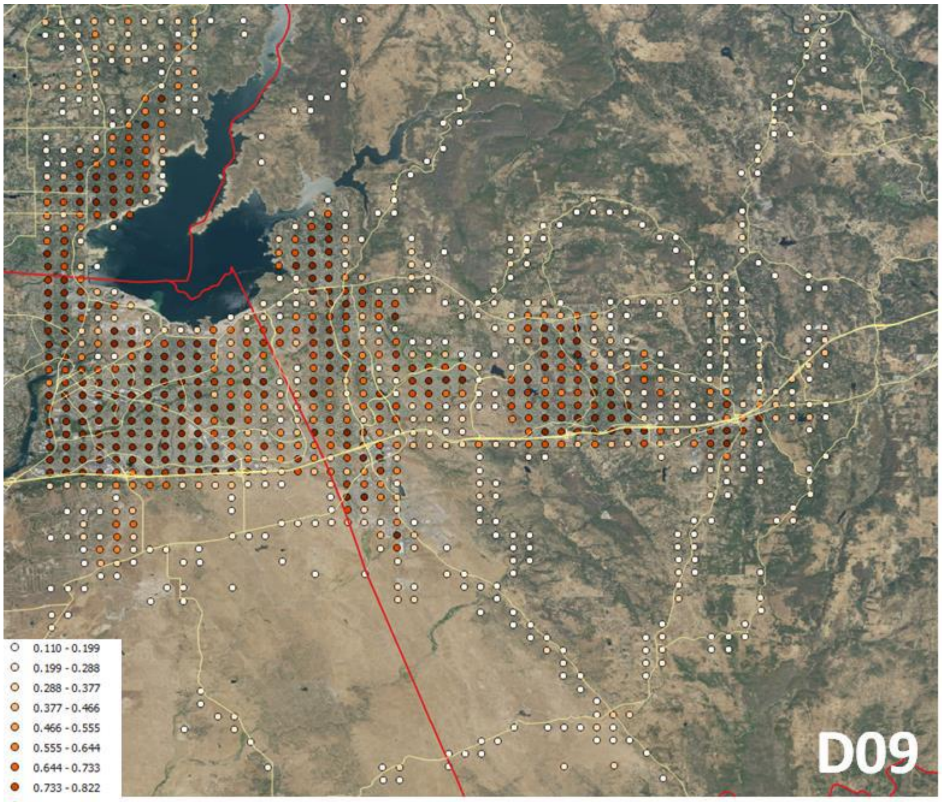

Urban Fraction (1022 trigger cells) Folsom / El Dorado Hills area

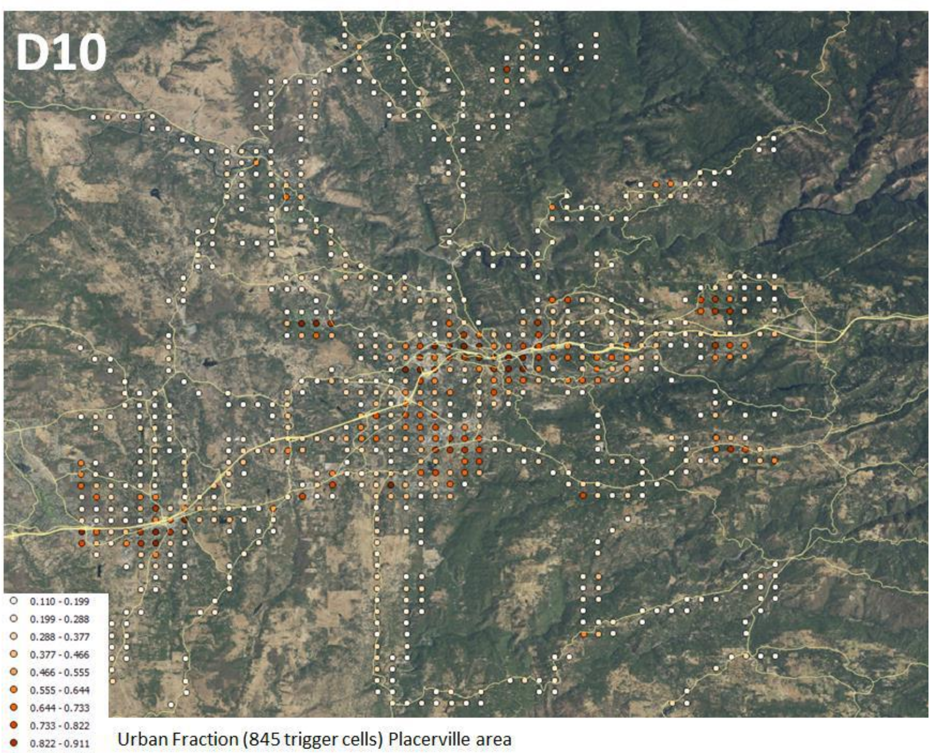

Urban Fraction (845 trigger cells) Placerville area

5.22 IMPACTS OF MITIGATION MEASURES AT THE COMMUNITY LEVEL

In this section, results from the fine-scale, community- or neighborhood-level simulations are presented. The analysis provides a quantification of effects from UHI-mitigation measures at the 500-m scale.

5.22.1 DOMAIN D05 (Yuba City / Marysville)

Figure 5-44 depicts the MTP project locations and other areas of interest that were modeled to evaluate the local-scale impacts of mitigation measures in domain D05. The yellow line defines downtown Marysville, an area of interest per project TAC, the orange lines are roadway and bridge projects identified by the City of Yuba City, and the red lines are MTP projects including point projects identified by WSP. The major highways of interest for electrification scenarios are also highlighted with bold black lines.

Figure 5-44: Locations of roadway projects and areas of interest in the Yuba City / Marysville domain.

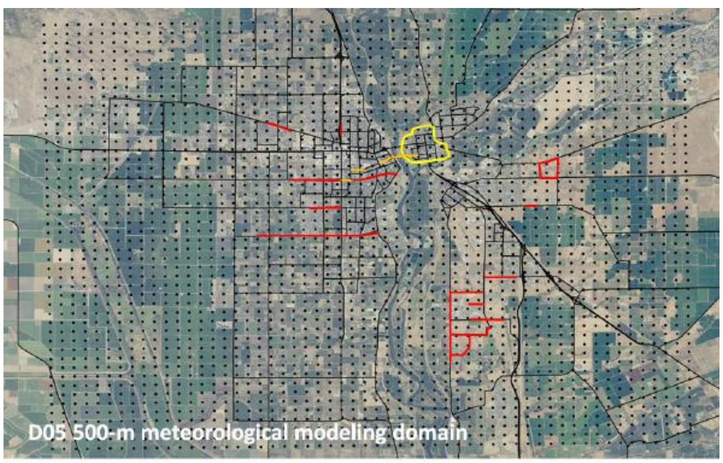

Scenario AA

Figure 5-45 depicts the urban-canopy air-temperature impacts of implementing caseAA (defined earlier) for a sample interval. In downtown Marysville, both cool roofs and pavements are implemented but in the MTP roadway project areas, only cool pavements are used. In the areas of interest (defined above), the urban canopy is cooled by up to a maximum of 4.5 °C, as an average over all 1500-PDT hours in the period August 1 – 15, 2016 (in this example). The largest cooling is seen in the downtown Marysville area and the MTP roadway projects in the southern part of the domain. These cooling effects are larger than the regional effects discussed earlier in Sections 5.10 and 5.13, as the former were averaged over 2 km whereas here, the effects are localized, at finer scales, and within the urban canopy. The roadway-temperature impacts of implementing cool pavements are shown in Figure 5-46. The average maximum cooling (i.e., averaged over all 1500-PDT hours) in the period August 1 – 15, 2016 is 11.0 °C. The spatial pattern of the affected areas is similar to that in Figure 5-45 (since the measures are implemented at the same locations) but the temperature reductions are different.

Figure 5-45: Change in urban-canopy air temperature from cool roofs and pavements in the Yuba City / Marysville area. Example: average changes at 1500 PDT, August 1 – 15, 2016. Maximum average cooling is 4.5 °C (darkest blue).

Figure 5-46: Change in roadway temperature from cool pavements in the Yuba City / Marysville area. Example: average changes at 1500 PDT, August 1 – 15, 2016. Maximum average cooling is 11.0 °C (darkest blue).

Scenario BBevapo

The air-temperature impacts of implementing vegetation canopy-cover increases in the downtown Marysville area were computed and an example is shown in Figure 5-47. The 24-hour average cooling (in the sample interval June 1 – 15, 2015) reaches up to 1.8 °C in the north-central parts of downtown.

Figure 5-47: Change in air temperature from canopy in Marysville. Example: all-hour average change in the interval June 1 – 15, 2015. Maximum average cooling is 1.8 °C (darkest blue).

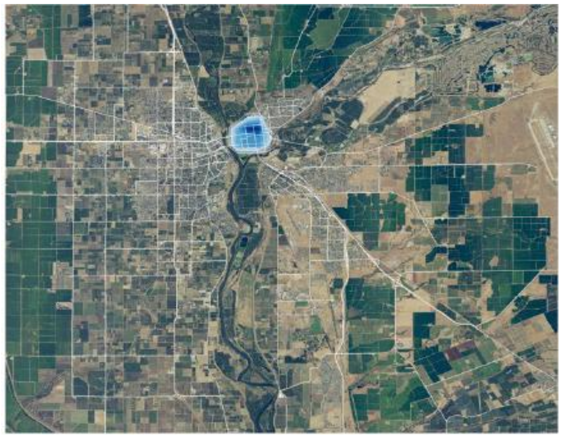

Scenario QF2

Figure 5-48 shows the near-surface temperature effects of vehicle electrification (25% EV ownership) along the major highways in the area, namely, HWY 20, HWY 99, HWY 70, and HWY 65. The 1700-PDT (rush-hour) average reduction reaches up to 1.8 °C, during the sample interval depicted in the figure (July 1 – 15, 2013). The largest cooling can be seen along highways 99 (N-S direction) and 20 (E-W direction) in Yuba City, as well as in the downtown Marysville area.

Figure 5-48: Change in near-surface temperature from vehicle electrification in the Yuba City / Marysville area. Example: 1700-PDT (rush-hour) average change in the interval July 1 – 15, 2013. Maximum average cooling is 1.8 °C (darkest blue).

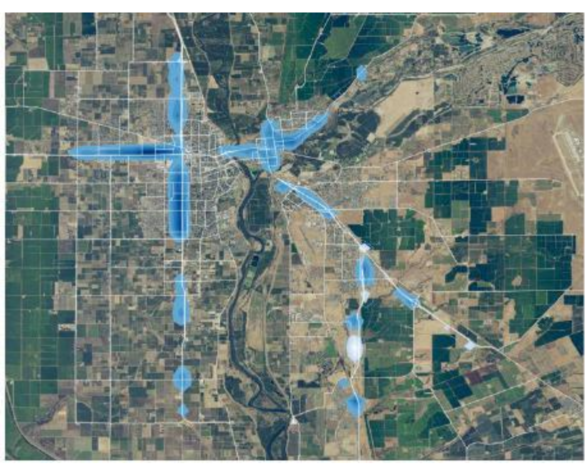

Thus, whereas the figures above provide samples of temperature impacts at selected hours during example time periods, Table 5-17 is a summary of temperature changes averaged (for various given hours or range of hours) over all modeled periods identified earlier in Section 5.20. As with the preceding analysis, the summaries in Table 5-17 are for localized effects only (no advective effects are accounted for). Later in this report, both localized and advective (transported) effects will be discussed and compared

It is important to note here (and in similar subsequent tables) that, unlike cool pavements and roofs, canopy cover affects air temperature above the canopy as well as both air temperature and surface temperature below the canopy. Similarly, for the electrification scenarios, the tail pipe exhaust occurs closer to the ground than to the upper parts of the urban canopy layer. Thus, for both canopy-cover and electrification scenarios, it is more accurate to account for (e.g., average) both air and surface temperature changes as will be shown later in the temperature summaries. However, for the purpose of Table 5-17 (and similar ones), the effects are reported separately.

Table 5-17: Changes in temperature as area-wide and time averages per given hour or range of hours (averaged over the 3 intervals defined earlier) for the Yuba City / Marysville area. In case of canopy cover and electrification scenarios, a better indicator of the effects is to average Tair and Tsfc (see text for explanation).

D05					
Marysville / Yuba City			Albedo scenario (avg. change in °C)		Canopy scenario (avg. change in °C)
0600 PDT					
	Tair	roofs and pavements	-0.24		-0.34
		roadways	-0.17		
	Tsf	roofs and pavements	-0.46		-2.23
		roadways	-0.35		
1300 PDT					
	Tair	roofs and pavements	-3.07		-0.43
		roadways	-2.09		
	Tsf	roofs and pavements	-8.28		-2.56
		roadways	-5.53		
1500 PDT					
	Tair	roofs and pavements	-2.68		-0.40
		roadways	-2.46		
	Tsf	roofs and pavements	-7.45		-2.50
		roadways	-6.33		
all hours					
	Tair	roofs and pavements	-1.38		-0.49
		roadways	-1.11		
	Tsf	roofs and pavements	-3.57		-2.87
		roadways	-2.68		

D05		
Marysville / Yuba City		Electrification scenario (avg. change in °C)
0700 PDT		
	Tair	-0.05
	Tsfc	-0.18
1700 PDT		
	Tair	-0.05
	Tsfc	-0.37
all hours		
	Tair	-0.04
	Tsfc	-0.24

5.22.2 DOMAIN D06 (Woodland)

In Figure 5-49, the yellow line highlights an area of interest (per TAC) in the northwestern part of Woodland where additional future urbanization is expected to occur. The red lines depict the MTP roadway projects including points identified by WSP. The highways of interest in electrification scenarios are highlighted with black lines.

Figure 5-49: Locations of roadway projects and areas of interest in the Woodland area.

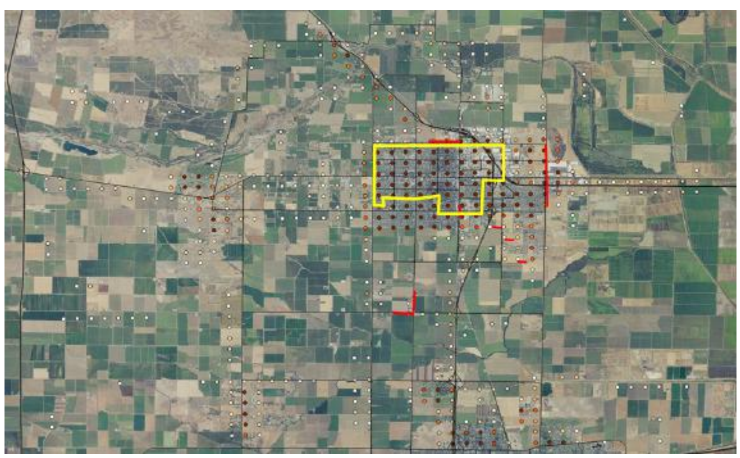

Scenario AA

Figure 5-50 shows the urban-canopy air-temperature impacts of implementing cool surfaces (as defined earlier) for a sample interval. Within the area defined by yellow boundaries (in Figure 5-49), both cool pavements and roofs are applied. In the roadway-project areas (red lines) only cool pavements are assumed to be implemented, as define earlier in Section 5-19. The urban canopy in these areas is cooled by up to a maximum of 4.5 °C, as an average over all 1500-PDT hours in the sample period August 1 – 15, 2016. The largest cooling occurs in the northern part of the city (Figure 5-50). Again, and as discussed earlier, these cooling effects are larger than the regional ones, as the latter were averaged over 2 km whereas here the effects are localized.

The roadway-temperature impacts of implementing cool pavements are shown in Figure 5-51. The average maximum cooling (averaged over all 1500-PDT hours) in the period August 1 – 15, 2016 is 10.9 °C. The larger cooling occurs in the northern parts of Woodland as well as at the locations of the roadway projects. Figures 5-50 and 5-51 show the same spatial pattern in temperature change (as the different measures are implement in similar areas) but the magnitudes of the changes differ.

Figure 5-50: Change in urban-canopy air temperature from cool roofs and pavements in Woodland. Example: average changes at 1500 PDT, August 1 – 15, 2016. Maximum average cooling is 4.5 °C (darkest blue).

Figure 5-51: Change in roadway temperature from cool pavements in Woodland. Example: average changes at 1500 PDT, August 1 – 15, 2016. Maximum average cooling is 10.9 °C (darkest blue).

Scenario BBevapo

Figure 5-52 depicts the air-temperature impacts of increasing vegetation canopy-cover in the downtown Woodland area. The 24-hour average cooling (in the sample interval June 1 – 15, 2015) reaches up to 1.4 °C in the north-eastern parts of the urban area that was defined with yellow boundaries in Figure (5-49).

Figure 5-52: Change in air temperature from canopy in Woodland. Example: all-hour average change in the interval June 1 – 15, 2015. Maximum average cooling is 1.4 °C (darkest blue).

Scenario QF3

Figure 5-53 shows the near-surface temperature effects of vehicle electrification (25% EV ownership) in the Woodland area. The effects are quantified along the major highways in the area, namely, I-5, HWY 22/16, and HWY 113. The rush-hour (1700-PDT) average reduction in temperature reaches up to 2.2 °C during the sample interval depicted in the figure (July 1 – 15, 2013). The largest cooling is seen along highways 22/16, as well as in a central section of HWY 113.

Figure 5-53: Change in near-surface temperature from vehicle electrification in the Woodland area. Example: 1700-PDT (rush-hour) average change in the interval July 1 – 15, 2013. Maximum average cooling is 2.2 °C (darkest blue).

Table 5-18 provides a summary of temperature changes averaged (for various given hours or range of hours) over the three modeled periods identified in Section 5.20. Again, the summary is for localized effects only (both the localized and advective effects will be discussed later in this report). As explained above, for canopy-cover and electrification scenarios, both air and surface temperature changes should be accounted for, but are reported separately in Table 5-18.

Table 5-18: Changes in temperature as area-wide and time averages per given hour or range of hours (averaged over the 3 intervals defined earlier) for the Woodland area. For canopy cover and electrification scenarios, a better indicator of the effects is to average both Tair and Tsfc (see text for explanation).

D06					
Woodland			Albedo scenario (avg. change in °C)		Canopy scenario (avg. change in °C)
0600 PDT					
	Tair	roofs and pavements	-0.25		-0.29
		roadways	-0.26		
	Tsf	roofs and pavements	-0.42		-1.73
		roadways	-0.46		
1300 PDT					
	Tair	roofs and pavements	-2.74		-0.23
		roadways	-3.31		
	Tsf	roofs and pavements	-6.61		-1.31
		roadways	-8.60		
1500 PDT					
	Tair	roofs and pavements	-2.51		-0.19
		roadways	-2.92		
	Tsf	roofs and pavements	-6.14		-1.70
		roadways	-7.55		
all hours					
	Tair	roofs and pavements	-1.29		-0.33
		roadways	-1.47		
	Tsf	roofs and pavements	-2.94		-2.01
		roadways	-3.66		

D06		
Woodland		Electrification scenario (avg. change in °C)
0700 PDT		
	Tair	-0.05
	Tsfc	-0.26
1700 PDT		
	Tair	-0.01
	Tsfc	-0.40
all hours		
	Tair	-0.04
	Tsfc	-0.25

5.22.3 DOMAIN D07 (Sacramento)

Figure 5-54 identifies the locations of MTP project and other areas of interest for modeling and analysis in the Sacramento area. The yellow zones are AB617 communities defined by SMAQMD that also are of interest to the project TAC and the cities in this area. The red lines are MTP projects including those identified by WSP and the major highways of interest in electrification scenarios are highlighted with bold black lines.

Figure 5-54: Locations of roadway projects and areas of interest in the Sacramento region.

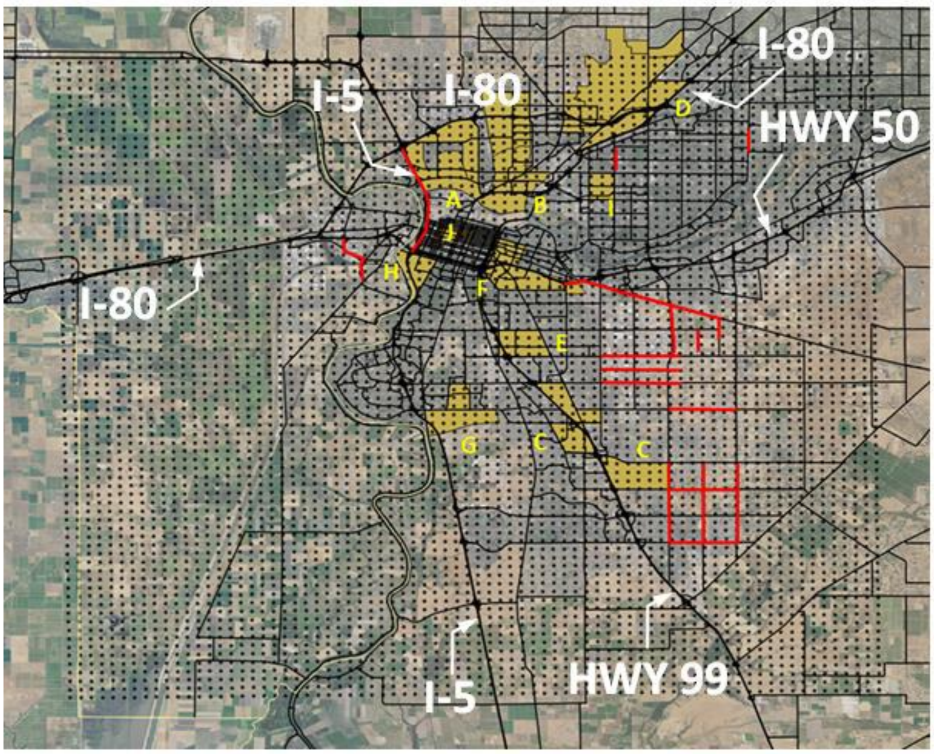

Scenario AA

In Figure 5-55, the urban-canopy air-temperature impacts of implementing caseAA (defined earlier) are shown for the sample interval August 1 – 15, 2016. It is assumed that in the AB617 communities (yellow areas in Figure 5-54), both cool roofs and cool pavements are implemented, whereas in the roadway project corridors (red lines), only cool pavement are applied. The average cooling in the urban canopy reaches up to a maximum of 5.2 °C as a result of implementing cool roofs and pavements (as an average over all 1500-PDT hours in this period). The largest cooling is seen in various parts of the AB617 communities as well as along the MTP roadway projects (Figure 5-55). Again, it should be recalled that these cooling effects are significantly larger than those at the 2 km scale because they are very localized and averaged over much smaller areas.

Figure 5-56 shows the roadway-temperature impacts of implementing cool pavements. The maximum average cooling of the roadways over all 1500-PDT hours in the period August 1 – 15, 2016 is 13.2 °C.

Figure 5-55: Change in urban-canopy air temperature from cool roofs and pavements in the Sacramento area. Example: average changes at 1500 PDT, August 1 – 15, 2016. Maximum average cooling is 5.2 °C (darkest blue).

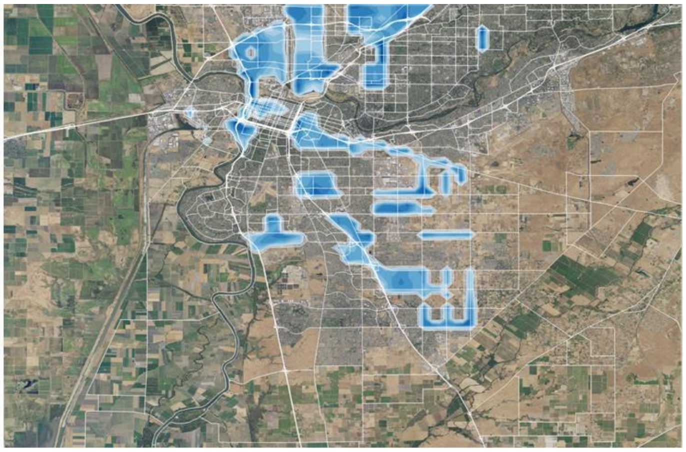

Figure 5-56: Change in roadway temperature from cool pavements in the Sacramento area. Example: average changes at 1500 PDT, August 1 – 15, 2016. Maximum average cooling is 13.2 °C (darkest blue).

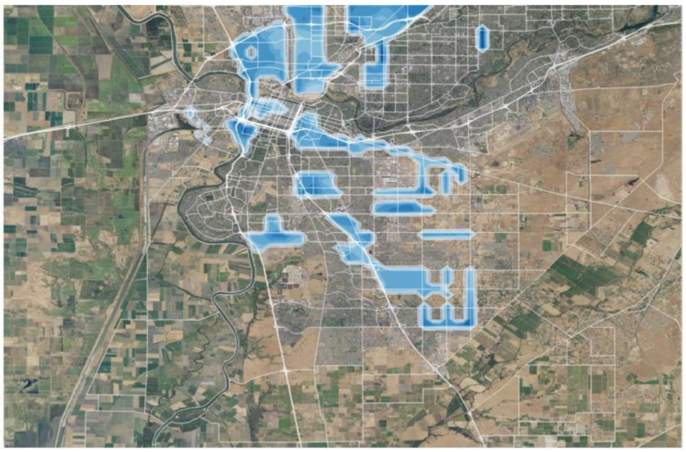

Scenario BBevapo

The increases in canopy cover were assumed to be implemented in AB627 communities "A" in the north and "C" in the south of this domain. Figure 5-57 shows the air-temperature impacts of increasing vegetation canopy-cover in these two areas. The 24-hour average cooling (during the sample interval June 1 – 15, 2015) reaches up to 1.4 °C in community "C" and is larger than the cooling attained in community "A".

Figure 5-57: Change in air temperature from canopy cover in the Sacramento area. Example: all-hour average change in the interval June 1 – 15, 2015. Maximum average cooling is 1.4 °C (darkest blue).

Scenario QF2

In terms of near-surface temperature effects from electrification (again, at the 25% level of EV ownership) in the Sacramento area, model results are shown in Figure 5-58. The effects are quantified along the major highways – I-80, HWY 50, I-5, and HWY 99. The 1700-PDT (rush-hour) average reduction in temperature reaches up to a maximum of 2.4 °C, during the sample interval depicted in the figure (July 1 – 15, 2013). The largest cooling occurs along HWY 50 and HWY 99, although all major highways do see significant cooling at different locations (see Figure 5-58).

Figure 5-58: Change in near-surface temperature from vehicle electrification in the Sacramento area. Example: 1700-PDT (rush-hour) average change in the interval July 1 – 15, 2013. Maximum average cooling is 2.4 °C (darkest blue).

Table 5-19 provides a summary of temperature changes averaged (for various given hours or range of hours) over the three modeled periods identified in Section 5.20. Again, the summaries are for localized, non-advective effects only and, as explained above, for canopy-cover and electrification scenarios, both air and surface temperature changes should be accounted for. For the purpose of this table, however, the effects are reported separately.

Table 5-19: Changes in temperature as area-wide and time averages per given hour or range of hours (averaged over the 3 intervals defined earlier) for the Sacramento area. For canopy cover and electrification scenarios, a better indicator of the effects is to average both Tair and Tsfc (see text for explanation).

D07					
Sacramento area			Albedo scenario (avg. change in °C)		Canopy scenario (avg. change in °C)
0600 PDT					
	Tair	roofs and pavements	-0.25		-0.39
		roadways	-0.24		
	Tsf	roofs and pavements	-0.44		-2.25
		roadways	-0.45		
1300 PDT					
	Tair	roofs and pavements	-2.79		-0.14
		roadways	-3.14		
	Tsf	roofs and pavements	-6.98		-1.52
		roadways	-7.90		
1500 PDT					
	Tair	roofs and pavements	-2.67		-0.21
		roadways	-2.90		
	Tsf	roofs and pavements	-6.70		-2.03
		roadways	-7.39		
all hours					
	Tair	roofs and pavements	-1.31		-0.41
		roadways	-1.45		
	Tsf	roofs and pavements	-3.08		-2.54
		roadways	-3.46		

D07		
Sacramento area		Electrification scenario (avg. change in °C)
0700 PDT		
	Tair	-0.04
	Tsfc	-0.39
1700 PDT		
	Tair	-0.11
	Tsfc	-0.69
all hours		
	Tair	-0.07
	Tsfc	-0.43

5.22.4 DOMAIN D08 (Sacramento – Roseville – Granite Bay)

For the Sacramento – Roseville – Granite Bay areas, Figure 5-59 depicts the MTP project locations and areas of interest for analysis per project TAC recommendations. The yellow area is AB617 community "D" defined by SMAQMD. The red lines are MTP projects including those identified by WSP, and the major highways of interest in electrification scenarios are highlighted with white lines. The approximate outlines of the cities of Roseville and Granite Bay also are shown in the figure (with yellow and white lines, respectively).

Figure 5-59: Locations of roadway projects and areas of interest in the Sacramento – Roseville – Granite Bay area.

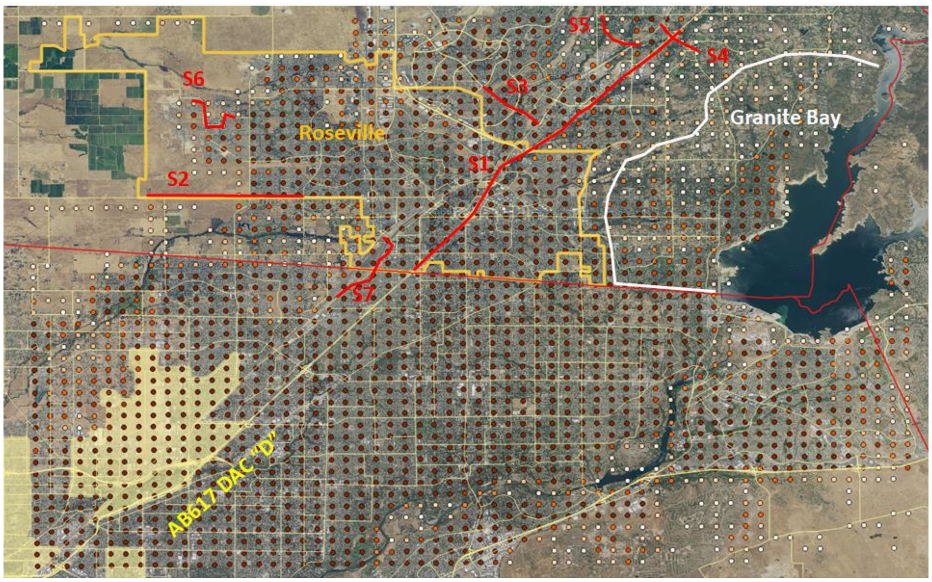

Scenario AA

In Figure 5-60, the urban-canopy air-temperature impacts of implementing caseAA (defined earlier) are shown for a sample interval. Again, it is assumed that in the AB617 community "D" (yellow area in Figure 5-59), both cool roofs and cool pavements are implemented, whereas in the roadway project areas (red lines), only cool pavement are applied. Thus, in the areas of interest, the urban canopy is cooled by up to a maximum of 4.6 °C as a result of implementing cool roofs and pavements, as an average over all 1500-PDT hours in the period August 1 – 15, 2016. The largest cooling effects are distributed throughout the modified urban area and along the major highways.

Figure 5-61 shows the roadway-temperature impacts of implementing cool pavements. The maximum averaged cooling of the roadways over all 1500-PDT hours in the period August 1 – 15, 2016 is 13.7 °C. The largest cooling, as expected, is seen relatively more along the main roadways in the area.

Figure 5-60: Change in urban-canopy air temperature from cool roofs and pavements in the Sacramento – Roseville – Granite Bay area. Example: average changes at 1500 PDT, August 1 – 15, 2016. Maximum average cooling is 4.6 °C (darkest blue).

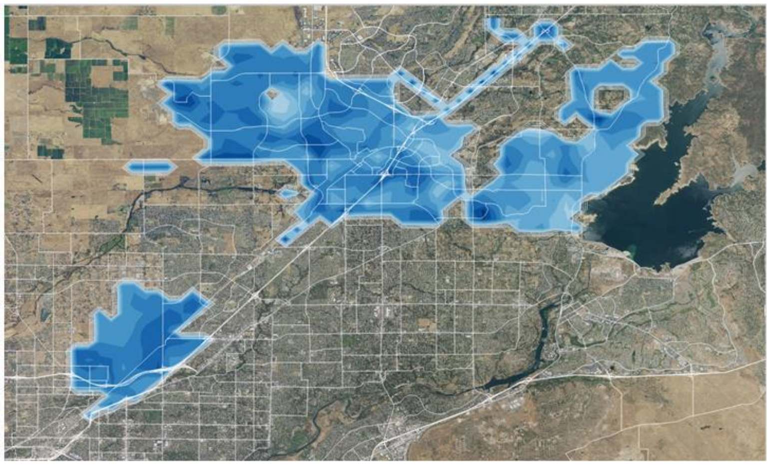

Figure 5-61: Change in roadway temperature from cool pavements in the Sacramento – Roseville – Granite Bay area. Example: average changes at 1500 PDT, August 1 – 15, 2016. Maximum average cooling is 13.7 °C (darkest blue).

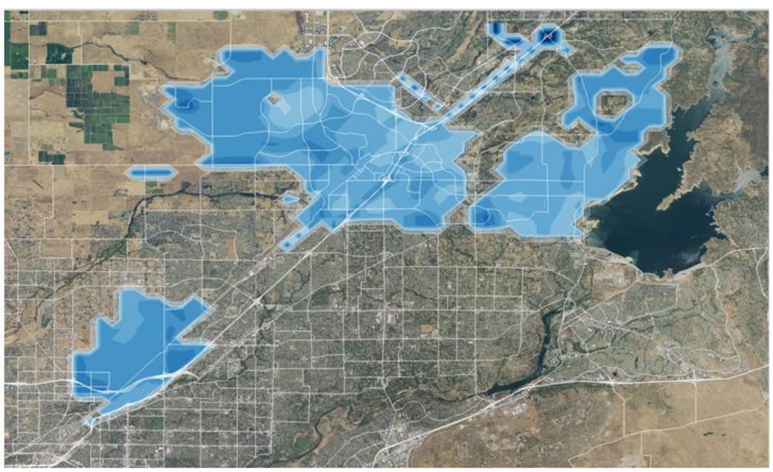

Scenario BBevapo

The scenario of increased canopy cover was assumed to be implemented in the AB617 community "D" identified by the SMAQMD. Figure 5-62 depicts the air-temperature impacts of implementing vegetation canopy-cover increases during the sample interval June 1 – 15, 2015. The 24-hour average cooling (during this interval) reaches up to 0.9 °C mostly in the eastern and north-eastern parts of this community.

Figure 5-62: Change in air temperature from canopy in Sacramento AB-617 community "D": all-hour average change in the interval June 1 – 15, 2015. Maximum average cooling is 0.9 °C (darkest blue).

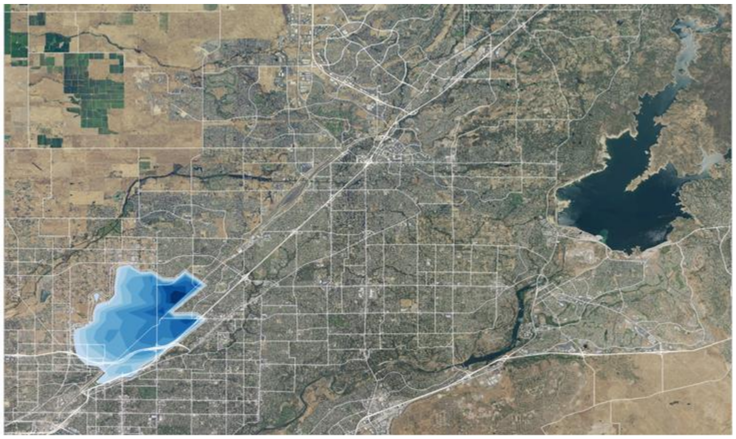

Scenario QF3

Figure 5-63 shows the near-surface temperature effects of automobile electrification (at the 25% level of EV ownership) in the Sacramento –Roseville – Granite Bay areas. The effects are quantified along the major highways in this region – I-80, HWY 65, HWY 50, and route E2. The 1700-PDT (rush-hour) average reduction in temperature reaches up to 2.3 °C, during the sample interval July 1 – 15, 2013. The largest average cooling occurs along HWY 50 and I-80.

Figure 5-63: Change in near-surface temperature from vehicle electrification in the Sacramento – Roseville – Granite Bay area. Example: 1700-PDT (rush-hour) average change in the interval July 1 – 15, 2013. Maximum average cooling is 2.3 °C (darkest blue).

Finally, Table 5-20 provides a summary of temperature changes averaged (for various given hours or range of hours) over the three modeled periods identified in Section 5.20. As before, the summaries in Table 5-20 are only for the localized, non-advective effects. It is reiterated again that for canopy-cover and electrification scenarios, both air and surface temperature changes need to be accounted for, e.g., averaged together. In Table 5-20, however, the effects are reported separately.

Table 5-20: Changes in temperature as area-wide and time averages per given hour or range of hours (averaged over the 3 intervals defined earlier) in the Sacramento – Roseville – Granite Bay areas. For canopy cover and electrification scenarios, a better indicator of the effects is to average both Tair and Tsfc (see text for explanation).

D08					
Sacramento – Roseville – Granite Bay			Albedo scenario (avg. change in °C)		Canopy scenario (avg. change in °C)
0600 PDT					
	Tair	roofs and pavements	-0.29		-0.34
		roadways	-0.36		
	Tsf	roofs and pavements	-0.49		-1.92
		roadways	-0.63		
1300 PDT					
	Tair	roofs and pavements	-3.02		-0.18
		roadways	-3.63		
	Tsf	roofs and pavements	-7.76		-1.57
		roadways	-10.04		
1500 PDT					
	Tair	roofs and pavements	-2.90		-0.22
		roadways	-3.61		
	Tsf	roofs and pavements	-7.35		-1.79
		roadways	-9.77		
all hours					
	Tair	roofs and pavements	-1.42		-0.34
		roadways	-1.72		
	Tsf	roofs and pavements	-3.43		-2.22
		roadways	-4.45		

D08		
Sacramento – Roseville – Granite Bay		Electrification scenario (avg. change in °C)
0700 PDT		
	Tair	-0.09
	Tsfc	-0.52
1700 PDT		
	Tair	-0.10
	Tsfc	-0.85
all hours		
	Tair	-0.08
	Tsfc	-0.55

5.22.5 DOMAIN D09 (Folsom – El Dorado Hills)

Figure 5-64 depicts the roadway projects and areas of interest in the Folsom – El Dorado Hills region that were modeled to evaluate the local-scale impacts of mitigation measure. As before, the red lines depict the MTP roadway projects including those identified by WSP and the approximate boundaries of the cities of Folsom and El Dorado Hills are highlighted with blue and yellow lines, respectively. The highways of interest to the electrification scenarios are also highlighted in white.

Figure 5-64: Locations of roadway projects and areas of interest in the Folsom – El Dorado Hills area.

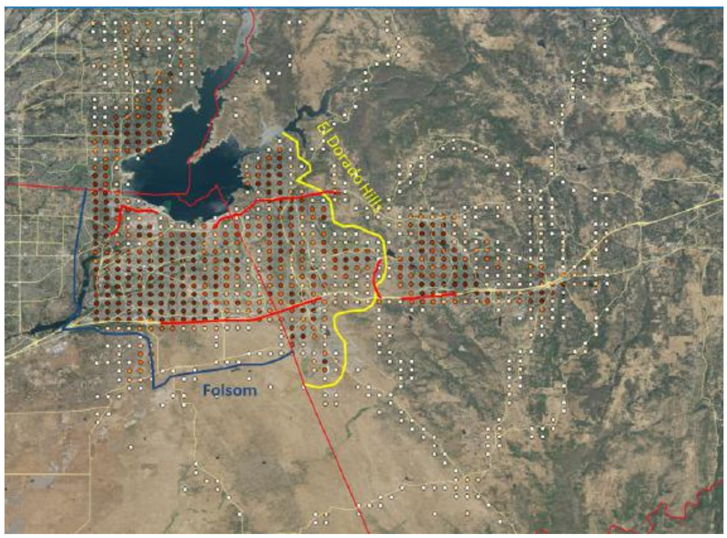

Scenario AA

In Figure 5-65 the urban-canopy air-temperature impacts of implementing caseAA (defined earlier) are shown for a sample interval. It is assumed in this scenario that both cool roofs and cool pavements are implemented throughout the urban areas whereas in the roadway project corridors (red lines), only cool pavement are applied. However, the roadway projects also occur within the urban areas that are modified and, as such, there is overlap in the reporting of effects. The urban canopy in these areas is cooled by up to a maximum of 4.9 °C as a result of implementing cool roofs and pavements, i.e., the largest average cooling over all 1500-PDT hours in the period August 1 – 15, 2016.

Figure 5-66 shows the roadway-temperature impacts of implementing cool pavements in the urban areas and at the locations of the MTP roadway projects. The average maximum cooling of the roadways over all 1500-PDT hours in the period August 1 – 15, 2016 is 12.6 °C. As expected, the largest cooling occurs in areas with higher densities of roadways (with larger modifications) as well as along major routes such as HWY 50.

Figure 5-65: Change in urban-canopy air temperature from cool roofs and pavements in the Folsom – El Dorado Hills area. Example: average changes at 1500 PDT, August 1 – 15, 2016. Maximum average cooling is 4.9 °C (darkest blue).

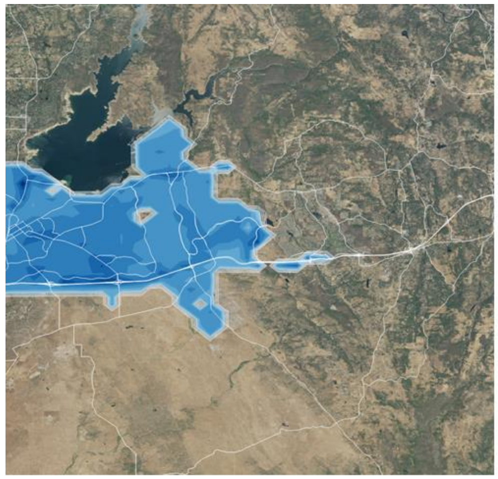

Figure 5-66: Change in roadway temperature from cool pavements in the Folsom – El Dorado Hills area. Example: average changes at 1500 PDT, August 1 – 15, 2016. Maximum average cooling is 12.6 °C (darkest blue).

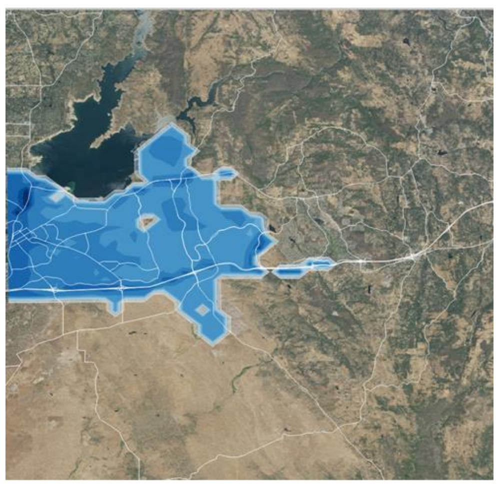

Scenario BBevapo

The scenario of increased canopy cover was assumed to be implemented throughout the Folsom and El Dorado Hills urban areas, assuming an increase in cover that is proportional to the level of urbanization in each city. Figure 5-67 shows the air-temperature impacts of implementing vegetation canopy-cover during the sample interval June 1 – 15, 2015. The 24-hour average cooling (in this interval) reaches up to 1.5 °C mostly in the eastern parts of this urban area, and is relatively larger in the more urbanized parts in south Folsom and El Dorado Hills.

Figure 5-67: Change in air temperature from canopy in the Folsom – El Dorado Hills area: all-hour average change in the interval June 1 – 15, 2015. Maximum average cooling is 1.5 °C (darkest blue).

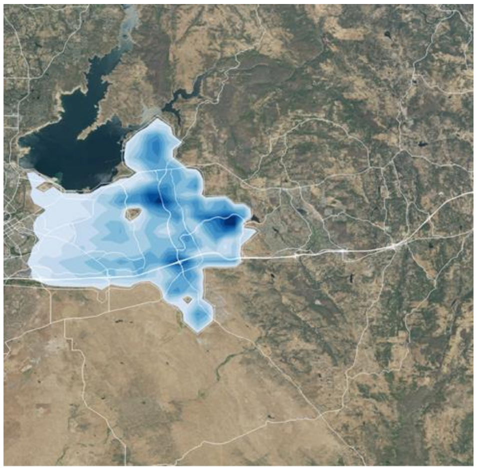

Scenario QF3

Figure 5-68 shows the near-surface temperature effects of automobile electrification (25% EV ownership) in the Folsom – El Dorado Hills area. The effects are quantified along the major highways – HWY 50 (running E-W in the figure), Folsom Blvd. (the left N-S route) and El Dorado Hills Blvd. (right N-S route in the figure). The 1700-PDT (rush-hour) average reduction in temperature reaches up to 1.8 °C, during the sample interval depicted in the figure (July 1 – 15, 2013). The largest cooling is seen along HWY 50.

Figure 5-68: Change in near-surface temperature from vehicle electrification in the Folsom – El Dorado Hills area. Example: 1700-PDT (rush-hour) average change in the interval July 1 – 15, 2013. Maximum average cooling is 1.8 °C (darkest blue).

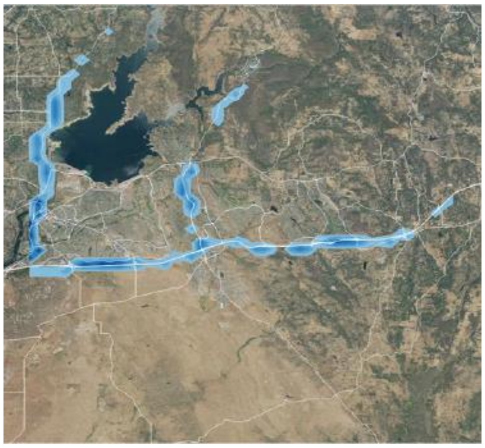

Table 5-21 provides a summary of temperature changes averaged (for various given hours or range of hours) over the three modeled periods identified in Section 5.20. While the summaries in this table are for localized effects only, the advective effects will be discussed later in this report. As explained above, for canopy-cover and electrification scenarios, both air and surface temperature should be accounted for, i.e., averaged, but are reported separately in Table 5-21.

Table 5-21: Changes in temperature as area-wide and time averages per given hour or range of hours (averaged over the 3 intervals defined earlier) in the Folsom – El Dorado Hills. For canopy cover and electrification scenarios, a better indicator of the effects is to average both Tair and Tsfc (see text for explanation).

D09					
Folsom / El Dorado Hills			Albedo scenario (avg. change in °C)		Canopy scenario (avg. change in °C)
0600 PDT					
	Tair	roofs and pavements	-0.27		-0.35
		roadways	-0.29		
	Tsf	roofs and pavements	-0.50		-1.71
		roadways	-0.54		
1300 PDT					
	Tair	roofs and pavements	-3.04		-0.21
		roadways	-3.46		
	Tsf	roofs and pavements	-8.10		-1.32
		roadways	-9.29		
1500 PDT					
	Tair	roofs and pavements	-3.15		-0.22
		roadways	-3.54		
	Tsf	roofs and pavements	-8.14		-1.52
		roadways	-9.18		
all hours					
	Tair	roofs and pavements	-1.49		-0.35
		roadways	-1.70		
	Tsf	roofs and pavements	-3.72		-1.86
		roadways	-4.30		

D09		
Folsom / El Dorado Hills		Electrification scenario (avg. change in °C)
0700 PDT		
	Tair	-0.06
	Tsfc	-0.32
1700 PDT		
	Tair	-0.08
	Tsfc	-0.53
all hours		
	Tair	-0.05
	Tsfc	-0.34

5.22.6 DOMAIN D10 (Placerville – Diamond Springs)

Finally, Figure 5-69 depicts the roadway project locations and areas of interest in the Placerville – Diamond Springs region that were modeled to evaluate the local-scale impacts of mitigation measures. As before, the red lines depict the MTP roadway projects including project point locations identified by WSP and the yellow lines delineate the urban areas of interest in (from north to south) Placerville, Diamond Springs, and El Dorado. The highways of interest to electrification scenarios are also identified.

Figure 5-69: Locations of roadway projects and areas of interest in Placerville – Diamond Springs area.

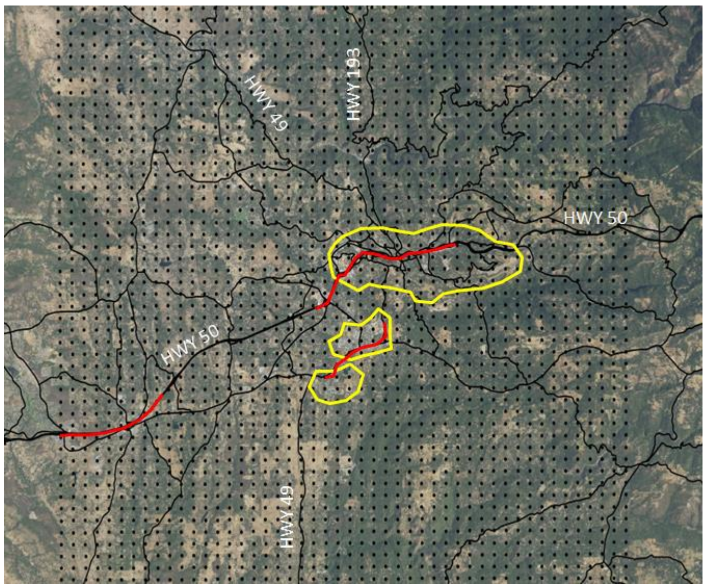

Scenario AA

In Figure 5-70 the urban-canopy air-temperature impacts of implementing caseAA (defined earlier) are shown for a sample interval. It is assumed in this scenario that both cool roofs and cool pavements are implemented throughout the above-defined urban areas whereas in the roadway project corridors (red lines), only cool pavement are applied. Since the roadway projects also occur in some of the urban areas that are modified, there is also an overlap in reporting the resulting effects. The urban canopy in these areas is cooled by up to a maximum of 4.4 °C as a result of implementing cool roofs and pavements, as an average over all 1500-PDT hours in the period August 1 – 15, 2016.

Figure 5-71 shows the roadway-temperature impacts of implementing cool pavements throughout the urban areas and at the locations of the MTP projects in the Placerville – Diamond Springs – El Dorado region. The average maximum cooling of the roadways over all 1500-PDT hours in the period August 1 – 15, 2016 is 12.4 °C. The largest cooling occurs in areas with higher densities of roadways as well as along major routes such as HWY 50.

Figure 5-70: Change in urban-canopy air temperature from cool roofs and pavements in the Placerville – Diamond Springs area. Example: average changes at 1500 PDT, August 1 – 15, 2016. Maximum average cooling is 4.4 °C (darkest blue).

Figure 5-71: Change in roadway temperature from cool pavements in the Placerville – Diamond Springs area. Example: average changes at 1500 PDT, August 1 – 15, 2016. Maximum average cooling is 12.4 °C (darkest blue).

Scenario BBevapo

The scenario of increased canopy cover was assumed to be implemented throughout the Placerville, Diamond Springs, and El Dorado urban areas delineated in Figure 5-69, assuming that the increase in cover is proportional to the level of urbanization in each area. Figure 5-72 shows the air-temperature impacts of implementing vegetation canopy-cover during the sample interval

June 1 – 15, 2015. The 24-hour average cooling (in this interval) reaches up to 1.4 °C mostly in the central parts of Placerville.

Figure 5-72: Change in air temperature from canopy in Placerville – Diamond Springs – El Dorado area: all-hour average change in interval June 1 – 15, 2015. Maximum average cooling is 1.4 °C (darkest blue).

Scenario QF2

Figure 5-73 shows the near-surface temperature effects of automobile electrification (25% EV ownership) in the Placerville – Diamond Springs – El Dorado area. The effects are shown along the major highways – HWY 50, HWY 49, and HWY 193. The 1700-PDT (rush-hour) average reduction in near-surface temperature reaches up to 2.0 °C, during the sample interval depicted in the figure (July 1 – 15, 2013). The largest average cooling is seen along HWY 50 in the Placerville area (see Figure 5-69).

Figure 5-73: Change in near-surface temperature from vehicle electrification in the Placerville – Diamond Springs – El Dorado area. Example: 1700-PDT (rush-hour) average change in the interval July 1 – 15, 2013. Maximum average cooling is 2.0 °C (darkest blue).

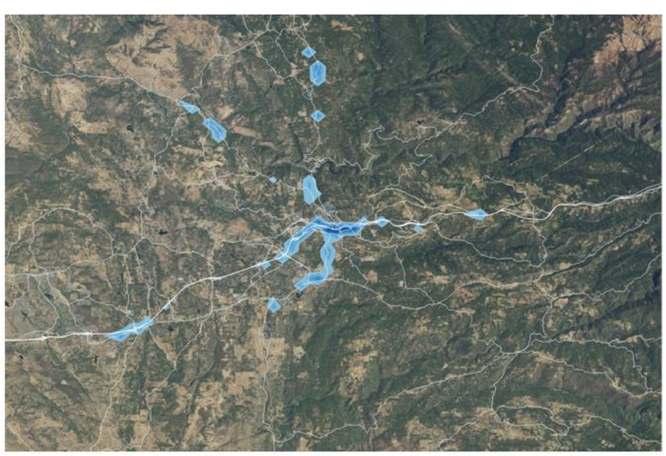

Finally, Table 5-22 provides a summary of temperature changes averaged (for various given hours or range of hours) over the three modeled periods identified in Section 5.20, above. The summaries in for localized effects only. Later in this report, the localized and advective (transported) effects will be discussed. As explained above, for canopy-cover and electrification scenarios, both air and surface temperature changes are accounted for. For the purpose of this table, the effects are reported separately.

Table 5-22: Changes in temperature as area-wide and time averages per given hour or range of hours (averaged over the 3 intervals defined earlier) in the Placerville – Diamond Springs – El Dorado area. For canopy cover and electrification scenarios, a better indicator of the effects is to average both Tair and Tsfc.

D10					
Placerville			Albedo scenario (avg. change in °C)		Canopy scenario (avg. change in °C)
0600 PDT					
	Tair	roofs and pavements	-0.23		-0.44
		roadways	-0.33		
	Tsf	roofs and pavements	-0.47		-2.19
		roadways	-0.61		
1300 PDT					
	Tair	roofs and pavements	-2.51		-0.17
		roadways	-3.23		
	Tsf	roofs and pavements	-6.93		-1.36
		roadways	-8.93		
1500 PDT					
	Tair	roofs and pavements	-2.51		-0.29
		roadways	-3.21		
	Tsf	roofs and pavements	-6.77		-1.81
		roadways	-8.61		
all hours					
	Tair	roofs and pavements	-1.21		-0.39
		roadways	-1.57		
	Tsf	roofs and pavements	-3.12		-2.12
		roadways	-4.02		

D10		
Placerville		Electrification scenario (avg. change in °C)
0700 PDT		
	Tair	-0.02
	Tsfc	-0.17
1700 PDT		
	Tair	-0.06
	Tsfc	-0.27
all hours		
	Tair	-0.02
	Tsfc	-0.15

5.23 TEMPERATURE SUMMARIES AND ATTAINMENT OF THE UHII

In this section, results from the modeling of localized cooling measures at community level (500-m scale) are summarized and compared to the local all-hours UHII computed for current climate conditions and urbanization levels. The goal here is to evaluate the effectiveness of local actions and the resulting microclimatic (e.g., temperature) changes at community scale in offsetting the area's UHII.

The local attainment of the UHII via each mitigation measures was evaluated for two situations, as shown in Table 5-23: (1) a scenario where only the community implements UHI-mitigation measures (which was presented in Section 5.22) and (2) a scenario where both the community and its neighbors implement the measures. In this second situation, the community also benefits from cooler air transported from upwind areas in addition to the local cooling resulting from the implementation of its own heat-mitigation measures. The length scale, or upwind distance of relevance to transport of cooler air, was defined as an average of 2 – 4 km per analysis in Section 5.8.

As discussed in previous sections, the attainment levels from implementing cool roofs and cool pavements were based on assessment of air temperature changes whereas attainment levels from vegetation-cover and vehicles-electrification measures were based on changes in both air and surface temperatures to more accurately capture their effects near the ground.

In Table 5-23, the all-hours UHII and the all-hours 500-m attainment of UHII were averaged over the same representative periods defined earlier in Section 5.20. The evaluations (in the table) are for each measure in standalone mode. The total effects of combinations of measures are non-linear (i.e., cannot be computed as simple sum of parts) and are typically smaller than the sum of the components (Taha 2015a,b). Still, the information in Table 5-23 can provide Caltrans and urban planners with rough information as to potential magnitudes of effects that can be anticipated if measures were combined.

From the summary table, it can readily be seen that (1) some measures, even in standalone fashion, can completely offset the UHII, with or without transport of cooler air from upwind urban areas and (2) when neighboring communities also implement UHI mitigation measures, the local benefits increase significantly (doubling, in general, but of course varying from one measure and location to another).

It is to be re-emphasized that these are localized effects, i.e., temperature changes at or near the surface of the modified roadways or he air temperature within the urban canyons of the selected communities. Hence, the cooling effects of pavements alone (in some locations) can be larger than the effects of pavements and roof albedo modifications because the levels of increase in pavement albedo for the main highways and freeways are larger than those for the local roadways in the selected communities (for the reasons stated in Section 5.6.4). In addition, there is a shading effect in the canyons that reduces the effectiveness of cool pavement measures there (Taha 2008a-c; Rosado et al. 2017). Refer, again, to the definitions of the scenarios in Section 5.19.

Table 5-23: Mitigation potential of local projects vs. regional all-hours UHII.

Project area	All-hours Tair UHII (°C)**		Localized/no advection UHII attainment local mitigation only	Localized+advection UHII attainment local mitigation+advection
D05 Yuba City / Marysville Downtown YC and M	2.41	Cool roofs / pavements	-58%	-82%
		Cool pavements	-46%	-70%
		Electric vehicles	-7%	-31%
		Vegetation cover	-71%	-95%
D06 Woodland DAC census tracts	2.14	Cool roofs / pavements	-60%	-93%
		Cool pavements	-69%	-101%
		Electric vehicles	-7%	-39%
		Vegetation cover	-51%	-84%
D07 Sac / SE Sac AB617 A, B, D	4.48	Cool roofs / pavements	-29%	-63%
		Cool pavements	-31%	-65%
		Electric vehicles	-6%	-39%
		Vegetation cover	-33%	-67%
D07 Sac / SE Sac AB617 C, E, G	2.33	Cool roofs / pavements	-56%	-93%
		Cool pavements	-60%	-97%
		Electric vehicles	-11%	-48%
		Vegetation cover	-63%	-101%
D08 Granite Bay	5.07	Cool roofs / pavements	-28%	-48%
		Cool pavements	-34%	-54%
		Electric vehicles	-6%	-27%
		Vegetation cover	-21%	-41%
D08 Roseville	5.83	Cool roofs / pavements	-24%	-52%
		Cool pavements	-30%	-57%
		Electric vehicles	-5%	-33%
		Vegetation cover	-18%	-46%
D09 El Dorado Hills	4.91	Cool roofs / pavements	-30%	-47%
		Cool pavements	-34%	-51%
		Electric vehicles	-4%	-20%
		Vegetation cover	-23%	-39%
D09 Folsom	4.86	Cool roofs / pavements	-31%	-52%
		Cool pavements	-35%	-56%
		Electric vehicles	-4%	-25%
		Vegetation cover	-23%	-44%
		Doubled cover increase	-40%	-61%
D10 Placerville / Diamond Springs / El Dorado City	1.36	Cool roofs / pavements	-88%	-113%
		Cool pavements	-118%	-143%
		Electric vehicles	-6%	-31%
		Vegetation cover	-96%	-121%

5.24 ADDITIONAL COMMUNITY-LEVEL SIMULATIONS

The following additional modeling at 500-m resolution was carried out per requests from the project TAC, SMAQMD, LGC, and participating cities and communities, in no particular order:

- Solar PV deployment and interactions with effects of cool surfaces;
- Cool walls and their incremental impacts on combined mitigation measures;
- Combinations of measures (cool roofs, cool pavements, increased canopy cover, and fleet electrification); and
- Electrification of motor vehicles per SMAQMD's ZEV Readiness Plan.

5.24.1 Impacts of vehicles electrification

This set of simulations was undertaken to evaluate the potential temperature impacts from heat-emission reductions following the SMAQMD's ZEV Readiness Plan. The locations of charging facilities (per SMAQMD) are shown as black points in Figure 5-74 superimposed over the UHII tiles in the Capital region for a random time period (in this example for July 16 – 31, 2015).

Figure 5-74: Charging/H2 stations vs. UHII composite tiles for July 16-31, 2015.

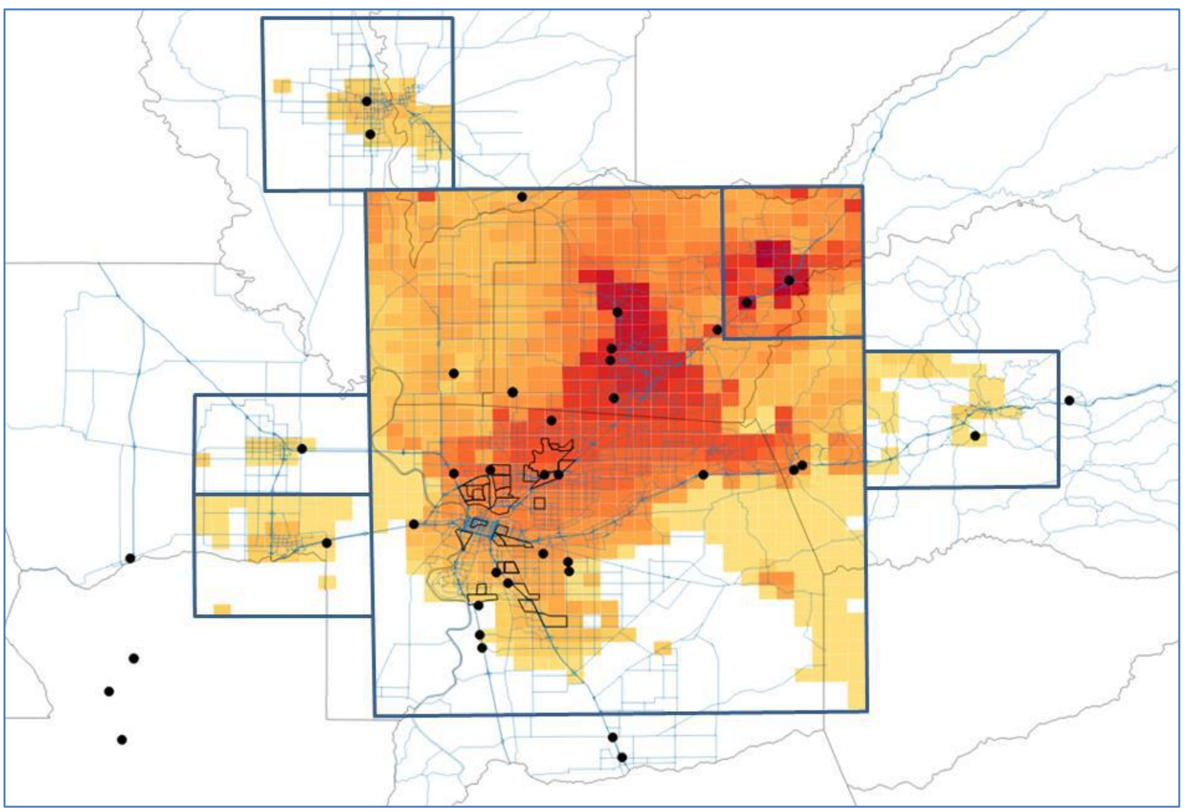

To calculate the reductions in heat emissions from this scenario, it was assumed in this study that maximum electrification would occur at and near the locations of the charging stations and decrease radially outwards following a Cressman weighting scheme:

$$W_{p,i} = \frac{R^2 - d_{p,i}^2}{R^2 + d_{p,i}^2} \qquad (5-11)$$

for $d_{p,i} \leq R$, and $W_{p,i} = 0$ for $d_{p,i} > R$.

In Eq. (5-11), $W_{p,i}$ is the weighting factor applied to heat emission rates (from mobile sources, in this case) at a model grid point, i, relative to a charging station point, p; R is a pre-determined radius of influence (e.g., 10 km); and $d_{p,i}$ is the distance from the grid point, i, to the charging station (point p). Note that heat emissions are not only weighted by this scheme, but also by land-use type, urban fraction, and the time of day relative to peak times, e.g., at 1700 PDT. The hourly profile for heat emissions was discussed in Section 5-19.

Thus, at the charging-station locations, electrification was assumed to be 25% and decreasing outwards until reaching zero at the 10 km radii of influence, as seen in Figure 5-75.

Figure 5-75: Charging/H2 stations vs. UHII composite tiles for July 16-31, 2015, and 10-km radii of influence. Source of station locations: SMAQMD / Frontier Energy ZEV Readiness Plan (2019).

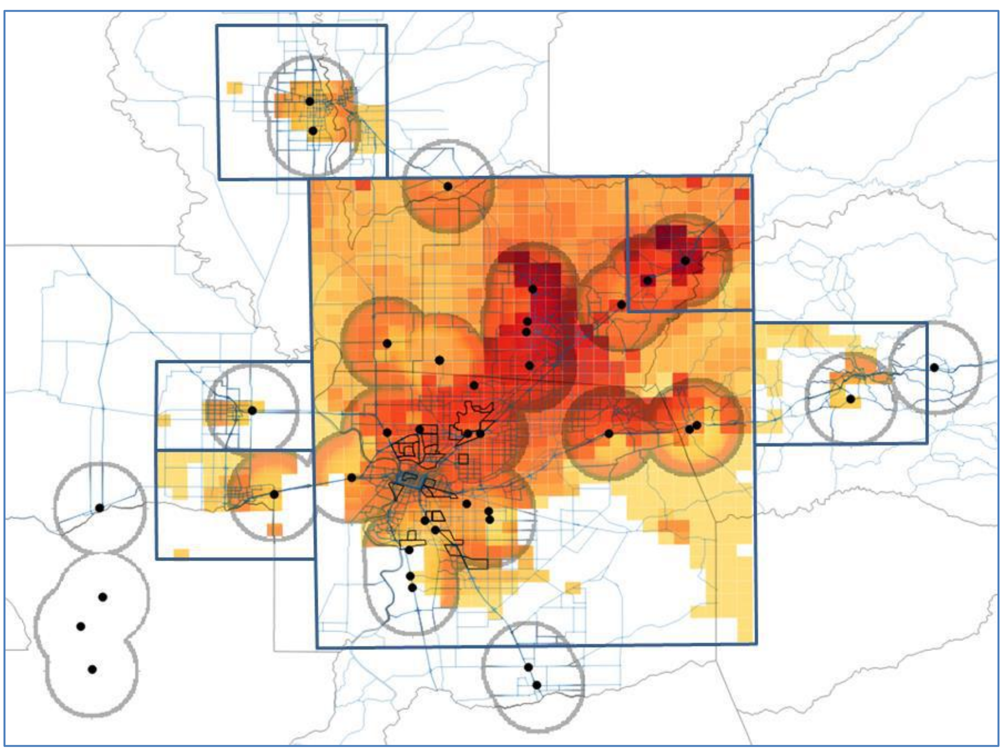

Figure 5-76: Charging stations and their locations relative to domains D07 and D08.

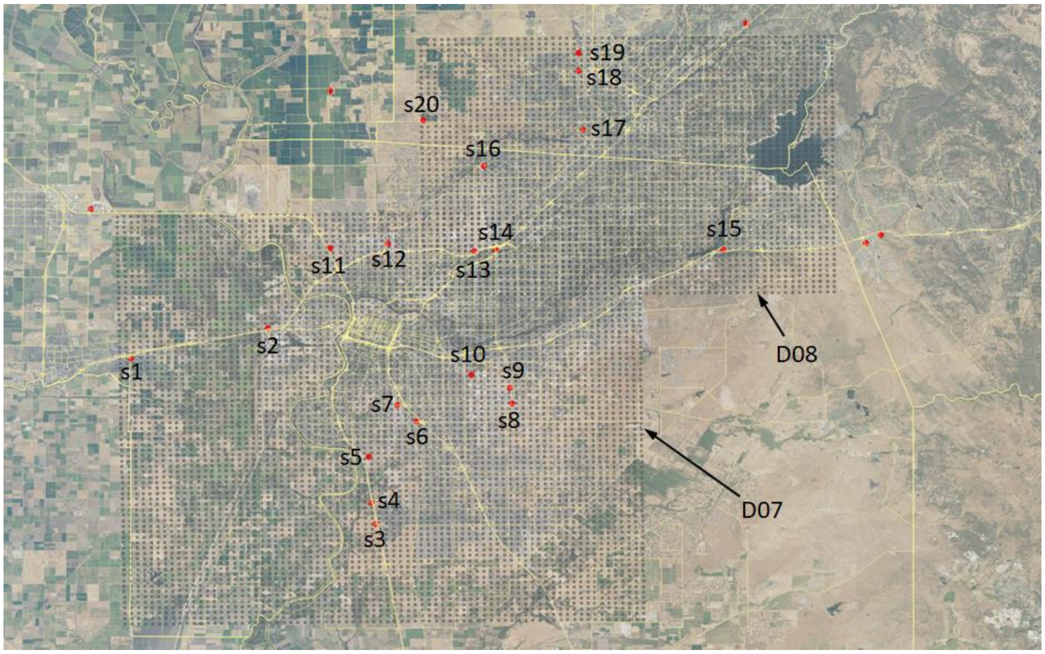

The simulations of this measure were carried out for domains D07 and D08, shown in Figure 5-76. Figure 5-77 depicts the resulting weighting ($W_{p,i}$, from Equation 5-11) for each grid cell as a function of distance from the charging stations. Thus, maximum electrification (25% EV ownership), i.e., $W_{p,i}$=1, is found at stations locations (black triangles) and zero electrification, i.e., $W_{p,i}$=0, at the perimeters of influence circles (no color).

Table 5-24 summarizes the results from this scenario (SMAQMD ZEV plan) as average reductions in 1700-PDT and all-hour temperature averages, that is, averaged over the time periods identified earlier and also averaged over all grid cells that were perturbed per given scenario. The results are presented for domains D07 and D08.

As previously discussed, surface temperature (Tsfc) may be a better indicator than Tair for the effects of tailpipe heat-emission reductions. Or, at the least, averaging both Tair and Tsfc should be done to more accurately capture those effects. However, in Table 5-24, these effects are still reported separately for Tair and Tsfc. The "average max cooling" column in the table is the average of the largest daily cooling over all days in the given period. The 1700 PDT averages columns are the averages of all 1700 PDT hours in the given period and the "all-hours" averages are averaged over every hour in the given period.

Figure 5-77: Charging stations and their locations relative to domains D07 (bottom-left) and D08 (top-right). The Cressman weight ranges from W=1 (maximum electrification) at the black triangles to W=0 (no electrification) at the yellow-white grid points.

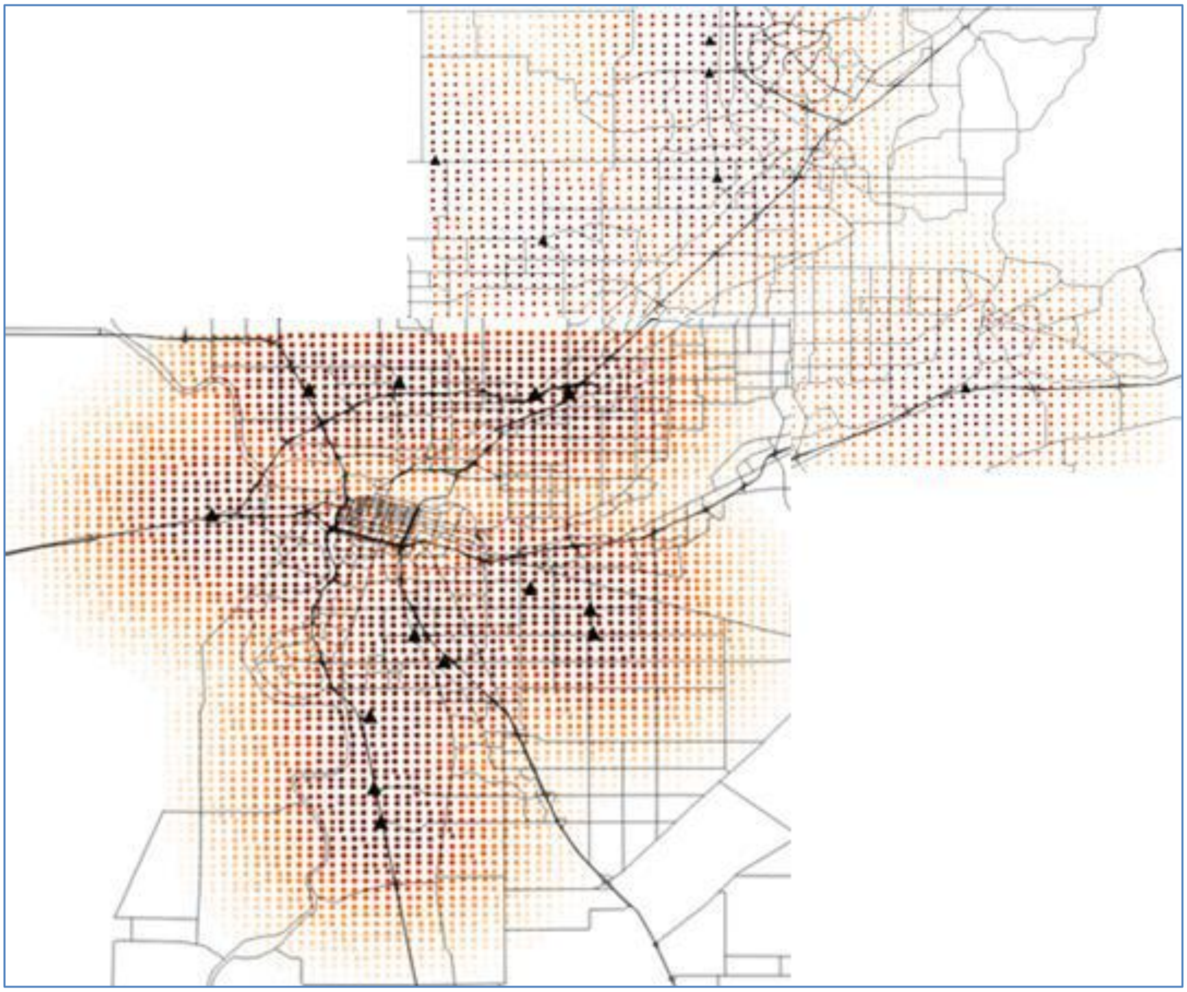

Table 5-24: SMAQMD ZEV measures impacts on temperature (changes in °C)

Domain and interval	1700 PDT			all hours		
	averages		average max. cooling (Tsfc)	averages		average max. cooling (Tsfc)
	Tair	Tsfc		Tair	Tsfc	
D07						
2013_int3	-0.32	-0.55	-2.97	-0.17	-0.28	-0.87
2015_int1	-0.20	-0.37	-2.81	-0.16	-0.27	-0.84
2016_int5	-0.24	-0.41	-3.34	-0.16	-0.27	-0.86
D08						
2013_int3	-0.27	-0.44	-1.58	-0.18	-0.29	-0.73
2015_int1	-0.25	-0.42	-2.17	-0.17	-0.27	-0.74
2016_int5	-0.26	-0.45	-1.79	-0.18	-0.30	-0.74

Figure 5-78 is a random sample showing the temperature effects from potential heat-emission reductions as a result of implementing the SMAQMD ZEV Readiness Plan in domains D07 and D08. For each domain, two examples are provided: (1) average change in Tsfc at 1700 PDT for sample periods and (2) all-hours average change in Tsfc (other intervals and averages are provided in Appendixes C-1 and C-2).

Surface temperature (Tsfc) in these examples can be reduced by up to a maximum of 2.81 ºC as a 1700-PDT average and up to 0.84 ºC as a 24-hour average in D07. In D08, the 1700-PDT average cooling reaches up to 1.58 ºC and the 24-hour average cooling up to 0.73 ºC. As stated above, the spatial temperature-reduction pattern is not only a result of the Cressman weighting scheme, but also affected by the LULC properties, urbanization density, locations of the major transportation routes, and other factors.

Note that the following figures are not to the same scale.

Figure 5-78: Samples from analysis of temperature impacts from the SMAQMD ZEV Readiness Plan. All other figures are included in Appendix C-1 and Appendix C-2. Caption below each figure provides additional information on content.

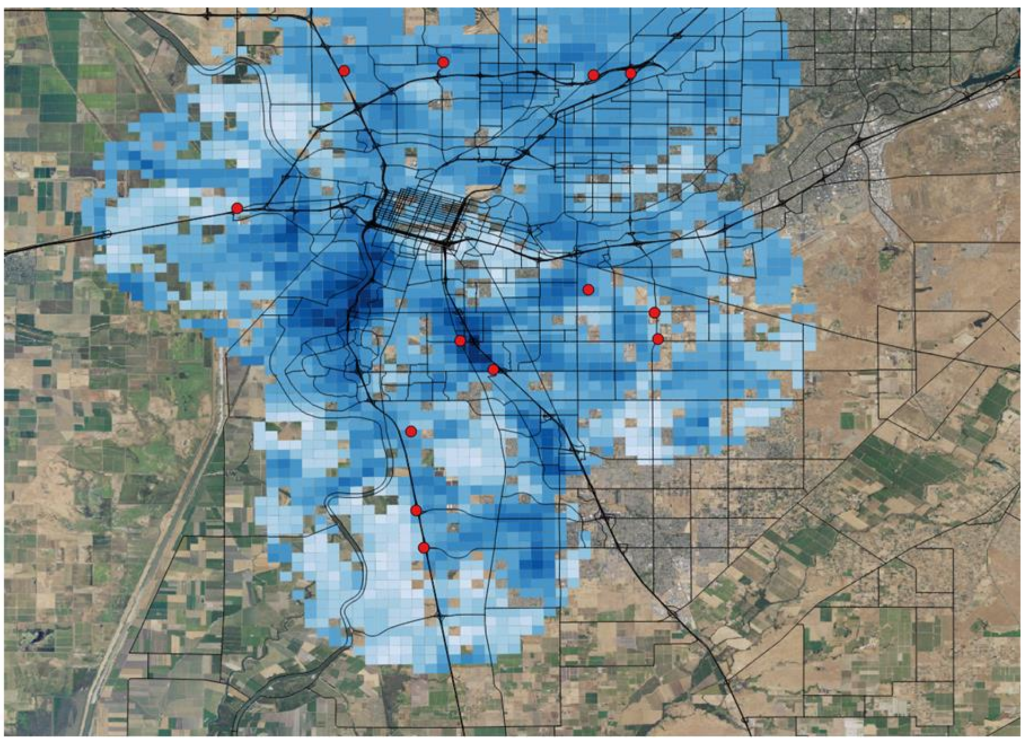

D07, average change in Tsfc at 1700 PDT, 2015_int1. Average maximum cooling: 2.81 °C (darkest blue), color step is 0.25 °C.

Figure 5-78, continued.

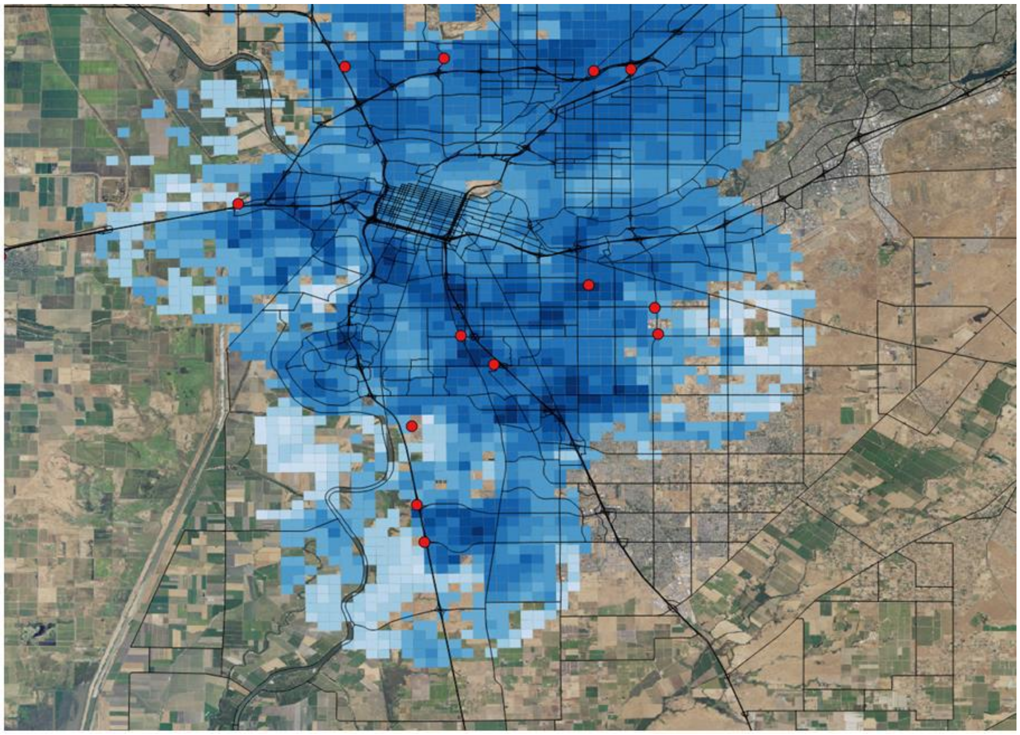

D07, all-hours average change in Tsfc, 2015_int1. Average maximum cooling: 0.84 °C (darkest blue), color step is 0.10 °C.

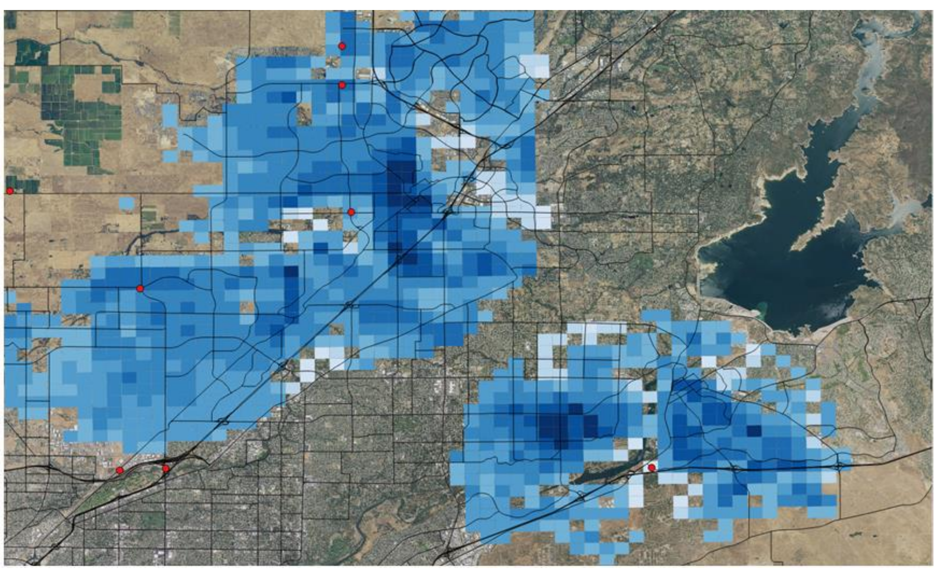

D08, average change in Tsfc at 1700 PDT, 2013_int3. Average maximum cooling: 1.58 °C (darkest blue), color step is 0.25 °C.

Figure 5-78, continued.

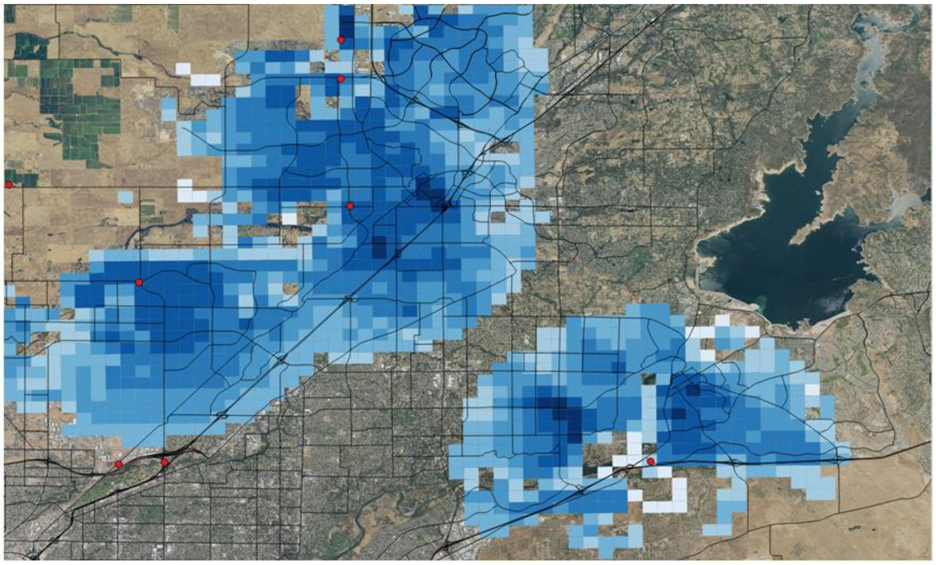

D08, all-hours average change in Tsfc, 2013_int3. Average maximum cooling: 0.73 °C (darkest blue), color step is 0.10 °C.

5.24.2 Solar photovoltaics

The City of Folsom and the SMAQMD expressed interest in evaluating the potential impacts of solar PV measures on air temperature near the ground and comparing their effects with those from tree cover on parking lots and from reflective materials. For this purpose, PV scenarios were modeled for domain D09, focusing on the City of Folsom.

Various parameters were considered in evaluating the standalone effects of ground-based (e.g., parking lots) and roof-based solar PV. While there are various approaches and levels of details involved in evaluating the effects of various solar PV configurations (e.g., Salamanca et al. 2016; Masson et al. 2014), Taha (2012) shows that, in general, the overall change in albedo after installation of a solar PV array can be estimated by:

$$\alpha_s' = \alpha_s (1-c) + (\rho + \varepsilon) c \qquad (5-12)$$

where α'_s is the new albedo of the surface *s*, e.g., roof, parking lot, wall, etc., α_s is the original albedo of the surface, in other words, the albedo of the surface upon which the solar PV is installed, *c* is the fraction of the surface *s* that is covered with the solar PV panels, ρ is the reflectivity of the solar panel, and ε is its conversion efficiency. As discussed in Taha (2012), ε typically ranges from an average of 0.15 currently to 0.30 in the near future. Thus, these two values were used as examples in the parameterizations examined here. For ρ, an average value is 0.08 and, from an evaluation of aerial imagery, *c* was found to range from 20% to 80% on residential and commercial roofs and from 50% to 100% on parking lots.

In the simulations discussed here, the current albedo (α_S) of various surfaces, e.g., roofs and pavements, were established based on the grid-cell-specific values obtained from the LULC and remote-sensed data analysis of albedo for each of the study domains (Section 2). Future values of albedo (α_S), to reflect scenarios of widespread implementation of cool roofs and cool pavements were assumed to be capped at 0.50 and 0.3, respectively. These realistic and feasible values are similar to those used in caseAA for the simulations discussed above (and defined in Section 5.19).

As there can be a large number of possible combinations of these parameters as well as their evolution over time, Table 5-25 identifies the scenarios that are discussed in this section. Table 5-26 presents a brief summary of the results followed by sample maps depicting the spatial characteristics of the temperature changes from widespread solar-PV deployment in the Folsom area.

Table 5-25: Scenarios of PV implementation.

	Surface = roof (#0)			Surface = paved / parking lot (0#)		
Scenario	roof albedo	ε	c	paved albedo	ε	c
casePV10	f(LULC) ~ 0.17 – 0.20	0.15	40%	-	-	-
casePV20	f(LULC) ~ 0.17 – 0.20	0.30	40%	-	-	-
casePV30	0.50	0.30	60%	-	-	-
casePV01	-	-	-	f(LULC) ~ 0.10 – 0.12	0.15	60%
casePV02	-	-	-	f(LULC) ~ 0.10 – 0.12	0.30	60%
casePV03	-	-	-	0.30	0.30	80%
casePV22	f(LULC) ~0.17 – 0.20	0.30	40%	f(LULC) ~ 0.10 – 0.12	0.30	60%

Table 5-26: Changes in near-surface temperatures (°C) resulting from various solar PV scenarios in the Folsom area. Note that scenarios PV03 and PV30 also include significant increases in background albedo, not just installation of solar PV.

	PV scenario							
	PV01	PV02	PV03	PV10	PV20	PV30	PV22	PV30vsAA
1500 PDT average								
Near-surface temperature	-1.17	-2.44	-4.04	-0.03	-0.08	-0.20	-2.49	+0.18
All hours average								
Near-surface temperature	-0.52	-1.18	-1.89	-0.01	-0.03	-0.09	-1.19	+0.08

As expected, the effects of solar PV on near-ground temperature are larger when the panels are implemented at ground level (ground-based) – e.g., over parking lots – than at roof level. This is because (1) rooftop modifications from solar PV occur at generally higher elevations above ground (or urban canyon) and as such, have smaller impacts on temperature in the lower parts of the urban canopy layer, (2) the albedo of roofs and effective albedo of solar panels are relatively similar and both larger than the albedo of pavements (e.g., parking lots), and (3) the effects of shading over parking lots (on near-surface temperature) are larger than the effects of shading at roof level (which is non-existent in some cases). Near the top of the canopy layer, on the other hand, both roof-based and ground-based solar PV have large effects on temperature.

With respect to current urban conditions, i.e., current typical albedo of roofs and pavements, the solar PV scenarios PV01 and PV02 (ground-based) produce average all-hours near-ground reduction (localized cooling) of 0.52 and 1.18 °C, respectively. This can reach a maximum of 1.17 and 2.44 °C, respectively, during peak hours. The larger cooling in case PV02 relative to that in case PV01 is entirely due to increased conversion efficiency (ε) and represents the range of possible cooling using today's technology in today's typical albedo ranges in urban areas.

The reductions in near-ground temperature as a result of roof-based solar PV installation (cases PV10 and PV20) are smaller, roughly up to 0.1 ºC, for the reasons listed above. Nevertheless, these numbers show that the benefits from solar PV installations (electricity) at roof level can be attained without incurring negative atmospheric effects, i.e., increasing air temperature at street level. The averaged effects of scenarios PV01 and PV10 (i.e., cooling of 0.6 ºC at 1500 PDT and 0.26 ºC as all-hours average) are generally comparable to those from other studies, e.g., Salamanca et al. (2016) and Masson (et al. (2013) for rooftop PV effects, but the ground-based PV scenarios evaluated in this study produce larger cooling (which was not evaluated in those other studies).

The study by Salamanca et al. (2016), via detailed panel-level energy-balance calculations, estimated that the cooling effects of rooftop PV can be as large as 0.2 – 0.4 ºC during the daytime. Using a relatively similar approach, Masson et al. (2014) estimated that the daytime cooling from solar PV reaches up to 0.2 ºC. However, it is reiterated here that the cooling effects discussed in this section are for ground-based PV (not rooftop) and were quantified to evaluate the impacts on near-ground temperatures so as to compare with the effects of tree canopies on parking lots.

In a scenario where both roof and ground-based solar PV are implemented, e.g., case PV22, the cooling is slightly larger than in case PV02, but by a small amount. In this scenario, reductions in 1500-PDT and all-hours near-surface temperatures of 2.49 and 1.19 °C, respectively, are predicted. In cases PV03 and PV30, the background albedo (of roofs and pavements) was also increased significantly in addition to installing solar PV – hence the resulting larger cooling effects are attributable mostly to the increase in background albedo. These scenarios represent future conditions where roof albedo, pavement albedo, and solar PV cover (ground-based and roof-based) are all increased.

Finally, case PV30vsAA demonstrates the potential negative effects of solar PV if implemented widely in the future when cool roofs and cool pavements also would have been implemented at a large scale (a hypothetical scenario, at this time). In this case, the installation of solar PV can have the potential to increase air temperature by an average of 0.08 °C (all-hours) and 0.18 °C at the time of the peak (1500 PDT) relative to if only cool roofs and pavements were installed -- although still much cooler than the base scenario.

Another aspect of interest to the City of Folsom is evaluating the relative potential cooling benefits from ground-based solar PV versus increasing tree canopy cover on parking lots. As discussed elsewhere in this report (Section 5-23), the local cooling effects (not taking advection into consideration) of canopy cover in the Folsom area are an average of 1.11 °C (23% attainment of the all-hours averaged UHII). As seen in Table 5-26, the cooling potential from ground-based solar PV (local non-advective effects) is an all-hours average of 0.52 °C at $\varepsilon = 0.15$, under current conditions. Thus, ground-based solar PV at 60% cover are one half as effective as an increase of 8 – 12% in vegetation cover over parking lots (see definitions of case01 in Section 5.5 and case_BBevapo in Section 5.18). It is to be emphasized that these results and equivalences vary significantly from one area to another.

Figure 5-79 shows sample results for a random interval (July 1 – 15, 2013) for scenarios PV01, PV02, PV03, and PV22 in terms of changes in the all-hours near-surface temperature averages in the Folsom – El Dorado Hills area (domain D09).

Figure 5-79: All-hour average near-surface temperature change from implementation of solar PV measures in the Folsom – El Dorado Hills area. Maximum cooling is in dark blue areas.

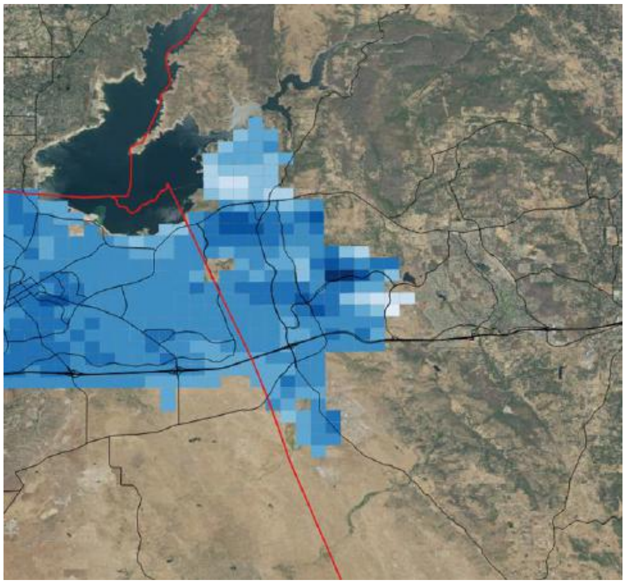

PV01: All-hours average impacts on near-surface temperature, 2013_int3. Range from white to dark blue: 0.0 to -0.90 ºC.

Figure 5-79, continued.

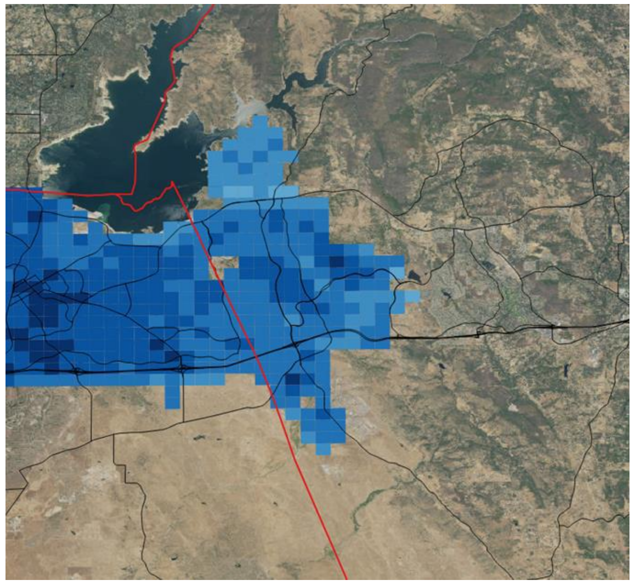

PV02: All-hours average impacts on near-surface temperature, 2013_int3. Range from white to dark blue: 0.0 to -1.6 ºC.

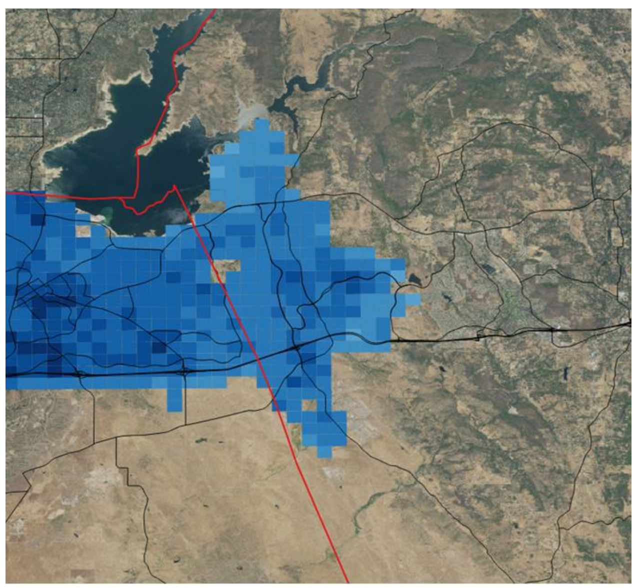

PV03: All-hours average impacts on near-surface temperature, 2013_int3. Range from white to dark blue: 0.0 to -2.6 ºC. This scenario also includes changes in background albedo.

Figure 5-79, continued.

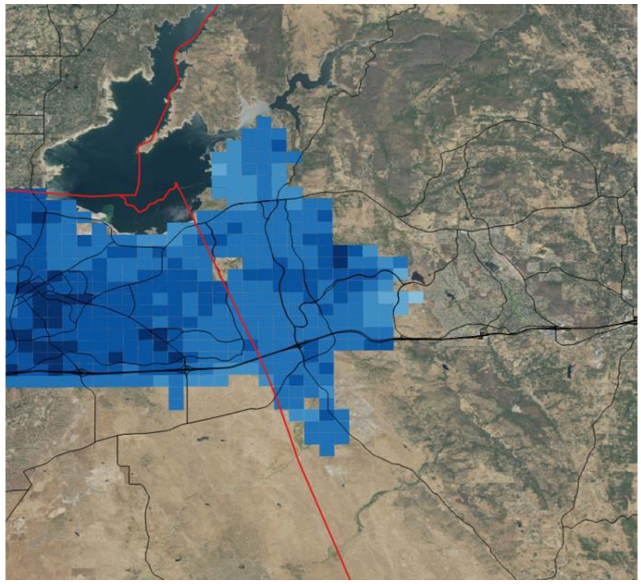

PV22: All-hours average impacts on near-surface temperature, 2013_int3. Range from white to dark blue: 0.0 to -1.64 ºC.

5.24.3 Combinations of measures

As discussed above, several mitigation measures were evaluated at the community scale (500-m resolution) in standalone mode. Combinations of measures were not presented as they would be arbitrary. However, per interest from the City of Elk Grove, an example of a combination scenario is provided (Figure 5-80).

This scenario was evaluated based on fine-scale modeling of the combined measures in domain D07, containing the City of Elk Grove. The results indicate that the combination measures provide significantly larger cooling benefits than each measure alone but, with two small exceptions, the total cooling (from combined measures) is smaller than the simple sum of the individual components (cooling from each standalone measure). In this domain, and for the modeled periods, the total cooling effects in the combination scenario are 5 – 15% smaller than the simple sum of the individual cooling effects.

Figure 5-80 summarizes some example findings and also shows the significant cooling benefits for the roadway surfaces ("Roadway temperature" column) during daytime hours, as well as for the 24 hours average. The other columns in this figure: "UCL temperature" is the air temperature within the urban canopy layer (canyon) and "surface temperature" is the average temperature of various surfaces making up the ground cover.

Figure 5-80: Temperature effects of combination of measures in D07. Vertical axis is change in temperature in degrees C.

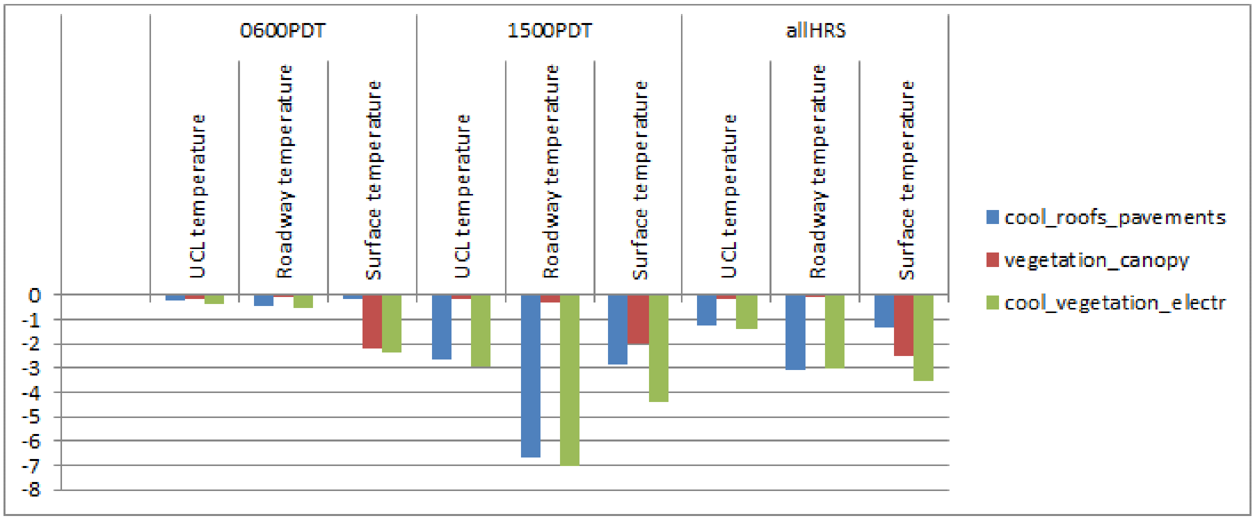

5.24.4 Cool walls

The potential impacts of cool walls were quantified for a scenario where wall albedo was increased from a current average of 0.15 to a maximum value of (capped at) 0.40. Figure 5-81 shows the cooling effects as averaged over time intervals (periods) of interest, representing various summer conditions in the City of Elk Grove. As expected, the albedo effects are largest during the daytime reaching up to a maximum average cooling of 1.4 ºC. The smaller effects in June 1 – 15, 2015, averaged 1500 PDT are caused by relatively larger cloud cover during this interval (first two weeks of June) relative to the other two intervals (which is also the reason behind the relatively lower air temperatures during that interval).

Figure 5-81: Averaged temperature effects of cool walls.

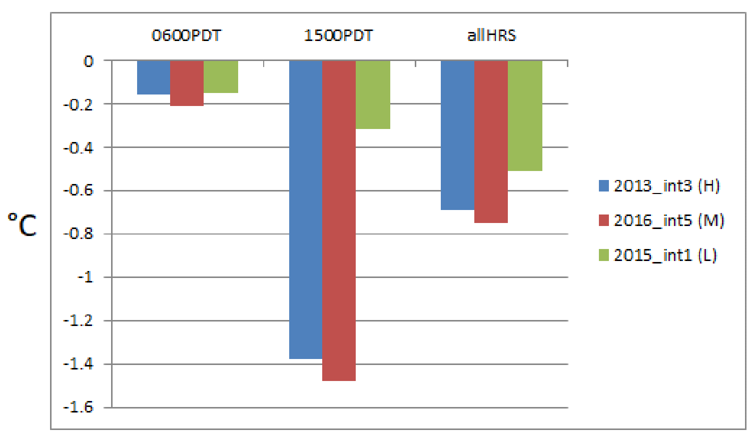

6. EFFECTS OF MITIGATION MEASURES IN FUTURE CLIMATE AND LAND USE

6.1 OBJECTIVES OF MODELING MITIGATION MEASURES IN FUTURE CLIMATE AND LAND USE

The goal of this task was to evaluate how urban heat and its indicators (e.g., UHI, UHII, and various metrics) are altered by changes in (1) climate and (2) urbanization levels. This is then followed by an evaluation of whether the proposed heat-mitigation measures would still be effective under those future conditions. For this purpose, the year 2050 was selected per input from SMAQMD, LGC, and the project TAC.

The objectives were to:

- Develop future climate scenarios via dynamical downscaling of CMIP5 / CCSM4 climate model with the Altostratus Inc.-customized urbanized WRF model and parameterizations;
- Develop future-year hourly meteorological initial and boundary conditions;
- Develop future physical urban surface properties characterizations based on LULC and urban morphology projections, future changes in the transportation system, roadways, and infrastructure (as available);
- Carry out future urban-climate simulations for year 2050 and two representative concentration pathways (RCP 4.5 and RCP 8.5);
- Characterize future climates in the 6-counties Capital region.;
- Evaluate changes in intra-urban climate variability, metrics, and thresholds under future conditions (of climate and land use) relative to present conditions; and
- Compute derivatives and metrics for heat health and the transportation system under future conditions.

6.2 EMISSIONS SCENARIOS

The representative concentration pathways (RCP, units of W m^{-2}) are indicators to the magnitudes of changes in radiative forcing. Four of the pathways, or scenarios, are defined as follows:

RCP 2.6:

This is the best scenario for limiting anthropogenic climate change, but likely unrealistic as it requires action very soon. CO_2 emissions peak by 2020 and decline to around zero by 2080. Atmospheric CO_2 peaks at 440 ppm in midcentury and then starts declining (Van Vuuren et al. 2011).

RCP 4.5:

In this scenario, emissions peak around mid-century at 50% higher than 2000 levels and then decline over 30 years to stabilize at half of 2000 levels. CO_2 concentrations rise to 520 ppm by 2070 beyond which the increase is much slower (Clarke et al. 2007).

RCP 6.0:

In this scenario, emissions double by 2060 and then decrease but stay above current levels. CO_2 concentrations increase to 620 ppm by 2100 but at a relatively slow rate (Hijioka et al. 2008).

RCP 8.5:

This is a scenario whereby emissions continue to increase. Atmospheric CO_2 concentrations reach 950 ppm by 2100 and continue increasing beyond that (Riahi et al. 2011).

In this modeling study, RCP 4.5 and RCP 8.5 were used. Output from the CCSM4 climate model (Bruyere et al. 2014) for these two scenarios was dynamically downscaled for the year 2050 using Altostratus Inc.'s modified urban models (AREAMOD and modUCM) discussed earlier in this report.

6.3 PROJECTIONS OF FUTURE URBANIZATION

In this study, the USGS LUCAS land-use projections of Sleeter et al. (2017a,b) were used to develop surface characterization input to the atmospheric model, including the development of surface physical properties in the new urban areas by 2050. The LUCAS dataset defines one business-as-usual (BAU) scenario and three other scenarios with population decrease, i.e., migration out of California. In this study, the BAU scenario was used in developing the model input for year 2050.

Figure 6-1 shows the expected urbanization levels in the Capital region by the 2050 under the BAU scenario per LUCAS. The green color-coded grid cells are current urban land use and the pink color-coded cells are new urban areas by 2050. These areas were developed in this study by vectorizing and remapping the LUCAS land-use datasets onto the model's 2-km domain. In this domain (D04), the urbanized area in 2050 is 1.68 times the urbanized area in 2015 (a 68% growth). In other words, the urban area in 2015 is 9.5% of the domain area whereas in 2050, the total urban area is 16% of the 2-km domain (dotted area in Figure 6-1).

In this project, the current land-use and land-cover distributions, including current urban cover (green areas), were derived from NLCD 2011 / 2016 datasets (MRLC 2011). This was then merged with the projected changes in urbanization from LUCAS to arrive at the 2050 urban LULC input to the atmospheric models.

The changes in land use corresponding to the BAU scenario, as defined by Sleeter et al. (2017a,b), include the following:

- Urban land cover will double by the year 2100, increasing by 182 $km^2\ yr^{-1}$ from 2001 to 2100;
- Agricultural expansion will occur at a rate of 155 $km^2\ yr^{-1}$; Agricultural contraction will occur at 127 $km^2\ yr^{-1}$; and
- Natural lands will decline by 13,842 km^2 by 2100.

Figure 6-2 is a translation of the BAU scenario (shown in Figure 6-1) into model grid-cell representations. The cells marked "1" represent current urban land use and those marked "99" represent expansion of urban land use by 2050. The number of urban cells in 2015 is 495, whereas in 2050 the number is 855 (i.e., 495+360).

Figure 6-1: Current (2015) and 2050 BAU urban land use scenario (per data from USGS LUCAS, Sleeter et al. 2017a,b and NLCD 2011).

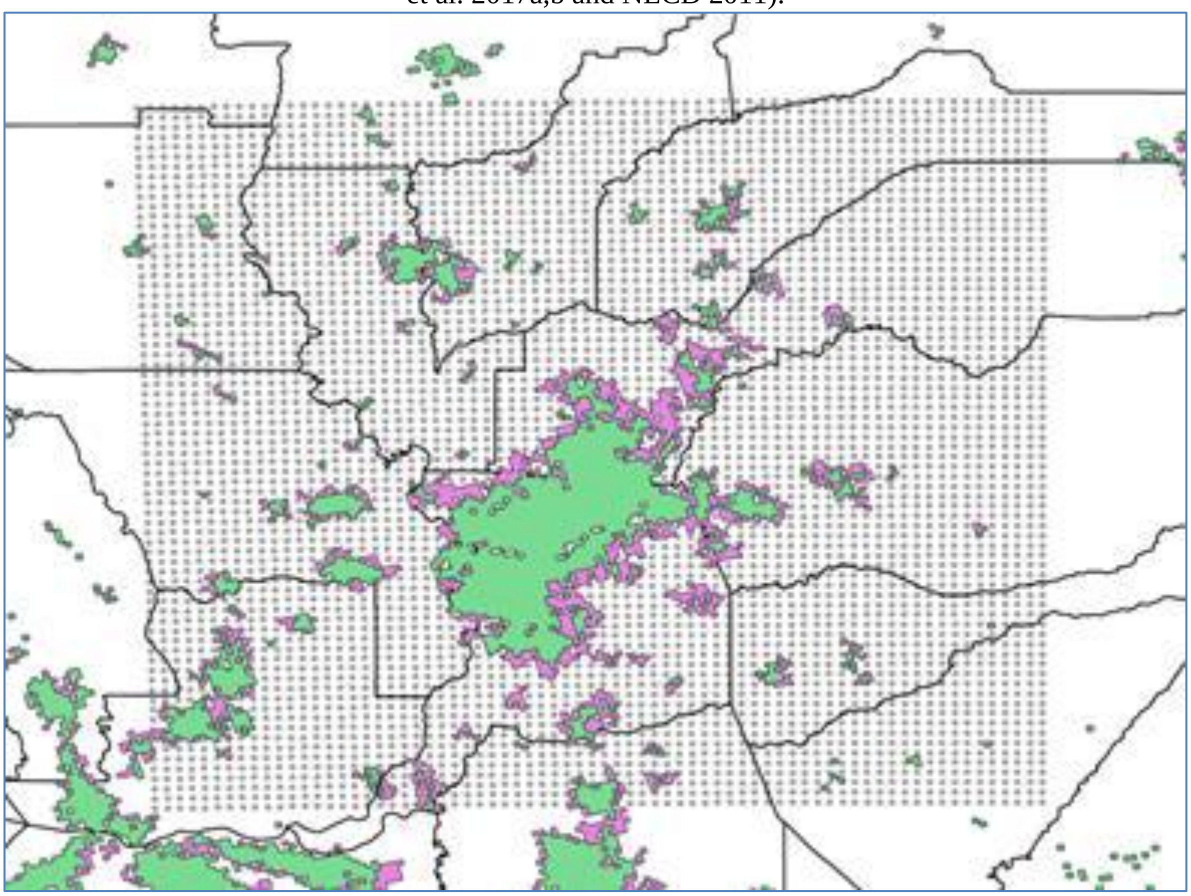

Figure 6-2: Translation of current and future urban land use into model-grid cell representations.

Having defined the new urban extent in 2050 (i.e., the pink areas in Figures 6-1 and 6-2), the next step was to develop a physical characterization for these urban areas to update the corresponding input to the land-surface and atmospheric models. Several properties were defined including (1) urban fraction, (2) various surface-cover types, vegetation, pervious / impervious cover, and (3) physical properties such as albedo, roughness length, etc., based on properties of nearby (current) urban areas. Since it is unknown what the physical and geometrical characteristics of these new urban areas would be, one way to characterize them is by extending the properties of existing nearby urban areas, i.e., near the outskirts of the current urban boundaries.

To do so, an algorithm was designed in this study to (1) "march" or "roam" through each and all new urban grid cells by 2050, (2) within a specified radius of influence, search for current urban cells and average their physical properties, then (3) project these properties onto the expanding, new urban areas (cells) based on average properties of current neighboring urban areas. In this analysis, the marching search window was assigned a radius of 6 km.

While the urban fractions and physical properties for the new urban areas by 2050 were derived based on neighboring-cells urban fractions (from 2015), the corresponding impervious fractions in 2050 were still needed in order to compute the changes in surface properties, e.g., albedo, roughness, soil moisture, etc., for developing the 2050 perturbation scenarios (mitigation measures). A first step in that direction was to evaluate whether some correlation exists (in current LULC conditions) between urban fraction and impervious fraction. If there were such correlation, then it could be used in deriving future gridded impervious fraction based on gridded urban fraction for those new urban cells by 2050.

A snapshot from this analysis is shown in Figure 6-3 where a correlation between current urban fraction and impervious fraction is evaluated.

Figure 6-3: Correlation between impervious (vertical axis) and urban fraction (horizontal axis) for current LULC (year 2015).

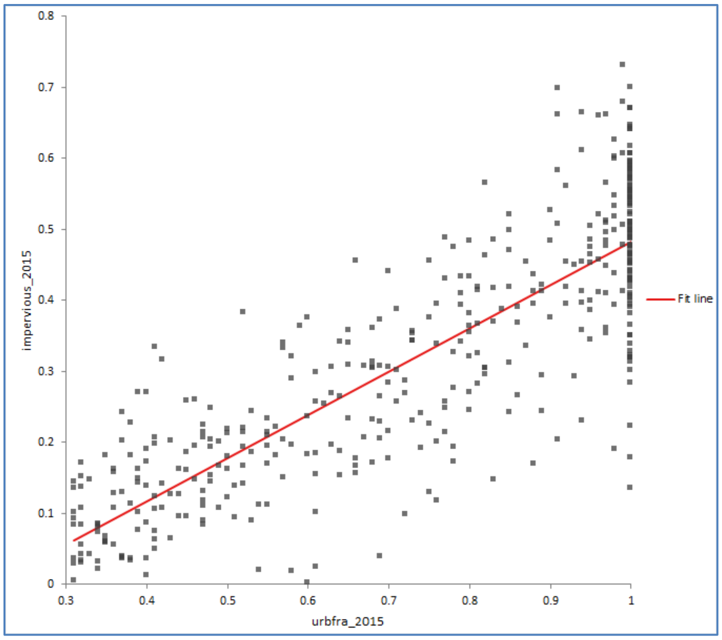

The analysis indicates that a reasonable correlation exists which can be used to estimate future impervious fraction from future urban fraction in 2050. In Figure 6-3, the correlation coefficient, R^2, is 0.7 and the P-value is <0.0001. The equation for the linear fit is:

$$I = -0.1257 + 0.6082\,U \qquad (6-1)$$

where I is the impervious fraction and U is the urban fraction as defined earlier, such as in Section 5.21 (equation 6-1 applies where $U > 0.30$). All projected thermo-physical properties were based on averages of current 2015 properties as discussed above and, where needed, weighted by urban fraction and / or impervious fraction as computed by equation 6-1.

Figures 6-4 and 6-5 show examples from characterizing the spatial distribution of changes in albedo for current (2015) and 2050 LULC (based on LUCAS), respectively. In both cases, the darkest color is the highest cell-level increase in albedo of +0.11. Contrasting the two figures also shows the larger extent of the urban area (and extent of albedo modifications) in 2050 relative to 2015.

Figure 6-4: Change in albedo for case10 in 2015

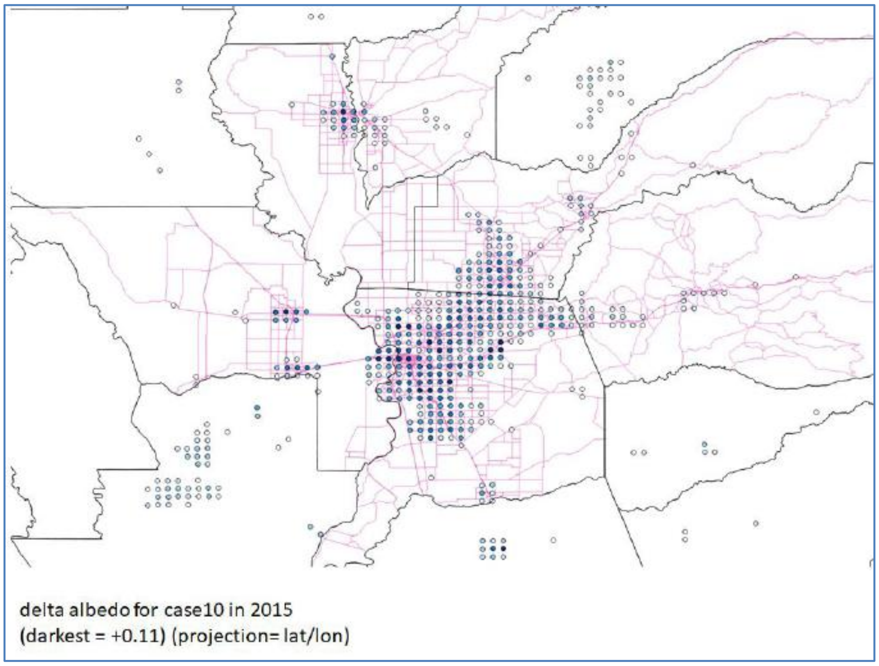

Figure 6-5: Change in albedo for case10 in 2050

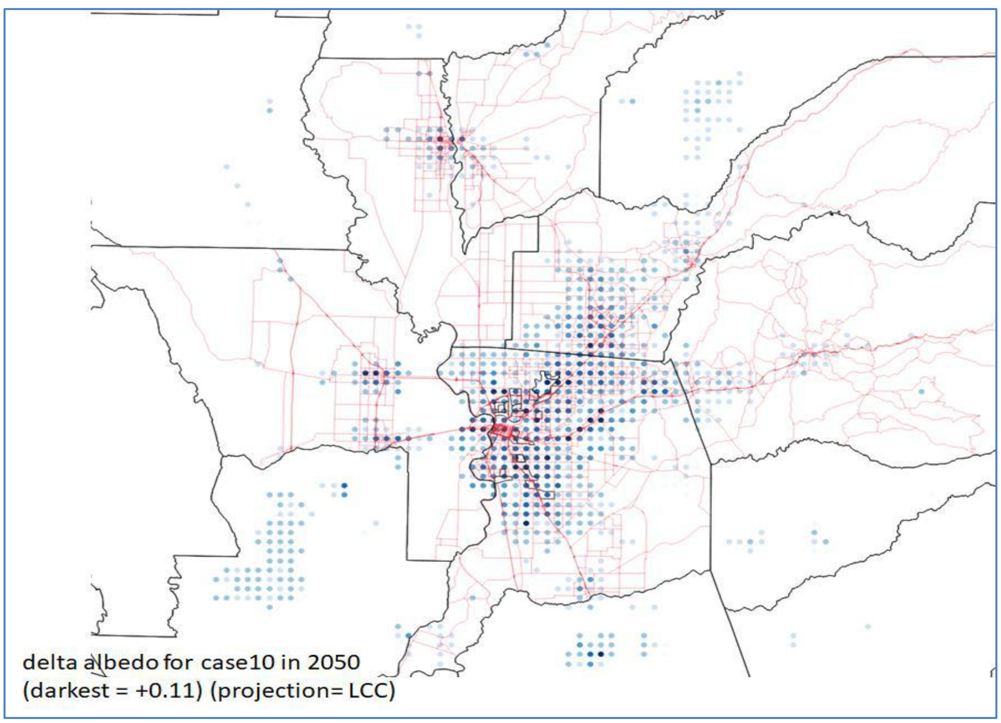

These changes in urban land-use properties were then used in the urban atmospheric model to dynamically-downscale the climate-model fields, i.e., with the Altostratus AREAMOD and modUCM approaches, and evaluate the combined impacts of climate and LULC changes on future meteorology in the study domains. The results are presented in the following sections. Here, two example snapshots are provided for the purpose of introducing this analysis.

In Figure 6-6, the temperature change (i.e., temperature equivalent DH hr^{-1} of the UHII) in 2050 RCP 8.5 at a random single hour (1600 PDT) relative to corresponding time and date in 2015 is presented. The range of change at that hour (dark green to dark red) is +1 to +5 °C. In the new urban areas (outskirts seen in pink in Figures 6-1 and 6-2), the change is up to +5 °C, which can be attributed to effects of both climate and LULC changes (urbanization), whereas the change in the existing (2015) urban areas is up to 3 °C, which is attributed to only the climate effects (since urbanization is assumed unchanged in these areas).

Thus, qualitatively at least, at this random hour, it can be said that the effects of climate are to warm the current urban areas by 3 °C whereas the effects of urbanization (changes in LULC only) are a warming of 2 °C (5 minus 3 °C). Thus this implies that (1) changes in urbanization and LULC are critical to account for and consider when developing regional land-use plans (since they have relatively similar local warming effects as the changes in climate) and (2) that UHI-mitigation measures will be critical in the future as they can locally offset the effects of climate change (e.g., in this case, 2 °C in potential cooling versus 3 °C in climate-induced urban warming).

Figure 6-6: Effects of climate and land-use changes at a random single hour. Example: Temperature equivalent, °C (DH hr^{-1}) difference between 2050 RCP 8.5 and current climate (2015) at 1600 PDT, July 27.

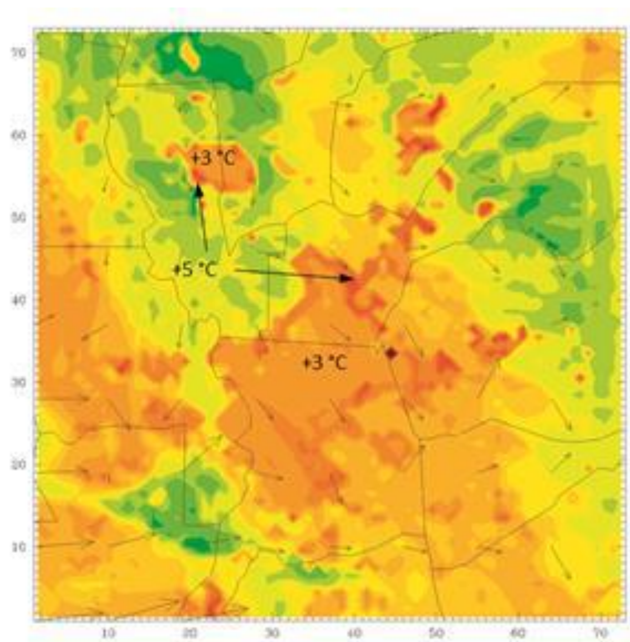

Figure 6-7: Temperature equivalent, °C (DH hr^{-1}) of the all-hours change in the UHII for all hours during the period July 16 – 31 of 2050 versus those in 2015.

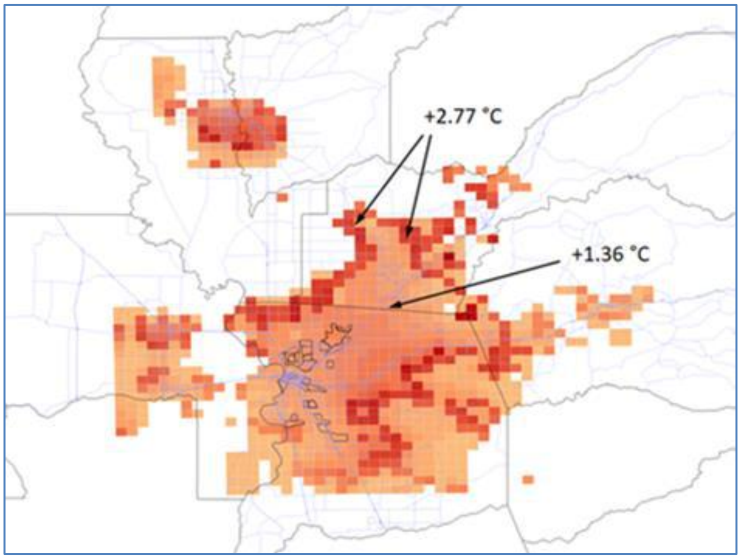

On the other hand, the examination of all intervals, not just a single hour as in the forgoing example, suggests that on the longer term, the local effects of changes in LULC and in climate on air temperature are of similar magnitudes. For example, Figure 6-7 shows the temperature equivalent (DH hr^{-1}) of the UHII change for all hours during the period July 16 – 31 of 2050 versus the same interval in 2015. In this case, the climate effect is +1.36 °C and the land-use effect is up to +1.41 °C (that is, 2.77 minus 1.36 °C), essentially of the same magnitude. Hence, the role of LULC change in warming and the role of UHI mitigation measures in cooling (under current and future climates) cannot be overstated in light of such similarities in magnitudes.

These are among a few points to bear in mind while the results are presented in more detail in the following sections.

6.4 MITIGATION MEASURES

The development of mitigation measures, e.g., increased albedo and canopy cover, among others, was discussed in Section 5.5, and needs not be repeated here. An example for increasing albedo was given above in Figure 6-5, where the darkest color represents the highest cell-level increase in albedo of +0.11. Similar patterns are seen in other mitigation measures that are proportional to technical potential. Because the urban area has expanded by 2050 (see Figures 6-1 and 6-2), there is increased technical potential as well, i.e., area available for implementation of albedo and canopy measures or, in other words, the modifiable urban area is larger. As will be discussed later in this report, this translates into larger potential cooling (because of the larger modified area) and thus provides a counterbalance to the warming effects from climate change and urbanization.

In addition to the scenarios defined in Section 5.5, this study also evaluated a scenario of smart growth whereby 15% less urbanization occurs in the future (2050) relative to the BAU scenario discussed above in Section 6.3. Figure 6-8 depicts the BAU scenario by 2050 (top) and the smart-growth scenario (bottom).

Figure 6-8: BAU (top) and smart growth (bottom) urbanization scenarios, by 2050, on the model 2-km grid (D04).

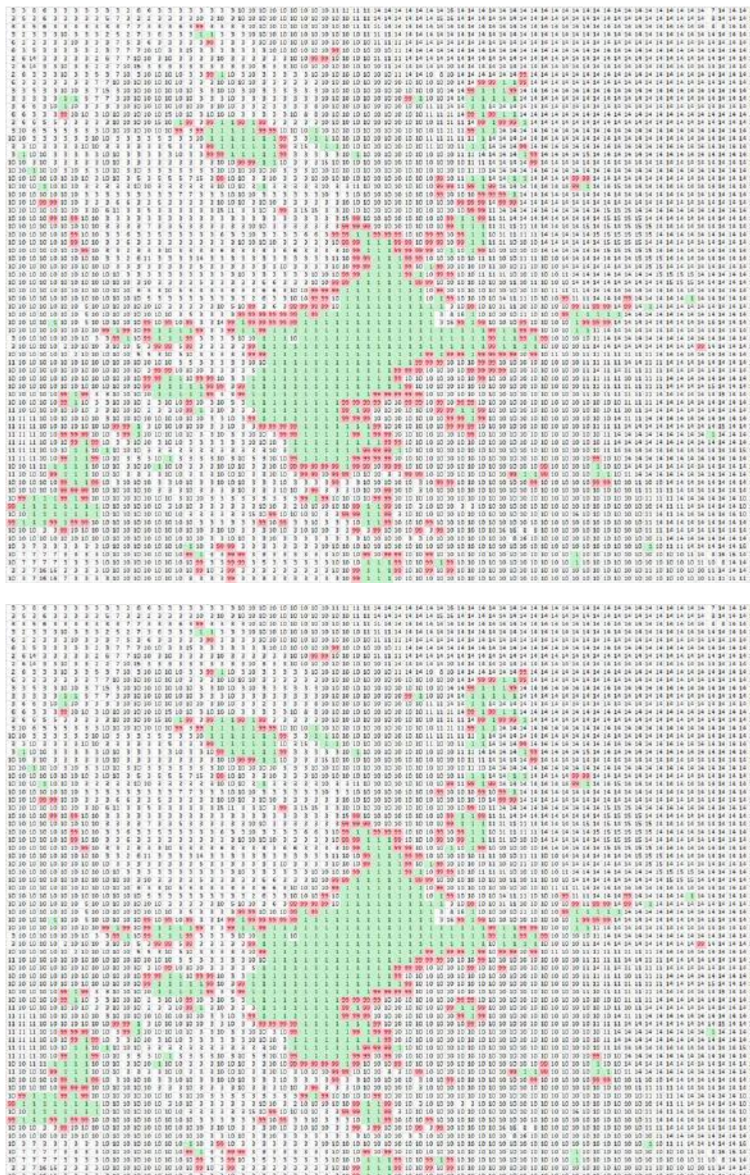

6.5 IMPACTS AND RANKING OF MITIGATION MEASURES IN FUTURE CLIMATE AND LAND USE

This discussion of the future impacts on the urban temperature field, UHI, UHII, and other metrics, largely follows the discussion of the same metrics for the current climate and land-use in Section 5-11. A such, definitions, concepts, and contexts will not be described again here.

6.5.1 Impact of mitigation measures on 0600 PDT temperature

In Figure 6-9, the average temperature reductions at 0600 PDT are presented, that is, temperature reductions averaged over all 0600 PDT hours (in each of the seven 2050 periods, int1 – int7) and over urban grid cells in each specified sub-domain. For each subdomain, two RCP scenarios are presented (RCP 4.5 and RCP 8.5, as defined in Section 6.2).

One can see from Figure 6-9 that the ranking (i.e., the order of measures' effectiveness) at this time interval is consistent and similar across all regions but that the magnitudes of reductions in temperature differ by location. This ranking (at this hour) is also exactly similar to the ranking (at 0600 PDT) in current climate.

As expected, the intra-measure differences within each area are different across the regions, i.e., how close or far apart the reductions are from different measures. Again, the caveat with case02 should be reiterated, i.e., an extreme canopy-cover increase scenario.

Figure 6-9: Average temperature reduction (°C) at 0600 PDT. Periods are identified on the horizontal axis and the ranking of measures on the right side of each graph.

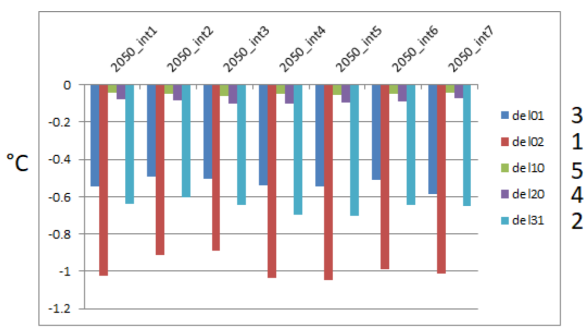

Auburn 2050 RCP 4.5

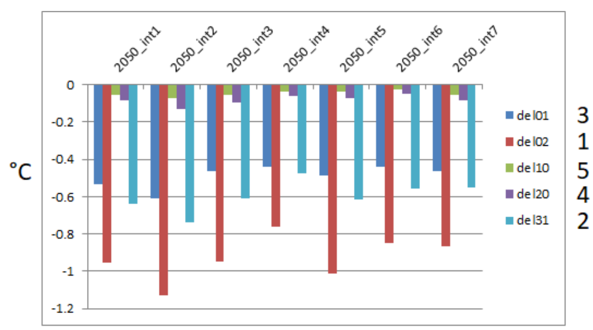

Auburn 2050 RCP 8.5

Figure 6-9, continued.

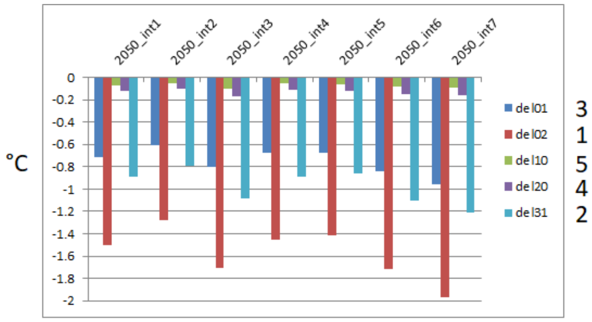

Davis 2050 RCP 4.5

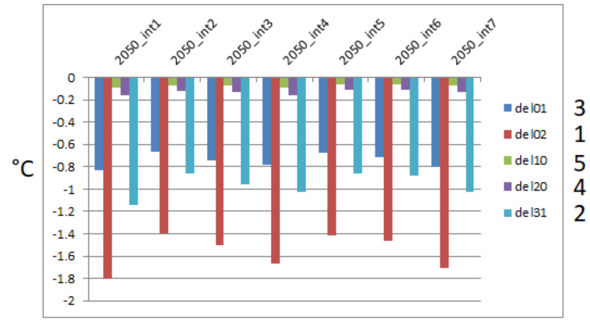

Davis 2050 RCP 8.5

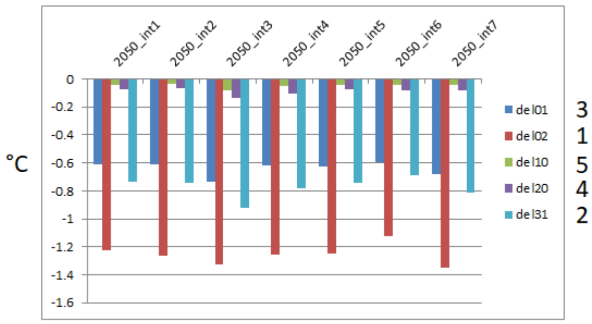

El Dorado Hills 2050 RCP 4.5

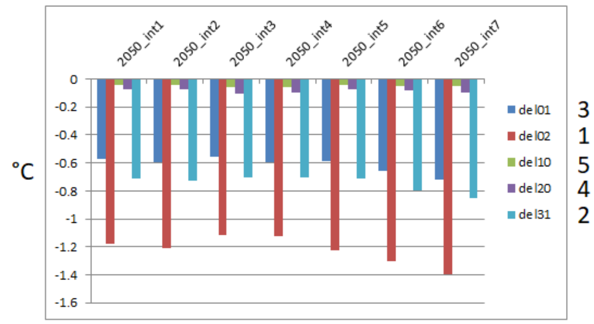

El Dorado Hills 2050 RCP 8.5

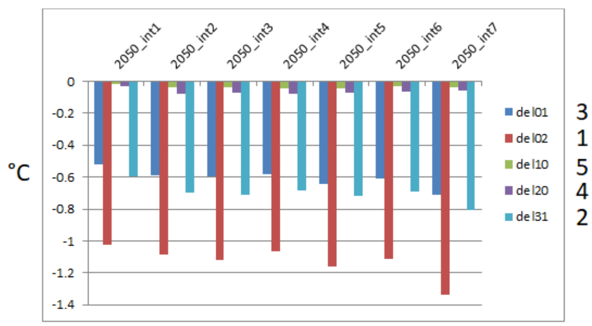

Placerville 2050 RCP 4.5

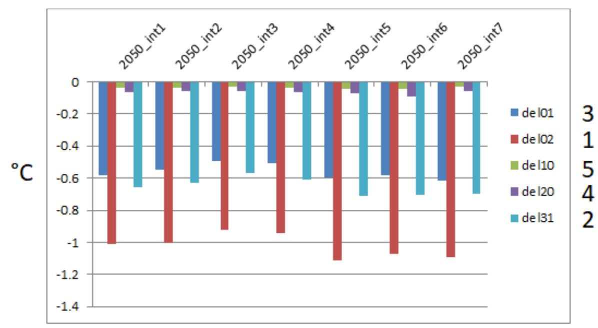

Placerville 2050 RCP 8.5

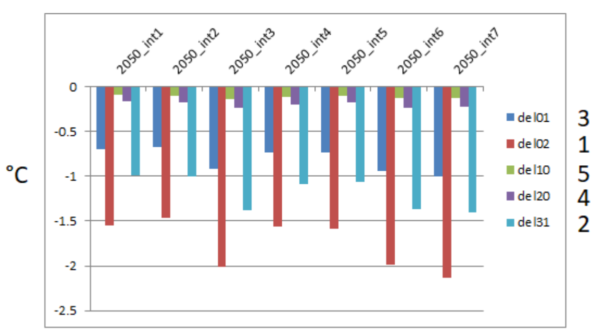

Sacramento 2050 RCP 4.5

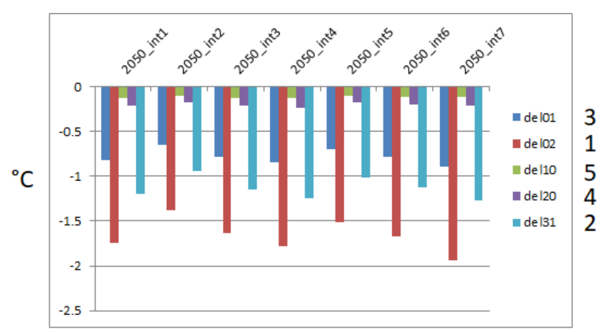

Sacramento 2050 RCP 8.5

Figure 6-9, continued.

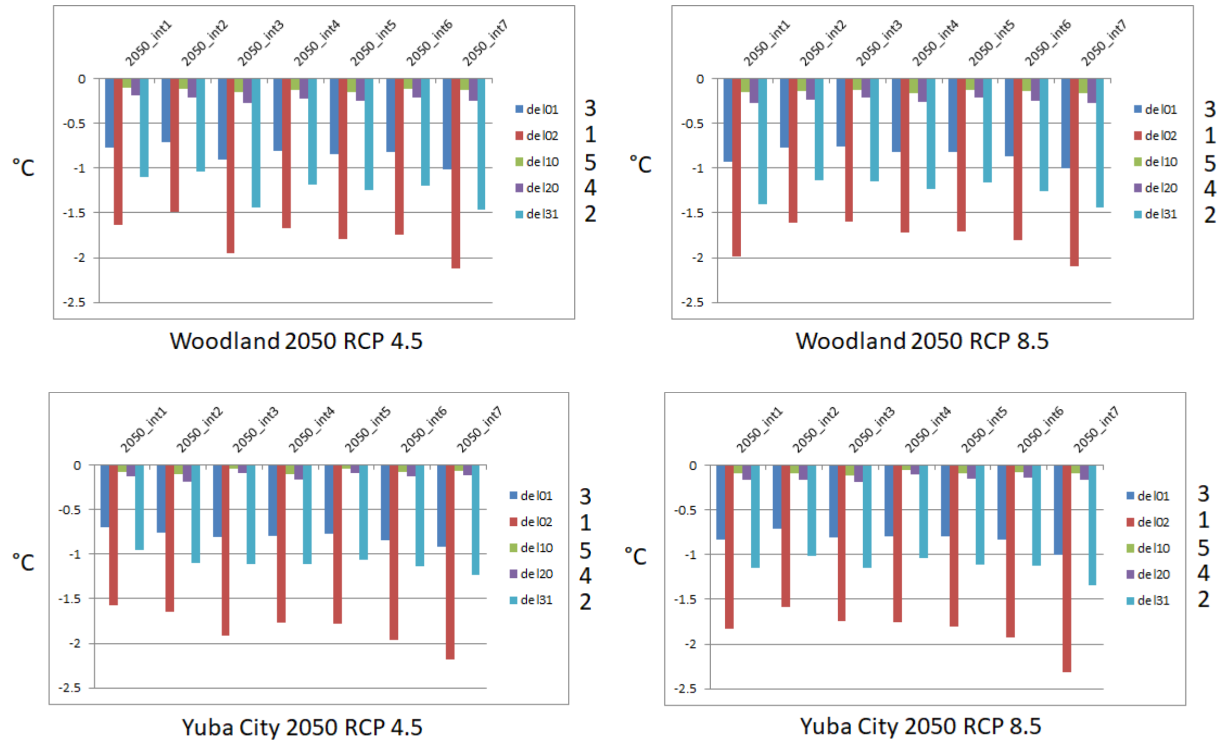

6.5.2 Impact of smart growth on 0600 PDT temperature

The impacts of the smart growth scenario defined in Section 6.4 were evaluated and compared against those of the BAU scenario in year 2050 (based on USGS LUCAS projections). While there are several ways these impacts could be quantified, including averaging over the entire region or each sub-domain, here the impacts are presented only for those locations (grid cells) where urbanization was prevented (compare the top and bottom parts of Figure 6-8). Clearly, applying this criterion would show much larger localized cooling impacts relative to, say, averaging over the entire domain including those areas that currently are urbanized (i.e., in 2013 – 2016).

Figure 6-10 shows that while there are variations by area and time interval, the overall average avoided warming at 0600 PDT is about 2 °C in the areas where urbanization was prevented. On the other hand, if averaged over each subdomain (not shown here), the effects of smart growth are smaller, as expected, i.e., an avoided warming of between 0.05 and 0.15 °C region-wide.

Figure 6-10: Impacts of smart growth on 0600-PDT air temperature in 2050: Avoided warming (°C) at new urban locations for RCP 4.5 and 8.5.

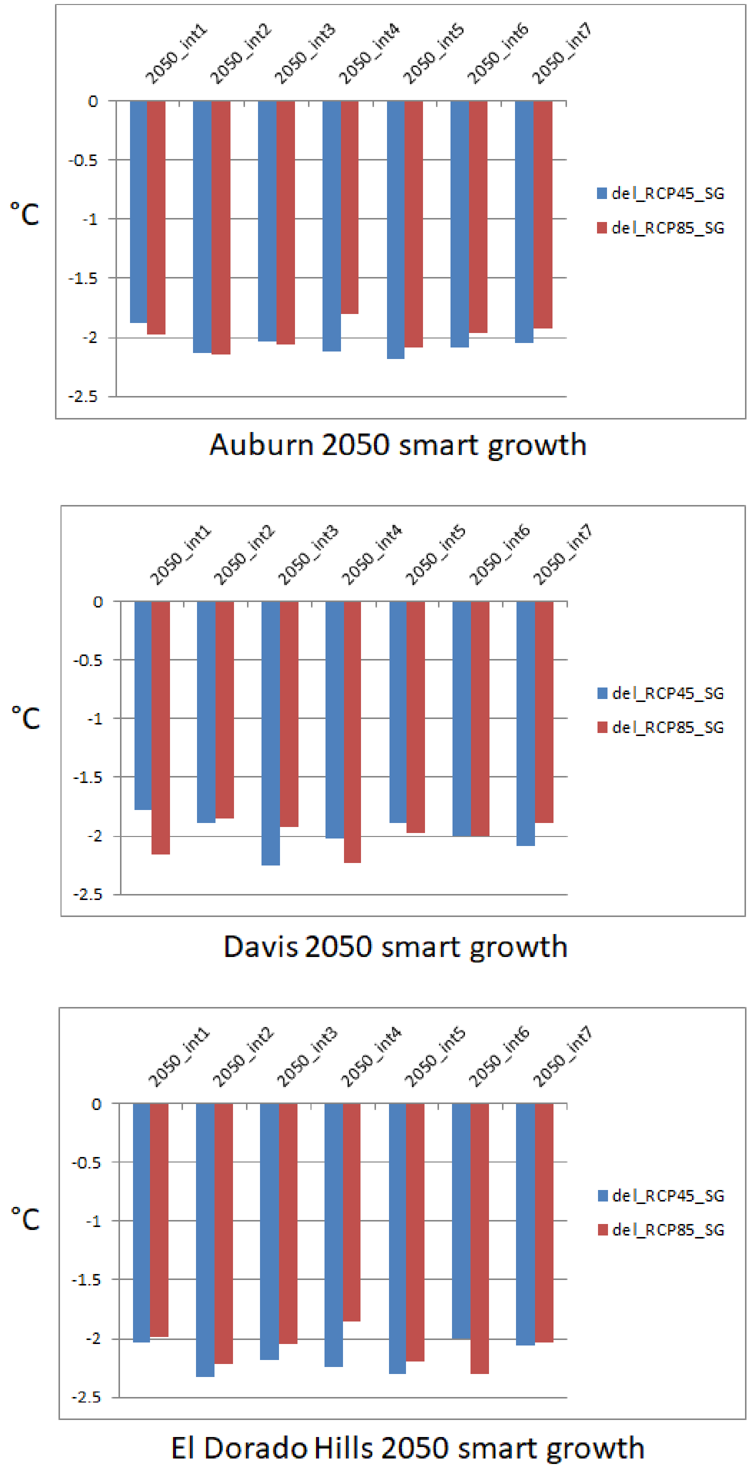

Figure 6-10, continued.

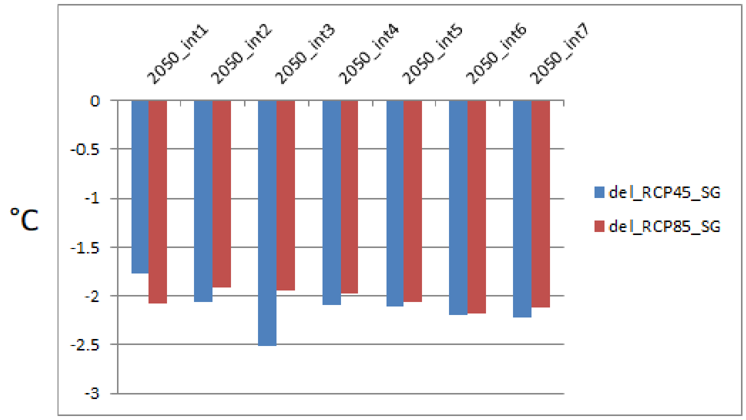

Sacramento 2050 smart growth

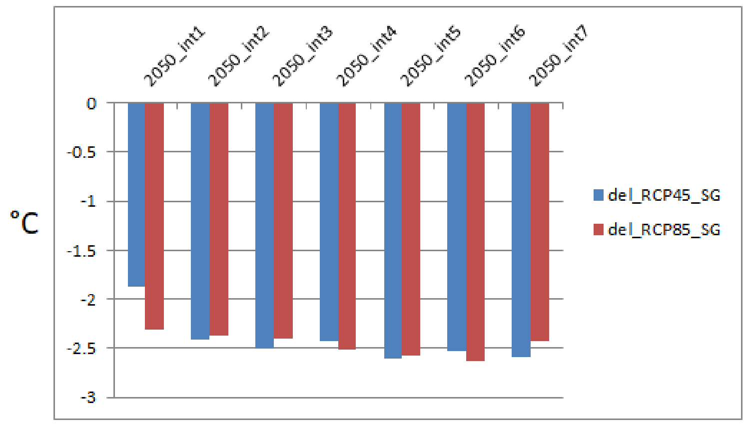

Yuba City 2050 smart growth

6.5.3 Impacts of mitigation measures on 1300 PDT temperature

In Figure 6-11, the average temperature reductions at 1300 PDT are presented, that is, temperature reductions averaged over all 1300 PDT hours (in each of the seven 2050 periods) and over urban grid cells in each specified sub-domain. For each area, two RCP scenarios are presented in the figure (RCP 4.5 and RCP 8.5).

Figure 6-11 shows that the ranking (i.e., the order of measures' effectiveness) at this time interval (1300 PDT) is (1) different from that at 0600 PDT, discussed above, and (2) also varies across different regions, unlike at 0600 PDT where they were similar across all sub-domains. At this time interval (1300 PDT), the effects of albedo measures are larger than those of canopy cover, as explained earlier, especially if case02 is excluded from the analysis (as an extreme). Furthermore, at Davis, the ranking of the measures is different in 2050 (for both RCPs) from the ranking in current climate. The magnitudes of reductions in temperature differ by location and so do the intra-measure differences within each area, i.e., how close or far apart are the reductions resulting from different measures.

Figure 6-11: Average temperature reduction (°C) at 1300 PDT. Periods are identified on the horizontal axis and the ranking of measures on the right side of each graph.

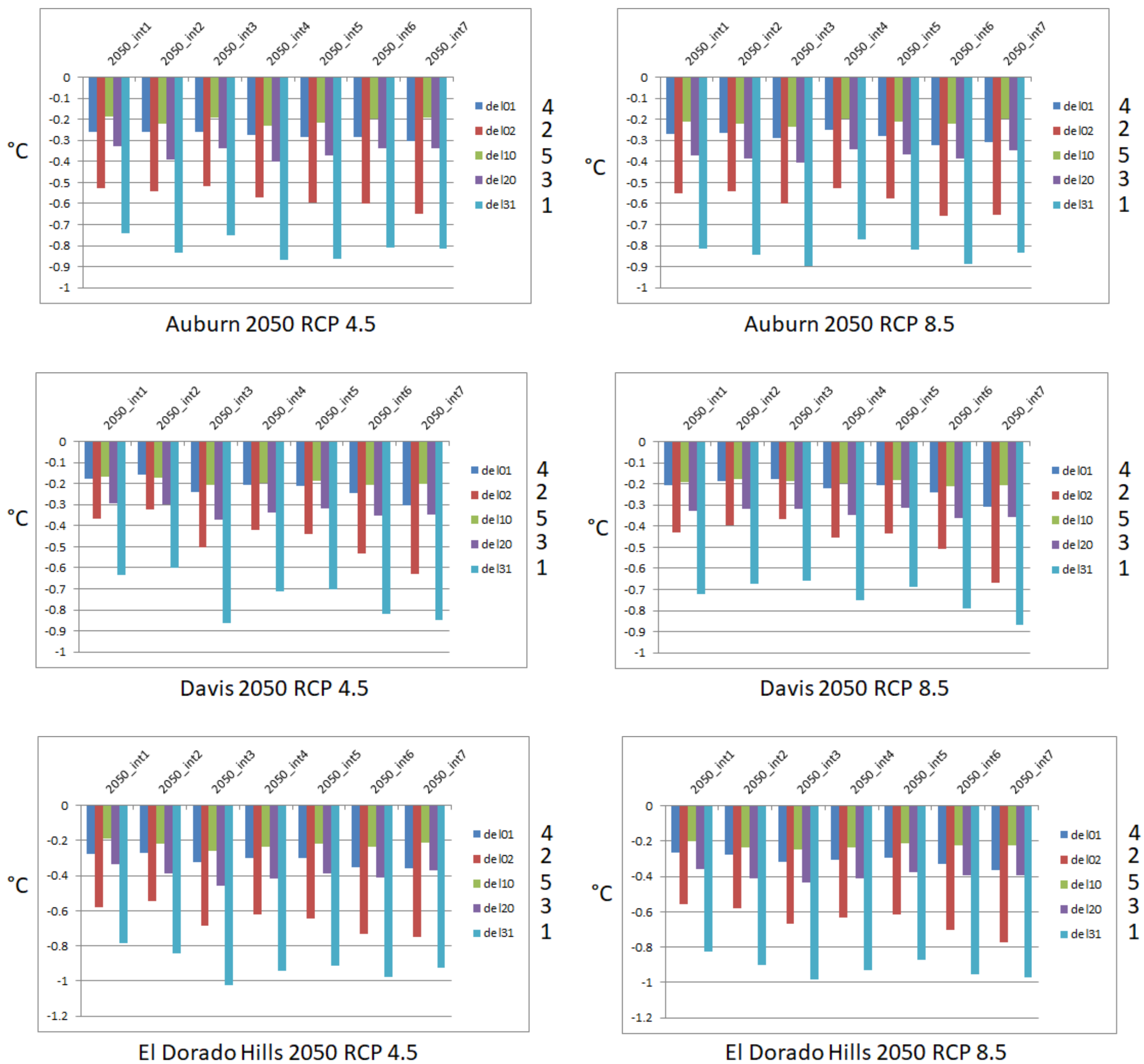

Figure 6-11, continued.

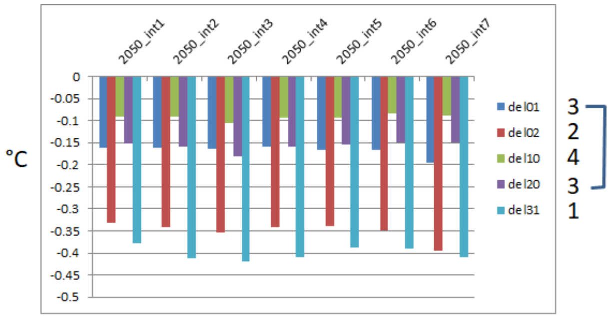

Placerville 2050 RCP 4.5

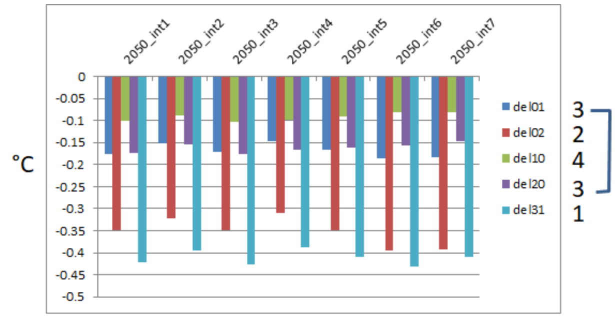

Placerville 2050 RCP 8.5

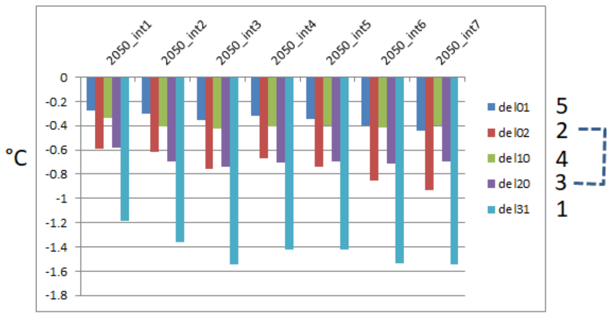

Sacramento 2050 RCP 4.5

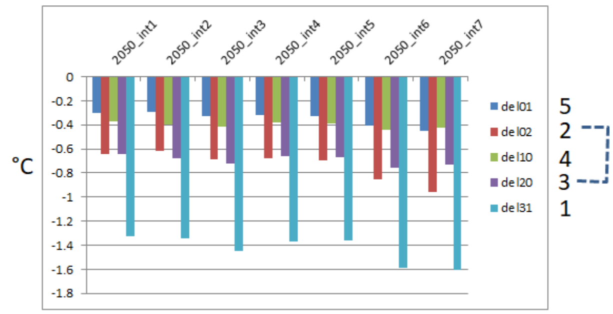

Sacramento 2050 RCP 8.5

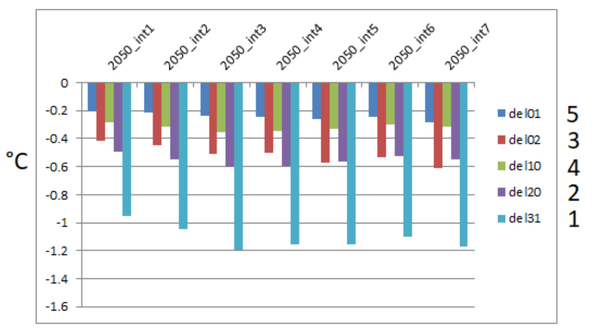

Woodland 2050 RCP 4.5

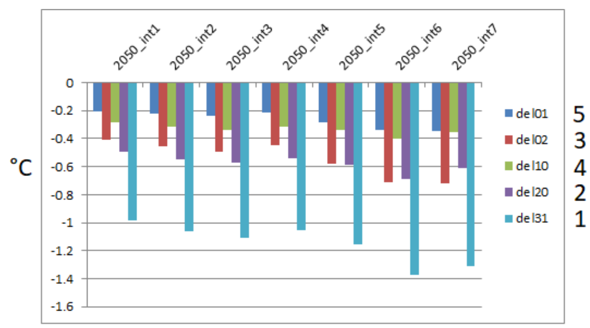

Woodland 2050 RCP 8.5

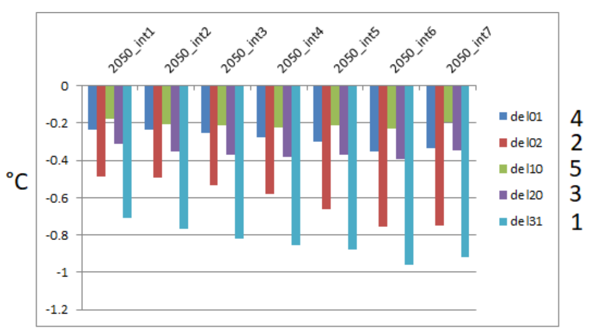

Yuba City 2050 RCP 4.5

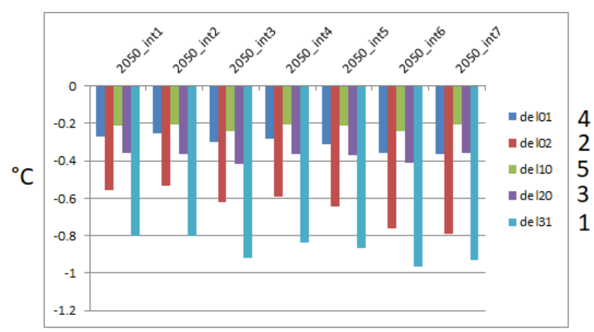

Yuba City 2050 RCP 8.5

6.5.4 Impacts of smart growth on 1300 PDT temperature

The smart growth scenario (defined above) was also evaluated in terms of air-temperature impacts compared to those of the BAU LULC scenario in year 2050 at 1300 PDT. As discussed earlier, the impacts are presented only at those locations (grid cells) where urbanization was prevented.

Figure 6-12 shows that there are more variations across the regions than was the case at 0600 PDT (where all regions had about a 2 °C average avoided warming). In this case (at 1300 PDT), the avoided warming ranges from an average of 0.05 °C in Davis to up to an average of 0.4 °C in Auburn. There also is a single instance of increase of up to 0.06 °C in temperature (in Davis) as a result of smart growth, but this is likely an anomaly. Again, if averaged over each subdomain, the effects of smart growth are small, e.g., avoided warming of between 0.05 and 0.1 °C region-wide.

Figure 6-12: Impacts of smart growth on 1300-PDT air temperature in 2050: Avoided warming (°C) at new urban locations for RCP 4.5 and 8.5.

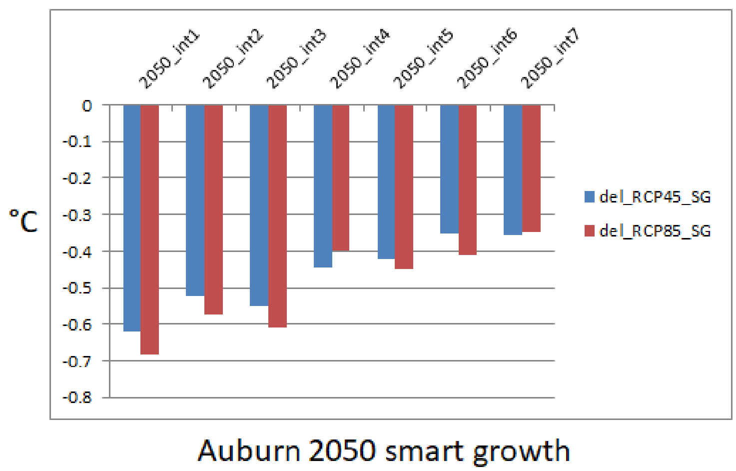

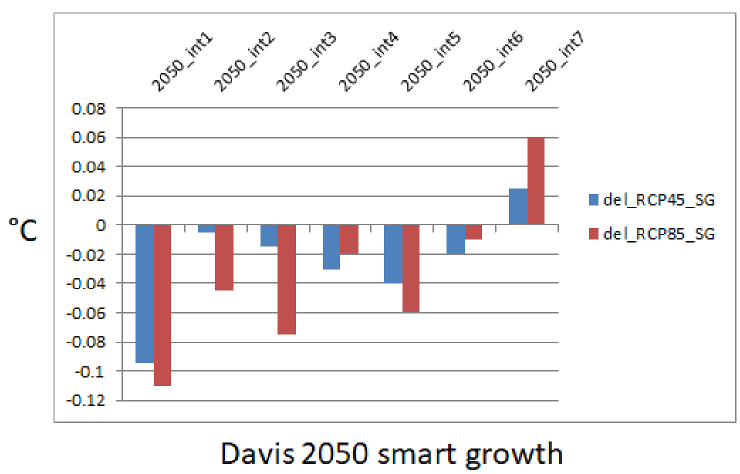

Figure 6-12, continued.

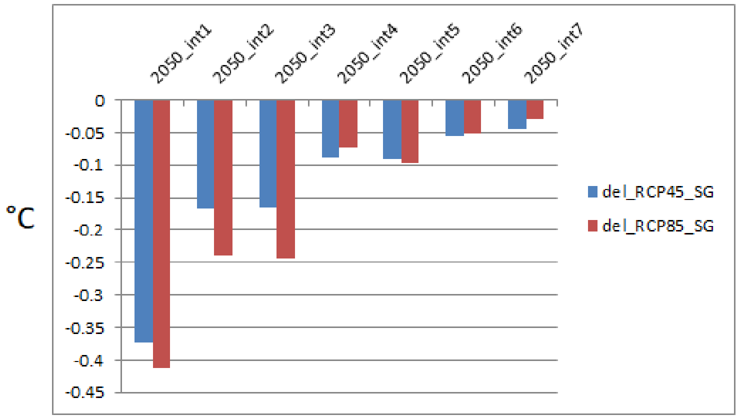

El Dorado Hills 2050 smart growth

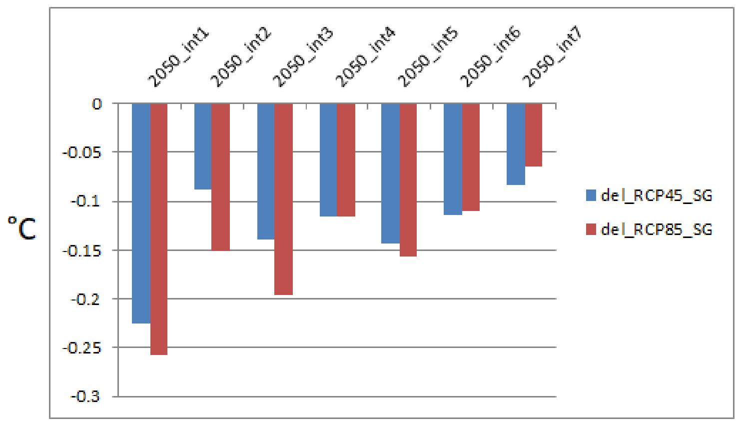

Sacramento 2050 smart growth

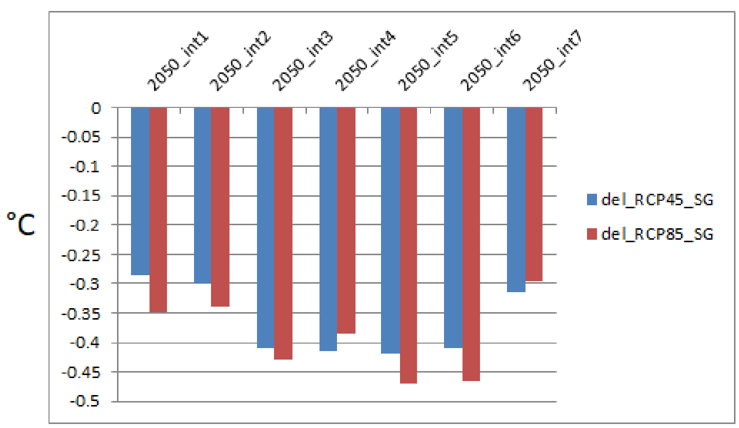

Yuba City 2050 smart growth

6.5.5 Impacts of mitigation measures on temperature during the period 1400 – 2000 PDT

Figure 6-13 shows the average temperature reductions for the interval 1400 - 2000 PDT (i.e., temperature reductions averaged over all 1400 to 2000 PDT hours in each period) and also averaged over urban grid cells in each specified sub-domain. As discussed earlier in the report, this range of hours is of interest to local utilities (SMUD) in peak-load planning and management.

Figure 6-13 shows that the ranking (i.e., the order of measures' effectiveness) at this time interval is (1) different from that at 0600 and 1300 PDT (although more similar to 1300 PDT) and (2) also varies across different regions, unlike at 0600 PDT. There is also the case in Woodland where the ranking of the mitigation measures in year 2050 differs from the ranking in current climate. At this time interval (1400 – 2000 PDT), the effects of albedo measures again are larger than those of canopy cover, excluding case02. The magnitudes of reductions in temperature and the intra-measure differences within each area differ by location, as was seen at hour 1300 PDT.

Figure 6-13: Average temperature reduction (°C) at 1400 - 2000 PDT. Periods are identified on the horizontal axis and the ranking of measures on the right side of each graph.

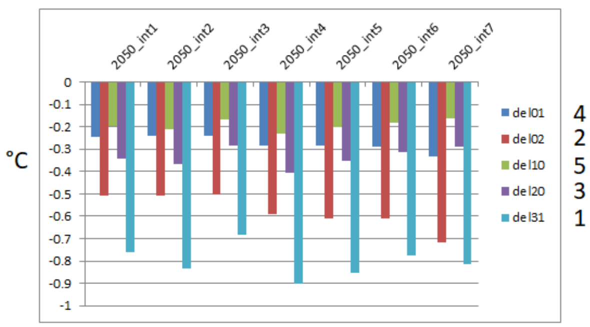

Auburn 2050 RCP 4.5

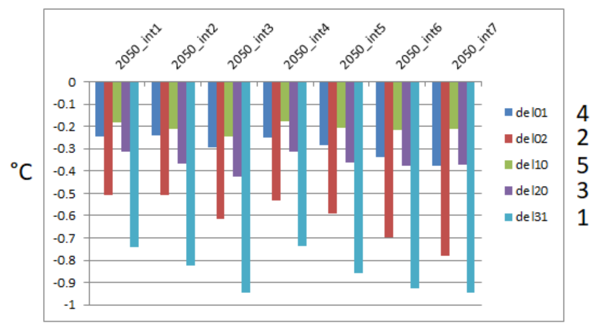

Auburn 2050 RCP 8.5

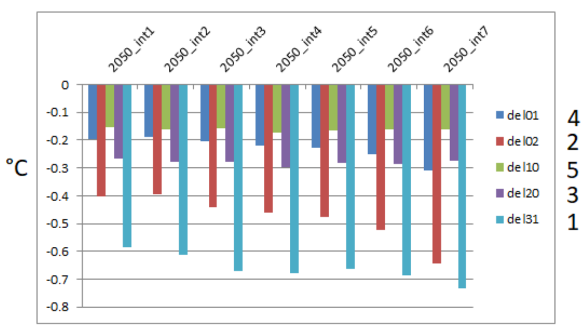

Davis 2050 RCP 4.5

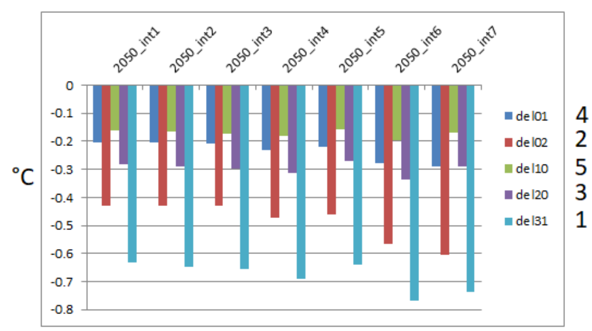

Davis 2050 RCP 8.5

Figure 6-13, continued.

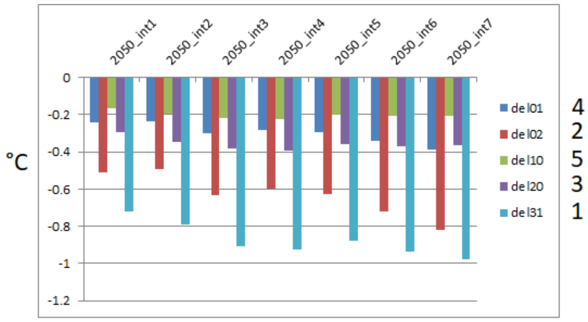

El Dorado Hills 2050 RCP 4.5

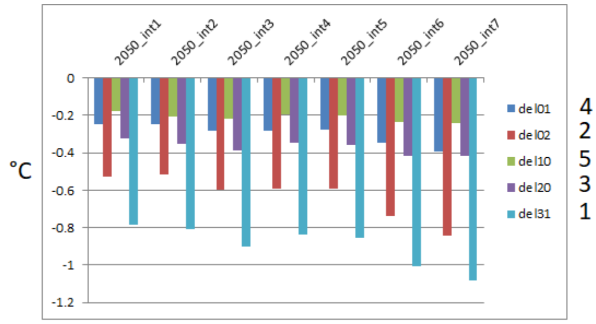

El Dorado Hills 2050 RCP 8.5

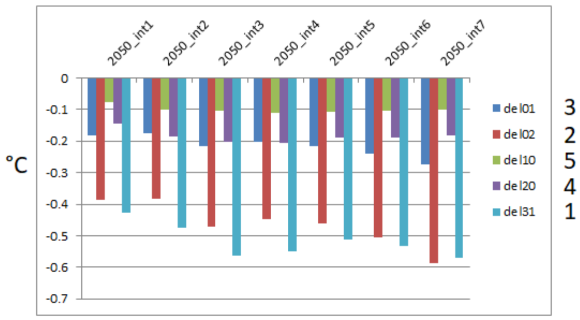

Placerville 2050 RCP 4.5

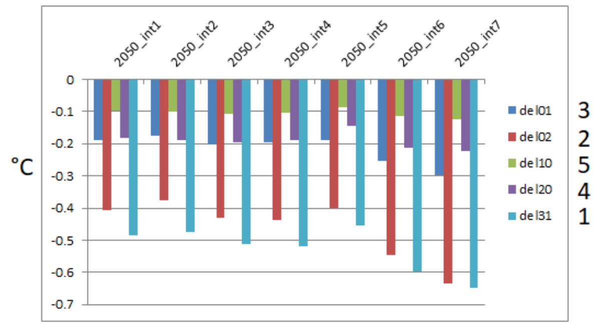

Placerville 2050 RCP 8.5

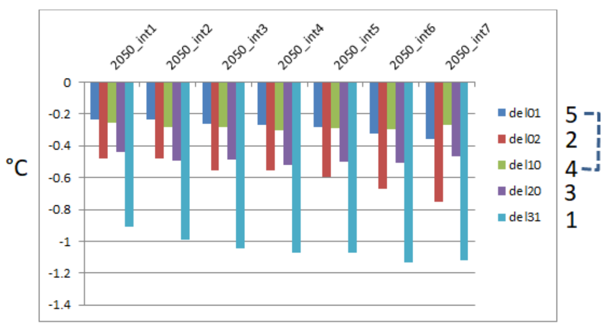

Sacramento 2050 RCP 4.5

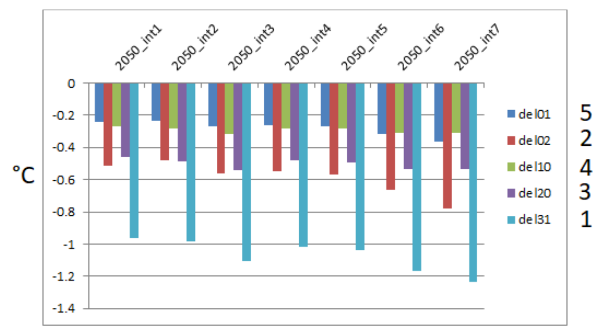

Sacramento 2050 RCP 8.5

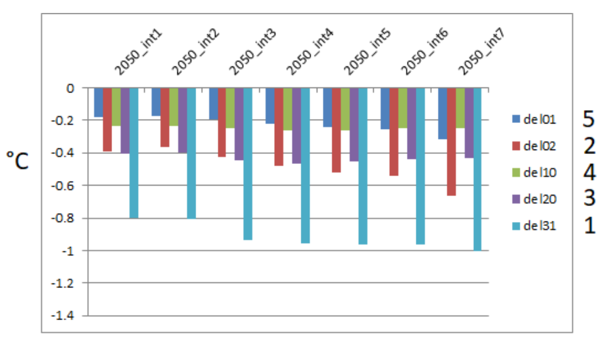

Woodland 2050 RCP 4.5

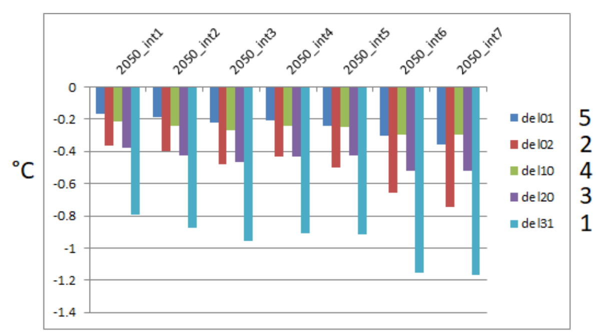

Woodland 2050 RCP 8.5

Figure 6-13, continued.

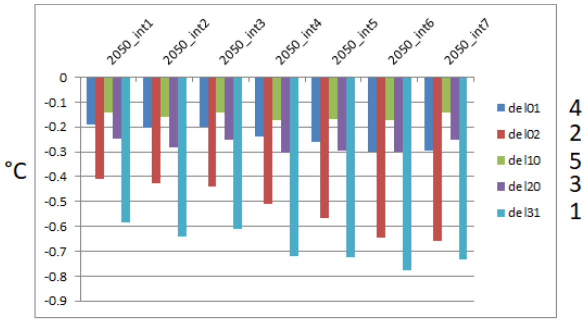

Yuba City 2050 RCP 4.5

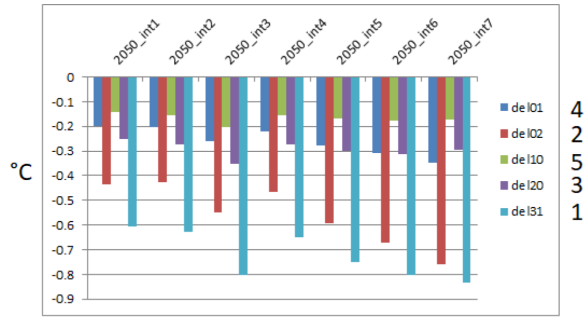

Yuba City 2050 RCP 8.5

6.5.6 Impacts of smart growth on 1400 - 2000 PDT temperature

As with the time intervals discussed earlier, the smart growth scenario was also evaluated in terms of air-temperature impacts during the hours 1400 – 2000 PDT and compared against those of the BAU scenario in year 2050 (based on USGS LUCAS projections). As before, the impacts are presented (in this section) at those locations (grid cells) where urbanization was prevented.

Figure 6-14 shows that, similar to 1300 PDT, there are more variations in avoided warming across the regions than was the case at 0600 PDT. At 1400 – 2000 PDT, the avoided warming ranges from an average of 0.6 °C in Davis to up to an average of 1.2 °C in Auburn. If averaged over each subdomain, the effects of smart growth are an avoided warming of between 0.05 and 0.15 °C region-wide

Figure 6-14: Impacts of smart growth on 1400- 2000 PDT air temperature in 2050: Avoided warming (°C) at new urban locations for RCP 4.5 and 8.5.

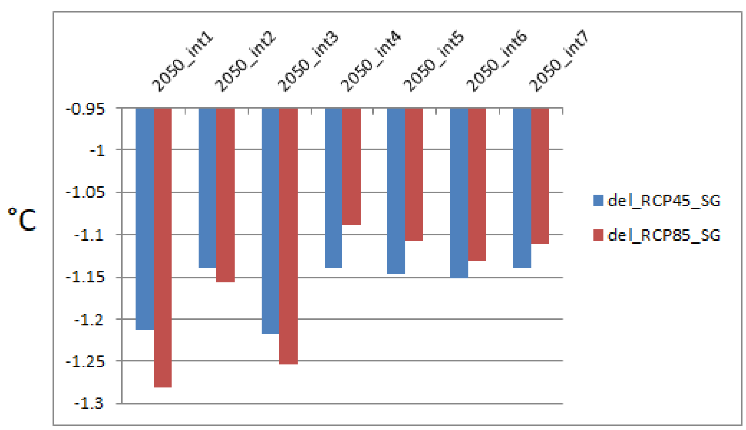

Auburn 2050 smart growth

Figure 6-14, continued.

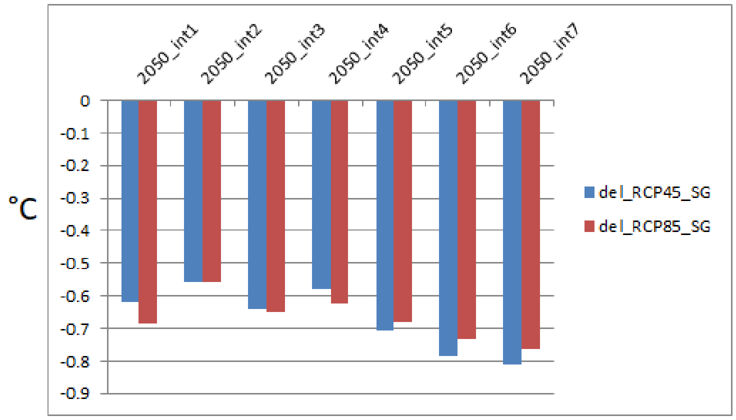

Davis 2050 smart growth

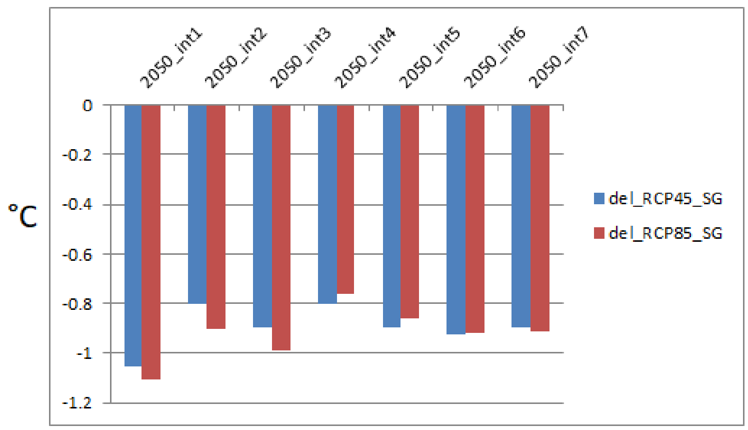

El Dorado Hills 2050 smart growth

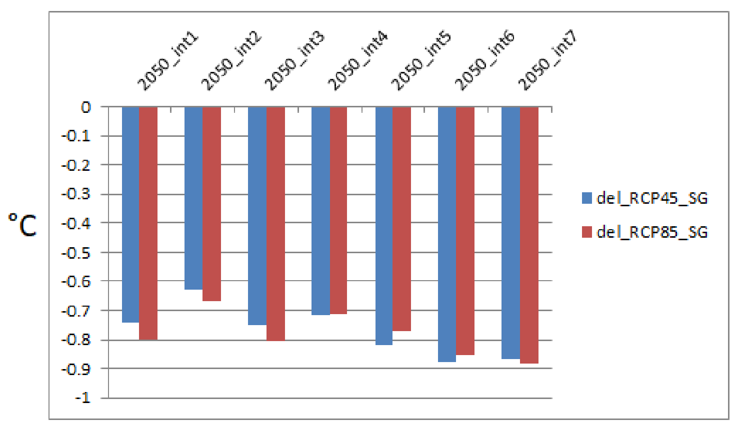

Sacramento 2050 smart growth

Figure 6-14, continued.

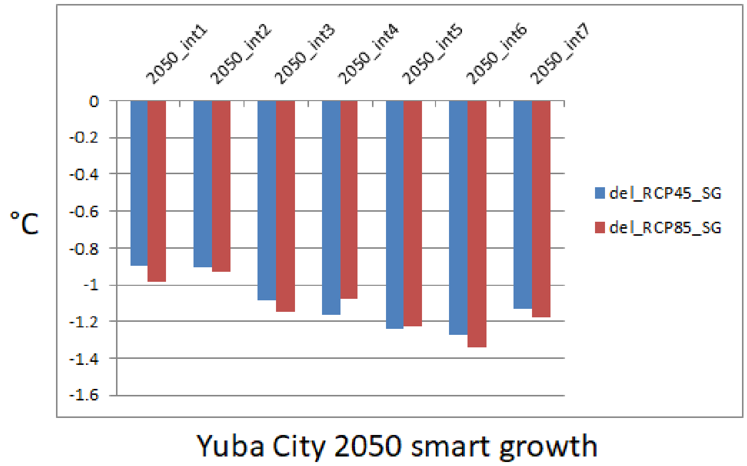

6.5.7 Impact of mitigation measures on 1500 PDT temperature

In Figure 6-15, the average temperature reductions at 1500 PDT are presented, i.e., temperature reductions averaged over all 1500 PDT hours in each of the seven 2050 periods and over urban grid cells in each specified sub-domain. As before, two RCP scenarios are shown (RCP 4.5 and RCP 8.5) for each sub-domain.

Figure 6-15 shows that the ranking (order of measures' effectiveness) at this time interval (1500 PDT) is generally similar to that at 1300 PDT but at different magnitudes. At this time interval (1500 PDT), the effects of albedo measures are larger than those of canopy cover, as explained earlier, especially if case02 is excluded from the analysis as an extreme. However, some albedo measures are still more effective even if case02 were included. Furthermore, in Auburn, Davis, El Dorado Hills, and Yuba City, the ranking of the measures is different in 2050 (both RCPs) from the ranking in current climate.

The magnitudes of reductions in temperature differ by location and so do the intra-measure differences within each area, i.e., how close or far apart are the reductions from different measures.

Figure 6-15: Average temperature reduction (°C) at 1500 PDT. Periods are identified on the horizontal axis and the ranking of measures on the right side of each graph.

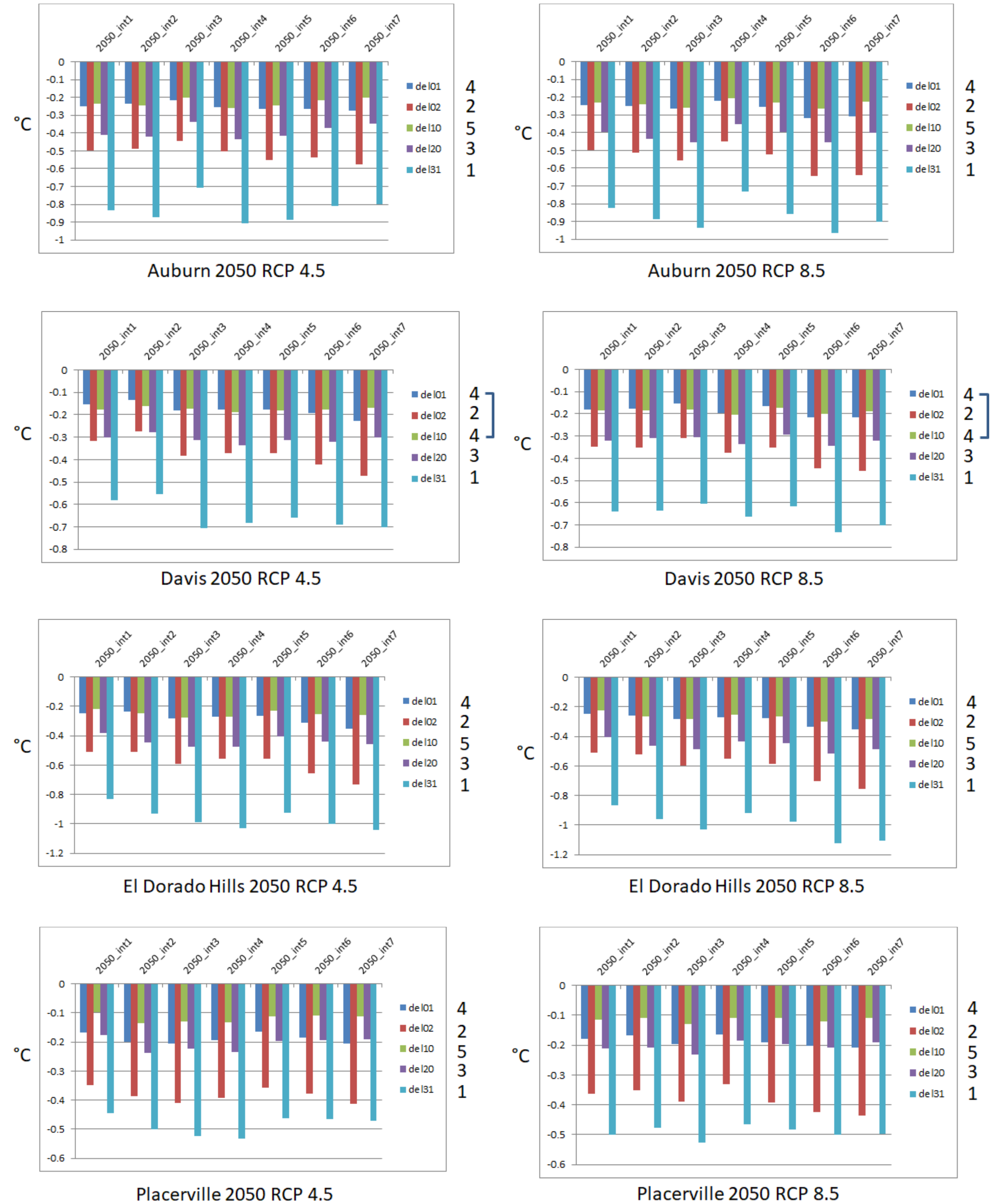

Figure 6-15, continued.

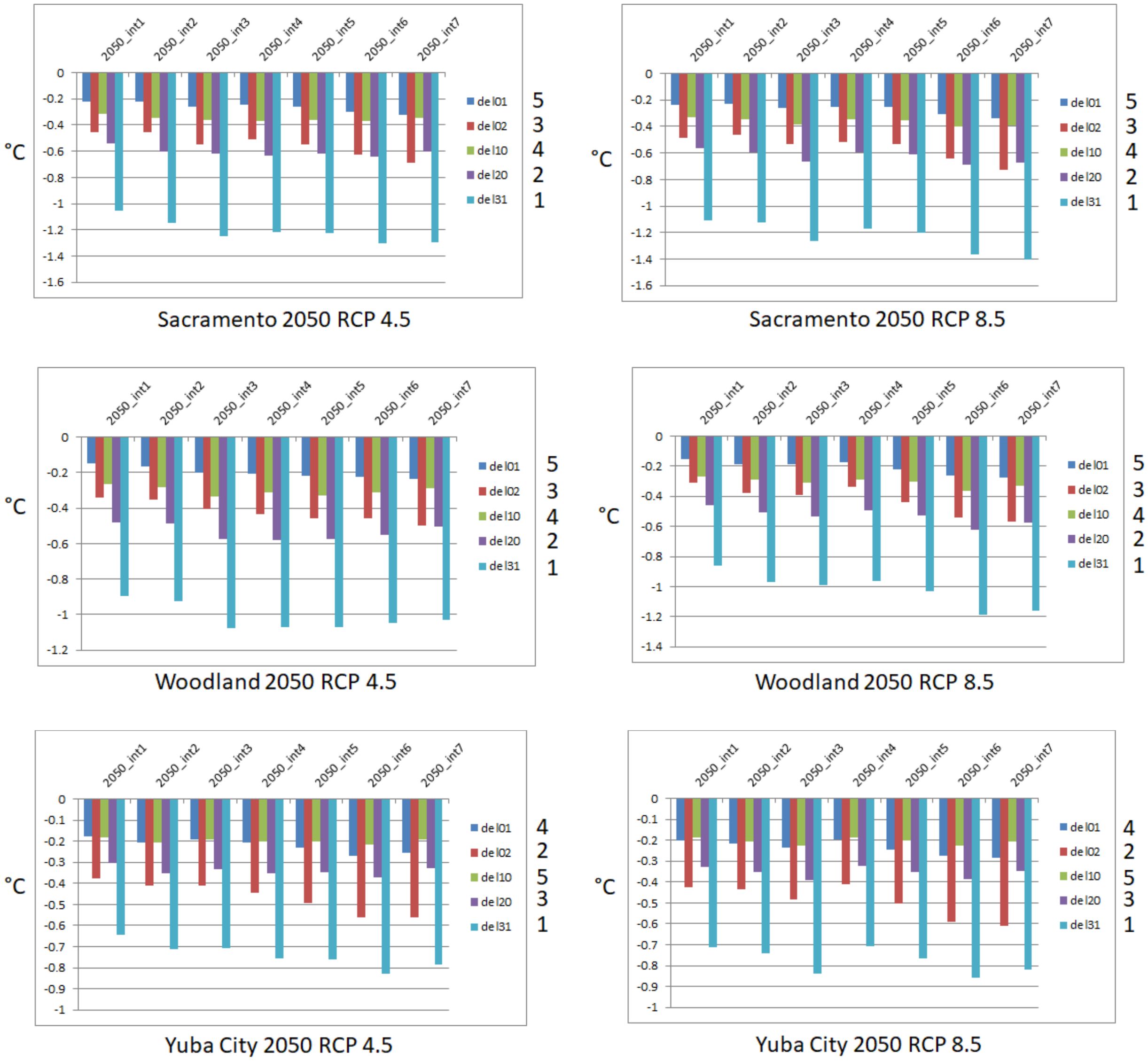

6.5.8 Impacts of smart growth on 1500 PDT temperature

The smart growth scenario (as defined earlier) was also evaluated in terms of air-temperature impacts and compared against those of the BAU scenario in year 2050 for the hour at 1500 PDT. As before, the impacts are presented here only for those grid cells where urbanization was avoided.

As with the hour at 1300 PDT, Figure 6-16 shows that there is significant variation across the regions. In this case, the avoided warming ranges from an average of 0.20 °C in Davis to up to an average of 0.6 °C in Auburn and Yuba City. However, if averaged over each subdomain, the effects of smart growth are smaller, e.g., an avoided warming of between 0.08 and 0.15 °C region-wide.

Figure 6-16: Impacts of smart growth on 1300-PDT air temperature in 2050: Avoided warming (°C) at new urban locations for RCP 4.5 and 8.5.

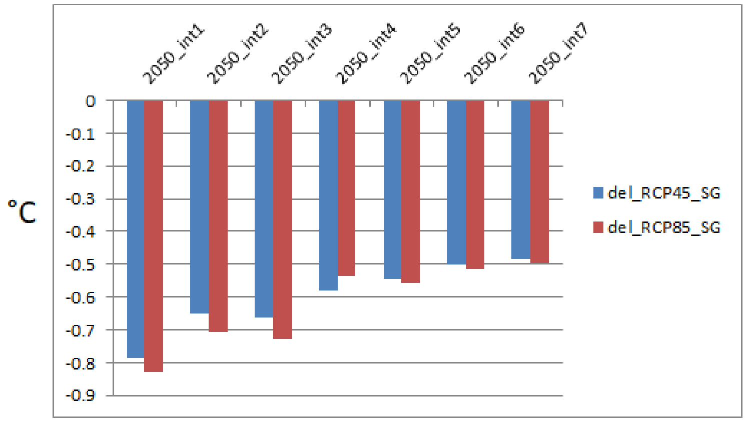

Auburn 2050 smart growth

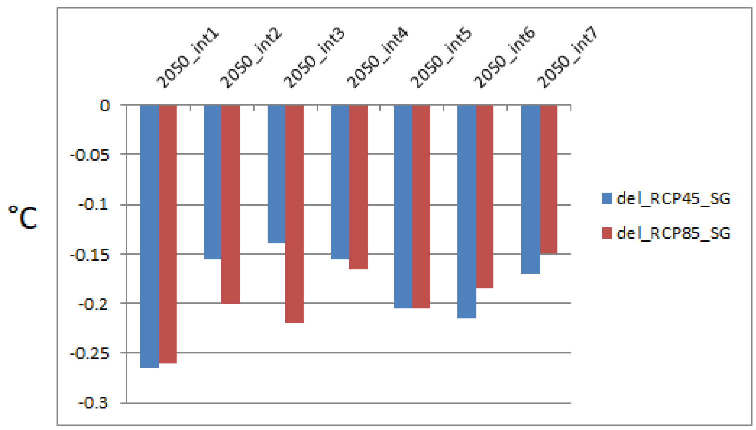

Davis 2050 smart growth

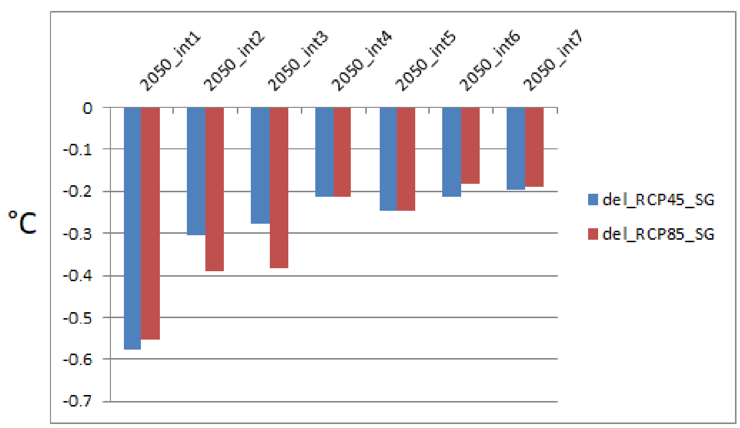

El Dorado Hills 2050 smart growth

Figure 6-16, continued.

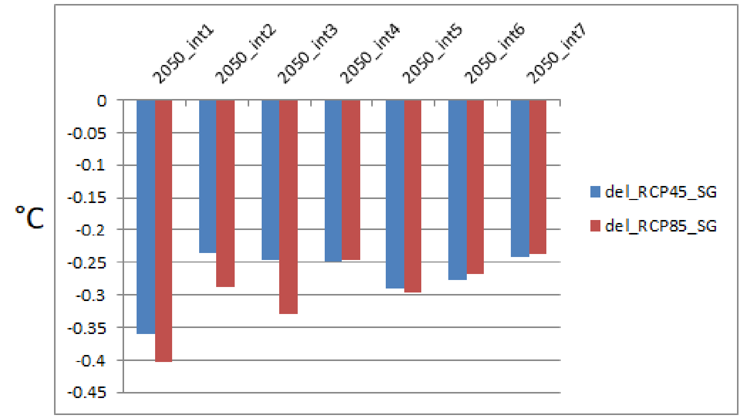

Sacramento 2050 smart growth

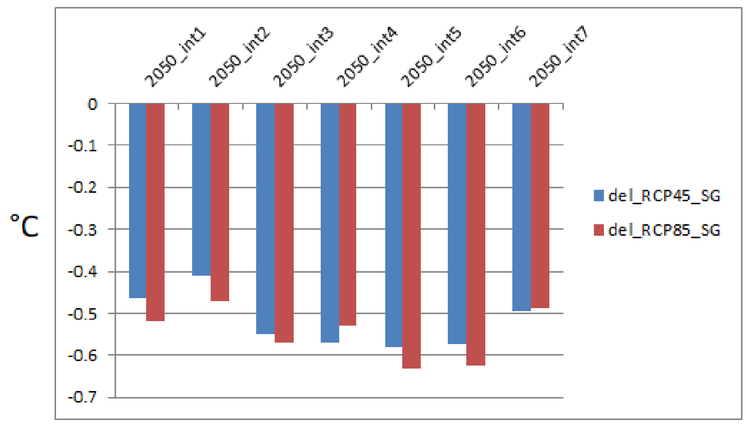

Yuba City 2050 smart growth

6.5.9 Impact of mitigation measures on all-hours average temperature

Figure 6-17 shows the all-hours average temperature reductions that are also averaged over urban grid cells in each specified sub-domain. It can be seen that the ranking of measures is uniform across all regions, but differs in Sacramento and Woodland. In the all-ours average, the effects of vegetation canopy cover are more dominant since this includes nighttime hours.

Figure 6-17: Average all-hours temperature reduction (°C). Periods are identified on the horizontal axis and the ranking of measures on the right side of each graph.

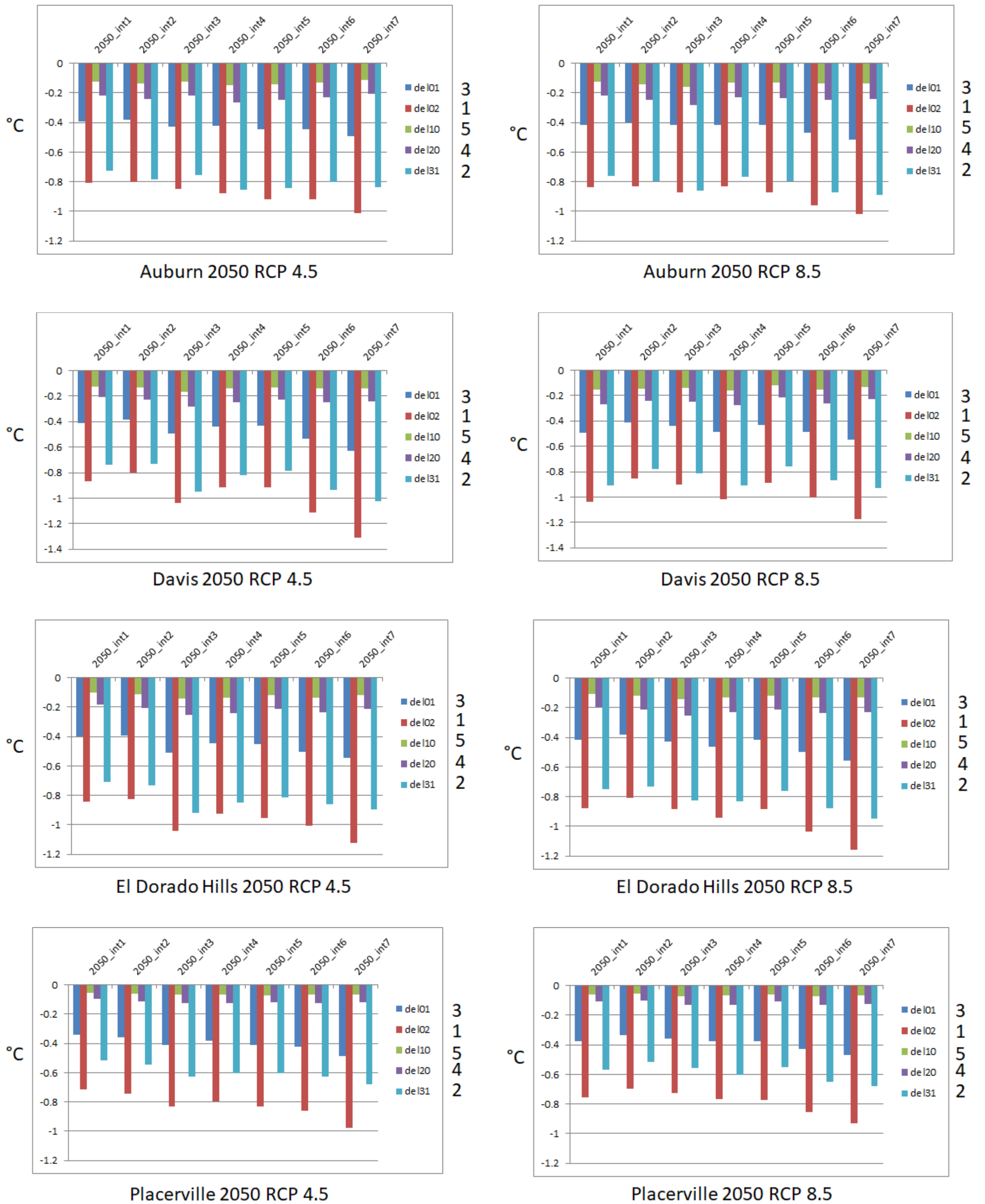

Figure 6-17, continued.

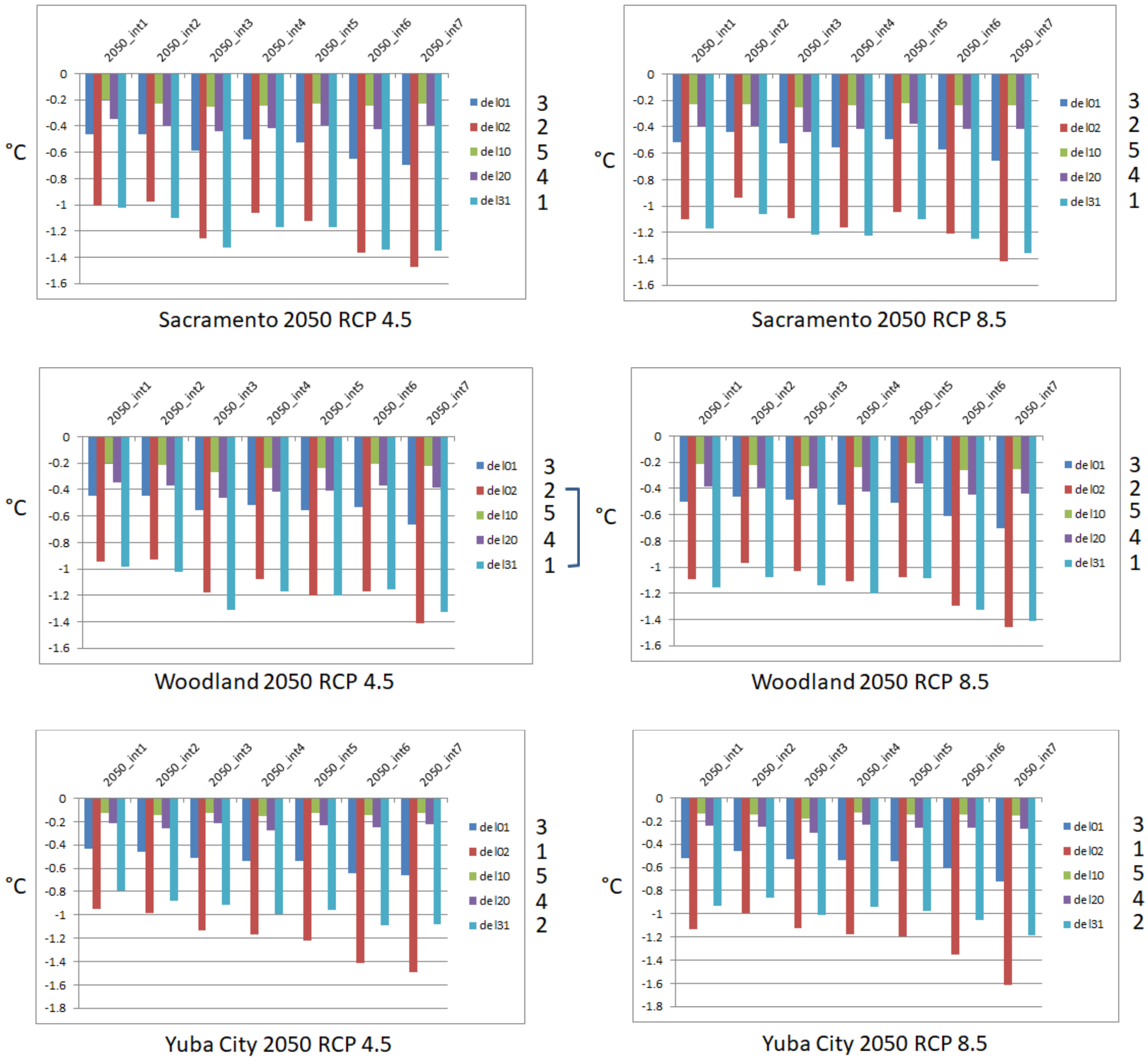

6.5.10 Impacts of smart growth on all-hours average temperature

Finally, the smart growth scenario was evaluated for the all-hours average impacts and compared against those of the BAU growth in year 2050. As before, the impacts are presented here only at those grid cells where urbanization was avoided. Figure 6-18 shows that except for Auburn and El Dorado Hills, there is less variation across the regions and a relatively similar avoided warming of between 1.2 and 1.6 °C. When averaged over sub-domains, the avoided warming is smaller, as discussed earlier.

Figure 6-18: Impacts of smart growth on all-hours average air temperature in 2050: Avoided warming (°C) at new urban locations for RCP 4.5 and 8.5.

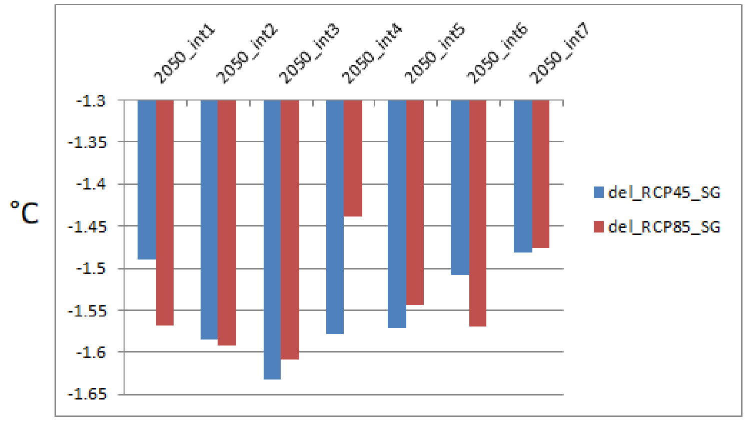

Auburn 2050 smart growth

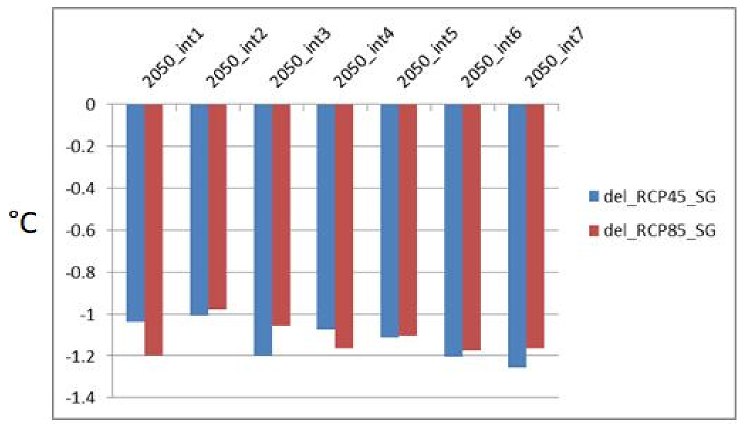

Davis 2050 smart growth

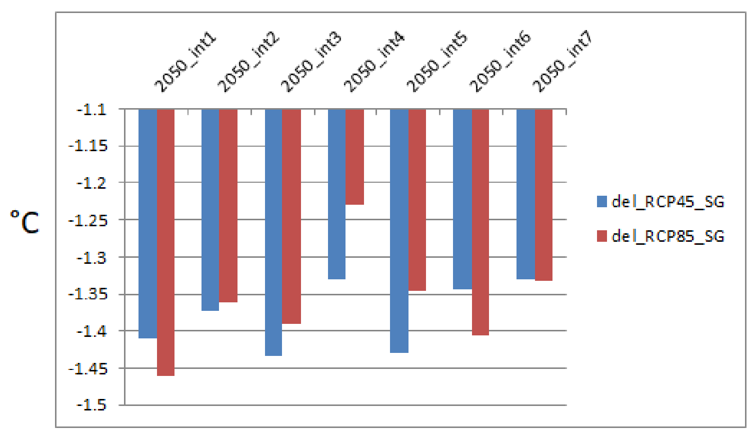

El Dorado Hills 2050 smart growth

Figure 6-18, continued.

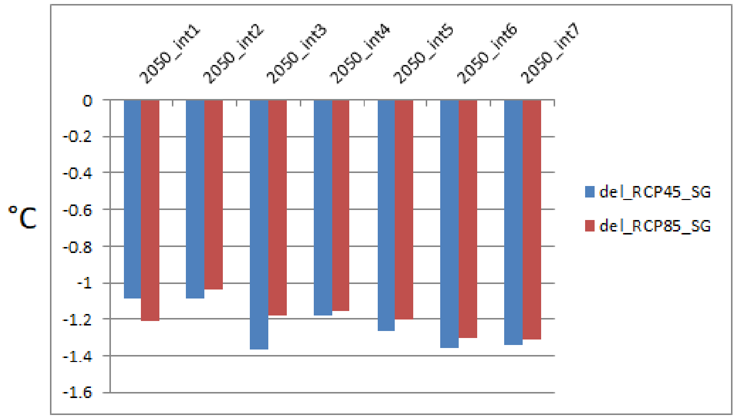

Sacramento 2050 smart growth

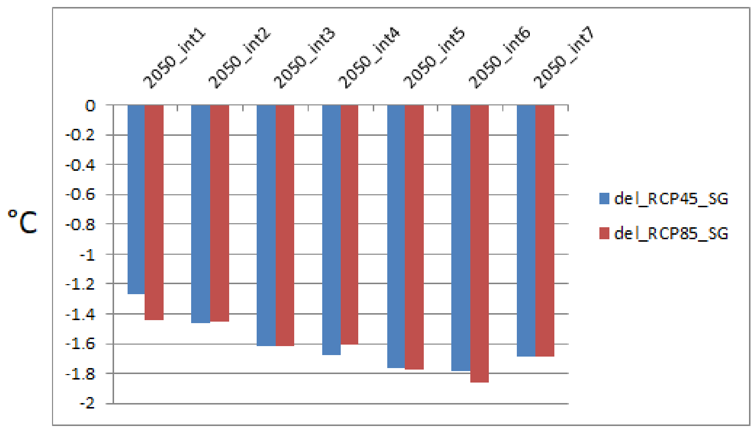

Yuba City 2050 smart growth

6.5.11 Summary of measures efficacies

Figure 6-19 summarizes the rankings of measures discussed above for 2050 RCP 4.5 and RCP 8.5 and provides a comparison with the efficacies under the current climate and land use. The chart is color-coded so that black is most effective measure (largest cooling) and near-white is smallest cooling effect. Note that these are impacts on air temperature, not the UHII. The following observations can be made:

1. For the 0600-PDT UHII:
    a. The rankings of mitigation measures (order) are similar and consistent across all regions.
    b. Within each region, the rankings are similar across current and future climates.
2. For the 1300-PDT UHII:
    a. The rankings are different across the regions.

    b. In Davis and Sacramento, the rankings are different in future climate than they are in current climate.
3. For the 1400 – 2000 PDT UHII:
    a. The rankings are different across the regions.
    b. In Woodland, the rankings are different in future climate than they are in current climate.
4. For the 1500 PDT UHII:
    a. The rankings are different across the regions.
    b. In Auburn, Davis, El Dorado Hills, and Yuba City, the rankings are different in future climate than they are in current climate.
5. For the all-hours UHII:
    a. The rankings are different across the regions.
    b. Within each region, the rankings are similar across current and future climates.

This type of information may be useful to planners if they specifically target certain times of day, e.g., peak temperatures, or are interested in mitigating all-hour UHII averages. In Figure 6-19, the various time bands may be of interest yo different applications. For example, the 0600 PDT and allHRS bands could be of interest from a heat-wave perspective, the 1400-2000 PDT band may be of interest to utilities, the 1500-PDT band could be used in relation to peak cooling demand analysis, and the band at 1300 PDT may be of relevance to assessments of measures around solar noon.

Figure 6-19: Ranking of measures case01 through case31 at the regional scale.

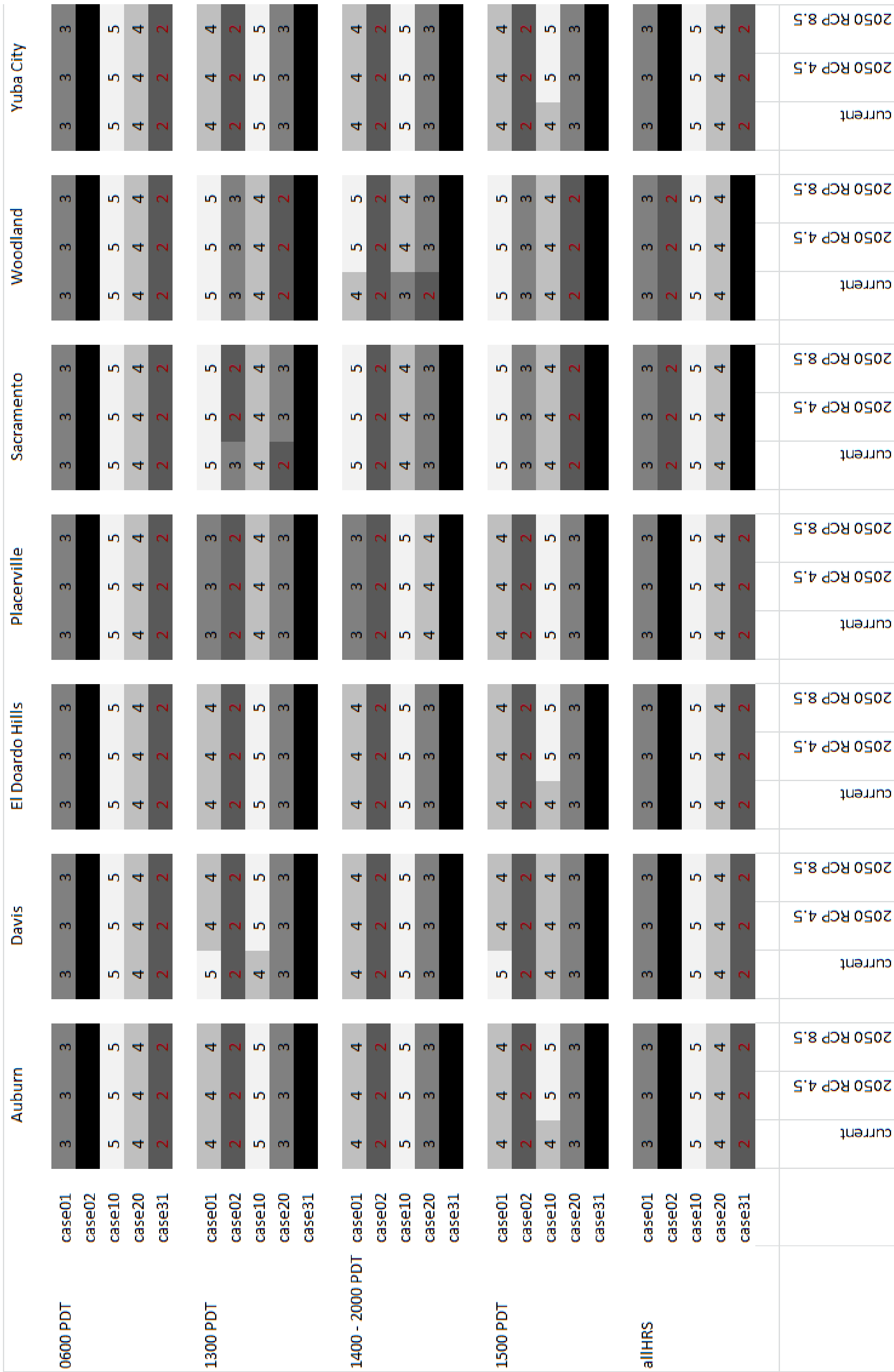

6.6 IMPACTS OF CLIMATE AND LAND-USE CHANGES ON THE UHII

As demonstrated earlier and shown in Figures 6-6 and 6-7, for example, both climate and LULC changes have significant impacts on the temperature field. Here, we continue that discussion in some additional detail, by examining the impacts on the local all-hours UHII.

The characteristics of the future UHII are dictated mainly by two aspects: (1) in areas currently urbanized, the main impacts on the future temperature field and the UHII are those from local climate-change effects, whereas (2) in areas that will be urbanizing between now and 2050, the impacts on future air temperature result from changes in land use (urbanization) and changes in climate. In general, the UHII in 2050 RCP 8.5 is larger than in RCP 4.5, as one would like to expect – however, there are a couple of deviations from this tendency, as explained in this section.

The effects of (1) climate and (2) LULC changes can be seen, for example, in Figure 6-20, for the period July 16 – 31, 2050, RCP 8.5. The temperature equivalent of the changes in all-hour UHII in currently-urbanized areas in the metro Sacramento region (for that period) is a warming of 1.36 °C. On the other hand, for those urbanizing areas on the outskirts, the temperature equivalent is a warming of 2.77 °C, which is larger as it includes both effects from climate and LULC changes occurring between now and 2050.

Figure 6-20: Change in the all-hours UHII (°C) from 2015 to 2050 RCP 8.5. Example for July 16 – 31.

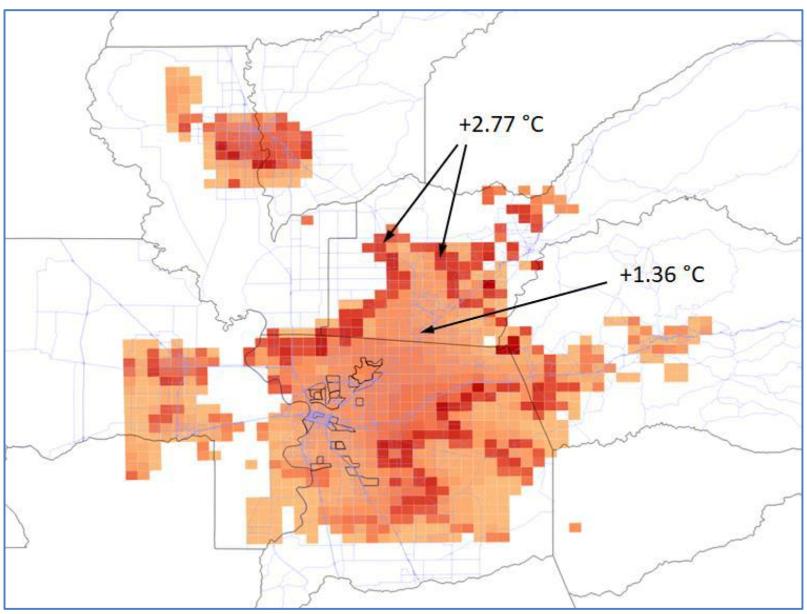

Table 6-1 provides a summary of the average all-hours UHII (averaged over all JJAS intervals 1 – 7, not just the sample period discussed above). It is noted from the table, and Figure 6-21, that the UHII is larger in 2050 RCP 4.5 than in current climates and is also larger in 2050 RCP 8.5 than it is in 2050 RCP 4.5, both of which are expected, except for domains D05 and D06. In these domains, the UHII in the RCP 8.5 scenario is still larger than in the current climate but is slightly smaller than in RCP 4.5. The reason is that the non-urban areas surrounding Yuba City / Marysville (in D05) and Woodland (in D06) warm up faster (on the long run) than the urban areas. This might be the result of lower vegetation cover in the non-urban areas in these two regions (see discussion of vegetation cover in Section 2.3.2). Since the non-urban areas warm up slightly faster than the urban ones in this case, the UHII, by definition, becomes slightly smaller – despite the fact that the absolute urban temperatures are higher in RCP 8.5 than in RCP 4.5. This phenomenon was also discussed in Taha (2017) for various areas in California. Figure 6-21 summarizes these changes in the UHII from current climate to 2050.

Table 6-1. All-hours UHII and changes (temperature equivalent in °C) at each sub-region (derived from the 2-km level for locations of sub-regions where 500-m domains D05-D10).

Domain	Area	All-hours UHII (temperature equivalent °C)		
		2013-2016	2050 RCP 4.5	2050 RCP 8.5
D05	Yuba City / Marysville	2.41	2.96	2.64
D06	Woodland	2.14	2.80	2.57
D07	Sacramento AB617 A, B, D	4.48	5.00	5.13
D07	Sacramento AB617 C, E, G	2.33	2.67	2.99
D08	Granite Bay	5.07	5.55	5.72
D08	Roseville	5.83	6.42	6.63
D09	El Dorado Hills	4.91	5.02	5.22
D09	Folsom	4.86	5.46	5.62
D10	Placerville	1.36	1.59	1.60

Figure 6-21: Changes in the UHII from current climate and LULC to 2050.

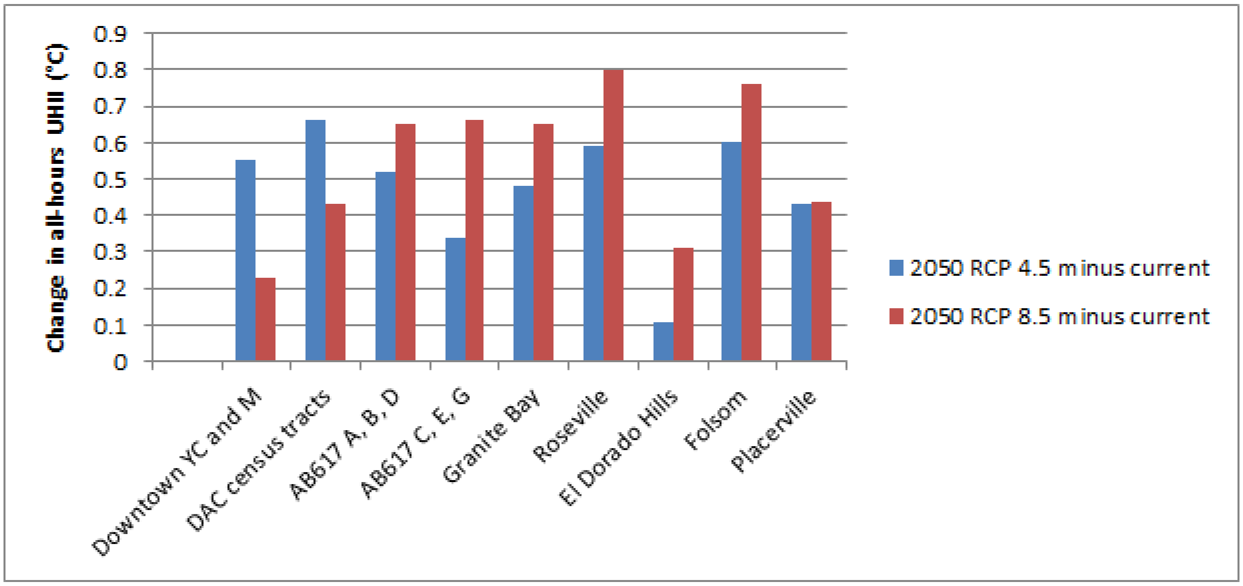

6.7 IMPACTS OF MITIGATION MEASURES ON THE 1300 PDT TEMPERATURE FIELD

As was done in Section 5.10, showing sample instantaneous effects of mitigation measures in current climate, a description of the spatial properties and distributions of the changes in the daytime UHII in 2050 as a result of heat-mitigation measures is provided in this section. Here, the instantaneous effects are presented, in Figure 6-22, for the random hour of 1300 PDT, July 27 or 28, of year 2050 (compared with the same dates in 2015, in Section 5.10, Figure 5-16).

Recall that this is the impact on the temperature field at sample hours (instantaneous impacts) not on the UHII per se or equivalent temperature. The scenarios (del##) presented in this figure were defined earlier in Section 5.5. The caption above each pair of graphs provides a description of the results and the potential cooling effects.

In general, the results show that the larger urban areas (i.e., total urbanization by 2050 relative to current) contribute to additional urban warming but at the same time provide increased technical potential, i.e., larger areas available for implementation of cooling measures – hence increased potential for cooling and canceling out the additional warming. A comparison between Figure 6-22 for 2050 (below) with Figure 5-16 (in Section 5.10 for current climate) shows a larger area affected by cooling in 2050 compared to 2013 – 2016.

Note that the cooling effect of vegetation canopy scenarios presented here is relatively the smallest (at the hour of 1300 PDT). It is shown here merely as an example to coincide with the same hour as the albedo effects shown in other figures but, as discussed earlier, the effects of urban greening are larger during later hours of the day and at night.

Figure 6-22: Example of instantaneous hourly impacts on temperature from mitigation measures at the 2-km level in the year 2050.

Case01. Left: 1300 PDT, July 27, 2050, RCP 4.5. Maximum cooling at this hour = 0.8 °C. Right: 1300 PDT, July 27, 2050, RCP 8.5. Maximum cooling at this hour = 0.9 °C.

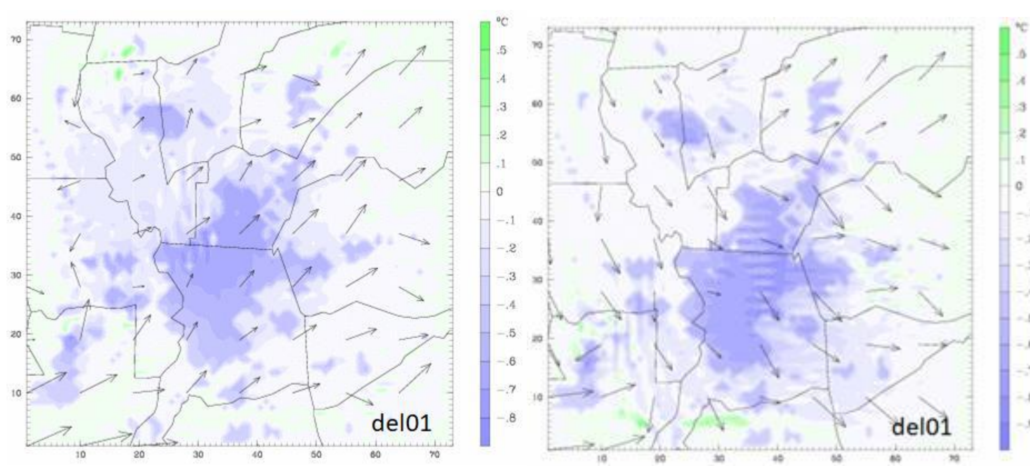

Case02. Left: 1300 PDT, July 27, 2050, RCP 4.5. Maximum cooling at this hour = 1.4 °C. Right: 1300 PDT, July 28, 2050, RCP 8.5. Maximum cooling at this hour = 1.6 °C.

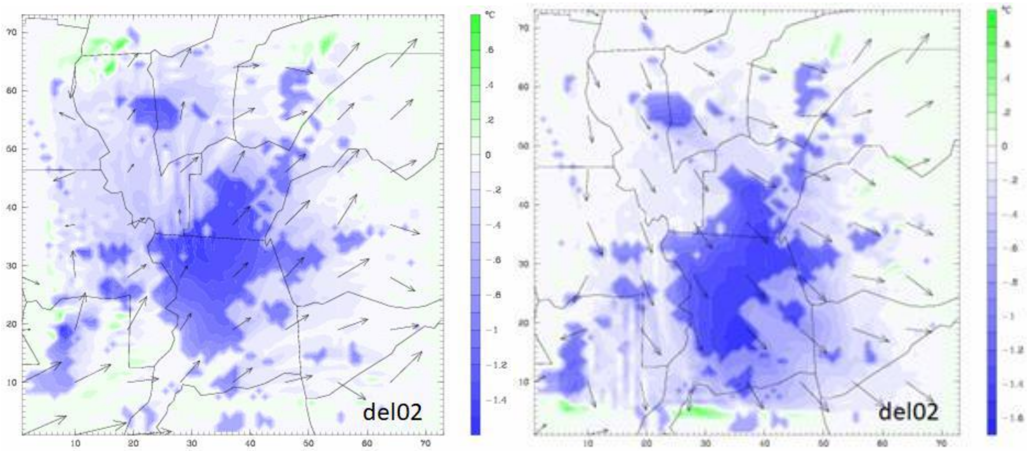

Case10. Left: 1300 PDT, July 27, 2050, RCP 4.5. Maximum cooling at this hour = 1.5 °C. Right: 1300 PDT, July 28, 2050, RCP 8.5. Maximum cooling at this hour = 1.3 °C.

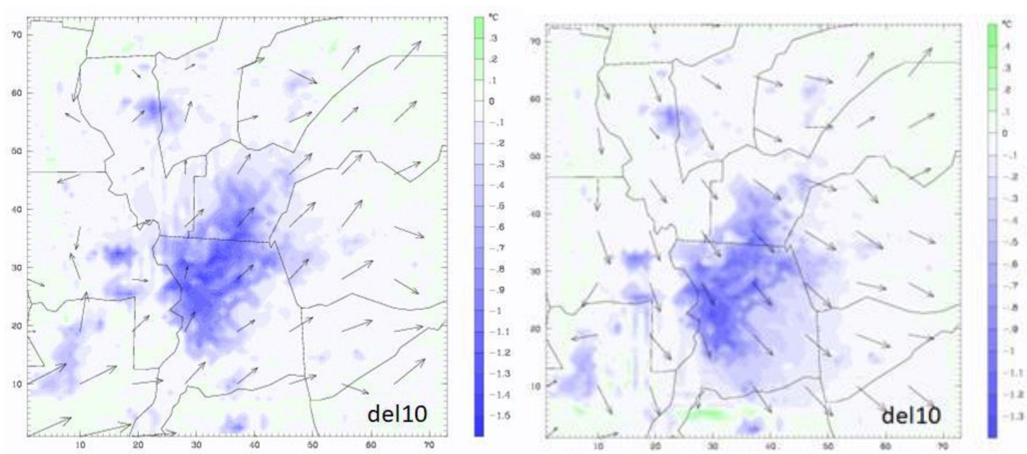

Case20. Left: 1300 PDT, July 27, 2050, RCP 4.5. Maximum cooling at this hour = 2.4 °C. Right: 1300 PDT, July 28, 2050, RCP 8.5. Maximum cooling at this hour = 2.2 °C.

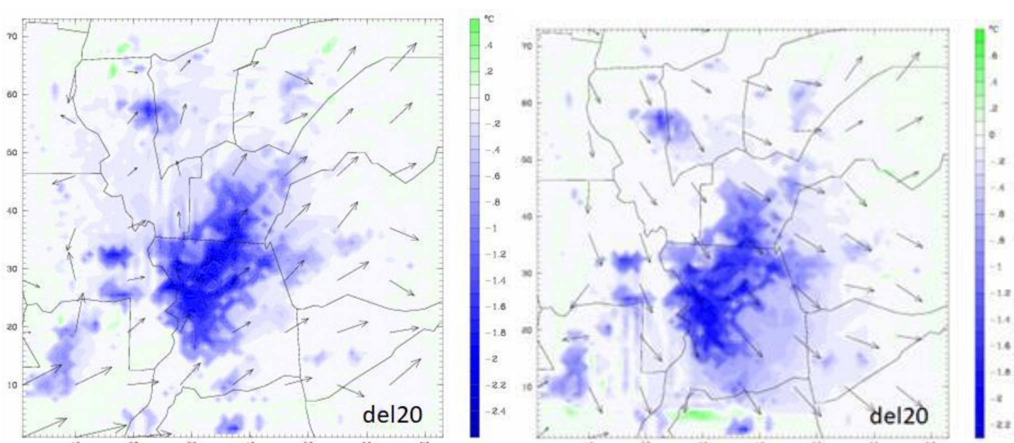

Case31. Left: 1300 PDT, July 27, 2050, RCP 4.5. Maximum cooling at this hour = 4.2 °C. Right: 1300 PDT, July 27, 2050, RCP 8.5. Maximum cooling at this hour = 4.2 °C.

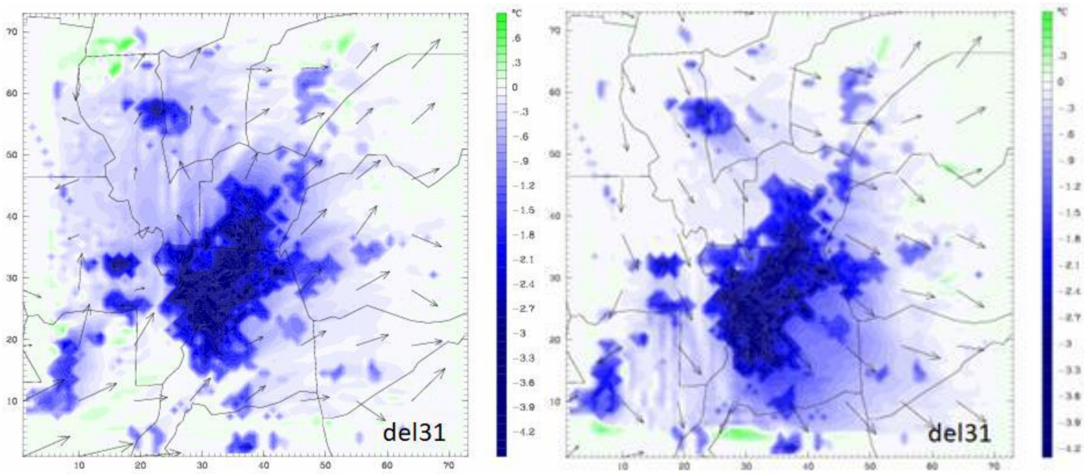

6.8 IMPACTS OF MITIGATION MEASURES ON THE UHI AND THE UHII IN FUTURE CLIMATE

6.8.1 Impact of mitigation measures on the 0600 PDT UHII in future climate

Figures 6-23 and 6-24 show the reductions (percentage-wise) in the 0600-PDT UHII averaged for all periods in 2050, for RCP 4.5 and RCP 8.5, respectively. Here, again, the caveat regarding case02 (as an extreme scenario) is to be born in mind.

The results show, in general, that the mitigation measures reduce the UHII in RCP 4.5 slightly more than in RCP 8.5 (because of the higher nighttime absolute temperatures in RCP 8.5 and the UHII definition as discussed earlier). The ranking of measures at the hour of 0600 PDT (including the extreme case02) is in the following order: 02, 31, 01, 20, and 10, in all sub-domains and in both RCP 4.5 and RCP 8.5. This ranking (order) of measures results from the larger nighttime effects of vegetation canopy cover relative to those from albedo modifications.

Figure 6-23: Impacts of mitigation measures on the 0600-PDT UHII in 2050 RCP 4.5. Vertical axis is percentage-wise reduction in the 0600-PDT UHII.

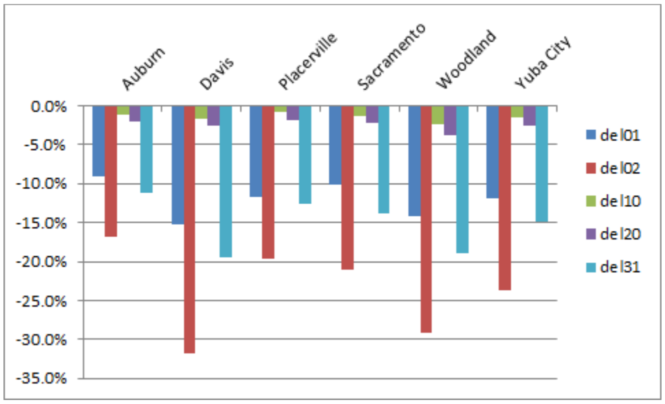

Figure 6-24: Impacts of mitigation measures on the 0600-PDT UHII in 2050 RCP 8.5. Vertical axis is percentage-wise reduction in the 0600-PDT UHII.

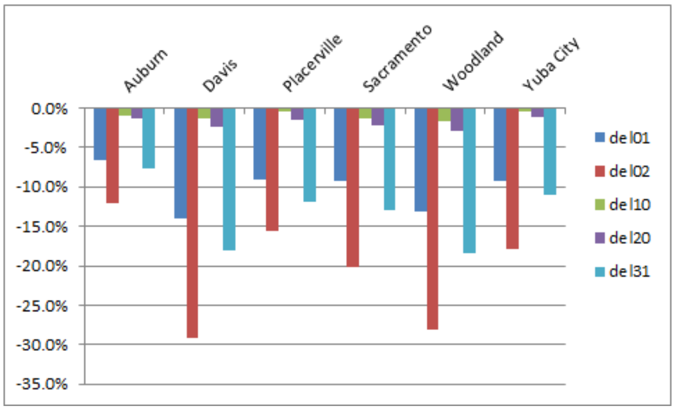

6.8.2 Impact of mitigation measures on the 1500 PDT UHII in future climate

Figures 6-25 and 6-26 summarize the reductions (percentage-wise) in the 1500-PDT UHII averaged for all periods in 2050, for RCP 4.5 and RCP 8.5, respectively.

The results from the 1500-PDT analysis show varying effects across scenarios and regions but also that, in general, the mitigation measures reduce the UHII in RCP 8.5 slightly more than in RCP 4.5 (which is the reverse of the effects during the hour at 0600 PDT). The ranking of measures at 1500 PDT (including the extreme case02) is in the following order: 31, 02, 20, then 10 and 01 tied, in all sub-domains and in both RCP 4.5 and RCP 8.5. This ranking (order) of measures is different from that at 0600-PDT (here the albedo measures are more effective) as this is for a daylight period.

Note that there is a single instance (anomaly) in Davis in RCP 4.5 where case10 causes a very small (1%) increase in the 1500-PDT UHII and a case in RCP 8.5 in Woodland where case01 has almost no effect on the UHII at this hour.

Figure 6-25: Impacts of mitigation measures on the 1500-PDT UHII in 2050 RCP 4.5. Vertical axis is percentage-wise reduction in the 1500-PDT UHII.

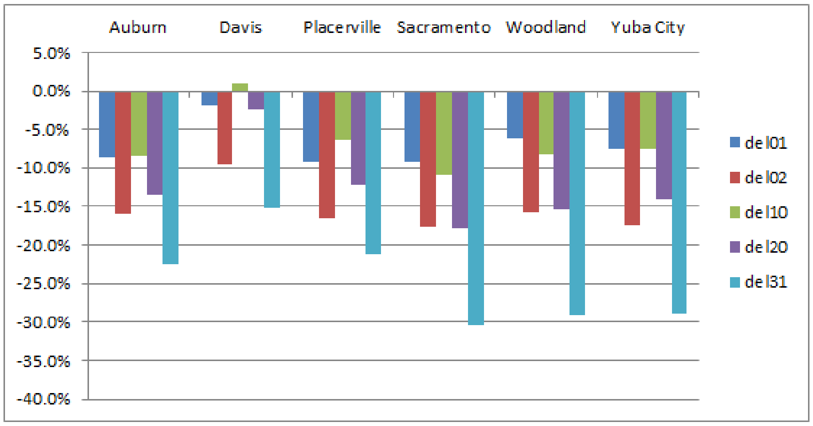

Figure 6-26: Impacts of mitigation measures on the 1500-PDT UHII in 2050 RCP 8.5. Vertical axis is percentage-wise reduction in the 1500-PDT UHII.

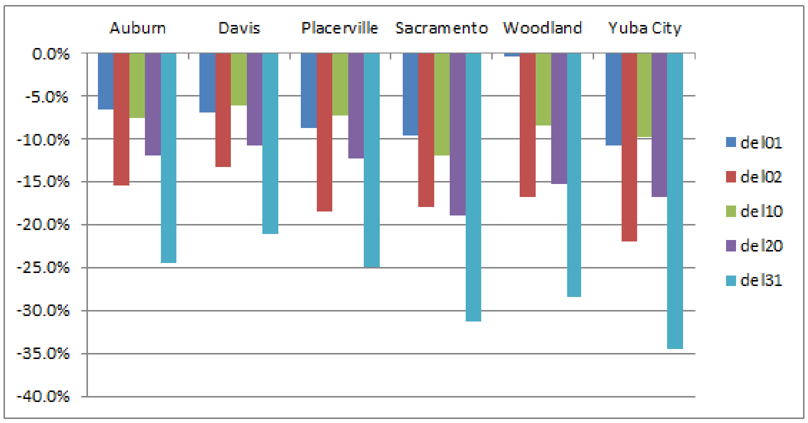

6.8.3 Impact of mitigation measures on the all-hours UHII in future climate

Finally, Figures 6-27 and 6-28 show the reductions (percentage-wise) in the all-hour UHII averaged for all periods in 2050, for RCP 4.5 and RCP 8.5, respectively.

The results indicate that the reductions are almost identical in RCP 4.5 and 8.5 (for each region) but that minor differences occur and that the reductions in RCP 8.5 are slightly smaller than those in RCP 4.5. The ranking of measures for the reduction in all-hours UHII (including extreme case02) is in the following order: 02, 31, 01, 20, and 10, in all sub-domains and in both RCP 4.5 and RCP 8.5. This order of measures is influenced by the effects of vegetation canopy cover, including the nighttime effect.

Figure 6-27: Impacts of mitigation measures on the all-hours UHII in 2050 RCP 4.5. Vertical axis is percentage-wise reduction in the all-hours UHII.

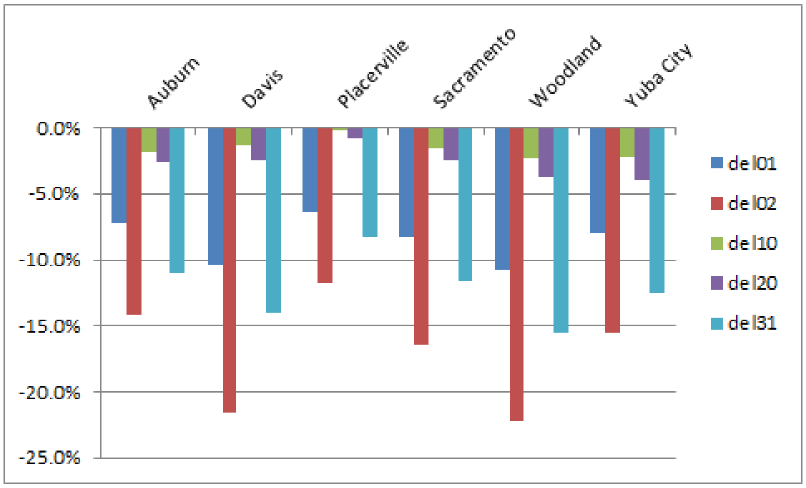

Figure 6-28: Impacts of mitigation measures on the all-hours UHII in 2050 RCP 8.5. Vertical axis is percentage-wise reduction in the all-hours UHII.

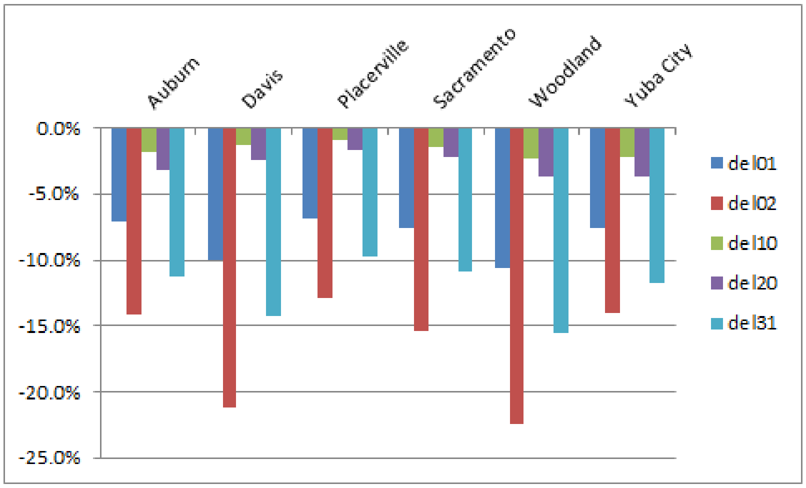

6.9 CHANGES IN THE NATIONAL WEATHER SERVICE HEAT INDEX (NWS HI) LEVELS IN FUTURE CLIMATE

Changes in the NWS HI warning levels resulting from changes in climate and urbanization, and the impacts of mitigation measures on the HI, were evaluated at the same probing locations defined in Section 5.15 (Figure 5-37). The analysis was carried out for all hours and ranges of hours. In this section, examples are provided for changes at 1700 PDT, i.e., averaged over all 1700 PDT hours in the period JJAS of 2050 for RCP 4.5 and RCP 8.5 for case00 and case31. The future-year NWS HI and its changes were also compared to the corresponding values in current climate (2013 – 2016) as seen in Figure 6-29 and Table 6-2, where the percentages of reductions in exceedances above specified NWS HI levels are given relative to thresholds "Danger", "Extreme caution", and "Caution".

Another goal of this analysis was to quantify the potential of heat-mitigation measures in "shifting down" the NWS HI from one warning level to a lower one, as was discussed in Section 5.15 for current climate. Several metrics are presented below that provide an assessment of these potential effects – some are specific to certain time intervals, others are more general indicators of averages.

In summary, it can be seen that the heat-mitigation measures can (1) shift down the NWS HI from one warning level to a lower one and (2) can offset the local-warming effects of urbanization and climate changes on the HI at all hours (compare the blue and red time series in Figure 6-29).

Figure 6-29: NWS HI and changes resulting from urban-cooling measures (case31) for the hour at 1700 PDT, year 2050, JJAS for RCP 4.5 and RCP 8.5.

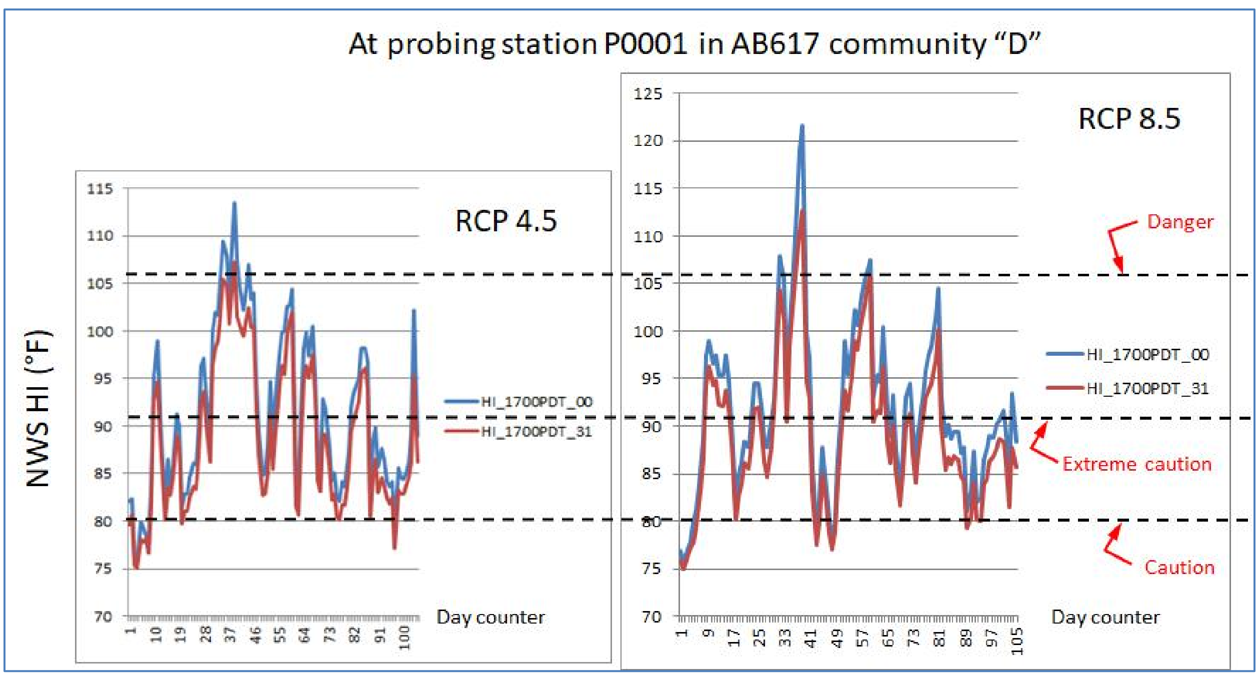

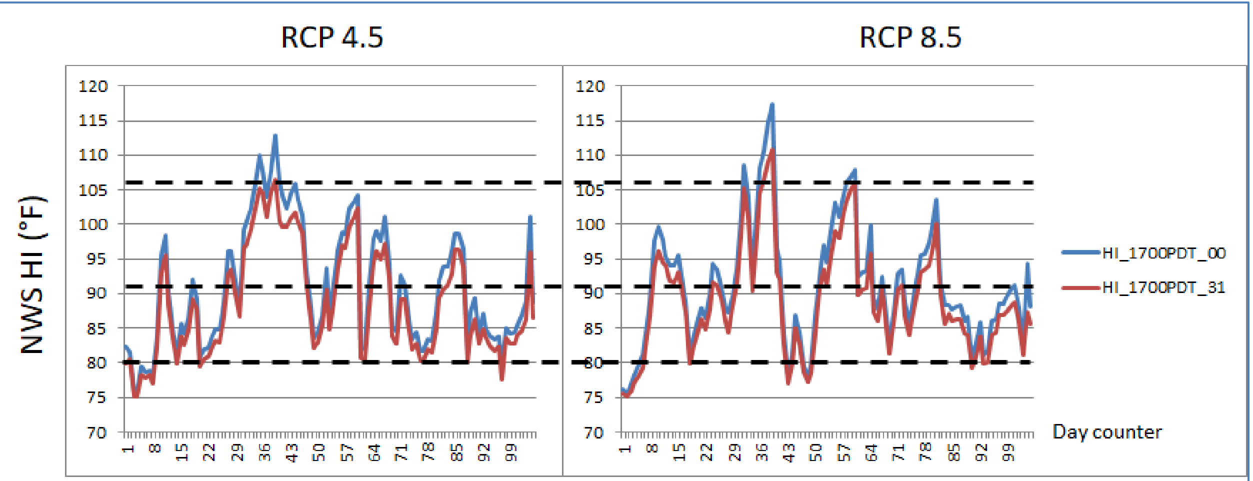

At probing station P0004 in AB617 community

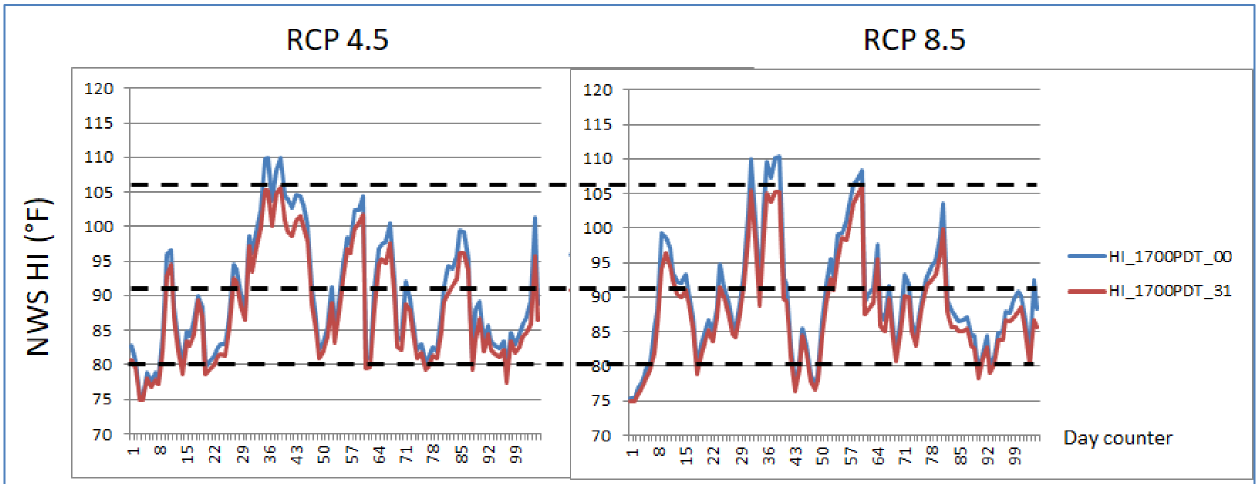

At probing station P0008 in AB617 community

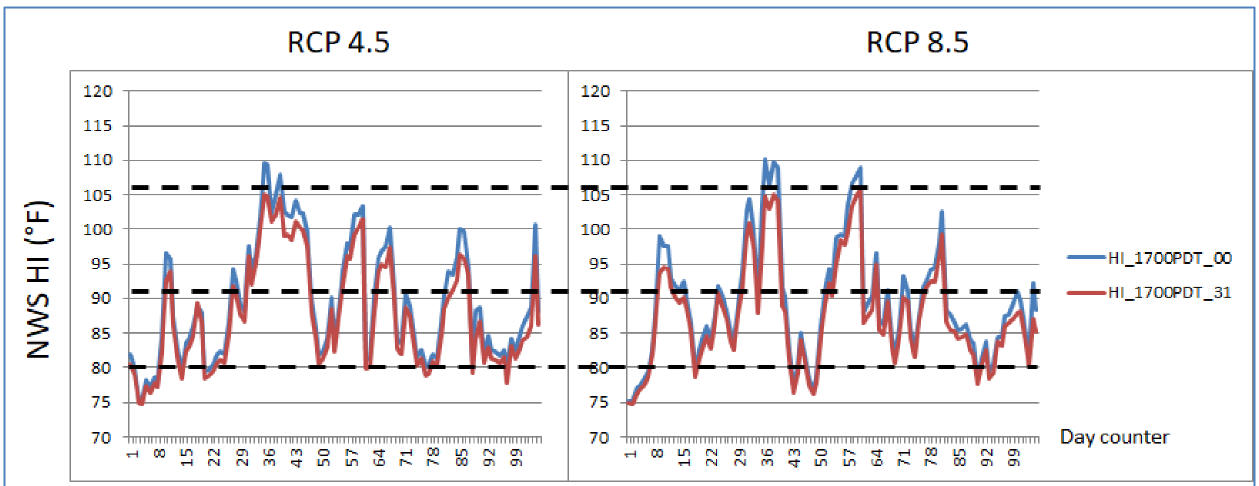

At probing station P0011 in AB617 community

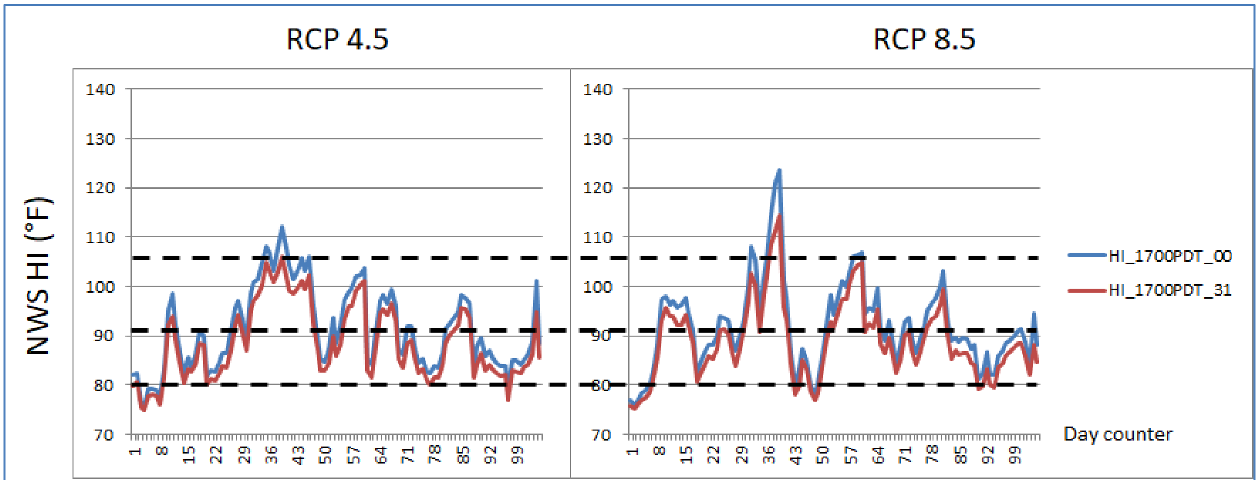

At probing station P0013 in Citrus Heights

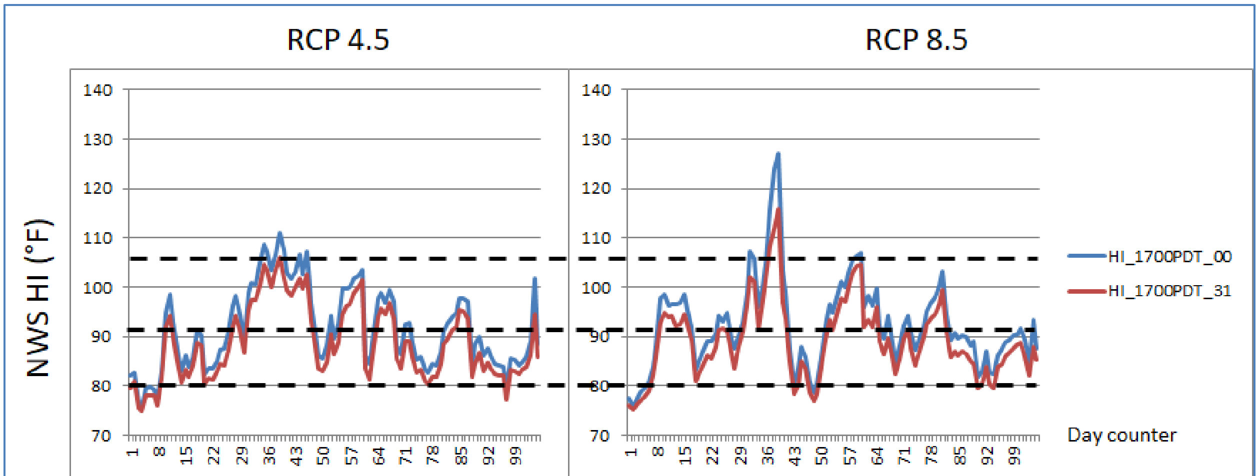

At probing station P0014 in Roseville

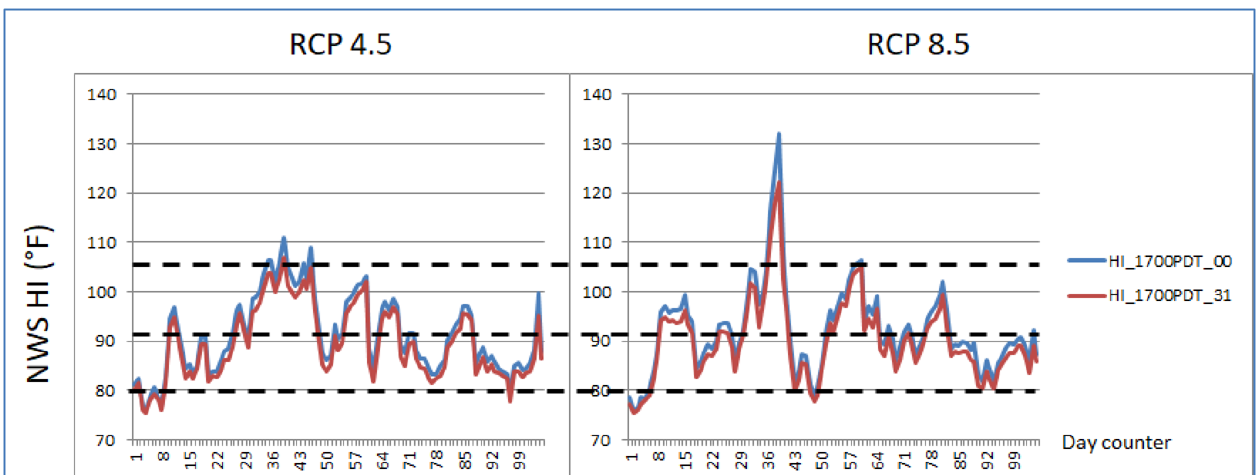

At probing station P0018 in Lincoln

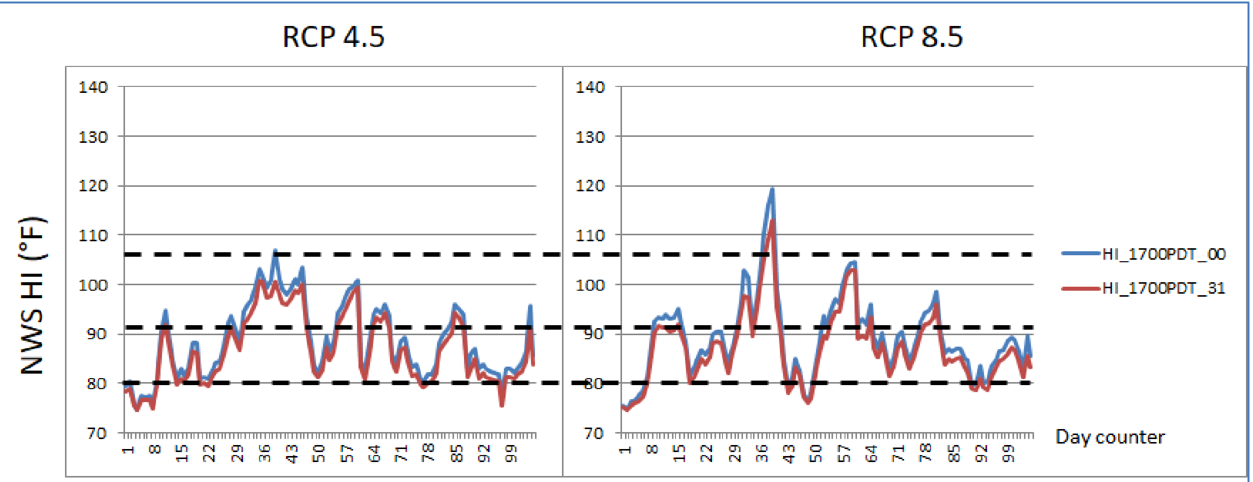

At probing station P0020 in El Dorado Hills

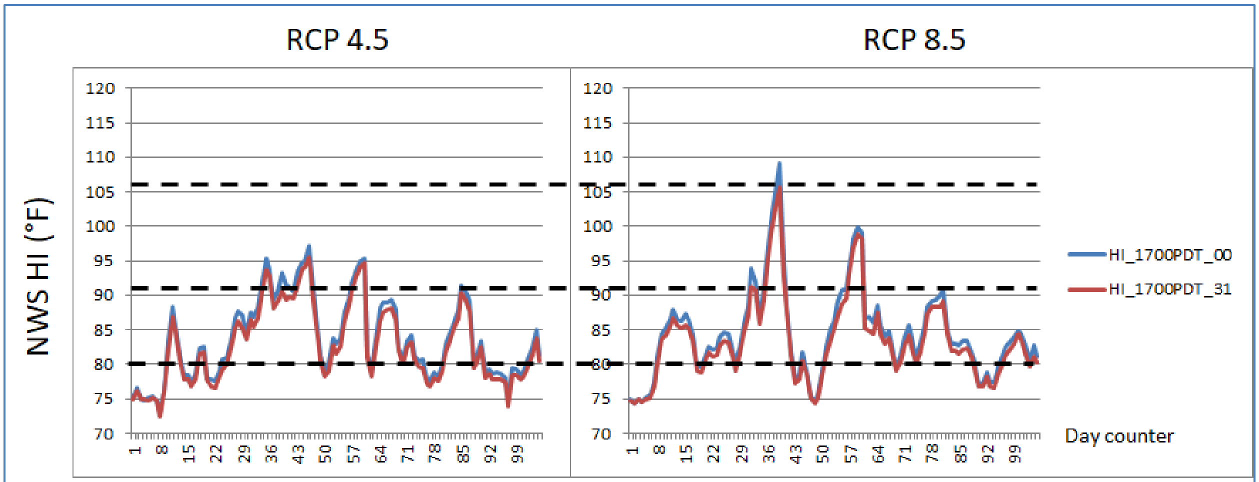

At probing station P0022 in Placerville

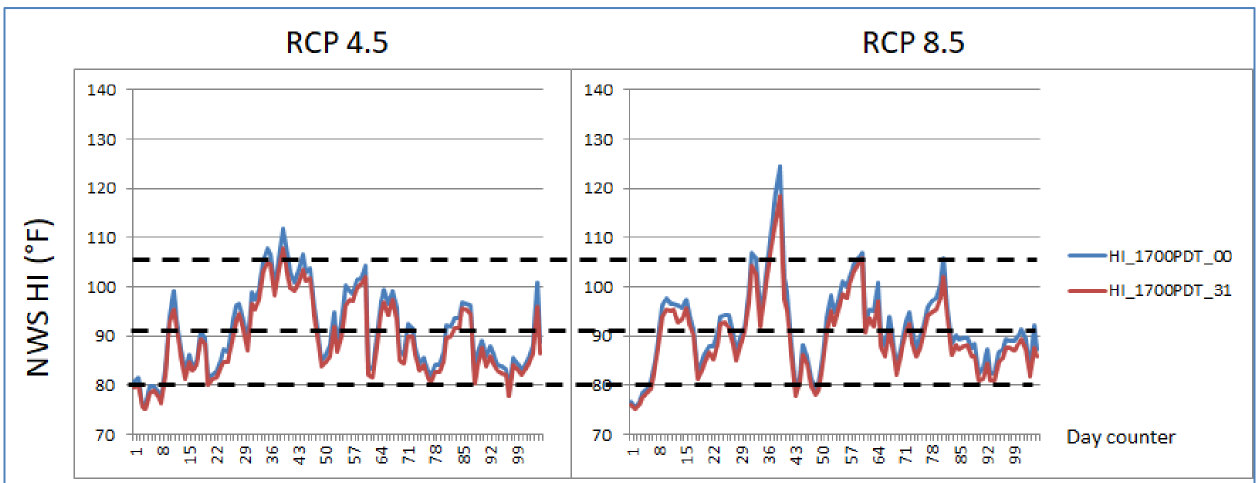

At probing station P0026 in Woodland

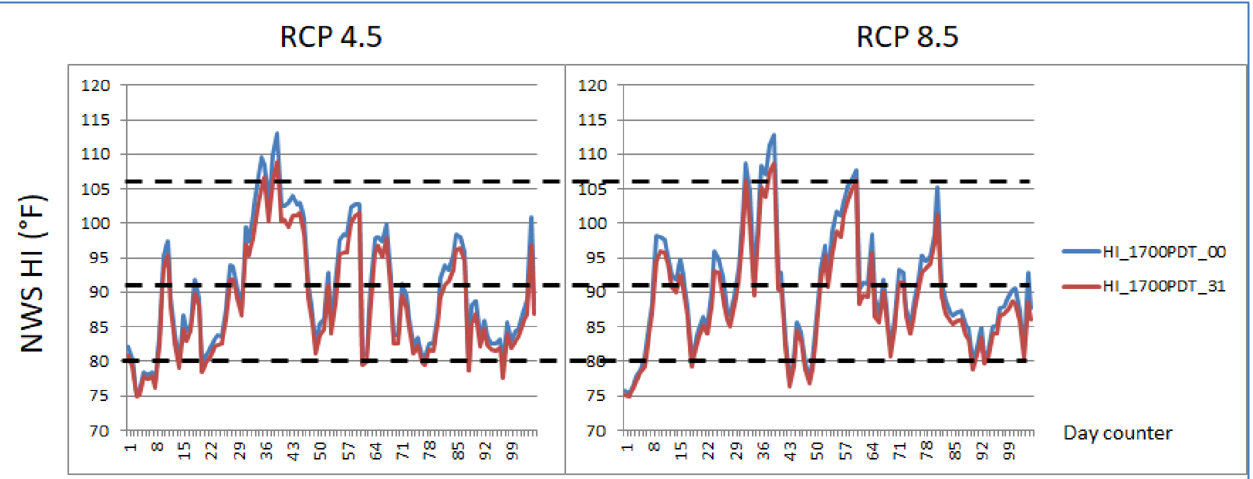

At probing station P0028 in Davis

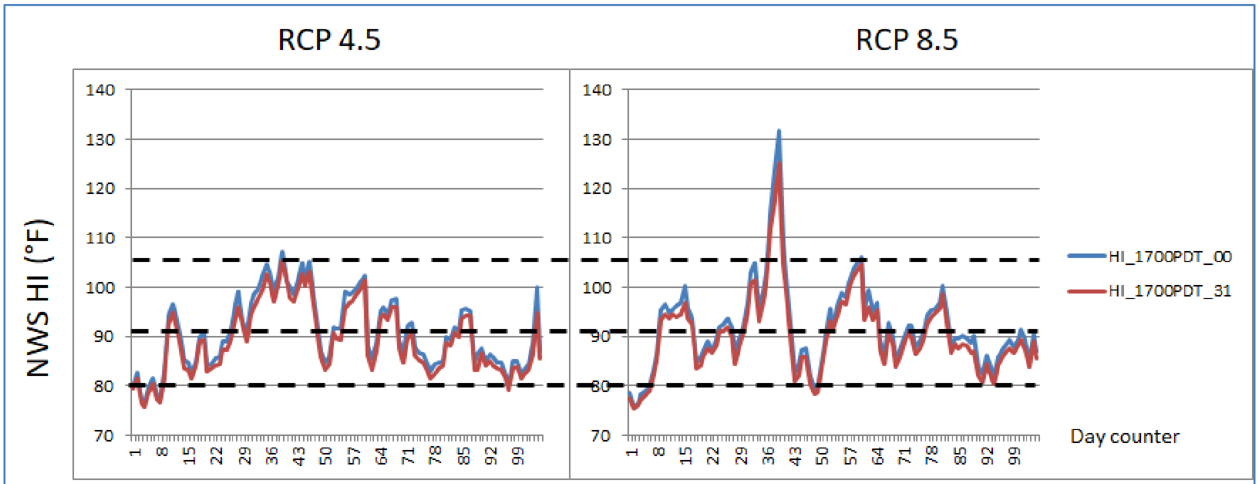

At probing station P0029 in Marysville

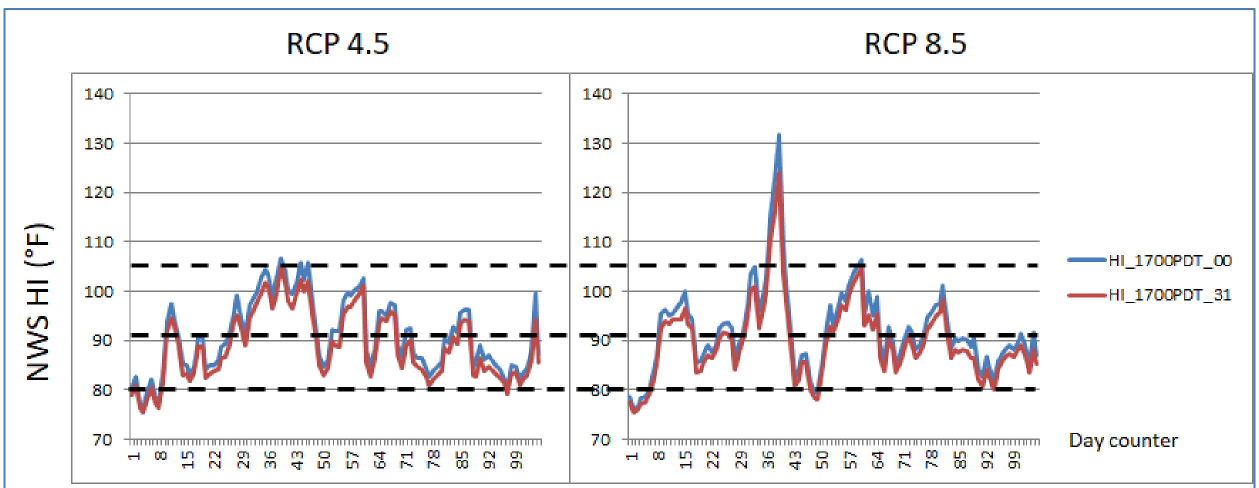

At probing station P0032 in Yuba City

Table 6-2: NWS HI and changes resulting from UHI-mitigation measures (case31) at hours 1700 PDT, year 2050, JJAS for RCP 4.5 and RCP 8.5. Current-climate NWS HI and changes are also provided for comparison.

P0001 AB617

NWS HI values at **1700 PDT** and exceedances above thresholds

P0001 AB617	Percent of DH (out of total) above threshold		
NWS HI thresholds	2013-2016	2050 RCP 4.5	2050 RCP 8.5
> 80 °F (caution)	93.0%	94.3%	93.5%
> 91 °F (extreme caution)	45.6%	49.8%	51.2%
> 106 °F (danger)	0.9%	6.8%	8.1%

Changes (reductions) in exceedances after deployment of case31

P0001 AB617	Decrease in exceedance following case31		
NWS HI thresholds	2013-2016	2050 RCP 4.5	2050 RCP 8.5
> 80 °F (caution)	-5.8%	-4.7%	-7.6%
> 91 °F (extreme caution)	-31.9%	-20.2%	-23.4%
> 106 °F (danger)	-66.2%	-83.6%	-57.7%

P0004 AB617

NWS HI values at **1700 PDT** and exceedances above thresholds

P0004 AB617	Percent of DH (out of total) above threshold		
NWS HI thresholds	2013-2016	2050 RCP 4.5	2050 RCP 8.5
> 80 °F (caution)	92.8%	94.3%	92.7%
> 91 °F (extreme caution)	43.5%	48.9%	49.4%
> 106 °F (danger)	0.6%	5.7%	8.1%

Changes (reductions) in exceedances after deployment of case31

P0004 AB617	Decrease in exceedance following case31		
NWS HI thresholds	2013-2016	2050 RCP 4.5	2050 RCP 8.5
> 80 °F (caution)	-5.0%	-5.2%	-7.1%
> 91 °F (extreme caution)	-28.6%	-22.3%	-27.8%
> 106 °F (danger)	-49.7%	-80.4%	-57.8%

Table 6-2, continued.

P0008 AB617

NWS HI values at **1700 PDT** and exceedances above thresholds

P0008 AB617	Percent of DH (out of total) above threshold		
NWS HI thresholds	2013-2016	2050 RCP 4.5	2050 RCP 8.5
> 80 °F (caution)	90.6%	92.6%	90.1%
> 91 °F (extreme caution)	36.0%	43.2%	43.6%
> 106 °F (danger)	0.3%	4.6%	9.2%

Changes (reductions) in exceedances after deployment of case31

P0008 AB617	Decrease in exceedance following case31		
NWS HI thresholds	2013-2016	2050 RCP 4.5	2050 RCP 8.5
> 80 °F (caution)	-5.2%	-9.6%	-4.1%
> 91 °F (extreme caution)	-30.5%	-13.8%	-33.2%
> 106 °F (danger)	-100.0%	-100.0%	-100.0%

P0011 AB617

NWS HI values at **1700 PDT** and exceedances above thresholds

P0011 AB617	Percent of DH (out of total) above threshold		
NWS HI thresholds	2013-2016	2050 RCP 4.5	2050 RCP 8.5
> 80 °F (caution)	90.1%	90.8%	89.2%
> 91 °F (extreme caution)	32.1%	40.2%	39.8%
> 106 °F (danger)	0%	3.5%	8.1%

Changes (reductions) in exceedances after deployment of case31

P0011 AB617	Decrease in exceedance following case31		
NWS HI thresholds	2013-2016	2050 RCP 4.5	2050 RCP 8.5
> 80 °F (caution)	-9.4%	-7.7%	-4.1%
> 91 °F (extreme caution)	-28.0%	-9.7%	-29.2%
> 106 °F (danger)	N/A	-100.0%	100.0%

Table 6-2, continued.

P0013 Citrus Heights

NWS HI values at **1700 PDT** and exceedances above thresholds

P0013 Citrus Heights	Percent of DH (out of total) above threshold		
NWS HI thresholds	2013-2016	2050 RCP 4.5	2050 RCP 8.5
> 80 °F (caution)	92.3%	94.3%	93.5%
> 91 °F (extreme caution)	44.8%	47.7%	51.2%
> 106 °F (danger)	1.4%	6.8%	7.1%

Changes (reductions) in exceedances after deployment of case31

P0013 Citrus Heights	Decrease in exceedance following case31		
NWS HI thresholds	2013-2016	2050 RCP 4.5	2050 RCP 8.5
> 80 °F (caution)	-4.9%	-3.9%	-8.6%
> 91 °F (extreme caution)	-33.5%	-21.0%	-25.4%
> 106 °F (danger)	-79.8%	-100.0%	-50.9%

P0014 Roseville

NWS HI values at **1700 PDT** and exceedances above thresholds

P0014 Roseville	Percent of DH (out of total) above threshold		
NWS HI thresholds	2013-2016	2050 RCP 4.5	2050 RCP 8.5
> 80 °F (caution)	93.4%	94.3%	95.2%
> 91 °F (extreme caution)	47.7%	49.6%	52.2%
> 106 °F (danger)	1.7%	7.9%	7.1%

Changes (reductions) in exceedances after deployment of case31

P0014 Roseville	Decrease in exceedance following case31		
NWS HI thresholds	2013-2016	2050 RCP 4.5	2050 RCP 8.5
> 80 °F (caution)	-6.1%	-4.1%	-8.7%
> 91 °F (extreme caution)	-36.2%	-20.3%	-23.4%
> 106 °F (danger)	-83.2%	-100.0%	-51.1%

Table 6-2, continued.

P0018 Lincoln

NWS HI values at **1700 PDT** and exceedances above thresholds

P0018 Lincoln	Percent of DH (out of total) above threshold		
NWS HI thresholds	2013-2016	2050 RCP 4.5	2050 RCP 8.5
> 80 °F (caution)	93.9%	95.1%	95.2%
> 91 °F (extreme caution)	52.7%	48.4%	52.1%
> 106 °F (danger)	2.0%	4.5%	6.1%

Changes (reductions) in exceedances after deployment of case31

P0018 Lincoln	Decrease in exceedance following case31		
NWS HI thresholds	2013-2016	2050 RCP 4.5	2050 RCP 8.5
> 80 °F (caution)	-4.7%	-2.9%	-5.8%
> 91 °F (extreme caution)	-27.0%	-15.8%	-15.0%
> 106 °F (danger)	-85.5%	-75.3%	-40.2%

P0020 El Dorado Hills

NWS HI values at **1700 PDT** and exceedances above thresholds

P0020 El Dorado Hills	Percent of DH (out of total) above threshold		
NWS HI thresholds	2013-2016	2050 RCP 4.5	2050 RCP 8.5
> 80 °F (caution)	89.0%	93.4%	90.9%
> 91 °F (extreme caution)	29.3%	37.8%	38.5%
> 106 °F (danger)	0.3%	1.1%	3.7%

Changes (reductions) in exceedances after deployment of case31

P0020 El Dorado Hills	Decrease in exceedance following case31		
NWS HI thresholds	2013-2016	2050 RCP 4.5	2050 RCP 8.5
> 80 °F (caution)	-4.8%	-8.5%	-7.1%
> 91 °F (extreme caution)	-31.9%	-12.8%	-30.2%
> 106 °F (danger)	-100.0%	-100.0%	-35.6%

Table 6-2, continued.

P0022 Placerville

NWS HI values at **1700 PDT** and exceedances above thresholds

P0022 Placerville	Percent of DH (out of total) above threshold		
NWS HI thresholds	2013-2016	2050 RCP 4.5	2050 RCP 8.5
> 80 °F (caution)	71.3%	68.2%	80.0%
> 91 °F (extreme caution)	10.4%	16.0%	12.2%
> 106 °F (danger)	0%	0%	1.2%

Changes (reductions) in exceedances after deployment of case31

P0022 Placerville	Decrease in exceedance following case31		
NWS HI thresholds	2013-2016	2050 RCP 4.5	2050 RCP 8.5
> 80 °F (caution)	-4.8%	-10.6%	-5.8%
> 91 °F (extreme caution)	-23.3%	-40.0%	-10.2%
> 106 °F (danger)	N/A	N/A	-100.0%

P0026 Woodland

NWS HI values at **1700 PDT** and exceedances above thresholds

P0026 Woodland	Percent of DH (out of total) above threshold		
NWS HI thresholds	2013-2016	2050 RCP 4.5	2050 RCP 8.5
> 80 °F (caution)	94.1%	94.3%	94.4%
> 91 °F (extreme caution)	48.7%	48.7%	52.1%
> 106 °F (danger)	1.4%	5.6%	5.9%

Changes (reductions) in exceedances after deployment of case31

P0026 Woodland	Decrease in exceedance following case31		
NWS HI thresholds	2013-2016	2050 RCP 4.5	2050 RCP 8.5
> 80 °F (caution)	-4.2%	-2.9%	-4.9%
> 91 °F (extreme caution)	-22.3%	-13.9%	-16.7%
> 106 °F (danger)	-79.7%	-80.0%	-40.3%

Table 6-2, continued.

P0028 Davis

NWS HI values at **1700 PDT** and exceedances above thresholds

P0028 Davis	Percent of DH (out of total) above threshold		
NWS HI thresholds	2013-2016	2050 RCP 4.5	2050 RCP 8.5
> 80 °F (caution)	92.1%	91.8%	91.8%
> 91 °F (extreme caution)	38.2%	46.1%	48.4%
> 106 °F (danger)	0.3%	4.7%	8.0%

Changes (reductions) in exceedances after deployment of case31

P0028 Davis	Decrease in exceedance following case31		
NWS HI thresholds	2013-2016	2050 RCP 4.5	2050 RCP 8.5
> 80 °F (caution)	-4.8%	-7.4%	-5.6%
> 91 °F (extreme caution)	-18.7%	-18.8%	-29.7%
> 106 °F (danger)	-1.1%	-27.0%	-43.8%

P0029 Marysville

NWS HI values at **1700 PDT** and exceedances above thresholds

P0029 Marysville	Percent of DH (out of total) above threshold		
NWS HI thresholds	2013-2016	2050 RCP 4.5	2050 RCP 8.5
> 80 °F (caution)	94.6%	95.1%	93.5%
> 91 °F (extreme caution)	61.0%	47.3%	51.0%
> 106 °F (danger)	3.4%	1.1%	5.0%

Changes (reductions) in exceedances after deployment of case31

P0029 Marysville	Decrease in exceedance following case31		
NWS HI thresholds	2013-2016	2050 RCP 4.5	2050 RCP 8.5
> 80 °F (caution)	-2.6%	-2.6%	-2.0%
> 91 °F (extreme caution)	-22.1%	-17.9%	-20.5%
> 106 °F (danger)	-58.7%	-100.0%	-26.1%

Table 6-2, continued.

P0032 Yuba City

NWS HI values at **1700 PDT** and exceedances above thresholds

P0032 Yuba City	Percent of DH (out of total) above threshold		
NWS HI thresholds	2013-2016	2050 RCP 4.5	2050 RCP 8.5
> 80 °F (caution)	94.8%	95.9%	93.5%
> 91 °F (extreme caution)	62.5%	49.2%	53.0%
> 106 °F (danger)	3.4%	1.1%	6.1%

Changes (reductions) in exceedances after deployment of case31

P0032 Yuba CIty	Decrease in exceedance following case31		
NWS HI thresholds	2013-2016	2050 RCP 4.5	2050 RCP 8.5
> 80 °F (caution)	-3.5%	-4.0%	-3.4%
> 91 °F (extreme caution)	-29.5%	-21.5%	-22.1%
> 106 °F (danger)	-75.2%	-100.0%	-40.0%

6.10 IMPACTS OF MITIGATION MEASURES ON THE UHII EXCEEDANCES RELATIVE TO A SPECIFIED TEMPERATURE THRESHOLD IN FUTURE CLIMATE

Figure 6-30 summarizes the percentage-wise reductions in the UHII (DH exceedances) relative to a specified temperature threshold of 35 °C (95 °F) which is a threshold commonly used by the electric utilities in calculating summertime cooling loads. This is shown in the figure for year 2050 and both RCP 4.5 and RCP 8.5.

The most effective measure at reducing the UHII above 35 °C is case31 (even if the extreme case02 is included in the analysis), followed by case02, then albedo (case20) and vegetation-canopy cover (case01) with relatively similar effects overall, and finally case10 (albedo). This order is seen across all regions and in both RCP 4.5 and RCP 8.5. The reductions are slightly larger in RCP 8.5 than in RCP 4.5 (as explained in the following section). The largest reductions (percentage-wise) are seen in Placerville because this area has only small UHII exceedances in the first place. It is important to reiterate again that the changes discussed in this section are changes in UHII not in absolute temperature.

Figure 6-30: Changes (percentage-wise) of the UHII exceedance above 35 C.

RCP 4.5

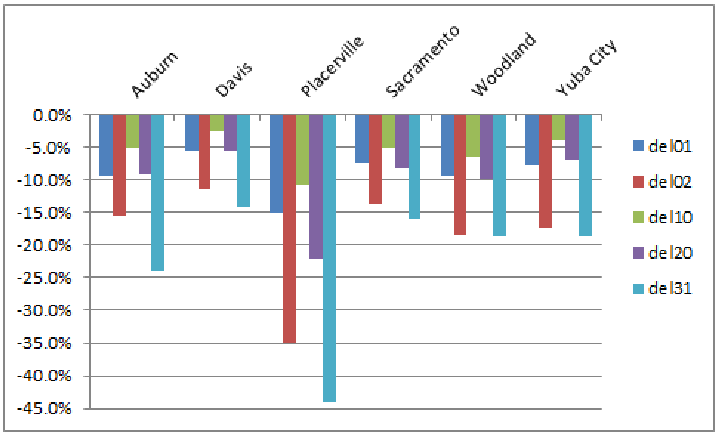

RCP 8.5

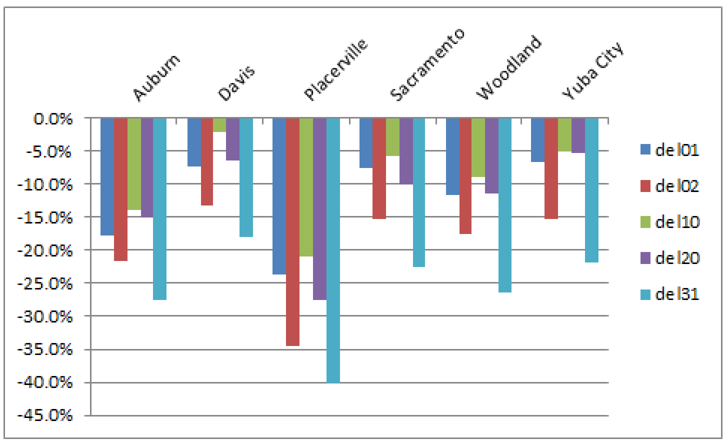

6.11 IMPACTS OF MITIGATION MEASURES ON TEMPERATURE EXCEEDANCES (DH) RELATIVE TO SPECIFIED THRESHOLDS IN FUTURE CLIMATE

In this section, the changes in temperature, e.g., cumulative DH, above certain thresholds, 35 and 38 °C, are discussed. It is noted here, again, that this analysis of temperature (DH) versus thresholds is different from a similar analysis of DH in terms of the NWS HI (discussed earlier, in Section 6.9) in that the NWS HI also includes humidity in the calculations whereas the analysis in this section is based only on dry-bulb temperature. This was also discussed in Section 5.14.

35 °C threshold

Figure 6-31 shows the percentage-wise changes in degree-hour (°C·hr) exceedances above 35 °C in sub-domains of interest, for all modeled time intervals (JJAS 2050), and for RCP 4.5 and RCP 8.5. For each time interval, the changes are presented for five scenarios or measures as an indication to their mitigation potentials relative to a corresponding base scenario. As before, the caveat related to case02 (as an extreme measure) should be reiterated.

Figure 6-31 shows that there is significant variation in the reduction of exceedances across different time intervals within each domain and variations from RCP 4.5 to RCP 8.5 within each region. There are also several cases (in different areas) where no exceedances occur above 35 °C in RCP 4.5 but significant exceedances are seen in RCP 8.5. As a result, the figures may be misleading in suggesting larger reductions in RCP 8.5 when there are none in RCP 4.5 (because there are no exceedances in RCP 4.5 to begin with).

The ranking (order) of measures in terms of effectiveness is as follows (applies to both RCP 4.5 and 8.5): in Auburn: 31, 02, 20, 01, 10; in Davis: 31, 02, 20, and 01/10 tied; in El Dorado Hills: 31, 02, 20, 01, 10; in Placerville: 31, 02, 20/01 tied, and 10; in Sacramento: 31, 02, 20, 01/10 tied; in Woodland: 31, 02/20 tied, 01/10 tied; and in Yuba City: 31, 02, 20/01 tied, then 10.

Figure 6-31: Changes in degree-hours above 35 °C

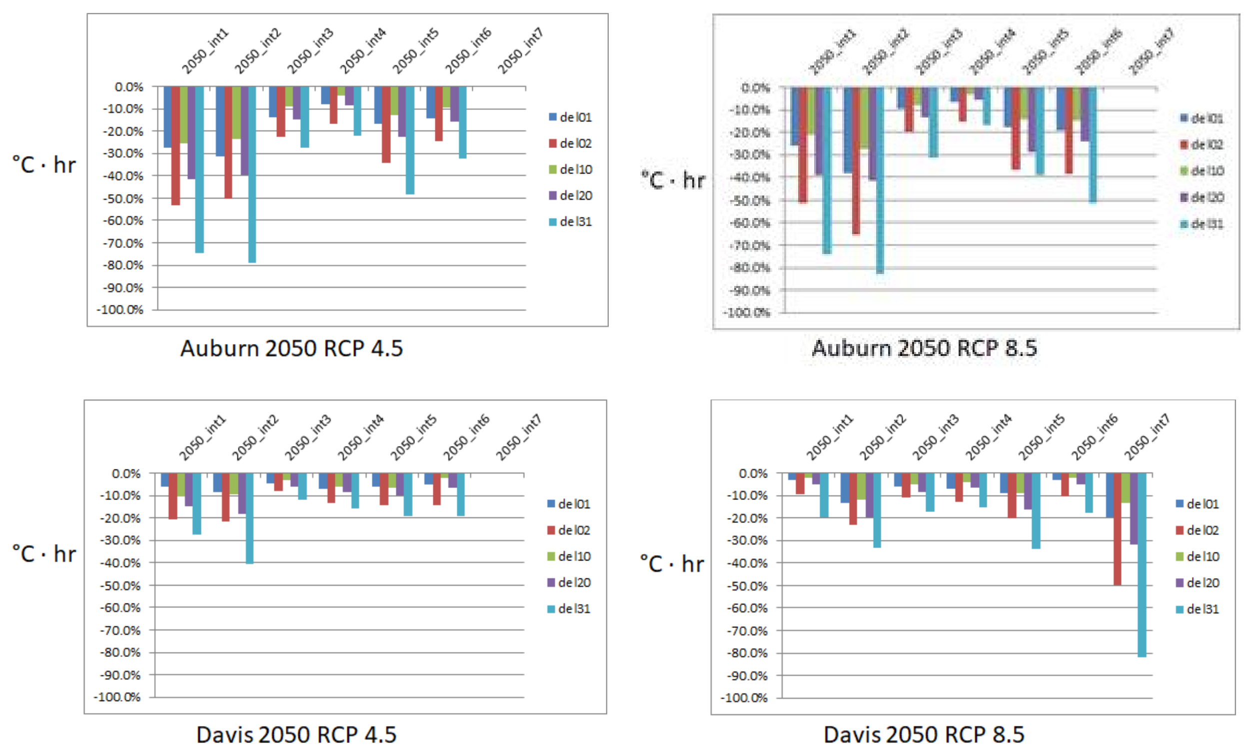

Figure 6-31, continued.

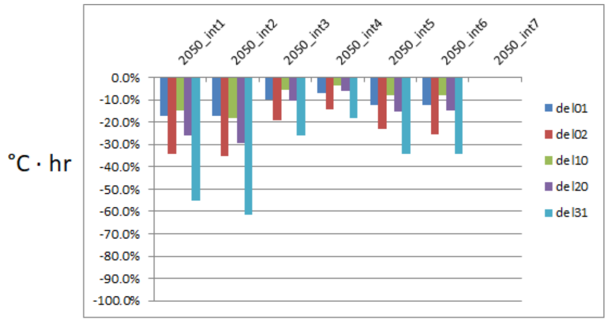

El Dorado Hills 2050 RCP 4.5

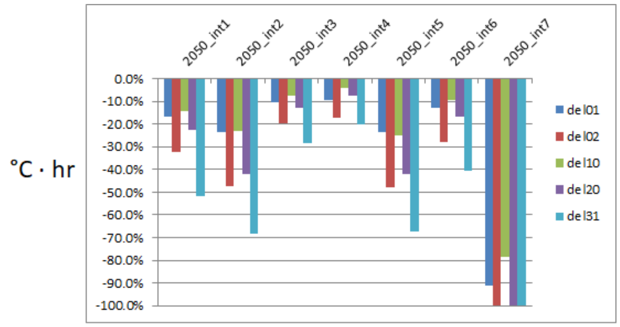

El Dorado Hills 2050 RCP 8.5

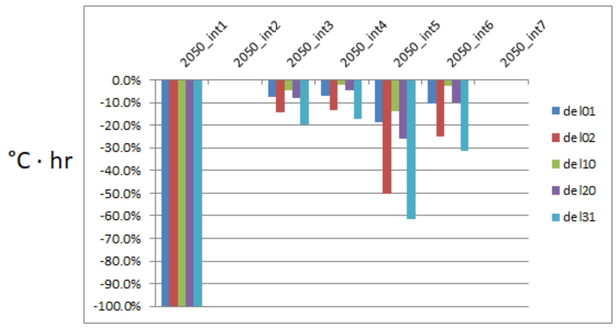

Placerville 2050 RCP 4.5

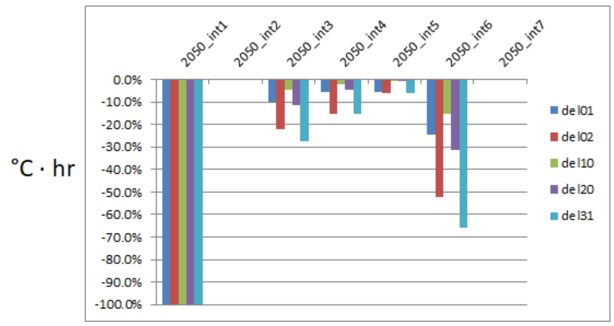

Placerville 2050 RCP 8.5

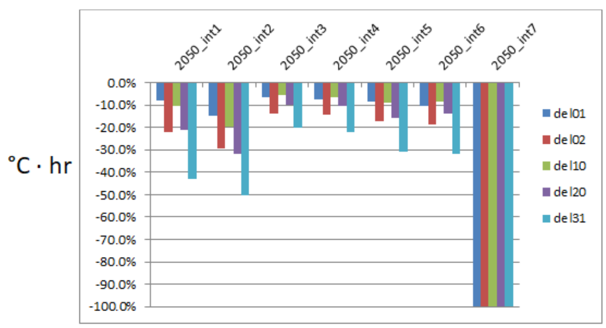

Sacramento 2050 RCP 4.5

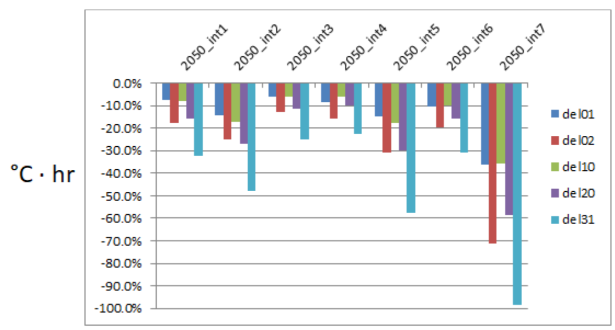

Sacramento 2050 RCP 8.5

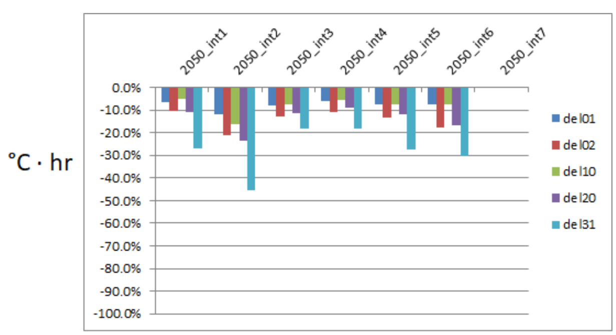

Woodland 2050 RCP 4.5

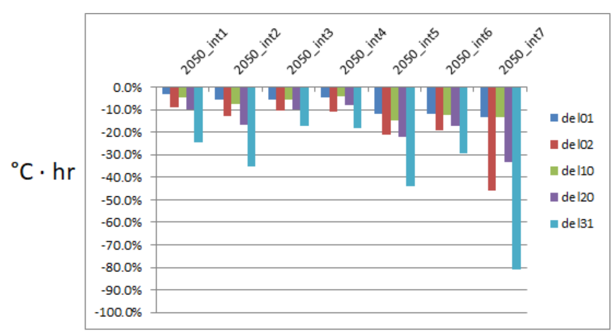

Woodland 2050 RCP 8.5

Figure 6-31, continued.

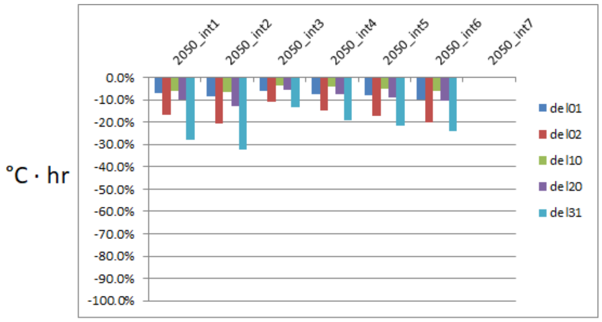

Yuba City 2050 RCP 4.5

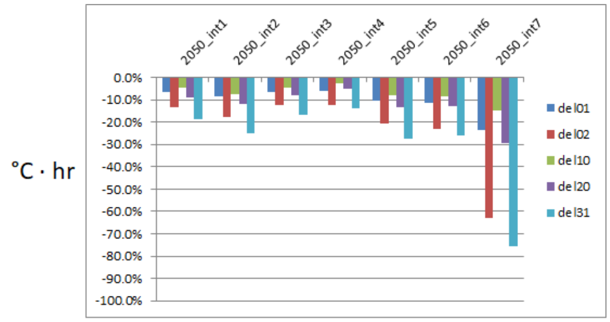

Yuba City 2050 RCP 8.5

38 °C threshold

The threshold of 38 °C is of interest to utilities in the region (SMUD) in planning for electric demand. The percentage-wise reductions in exceedances above 38 °C are smaller than the corresponding reductions over 35 °C, or non-existent in some cases, since there are fewer exceedances over 38 than over 35 °C to begin with (compare Figure 6-32 to Figure 6-31).

Figure 6-32 shows the changes (percentage-wise) in degree-hour (°C·hr) exceedances above 38 °C in sub-domains of interest, for all modeled time intervals (JJAS 2050), and for both RCP 4.5 and RCP 8.5. As with the 35 °C threshold, the changes are presented for five scenarios or measures to characterize their mitigation potentials relative to a corresponding base scenario.

The ranking (order) of measures in terms of effectiveness is slightly different from that for the 35 °C threshold, and is as follows (applies to both RCP 4.5 and RCP 8.5): in Auburn: 31, 02, 20, 01, 10; in Davis: 31, 02, 20, and 01/10 tied; in El Dorado Hills: 31, 02, 20, 01, 10; in Placerville: 31, 02, 20, 01, 10; in Sacramento: 31, 02/20 tied, 01/10 tied; in Woodland: 31, 20, 02, 10, 01; and in Yuba City: 31, 02, 20, 01, 10.

Figure 6-32: Changes in degree-hours above 38 °C

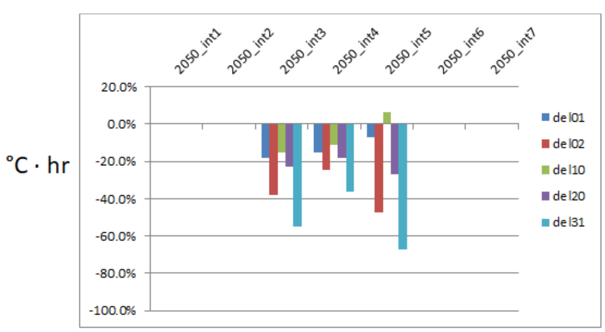

Auburn 2050 RCP 4.5

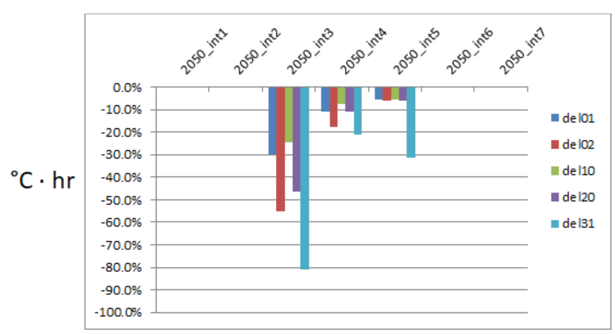

Auburn 2050 RCP 8.5

Figure 6-32, continued.

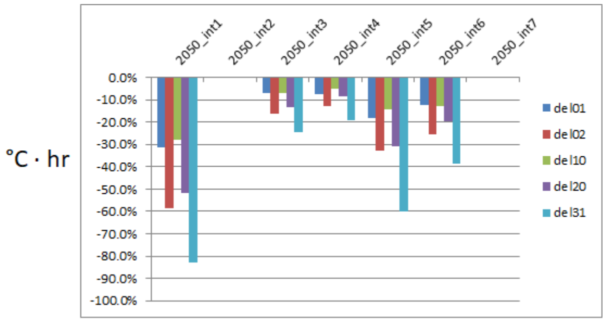

Davis 2050 RCP 4.5

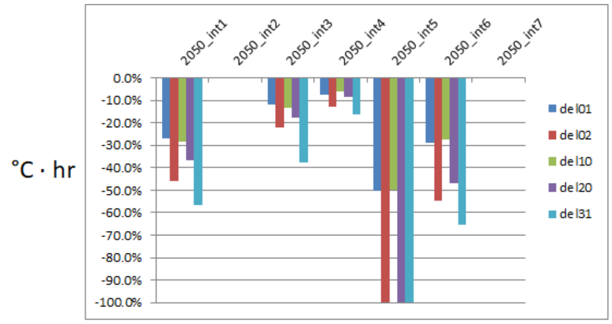

Davis 2050 RCP 8.5

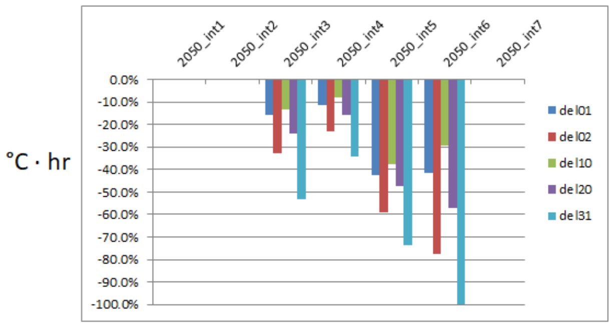

El Dorado Hills 2050 RCP 4.5

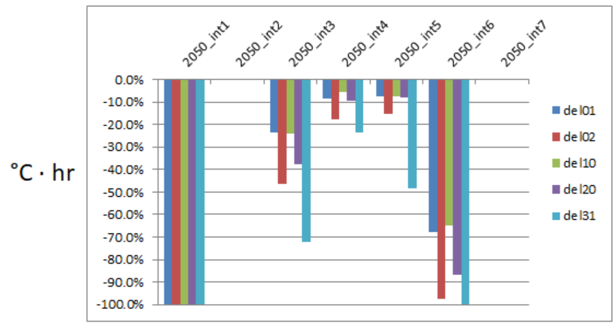

El Dorado Hills 2050 RCP 8.5

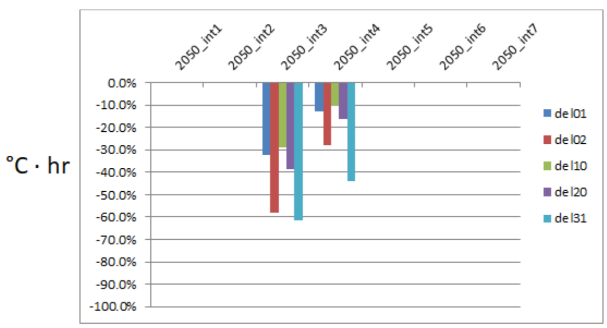

Placerville 2050 RCP 4.5

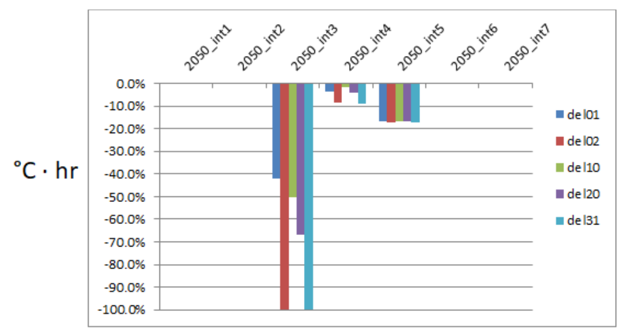

Placerville 2050 RCP 8.5

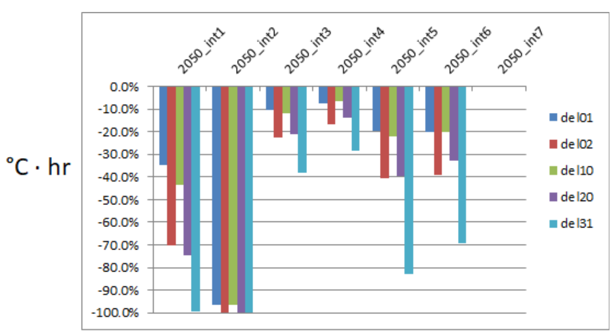

Sacramento 2050 RCP 4.5

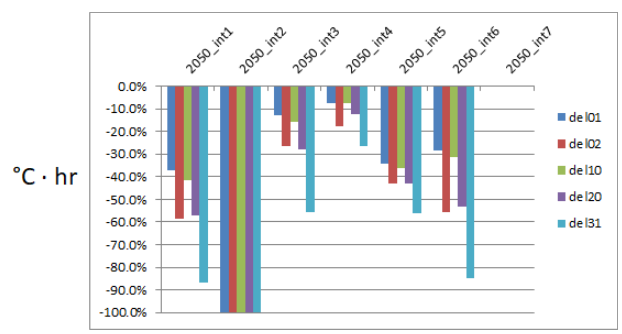

Sacramento 2050 RCP 8.5

Figure 6-32, continued.

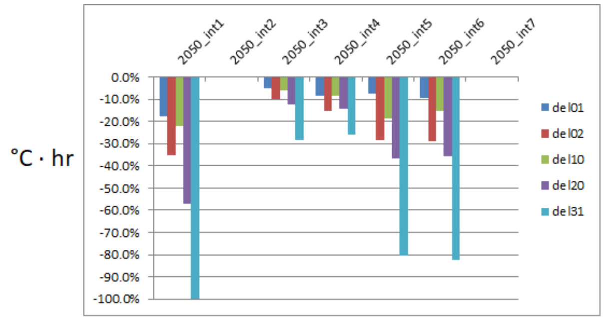

Woodland 2050 RCP 4.5

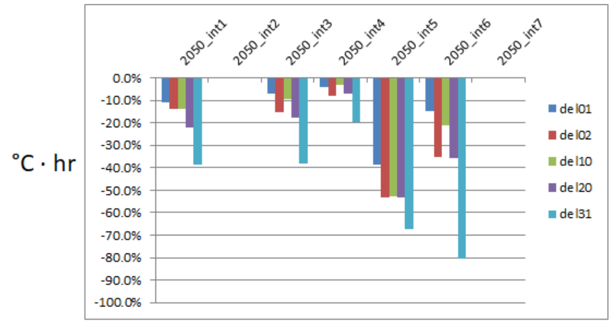

Woodland 2050 RCP 8.5

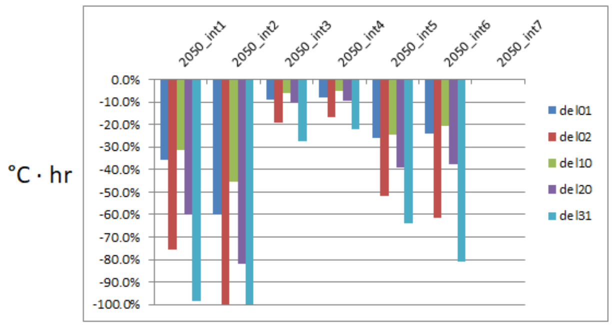

Yuba City 2050 RCP 4.5

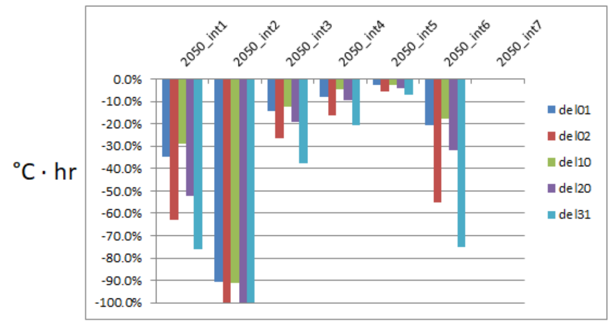

Yuba City 2050 RCP 8.5

6.12 IMPACTS OF SMART GROWTH ON TEMPERATURE EXCEEDANCES RELATIVE TO SPECIFIED THRESHOLDS.

The 2050 smart growth scenario defined earlier (in Section 6.4) was evaluated for impacts on exceedances (DH) above two thresholds (35 and 38 °C) and compared against those of the BAU scenario for year 2050 based on the USGS LUCAS projections defined in Section 6.3. As discussed earlier, the impacts are evaluated (in this section) only at those grid cells where urbanization was avoided. If averaging over whole sub-domains, the effects are much smaller.

Figure 6-33 provides a summary of these impacts, presented as percentage-wise reductions in degree-hours (DH) over the thresholds. The reason behind the apparent larger reductions in exceedances above 38 °C (right-side charts) than above 35 °C (left-side charts) is because there is initially less exceedance above 38 compared to above 35 °C, hence relatively easier to offset a larger fraction of the exceedance above 38 °C.

An examination of the results presented in Figure 6-33 suggests that as a crude overall average, the avoided exceedances (DH) as a result of smart growth are: (1) in Auburn: 35% avoided exceedances over 35 °C and 40% avoided exceedances over 38 °C; (2) in Davis, the avoided exceedances are 10% and 20%, respectively; (3) in El Dorado Hills, avoided exceedances are 25% and 35%, respectively; (4) in Sacramento, 20% and 40% respectively, and (5) in Yuba City, 30% and 60%, respectively.

Figure 6-33: Changes in degree-hours above 35 (left charts) and 38 °C (right charts) resulting from smart growth scenarios

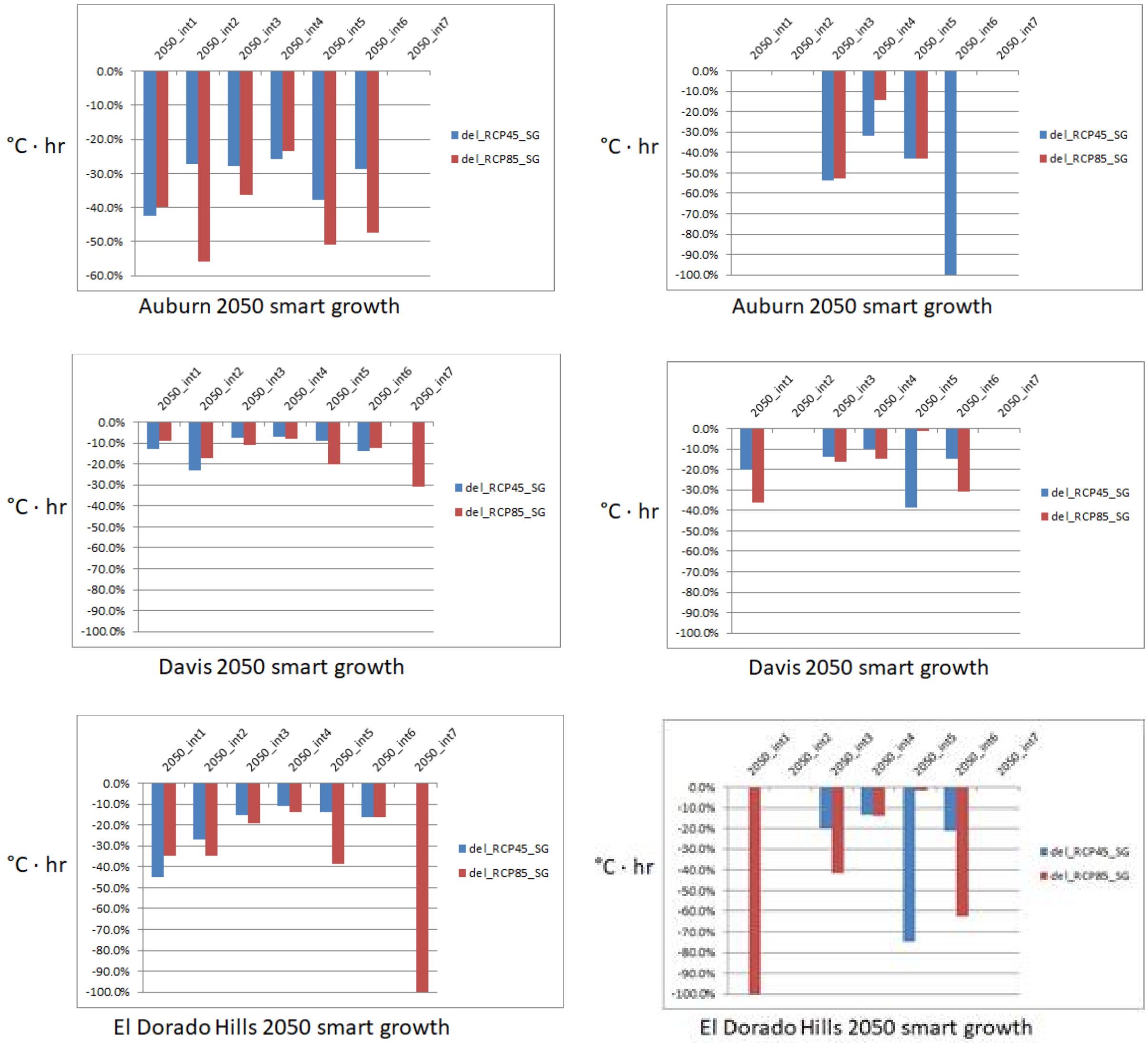

Figure 6-33, continued.

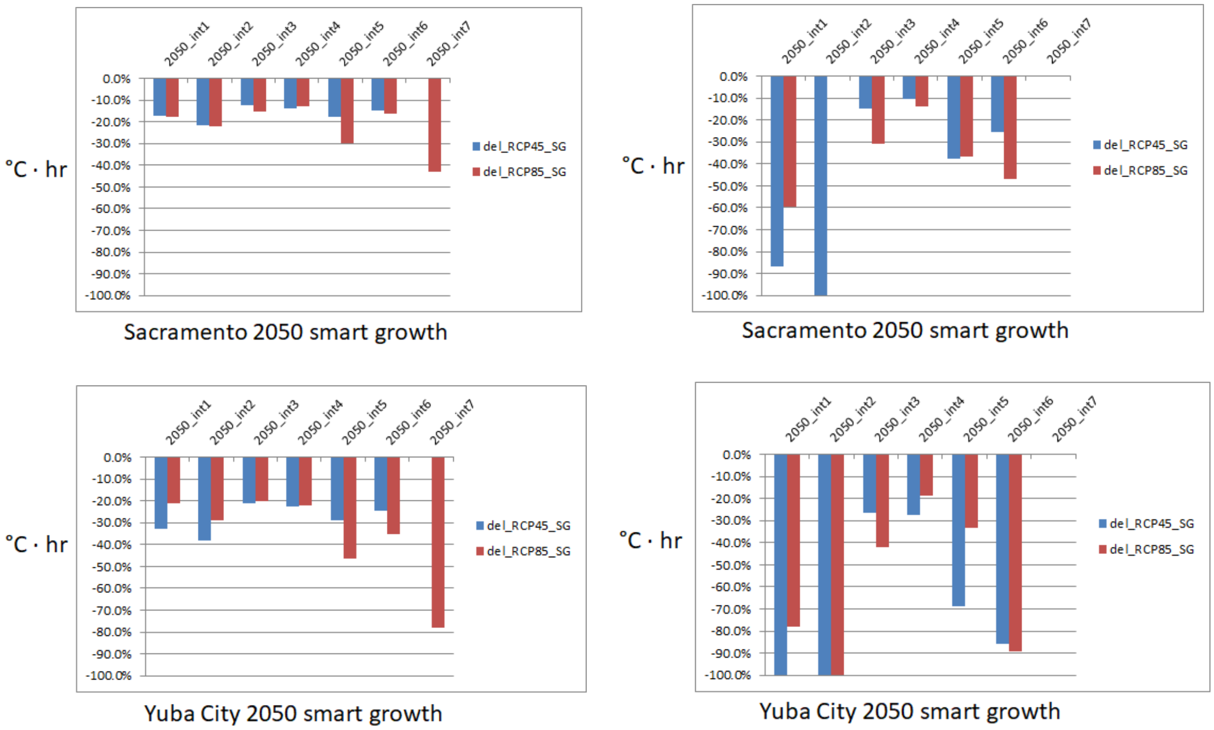

6.13 LOCAL OFFSETS TO THE UHII IN FUTURE CLIMATES

In this section, the 500-m simulations (discussed in Section 5) are revisited but this time in the context of future climate (2050). The goal is to evaluate the effectiveness of localized measures in offsetting the future-climate UHII that was characterized earlier in Section 6.6.

Tables 6-3 (for RCP 4.5) and 6-4 (for RCP 8.5) are structured in a manner similar to Table 5-23 (in Section 5.23), but for future climates. As before, these are the effects of mitigation measures in standalone mode of implementation at the geographical areas identified in the first column.

The model results show that the effectiveness of the mitigation measures in 2050 is generally similar to their effectiveness in current climate. In other words, the UHII attainment levels (percentages) for various measures are of the same magnitudes in 2050 (RCP 4.5 and RCP 8.5) as they are in current climate. Compare the last two columns in Tables 6-3 and 6-4 with the last two columns in Table 5-23. The reason, as explained earlier, is that increased urbanization, while contributing to additional local warming, also means an increase in technical potential, i.e., area available for the deployment of mitigation measures, thus keeping the UHII offset levels relatively similar to those in current climates or even slightly larger in some cases.

Table 6-3: 2050 RCP 4.5 temperature summaries and attainment of the UHII in future climate

Project area	All-hours Tair UHII (°C)**		Localized/no advection UHII attainment local mitigation only	Localized+advection UHII attainment local mitigation+advection
D05 Yuba City / Marysville Downtown YC and M	2.96			
		Cool roofs / pavements	-47%	-73%
		Cool pavements	-37%	-63%
		Electric vehicles	-6%	-31%
		Vegetation cover	-57%	-83%
D06 Woodland DAC census tracts	2.80			
		Cool roofs / pavements	-46%	-80%
		Cool pavements	-53%	-87%
		Electric vehicles	-5%	-39%
		Vegetation cover	-39%	-73%
D07 Sac / SE Sac AB617 A, B, D	5.00			
		Cool roofs / pavements	-26%	-62%
		Cool pavements	-28%	-64%
		Electric vehicles	-5%	-41%
		Vegetation cover	-30%	-66%
D07 Sac / SE Sac AB617 C, E, G	2.67			
		Cool roofs / pavements	-49%	-87%
		Cool pavements	-52%	-90%
		Electric vehicles	-9%	-47%
		Vegetation cover	-55%	-93%

Project area	All-hours Tair UHII (°C)**		Localized/no advection UHII attainment local mitigation only	Localized+advection UHII attainment local mitigation+advection
D08 Granite Bay	5.55			
		Cool roofs / pavements	-25%	-50%
		Cool pavements	-31%	-56%
		Electric vehicles	-6%	-30%
		Vegetation cover	-19%	-44%
D08 Roseville	6.42			
		Cool roofs / pavements	-22%	-54%
		Cool pavements	-27%	-59%
		Electric vehicles	-5%	-37%
		Vegetation cover	-16%	-48%
D09 El Dorado Hills	5.02			
		Cool roofs / pavements	-30%	-50%
		Cool pavements	-34%	-54%
		Electric vehicles	-4%	-24%
		Vegetation cover	-22%	-43%
D09 Folsom	5.46			
		Cool roofs / pavements	-27%	-53%
		Cool pavements	-31%	-57%
		Electric vehicles	-4%	-29%
		Vegetation cover	-20%	-46%
D10 Placerville / Diamond Springs / El Dorado City	1.59			
		Cool roofs / pavements	-75%	-99%
		Cool pavements	-101%	-125%
		Electric vehicles	-5%	-29%
		Vegetation cover	-82%	-106%

Table 6-4: 2050 RCP 8.5 temperature summaries and attainment of the UHII in future climate

Project area	All-hours Tair UHII (°C)**		Localized/no advection UHII attainment local mitigation only	Localized+advection UHII attainment local mitigation+advection
D05 Yuba City / Marysville Downtown YC and M	2.64	Cool roofs / pavements	-53%	-79%
		Cool pavements	-42%	-67%
		Electric vehicles	-6%	-32%
		Vegetation cover	-64%	-90%
D06 Woodland DAC census tracts	2.57	Cool roofs / pavements	-50%	-83%
		Cool pavements	-57%	-91%
		Electric vehicles	-6%	-39%
		Vegetation cover	-42%	-76%
D07 Sac / SE Sac AB617 A, B, D	5.13	Cool roofs / pavements	-25%	-61%
		Cool pavements	-27%	-63%
		Electric vehicles	-5%	-40%
		Vegetation cover	-29%	-64%
D07 Sac / SE Sac AB617 C, E, G	2.99	Cool roofs / pavements	-43%	-83%
		Cool pavements	-47%	-86%
		Electric vehicles	-8%	-47%
		Vegetation cover	-49%	-88%

Project area	All-hours Tair UHII (°C)**		Localized/no advection UHII attainment local mitigation only	Localized+advection UHII attainment local mitigation+advection
D08 Granite Bay	5.72	Cool roofs / pavements	-25%	-48%
		Cool pavements	-30%	-54%
		Electric vehicles	-5%	-29%
		Vegetation cover	-18%	-42%
D08 Roseville	6.63	Cool roofs / pavements	-21%	-53%
		Cool pavements	-26%	-57%
		Electric vehicles	-5%	-36%
		Vegetation cover	-16%	-47%
D09 El Dorado Hills	5.22	Cool roofs / pavements	-29%	-47%
		Cool pavements	-32%	-51%
		Electric vehicles	-4%	-22%
		Vegetation cover	-21%	-40%
D09 Folsom	5.62	Cool roofs / pavements	-27%	-51%
		Cool pavements	-30%	-55%
		Electric vehicles	-3%	-28%
		Vegetation cover	-20%	-44%
D10 Placerville / Diamond Springs / El Dorado City	1.6	Cool roofs / pavements	-75%	-100%
		Cool pavements	-100%	-125%
		Electric vehicles	-5%	-30%
		Vegetation cover	-81%	-106%

7. CONCLUDING REMARKS AND QUALITATIVE TAKEAWAYS

In concluding this report, a few qualitative takeaways are provided, in no particular order:

1. Significant urban-heat pollution exists in the 6-counties Capital region. The UHI and the UHII are larger in urban areas that (1) are more densely built up, (2) cover a larger geographical area, (3) located at the downwind end of an urban zone (trajectory-wise), (4) located at higher elevations, and (5) surrounded by non-urban areas that cool down significantly faster at night.
2. While temperature in the Capital region generally increases from current climate to future (e.g., to 2050 RCP 4.5 and then to 2050 RCP 8.5), the corresponding UHII also increases in this direction except for two urban areas where the UHII can be smaller in RCP 8.5 than in RCP 4.5 (although still larger than in current climate). This is a result of faster warming in the surrounding non-urban areas.
3. It is possible and highly feasible to mitigate the current UHI and offset the UHII (in some cases completely) using materials and practices that are reasonable and readily used throughout the 6-counties Capital region. The proposed UHI mitigation measures are reasonable – meaning they do not require hypothetical or extreme implementation levels, only what is already available and used in the current market and current construction and building practices.
4. Mitigation measures can offset the local UHII in standalone fashion, in some cases completely. Various combinations of measures can further attain or further offset the UHII, although the total effects of combinations of measures are not linear (not simple sums of individual cooling effects) and generally smaller than the sum of cooling effects from the individual UHI-mitigation measures.
5. The mitigation measures can have significant beneficial effects in terms of public heat health as indicated by their ability to lower the warning levels of the National Weather Service Heat Index (NWS HI). This was assessed by modeling various UHI-mitigation scenarios in this study.
6. The cooling measures can significantly reduce or completely erase the number of heat-wave days during several excessive-heat event periods identified in the study.
7. The mitigation measures are as effective under conditions of future climate and land use as they are under current conditions.
8. Different mitigation measures affect urban heat and temperature differently during different times of the day. Hence it is possible to target certain specific time intervals, e.g., peaks, night, day, or all hours (per a community or city's needs), if so desired, by choosing a specific mitigation measure or combinations of measures as suitable.
9. If, in addition to a community's own heat-mitigation actions, neighboring communities also implement UHI-mitigation measures, the local cooling effects could double (although there is a range of effects depending on location, time, specific measures, etc.).

10. Other measures that are not conventionally associated with urban cooling (or urban heat island mitigation), such as (1) vehicle electrification, (2) solar PV installations, and (3) smart urban growth, all appear to have significant urban-cooling effects.
11. The cooling effects are significant and beneficial across a range of urban areas in the Capital region, including AB617 and disadvantaged communities, which can help improve thermal comfort, reduce emissions of air pollutants, and improve air quality.
12. In this study, a ranking of measures' efficacy was done for each region, each measure, and each time interval (e.g., specific hours or a range of hours) for current and future climates and land use. Some areas or time intervals have a consistent ranking of measures, others vary by location, and, yet, others vary in future climate relative to current conditions. Some highlights are:
    a. For the 0600-PDT UHII:
        i. The rankings of mitigation measures (order) are similar and consistent across all regions.
        ii. Within each region, the rankings are similar across current and future climates.
    b. For the 1300-PDT UHII:
        i. The rankings are different across the regions.
        ii. In Davis and Sacramento, the rankings are different in future climate than they are in current climate.
    c. For the 1400 – 2000 PDT UHII:
        i. The rankings are different across the regions.
        ii. In Woodland, the rankings are different in future climate than they are in current climate.
    d. For the 1500 PDT UHII:
        i. The rankings are different across the regions.
        ii. In Auburn, Davis, El Dorado Hills, and Yuba City, the rankings are different in future climate than they are in current climate.
    e. For the all-hours UHII:
        i. The rankings are different across the regions.
        ii. Within each region, the rankings are similar across current and future climates.
13. Information generated in this modeling study can be used by Caltrans, SMAQMD, LGC, the cities and communities in the Capital region to prioritize projects and implementation of various measures or in the allocation of resources per urban-heat criteria under current climate conditions as well as in future climate and land use.

8. REFERENCES

Akbari H, Konopacki S, 2005. Calculating energy-saving potentials of heat-island reduction strategies. Energy Policy, 33, 721-756.

Akbari H, Rose S, Taha H, 1999. Characterizing the fabric of the urban environment: A case study of Sacramento, California. Lawrence Berkeley National Laboratory report LBNL-44688, Berkeley, California.

Alfaro E, Gershunov A, Cayan D, Steinemann A, Pierce D, Barnett T 2004. A method for prediction of California summer air surface temperature, EOS Transactions AGU, 85, 553–558 doi:10.1029/2004EO510001

Alfaro E, Gershunov A, Cayan D 2006. Prediction of summer maximum and minimum temperature over the central and western United States: The role of soil moisture and sea surface temperature. Journal of Climate 19, 1407-1421, doi: 10.1175/JCLI3665.1

Anderson JR, Hardy EE, Roach JT, Witmer RE, 2001. A land use and land cover classification system for use with remote sensor data. USGS Professional Paper 964, U.S. Government Printing Office, Washington, DC.

Ban-Weiss GA, Woods J, Millstein D, Levinson R, 2015. Using remote sensing to quantify albedo of roofs in seven California cities, Part 2: Results and application to climate modeling. Solar Energy, 115, 791-80, doi:10.1016/j.solener.2014.10.041

Benjamin M, Sudol M, Bloch L, Winer A, 1996. Low-emitting urban forests: A taxonomic methodology for assigning isoprene and monoterpene emission rates. Atmospheric Environment, 30, 1437 – 1452.

Berdahl P, Akbari H, Rose S, 2002. Aging of reflective roofs: Soot deposition. Applied Optics, 41, 2355. Also, Lawrence Berkeley National Laboratory Report No. 45367.

Berdahl P, Bretz S, 1997. Preliminary survey of the solar reflectance of cool roofing materials. Lawrence Berkeley National Laboratory Report No. 41294.

Bierwagen BG, Theobald DM, Pyke CR, Choate A, Groth P, Thomas JV, Morefield P 2010. National housing and impervious surface scenarios for integrated climate impacts assessments. PNAS 107, 20887-20892.

Bruyere C, Done JM, Holland GJ, Fredrick S, 2014. Bias corrections of global models for regional climate simulations of high-impact weather. Climate Dynamics, 43, 1847-1856, doi: 10.1007/s00382-013-2011-6

Burian S, Han WS, Brown M, 2003. Morphological analyses using 3-D building databases: Houston Texas. Department of Civil and Environmental Engineering, University of Utah.

Chen F, Kusaka H, Bornstein R, Ching J, Grimmond CSB, Grossman-Clarke S, Loridan T, Manning K, Martilli A, Miao S, Sailor D, Salamanca F, Taha H, Tewari M, Wang X, Wyszogrodzki A, Zhang C, 2010. The integrated WRF/urban modeling system: development, evaluation, and applications to urban environmental problems. International Journal of Climatology doi:10.1002/joc.2158.

Ching J, Brown M, Burian S, Chen F, Cionco R, Hanna A, Hultgren T, McPherson T, Sailor D, Taha H, Williams D, 2009. National urban database and access portal tool, NUDAPT. Bulletin of the American Meteorological Society doi:10.1175/2009BAMS2675.1

Clarke LE, Edmonds JA, Jacoby HD, Pitcher H, Reilly JM, Richels R, 2007. Scenarios of greenhouse gas emissions and atmospheric concentrations. Sub-report 2.1a of Synthesis and Assessment Product 2.1. Climate Change Science Program and the Subcommittee on Global Change Research, Washington DC.

Cooper CD, Alley FC, 1994. Air pollution control: A design approach. Waveland Press, Inc., Prospect Heights, IL, 694 pp.
Davey (2018). Urban tree canopy assessment, Sacramento, CA. Report prepared by Davey Resource Group for the City of Sacramento, pp. 56, Atascadero, California.
DuPont S, Mestayer PG, Guilloteau E, 2005. Parameterization of the urban water budget with the sub-mesoscale model. Journal of Applied Meteorology and Climatology, 45, 624 – 648.
Epstein SA, Lee S-M, Katzenstein AS, Carreras-Sospedra M, Zhang X, Farina SC, Vahmani P, Fine PM, Ban-Weiss G, 2017. Air-quality implications of widespread adoptions of cool roofs on ozone and particulate matter in southern California. PNAS August 7, 2017, https://doi.org/10.1073/pnas.1703560114.
Fallmann J, Forkel R, Emeis S, 2016. Secondary effects of urban heat island mitigation measures on air quality. Atmospheric Environment, 125, 199 – 211.
Fan H, Sailor DJ, 2005. Modeling the Impacts of Anthropogenic Heating on the Urban Climate of Philadelphia: A comparison of implementations in two PBL schemes. Atmospheric Environment, 39, 73-84.
Founda D, Santamouris M, 2017. Synergies between urban heat island and heat waves in Athens (Greece) during extremely hot summer (2012). Scientific Reports, 7: 10973. doi:10.1038/s41598-017-11407-6
Georgescu M, Morefield PE, Bierwage BG, Weaver CP. 2014. Urban adaptation can roll back warming of emerging metropolitan regions. Proceedings of the National Academy of Sciences 111, 2909-2914 doi: 10.1073/pnas.1322280111
Gershunov A, Cayan DR, Iacobellis SF, 2009. The great 2006 heat wave over California and Nevada: Signal of an increasing trend. Journal of Climate 22, 6181-6203.
Gery MW, Whitten GZ, Killus JP, 1988. Development and testing of the CBM-IV for urban and regional modeling. Report EPA-600/3-88-012, US EPA, Research Triangle Park, NC.
Gilbert HE, Rosado PJ, Ban-Weiss G, Harvey JT, Li H, Mandel BH, Millstein D, Mohegh A, Saboori A, Levinson RM, 2017. Energy and environmental consequences of a cool pavement campaign. Energy and Buildings, 157, 53-77, doi:10.1016/j.enbuild.2017.03.051
Grimmond CSB, Oke TR, 1999. Aerodynamic properties of urban areas derived from analysis of surface form. Journal of Applied Meteorology, 38, 1262-1292.
Hijioka Y, Matsuoka Y, Nishimoto H, Masui T, Kainuma M, 2008. Global GHG emission scenarios under GHG concentration stabilization targets. Journal of Global Environmental Engineering, 13, 97–108
Jacobson MZ, TenHoeve JE, 2011. Effects of urban surfaces and white roofs on global and regional climate. Journal of Climate, doi: 10.1175/JCLI-D-11-00032.1
Johnston B, Lehmer E, Gao S, Roth N, McCoy M. 2013. UPlan Land Use Allocation Model 2.6. University of California at Davis – Information Center for the Environment (http://ice.ucdavis.edu/project/uplan).
Kalkstein LS, Barthel CD, Green JS, Nichols MC,1996. A new spatial synoptic classification: Application to air-mass analysis. International Journal of Climatology, 16, 983-1004.
Kistler R, Kalnay E, Collins W, et al., 2001. The NCEP-NCAR 50-year reanalysis: Monthly means CDROM and documentation. Bulletin of the American Meteorological Society, 82, 247-267
Kusaka H, Kondo H, Kikegawa Y, Kimura F, 2001. A simple single-layer urban canopy model for atmospheric models: Comparison with multi-layer and slab models. Boundary-Layer Meteorology, 101, 329-358

Levinson R, Akbari H, Reilly JC, 2007. Cooler tile-roofed buildings with near-infrared-reflective non-white coatings. Energy & Buildings, 42, 2591-2605.

Levinson RM, Gilbert HE, Jin L, Harvey J, Kendall A, Li H, Mandel B, Millstein D, Rosado P, Saboori A, Lea J, Ban-Weiss G, Mohegh A, Santero N, 2017. Life-cycle assessment and co-benefits of cool pavements. Report prepared by the Lawrence Berkeley National Laboratory for the California Air Resources Board and the California Environmental Protection Agency under Contract 12-314.

Li D, Bou-Zeid E. 2013. Synergistic interactions between urban heat islands and heat waves: The impact in cities is larger than the sum of its parts. Journal of Applied Meteorology and Climatology 52, 2051-2064 doi: 10.1175/JAMC-D-13-02.1

Liu SC, Trainer M, 1988. Response of the tropospheric ozone and odd hydrogen radicals to column ozone change. Journal of Atmospheric Chemistry, 6, 221 – 233.

Macdonald RW, Griffiths RF, Hall DJ, 1998. An improved method for estimation of surface roughness of obstacle arrays. Atmospheric Environment, 32, 1857–1864

Martilli A, Clappier A, Rotach MW 2002. An urban surface exchange parameterization for mesoscale models. Boundary-Layer Meteorology, 104, 261-304

Masson V, Bonhomme M, Salagnac J-L, Briottet X, Lemonsu A, 2014. Solar panels reduce both global warming and urban heat island. Frontiers in Environmental Science, doi: 10.3389/fenvs.2014.00014

Multi-Resolution Land-Characteristics Consortium (MRLC) 2011. National Land Cover Databases. http://www.mrlc.gov/data/nlcd-2011-land-cover-conus-0

National Oceanic and Atmospheric Administration 2015. CM2 and CMIP5 models.

https://www.ncdc.noaa.gov/data-access/model-data/model-datasets/climate-prediction

NOAA/MADIS. National Oceanic and Atmospheric Administration / Meteorological Assimilation Data Ingest System (https://madis.ncep.noaa.gov/)

OEHHA 2013. California Communities Environmental Health Screening Tool, Version 1 (CalEnviroScreen 1.0) Guidance and Screening Tool. Office of Environmental Health Hazard Assessment Report, Sacramento, California, oehha.ca.gov/ej/pdf/042313CalEnviroScreen1.pdf

Pleim J, Xiu A, Finkelstein P, Otte T, 2001. A coupled land-surface and dry deposition model and comparison to field measurements of surface heat, moisture, and ozone fluxes. Water, Air, and Soil Pollution, 1, 243-252.

Pretzsch H, Biber P, Uhl E, Dahlhausen J, Rotzer T, Caldentey J, Koike T, van Con T, Chavanne A, Seifert T, du Toit B, Farnden C, Apuleit S, 2015. Crown size and growing space requirements of common tree species in urban center, parks, and forests. Urban Forestry & Urban Greening, 14, 466 – 479.

Riahi K, Krey V, Rao S, Chirkov V, Fischer G, Kolp P, Kindermann G, Nakicenovic N, Rafai P, 2011. RCP-8.5: exploring the consequence of high emission trajectories. Climatic Change, doi: 10.1007/s10584-011-0149-y

Rosado PJ, Ban-Weiss G, Mohegh A, Levinson RM, 2017. Influence of street setbacks on solar reflection and air cooling by reflective streets in urban canyons. Solar Energy 144, 144-157, doi:10.1016/j.solener.2016.12.026

Rose S, Akbari H, Taha H, 2003. Characterizing the fabric of the urban environment: A case study of Greater Houston, Texas. Lawrence Berkeley National Laboratory report LBNL-51448, Berkeley, California.

Sailor DJ, Lu L, 2004. A top–down methodology for developing diurnal and seasonal anthropogenic heating profiles for urban areas. Atmospheric Environment, 38, 2737 – 2748.

Salamanca F, Martilli A, 2009. A new building energy model coupled with an urban canopy parameterization for urban climate simulations – Part II: Validation with one dimension off-line simulations. Theoretical and Applied Climatology, 99, 345-356, doi: 10.1007/s00704-009-0143-8

Salamanca F, Georgescu M, Mahalov A, Moustaoui M, Martilli A, 2016. Citywide impacts of cool roofs and rooftop photovoltaic development on near-surface air temperature and cooling energy demand. Boundary-Layer Meteorology, 161, 203-221.

Seinfeld JS, 1975. Air pollution – Physical and chemical fundamentals. McGraw Hill, New York, NY.

Seinfeld JS, Pandis SN, 1998. Atmospheric Chemistry and Physics. John Wiley & Sons, Inc., New York, 1326 pp.

Simpson J, McPherson G, 2007. Preliminary evaluation of the potential air-quality benefits of trees within SIP guidelines. Center for Urban Forest Research, PSW, USDA Forest Service.

Skamarock W, Klemp J, Dudhia J, et al., 2008. A description of the Advanced Research WRF. NCAR Technical Note NCAR/TN-475+STR, National Center for Atmospheric Research, Boulder, Colorado.

Sleeter BM, Wilson TS, Sherba JT. 2017a. Land use and land cover projections for California's 4th Climate Assessment. US Geological Survey Data Release, doi: 10.5066/F7M61HFP. IP-083329.

Sleeter BM, Wilson TS, Sharygin E, Sherba JT, 2017b. Future scenarios of land change based on empirical data and demographic trends. Earth's Future, 5, 1068–1083, doi: 10.1002/2017EF000560

SMAQMD 2018. Final Assessment of Proposed Monitoring Locations for AB 617 Community Air Protection Action. Report prepared by the Sacramento Metropolitan Air Quality Management District, July 31, 2018.

Stern AC, Boubel RW, Turner DB, Fox DL, 1984. Fundamentals of air pollution. Academic Press, Inc., 530 pp.

Taha H, 2018. Intra-urban enhancements to probabilistic climate forecasting for the electric system. Contract CEC-15-070; report to be published online on the California Energy Commission Website.

Taha H, 2017. Characterization of urban heat and exacerbation: Development of a heat island index for California. Climate 5, 59. doi:10.3390/cli5030059.

Taha H, 2015a. Cool cities: counteracting potential climate change and its health impacts. Current Climate Change Reports, doi: 10.1007/s40641-015-0019-1.

Taha H, 2015b. Meteorological, air-quality, and emission-equivalence impacts of urban heat island control in California. Invited Paper, Sustainable Cities and Society, doi: 10.1016/j.scs.2015.03.009

Taha H, 2013a. Meteorological, emissions, and air-quality modeling of heat-island mitigation: Recent findings for California, U.S.A. International Journal of Low Carbon Technologies, doi: 10.1093/ijlct/ctt010

Taha H, 2013b. Multi-episodic and seasonal meteorological, air-quality, and emission-equivalence impacts of heat-island control and evaluation of the potential atmospheric effects of urban solar photovoltaic arrays. Final report prepared by Altostratus Inc. for the California Energy Commission, PIER Environmental Research Program, Sacramento, California.

http://www.energy.ca.gov/2013publications/CEC-500-2013-061/CEC-500-2013-061.pdf

Taha H, 2012. The potential for air-temperature impact from large-scale deployment of solar photovoltaic arrays in urban areas. Solar Energy, 91, 358 – 367.

Taha H, 2008a. Meso-urban meteorological and photochemical modeling of heat island mitigation. Atmospheric Environment, 42, 8795-8809, doi:10.1016/j.atmosenv.2008.06.036.

Taha H, 2008b. Episodic performance and sensitivity of the urbanized MM5 (uMM5) to perturbations in surface properties in Houston TX. Boundary-Layer Meteorology 127, 193-218. doi:10.1007/s10546-007-9258-6.

Taha H, 2008c. Urban surface modification as a potential ozone air-quality improvement strategy in California: A mesoscale modeling study. Boundary-Layer Meteorology, 127, 219-239 doi:10.1007/s10546-007-9259-5.

Taha H, 2007. Urban surface modification as a potential ozone air-quality improvement strategy in California -- Phase 2: Fine-resolution meteorological and photochemical modeling of urban heat islands. Final report prepared by Altostratus Inc. for the California Energy Commission, Sacramento, California, PIER Environmental Research. http://www.energy.ca.gov/2009publications/CEC-500-2009-071/CEC-500-2009-071.PDF

Taha H, 2005. Urban surface modification as a potential ozone air-quality improvement strategy in California -- Phase 1: Initial Mesoscale Modeling, Final report prepared by Altostratus Inc. for the California Energy Commission, Sacramento, California, PIER Environmental Research, 169 pp. http://www.energy.ca.gov/2005publications/CEC-500-2005-128/CEC-500-2005-128.PDF

Taha H, 2001. Potential impacts of climate change on tropospheric ozone in California: A preliminary assessment of the Los Angeles basin and the Sacramento valley. Lawrence Berkeley National Laboratory Report LBNL-46695, http://escholarship.org/uc/item/5s41x609

Taha H, 1999. Modifying a Mesoscale Meteorological Model to Better Incorporate Urban Heat Storage: A Bulk-Parameterization Approach. Journal of Applied Meteorology, 38, 466-473.

Taha H. 1997. Modeling the Impacts of Large-Scale Albedo Changes on Ozone Air Quality in the South Coast Air Basin. Atmospheric Environment, 31, 1667-1676.

Taha H, 1996. Modeling the Impacts of Increased Urban Vegetation on the Ozone Air Quality in the South Coast Air Basin. Atmospheric Environment, 30, 3423-3430.

Taha H, Levinson R, Mohegh A, Gilbert H, Ban-Weiss G, Chen S, 2018. Air-temperature response to neighborhood-scale variations in albedo and canopy cover in the real world: Fine-resolution meteorological modeling and mobile temperature observations in the Los Angeles climate archipelago. Climate 6, 53 (25 pp). https://doi.org/10.3390/cli6020053

Taha H, Freed T 2015. Creating and mapping an urban heat island index for California. Prepared by Altostratus Inc. for the California Environmental Protection Agency. https://calepa.ca.gov/wp-content/uploads/sites/34/2016/10/UrbanHeat-Report-Report.pdf

Taha H, Wilkinson J, Bornstein R, Xiao Q, McPherson G, Simpson J, Anderson C, Lau S, Lam J, Blain C, 2015. An urban–forest control measure for ozone in the Sacramento, CA Federal Non-Attainment Area (SFNA), Sustainable Cities and Society, 21, 51-65 doi: 10.1016/j.scs.2015.11.004.

Taha H, Wilkinson J, Bornstein R, 2011. Urban forest for clean air demonstration in the Sacramento Federal Non-Attainment Area: Atmospheric modeling in support of a voluntary control strategy. Project final report prepared by Altostratus Inc. for the Sacramento Metropolitan Air Quality Management District (SMAQMD), Sacramento, California.

Taha, H. and Sailor, D. 2010. “Evaluating the effects of radiative forcing feedback in modeling urban ozone air quality in Portland, Oregon: Two-way coupled MM5 - CMAQ simulations”. *Boundary-Layer Meteorology*, Volume 137, No. 2, (2010), pp. 291-305-- doi:10.1007/s10546-010-9533-9.

Taha, H., Konopacki, S., and Gabersek, S. 1999. "Impacts of large-scale surface modifications on meteorological conditions and energy use: A 10-region modeling study", *Theoretical and Applied Climatology*, Vol. 62, no. 3-4, pp. 175-185.

Tesche TW, McNally DE, Emery CA, Tai E 2001. Evaluation of the MM5 model over the Midwestern U.S. for three 8-hour oxidant episodes, Prepared for the Kansas City Ozone Technical Workgroup. Alpine Geophysics LLC and Environ Corp.

Thompson AM, 1991. Interaction of atmospheric chemicals and climate changes: Implications for tropospheric ozone. Chapter 4 in Sloane CS and Tesche TW (eds.) 1991. Atmospheric chemistry models and predictions for climate and air quality. Lewis Publishers, Inc. Michigan.

Thompson AM, 1992. The oxidizing capacity of the Earth’s atmosphere: Probable past and future changes. Science, 256, 1157 – 1165.

Van Vuuren DP, Stehfest E, Den Elzen MGJ, Deetman S, Hof A, Isaac M, Klein Goldewijk K, Kram T, Mendoza Beltran A, Oostenrijk R et al., 2011. RCP2.6: Exploring the possibility to keep global mean temperature change below 2°C. Climatic Change. doi: 10.1007/s10584-011-0152-3